



UNIVERSITAT DE
BARCELONA

Nanotechnology-mediated strategies targeting cancer stem cells for advanced cancer treatment

Sara Montero Martin

ADVERTIMENT. La consulta d'aquesta tesi queda condicionada a l'acceptació de les següents condicions d'ús: La difusió d'aquesta tesi per mitjà del servei TDX (www.tdx.cat) i a través del Dipòsit Digital de la UB (diposit.ub.edu) ha estat autoritzada pels titulars dels drets de propietat intel·lectual únicament per a usos privats emmarcats en activitats d'investigació i docència. No s'autoritza la seva reproducció amb finalitats de lucre ni la seva difusió i posada a disposició des d'un lloc aliè al servei TDX ni al Dipòsit Digital de la UB. No s'autoritza la presentació del seu contingut en una finestra o marc aliè a TDX o al Dipòsit Digital de la UB (framing). Aquesta reserva de drets afecta tant al resum de presentació de la tesi com als seus continguts. En la utilització o cita de parts de la tesi és obligat indicar el nom de la persona autora.

ADVERTENCIA. La consulta de esta tesis queda condicionada a la aceptación de las siguientes condiciones de uso: La difusión de esta tesis por medio del servicio TDR (www.tdx.cat) y a través del Repositorio Digital de la UB (diposit.ub.edu) ha sido autorizada por los titulares de los derechos de propiedad intelectual únicamente para usos privados enmarcados en actividades de investigación y docencia. No se autoriza su reproducción con finalidades de lucro ni su difusión y puesta a disposición desde un sitio ajeno al servicio TDR o al Repositorio Digital de la UB. No se autoriza la presentación de su contenido en una ventana o marco ajeno a TDR o al Repositorio Digital de la UB (framing). Esta reserva de derechos afecta tanto al resumen de presentación de la tesis como a sus contenidos. En la utilización o cita de partes de la tesis es obligado indicar el nombre de la persona autora.

WARNING. On having consulted this thesis you're accepting the following use conditions: Spreading this thesis by the TDX (www.tdx.cat) service and by the UB Digital Repository (diposit.ub.edu) has been authorized by the titular of the intellectual property rights only for private uses placed in investigation and teaching activities. Reproduction with lucrative aims is not authorized nor its spreading and availability from a site foreign to the TDX service or to the UB Digital Repository. Introducing its content in a window or frame foreign to the TDX service or to the UB Digital Repository is not authorized (framing). Those rights affect to the presentation summary of the thesis as well as to its contents. In the using or citation of parts of the thesis it's obliged to indicate the name of the author.



UNIVERSITAT DE BARCELONA

FACULTAT DE FARMÀCIA I CIÈNCIES DE L'ALIMENTACIÓ

Doctorat en Biomedicina

**NANOTECHNOLOGY-MEDIATED STRATEGIES TARGETING CANCER
STEM CELLS FOR ADVANCED CANCER TREATMENT**

Sara Montero Martin, 2021

NANOTECHNOLOGY-MEDIATED STRATEGIES TARGETING CANCER
STEM CELLS FOR ADVANCED CANCER TREATMENT

Memòria presentada per Sara Montero Martin per a optar al grau de doctor per
la Universitat de Barcelona

Programa de Doctorat en Biomedicina

Barcelona, 2021

Tesi realitzada sota la direcció del Dr. Simo Schwartz Navarro i la Dra. Diana Fernandes de Sousa Rafael, de l'Institut de Recerca de la Vall d'Hebron i sota la tutorització de la Dra. Veronica Noé Mata del Departament de Bioquímica i Fisiologia de la Universitat de Barcelona



Dr. Simo Schwartz Navarro



Dra. Diana Fernandes de Sousa Rafael



Dra. Veronica Noé Mata



Sara Montero Martin

Aquesta memòria de tesi doctoral titulada “*Nanotechnology-mediated strategies targeting cancer stem cells for advanced cancer treatment*” es presenta com a compendi de dues publicacions, on la doctoranda Sara Montero Martin consta com a primera autora i són fruit directe del seu treball de tesi. El Dr. Simo Schwartz Navarro i la Dra. Diana Fernandes de Sousa Rafael, com a directors de tesi, certifiquen que la memòria presentada per la Sara Montero Martin per a accedir al títol de Doctor en Biomedicina per la Universitat de Barcelona s’ha realitzat sota la seva supervisió i compleix els requisits formals i científics per a ser defensada davant del tribunal corresponent.

El treball ha estat realitzat al grup d’investigació Drug Delivery and Targeting de l’Institut de Recerca de la Vall d’Hebron.

ARTICLE 1: Montero S, *et al.* ZileutonTM loaded in polymer micelles effectively reduce breast cancer circulating tumor cells and intratumoral cancer stem cells. *Nanomedicine*. 2020;24:102106.

- DOI: 10.1016/j.nano.2019.102106
- IF 2020: 6.458; Quartile: Q1 in medicine, research and experimental.

ARTICLE 2: Montero S, *et al.* Intracellular delivery of Anti-SMC2 antibodies against cancer stem cells. *Pharmaceutics*. 2020;12(2):185.

- DOI: 10.3390/pharmaceutics12020185
- IF 2020: 6.321; Quartile: Q1 in pharmacology and pharmacy.

Barcelona, 2021

Dr. Simo Schwartz Navarro

Dra. Diana Fernandes de Sousa Rafael

A la meva gent.

A totes aquelles persones que han aportat alguna pedra,
per petita que hagi estat,
en aquest llarg camí.

Acknowledgements

Ja fa quasi quatre anys que va començar aquesta etapa que tot just ara finalitza. Durant aquest temps, com a la vida, hi ha hagut moments per a tot, però sobretot per a aprendre i millorar dia a dia professional i personalment. Han sigut moltes les persones que he conegut i han estat presents en aquest recorregut, que d'una manera o altra m'han ajudat i acompanyat en aquest camí. Tot l'esforç i dedicació que hi ha darrere d'aquestes pàgines és, en gran part, vostre. A totes elles, GRÀCIES, ha estat un plaer.

En primer lloc m'agradaria agrair al Dr. Simo Schwartz per haver-me donat l'oportunitat de poder realitzar la meua tesi doctoral al seu grup d'investigació, obrir-me les portes del seu laboratori i permetre'm aprendre tot el que avui sé.

Para as minhas colegas portuguesas, simplesmente não tenho palavras. Gracias por la comprensión, enorme generosidad y cantidad de momentos que hemos disfrutado tanto dentro como fuera del laboratorio. Diana, gracias por la infinidad de aprendizajes que me has aportado durante todos estos años, tanto a nivel laboral, personal, pero sobretodo de la vida en general. Creo que nunca podré devolverte todo lo que has hecho por mí. Fernanda, gracias a ti también por toda la ayuda, por tener siempre respuesta y solución a todo tipo de problemas, incluso en los momentos más críticos. Estar a tu lado es, sin duda, garantía de estar en constante formación. Muito obrigada pelo grande apoio, por estarem sempre disponíveis para ajudar.

Gracias Petra, por enseñarme a manejar y mover en un laboratorio, por ayudarme en mis inicios y aconsejarme cuando los resultados igual no eran los esperados. Gràcies Quim, per la teua implicació i predisposició sempre que ho he necessitat, tot i estar saturat de feina. Per les teves idees i propostes, sempre amb ganes de millorar. Als meus companys doctorands, Francesc i Patri, pel bon humor i bon rotllo creat al laboratori. Gràcies també per tots els viatges, països i experiències que hem pogut compartir; se'ns dubte, una de les meves parts preferides de tota aquesta etapa.

Laura, gràcies per posar una mica d'ordre al, a vegades, caòtic laboratori. Persones amb la teua incansable energia són necessàries per a que tot funcioni a perfecció.

Gràcies a tu també Mireia. Potser no t'ho sembla, però vas arribar en un moment clau i tenir la teua alegria rondant pel laboratori va ser essencial. Només puc desitjar-te moltíssima sort en aquest nou camí que recentment has començat.

Gràcies a totes les persones, que en algun moment o altre han format part del grup DDT, generant un bon ambient de treball i fent més agradable el dia a dia. Gràcies per haver-me fet sentir una més en tot això, ha estat un enorme plaer poder compartir laboratori amb tots vosaltres. Agrair també a totes les persones que formen part de la plataforma functional validation and preclinical research, fent possible tots els experiments in vivo.

Gràcies Verònica, per estar disponible sempre que ho he necessitat i rebre'm amb la teva bona energia.

Gracias familia, por estar siempre a mi lado, por todos los valores que me habéis transmitido y hacer de mi la persona que soy hoy en día. Sin vuestra ayuda y apoyo nada de todo esto habría sido posible. Gracias Joana, por esos paseos interminables, por aguantar mis charlitas (y yo las tuyas también), por estar siempre ahí. No sé en qué momento has pasado de ser mi hermana pequeña, a uno de los apoyos más importantes de mi vida. A tu lado todo parece mucho más sencillo. Estoy muy orgullosa de ti y de todo lo que logras día a día. Sin duda eres un gran ejemplo de superación.

Gràcies a totes aquelles persones que em coneixen perfectament, que saben aconsellar i acompanyar. Afortunadament, en tinc unes quantes al meu voltant, i no podria estar més agraïda.

Gràcies a les meves amigues, les de sempre, per seguir al meu costat. Gaudint i rient als bons moments, i fent-me costat sempre que les coses no han estat tan fàcils. Gràcies per compartir literalment tota la vida amb mi, des que tinc consciència, per sempre estar disposades a escoltar i ajudar quan ho he necessitat.

Gracias a las chicas del quinto, por este espacio llamado casa que estamos construyendo, por las risas y calorcito confortable que mejoran y relajan el día a día. Gracias por el soporte incondicional y hacerme sentir que todo es posible. De veras que me ha venido genial un lugar así para dar punto y final a esta etapa.

Abstract

Despite the latest advances in early diagnosis and increased resources employed to develop new therapeutic options, effective control of cancer disease remains a challenge. In fact, cancer is the second leading cause of death and represents a huge economic impact on global health. Furthermore, currently available therapies exhibit limited efficacy for metastasis, being advanced cancer still considered an incurable disease. In this context, it has been shown that metastatic spread, resistance to treatment, as well as aggressiveness of recurrent disease are supported by the presence of cancer stem cells (CSC) within the tumors, a small cell subpopulation that have the ability to regenerate them after chemo- or radiotherapy. Indeed, CSC are intrinsically drug-resistant, thus being responsible for many therapeutic failures. Therefore, in order to increase cancer patient survival, the development of new therapeutic strategies specifically targeting the CSC compartment is required to successfully overcome drug resistance and prevent subsequent tumor relapse. On the other side, conventional chemotherapy produces high systemic toxicity and presents dose-limiting issues due to its low solubility. Thus, difficulties in achieving the required efficacy in the clinical settings are common. Fortunately, tumors can act as therapeutic targets and be passively reached by nanomedicines through the well-known enhanced permeability and retention (EPR) effect. Hence, nanotechnology-based therapies with oncological indications have grown considerably in recent decades, increasing the number of approved products by regulatory agencies, as well as those enrolled in clinical trials. In this regard, the use of nanoparticles as nano-sized drug delivery systems (nano-DDS) is a potential option that provides the opportunity to increase the therapeutic efficacy of loaded agents, reduce harmful side effects and, most importantly, specifically target and eradicate the CSC fraction. Noteworthy, depending on the nano-DDS nature, it is possible to deliver a wide range of payloads, improving their pharmacokinetic patterns while evading the CSC characteristic resistance mechanisms and, consequently, achieving higher drug intracellular accumulation. In particular, polymeric micelles (PM) are nano-DDS widely used in the biomedical field due to their high stability, increased cargo bioavailability, biocompatibility and biodegradability. Moreover, PM can be manufactured through a simple and economic production method, which can be easily scaled-up for future clinical implementation.

Therefore, aiming to specifically eliminate the CSC subset, previous studies performed in our laboratory group were focused on the identification of characteristic CSC targets, namely the arachidonate 5-lipoxygenase (ALOX5) enzyme and the structural maintenance of chromosomes 2 (SMC2) protein. Herein, we have designed and developed two new anti-CSC therapeutic strategies based on blocking key molecular

pathways essential for CSC survival and proliferation, through the ALOX5 and SMC2 inhibition. In addition, combination therapy, which simultaneously eradicates both CSC and bulk tumor cells subpopulations, has also been assessed.

Specifically, two anti-CSC subpopulation therapeutic strategies have been developed, namely i) pharmacological approach, with the ALOX5 chemical inhibitor ZileutonTM; and ii) biotherapeutic approach, where the specific SMC2 blockade is achieved with antibodies anti-SMC2 (Ab-SMC2) protein. Aiming to allow their solubilization and to protect therapeutic agents from degradation, Pluronic® F127-based PM were designed to encapsulate ZileutonTM (PM-ZileutonTM) and Ab-SMC2 (PM-CON:SMC2). Both formulations were physicochemically characterized, and preclinically validated *in vitro* and *in vivo* breast and colon cancer models. The obtained results demonstrated that both proposed anti-CSC therapeutic strategies, PM-ZileutonTM and PM-CON:SMC2, improve their effectiveness *in vitro* compared to their free anti-cancer agent, particularly in the challenging fraction of CSC. Importantly, when conventional treatments showed strong resistance, both formulations were substantially effective in terms of cell viability reduction and colony formation impairment. Further, thanks to the great structural versatility provided by Pluronic® F127-based PM it was possible to perform combination therapy, mixing PM-CON:SMC2 with conventional chemotherapeutics such as Paclitaxel (PTX) and 5-Fluorouracil (5-FU) to treat not only the primary tumor, but also the resultant metastasis by targeting both CSC and differentiated tumor cells, respectively. Notably, the combined micelles showed higher efficacy than their free forms in terms of inhibition of tumorspheres formation. In addition, due to the preferred accumulation of PM at the tumor site and the specificity of ZileutonTM in CSC elimination, a significant intratumoral decrease of CSC *in vivo* after PM-ZileutonTM treatment was observed. Moreover, our results also showed a strong reduction of circulating tumor cells (CTC) and CSC in blood stream, and subsequent reduction of intravasation and invasion capacity of CSC, resulting in a significant reduction of lung metastasis in highly resistant MDA-MB-231 BC model. In conclusion, our data clearly suggest the anti-metastatic potential of PM-ZileutonTM, the effective intracellular release of antibodies targeting SMC2 protein and, furthermore, the opportunity to offer a multifunctional delivery system nanoplatfrom to improve overall therapeutic outcomes of metastatic cancer.

Keywords: Breast and colon cancer; Cancer stem cells (CSC); ALOX5 enzyme; SMC2 protein; ZileutonTM; Intracellular delivery of antibodies; Pluronic® F127-based polymeric micelles (PM); Circulating tumor cells (CTC); Combination therapy; Paclitaxel (PTX); 5-Fluorouracil (5-FU).

Resum

Tot i els darrers avenços en el diagnòstic precoç i l'augment de recursos emprats per a desenvolupar noves opcions terapèutiques, el control eficaç de la malaltia del càncer continua sent un repte. De fet, el càncer és la segona causa de mort arreu del món i representa un gran impacte econòmic pel que fa a la salut mundial. A més, les teràpies disponibles a dia d'avui presenten una eficàcia limitada per al tractament de les metàstasis, fent del càncer avançat una malaltia incurable. En aquest context, s'ha demostrat que la difusió metastàtica, la resistència al tractament i l'agressivitat dels tumors recurrents són degudes a la presència de cèl·lules mare del càncer (CMC) dins dels tumors, una petita subpoblació de cèl·lules que té la capacitat de regenerar-los després dels tractaments amb quimio- o radioteràpia. De fet, les CMC són intrínsecament resistents als fàrmacs i, per tant, responsables de molts dels fracassos terapèutics. Així, amb la finalitat d'incrementar la supervivència dels pacients amb càncer, és necessari el desenvolupament de noves estratègies terapèutiques dirigides específicament a la subpoblació de CMC, per a poder superar amb èxit la resistència farmacològica i, així, evitar la posterior recaiguda de la malaltia. D'altra banda, la quimioteràpia convencional produeix una alta toxicitat sistèmica a més de presentar limitacions a l'hora d'administrar-la degut a la seva baixa solubilitat. Per tant, són freqüents les dificultats per a aconseguir l'eficàcia necessària a la pràctica clínica. Afortunadament, els tumors poden actuar com a dianes terapèutiques i ser assolits passivament per les nanomedicines mitjançant el conegut efecte de permeabilitat i retenció millorada. És per aquest motiu que les teràpies basades en nanotecnologia amb indicacions oncològiques han crescut considerablement en els últims temps, augmentant tant el nombre de productes aprovats per les agències reguladores, com els inscrits a assajos clínics. Així, l'ús de nanopartícules com a sistemes de subministrament de fàrmacs de mida nanomètrica (nano-DDS) possibilita l'increment de l'eficàcia terapèutica dels agents anticancerígens administrats, reduint els efectes secundaris nocius i, el més important, eliminant específicament la fracció de CMC de dins dels tumors. És important destacar que segons la naturalesa dels nano-DDS és possible administrar una àmplia gamma de molècules terapèutiques, millorant els seus patrons farmacocinètics tot evitant els mecanismes de resistència característics de les CMC i, en conseqüència, aconseguir una major acumulació intracel·lular dels fàrmacs. Concretament, les micel·les polimèriques (MP) són nano-DDS àmpliament utilitzats al camp biomèdic degut a la seva elevada estabilitat, biocompatibilitat i biodegradabilitat. Altrament, aquestes nanopartícules es poden fabricar mitjançant un mètode de producció senzill, econòmic i fàcilment escalable per a una futura implementació clínica.

Així, amb l'objectiu d'eliminar específicament el subconjunt de CMC, els estudis previs realitzats al nostre grup de laboratori es van centrar en la identificació de dianes terapèutiques característiques de les CMC, com ara són l'enzim arachidonat 5-lipoxigenasa (ALOX5) i la proteïna estructural maintenance of chromosomes 2 (SMC2). En aquest treball, hem dissenyat i desenvolupat dues estratègies terapèutiques anti-CMC basades en el bloqueig de vies moleculars essencials per a la seva supervivència i proliferació, mitjançant la inhibició de l'ALOX5 i SMC2. També s'ha avaluat la teràpia combinada per tal de valorar l'efecte de l'erradicació simultània, eliminant d'aquesta manera tant la fracció de CMC, com les cèl·lules tumorals diferenciades.

Les estratègies proposades es fonamenten en dos mètodes d'inhibició diferenciats, concretament: i) l'opció farmacològica, amb l'inhibidor químic de l'ALOX5, el ZileutonTM; i ii) l'opció bioterapèutica, on el bloqueig específic de la proteïna SMC2 s'aconsegueix mitjançant anticossos anti-SMC2 (Ab-SMC2). En tots dos mètodes, s'han utilitzat MP produïdes amb el polímer amfifílic Pluronic® F127 per tal de millorar la solubilització de les molècules anti-CMC emprades, així com protegir-les d'una degradació prematura. D'aquesta manera, les micel·les s'han dissenyat per a encapsular el ZileutonTM i els Ab-SMC2, donant lloc a PM-ZileutonTM i PM-CON:SMC2, respectivament. Les dues formulacions es van caracteritzar fisicoquímicament i es van validar preclínicament en models de càncer de mama i còlon *in vitro* i *in vivo*. Els resultats obtinguts van demostrar que les dues estratègies terapèutiques anti-CMC proposades milloren la seva efectivitat *in vitro* en comparació amb el seu agent anticancerigen lliure, particularment a la fracció de les problemàtiques CMC. A més, quan els tractaments utilitzats regularment a la pràctica clínica van mostrar una forta resistència, ambdues formulacions van resultar ser significativament efectives pel que fa a la viabilitat cel·lular i impediment en la formació de colònies. D'altra banda, gràcies a la gran versatilitat estructural proporcionada per les MP de Pluronic® F127, es va poder provar l'efecte de la teràpia combinada barrejant PM-CON:SMC2 amb quimioteràpies d'ús convencionals com ara el Paclitaxel (PTX) i el 5-Fluorouracil (5-FU), amb l'objectiu de no només tractar el tumor primari, sinó també la metastàsis resultant tot dirigint-nos tant a les CMC com a les cèl·lules tumorals diferenciades, respectivament. Cal assenyalar que les micel·les combinades van mostrar una eficàcia superior a les seves formes lliures respecte a la inhibició de la formació d'esferes tumorals, model de creixement específic de les CMC. A més, degut a l'acumulació preferencial de les MP a la regió tumoral i l'especificitat del ZileutonTM eliminant les CMC, es va poder observar una disminució intratumoral significativa de CMC *in vivo* en models de càncer de mama després del tractament amb PM-ZileutonTM. Els resultats també van mostrar una forta reducció de cèl·lules tumorals

circulants (CTC) i CMC al torrent sanguini, donant lloc a una posterior reducció en la capacitat d'invasió de les CMC i, per tant, una disminució significativa de les metàstasis pulmonars al model de càncer de mama MDA-MB-231 altament resistent. Com a conclusió, les nostres dades demostren el potencial anti-metastàtic de les PM-ZileutonTM, així com un eficaç alliberament intracel·lular d'anticossos dirigits a la proteïna SMC2, a més d'oferir l'oportunitat de crear una nanoplataforma multifuncional, com a sistema d'administració, per tal de poder millorar els resultats terapèutics globals del càncer metastàtic.

Paraules clau: Càncer de mama i còlon; Cèl·lules mare del càncer (CMC); Enzim ALOX5; Proteïna SMC2; ZileutonTM; Alliberament intracel·lular d'anticossos; Micelles polimèriques (MP); Cèl·lules tumorals circulants (CTC); Teràpia combinada; Paclitaxel (PTX); 5-Fluorouracil (5-FU).

Table of contents

<i>Acknowledgements</i>	<i>viii</i>
<i>Abstract</i>	<i>xii</i>
<i>Resum</i>	<i>xvi</i>
<i>Table of contents</i>	<i>xxii</i>
<i>Abbreviations</i>	<i>xxvi</i>
<i>List of figures and tables</i>	<i>xxxii</i>
<i>Introduction</i>	<i>1</i>
<i>1. Cancer statistics and facts</i>	<i>3</i>
1.1. The complexity of cancer disease	<i>4</i>
1.1.1. The crucial role of tumor microenvironment	<i>7</i>
<i>2. Cancer Stem Cells</i>	<i>9</i>
2.1. Cancer stem cells models	<i>9</i>
2.2. Cancer stem cells properties	<i>11</i>
2.3. CSC role and impact in cancer disease treatment	<i>14</i>
2.4. CSC-specific targeting strategies	<i>14</i>
2.5. Combination therapy – the real solution for cancer treatment?	<i>16</i>
<i>3. Breast and colorectal cancers</i>	<i>18</i>
3.1. Breast cancer	<i>18</i>
3.2. Colorectal Cancer	<i>20</i>
3.3. Unmet needs in current cancer treatment	<i>23</i>
<i>4. Nanotechnology and nanomedicine in cancer field</i>	<i>24</i>
4.1. Advantages of using nano-DDS for cancer treatment	<i>26</i>
4.1.1. Passive vs. active targeting	<i>30</i>
4.2. Advantages of using nano-DDS for specific targeting against CSC	<i>31</i>
4.3. Different types of nanoparticles	<i>32</i>
4.3.1. Lipid-based nanoformulations	<i>33</i>

4.3.1.1. Liposomes	33
4.3.1.2. Solid Lipid Nanoparticles	34
4.3.1.3. Nanostructured Lipid Carriers	35
4.3.2. Polymer-based nanoformulations.....	35
4.3.2.1. Polymeric Micelles.....	35
4.3.2.2. Dendrimers.....	38
4.3.2.3. Polymeric Nanoparticles.....	39
4.3.3. Protein-based nanoformulations	40
4.4. Nanopharmaceuticals for cancer treatment	41
5. Different proposed nanotechnology-mediated strategies targeting CSC fraction	45
5.1. Targeting CSC: <i>in vitro</i> and <i>in vivo</i> fluorescent models.....	46
<i>Objectives</i>	49
<i>Results</i>	53
<i>Article 1</i>	55
<i>Article 2</i>	85
<i>Discussion</i>	113
<i>Conclusions</i>	131
<i>References</i>	135
<i>Annex</i>	157
<i>Article 3</i>	159

Abbreviations

5-DTAF	5-([4,6-dichlorotriazin-2-yl]amino)fluorescein hydrochloride
5-FU	5-Fluorouracil
ABC	Amphiphilic block copolymers
Ab-SMC2	Antibodies anti-SMC2
ABC transporters	ATP-binding cassette transporters
ABX	Abraxane
AgNPs	Silver nanoparticles
ALDH1A1	Aldehyde dehydrogenase 1A1
ALOX5	Arachidonate 5-lipoxygenase
AML	Acute myeloid leukemia
APC	Adenomatous Polyposis Coli
AuNPs	Gold nanoparticles
BC	Breast cancer
BLMH	Bleomycin hydrolase
BRAF	Serine/threonine-protein kinase B-Raf
CAFs	Cancer-associated fibroblasts
CIMP	CpG island DNA methylation phenotype
CIN	Chromosomal instability
CMC	Critical micellar concentration
CML	Chronic myeloid leukemia
CNTs	Carbon nanotubes
CRC	Colorectal cancer
CSC	Cancer stem cells
CTC	Circulating tumor cells
DLS	Dynamic light scattering
ECM	Extracellular matrix
EDC	(1-ethyl- 3-(3-dimethylaminopropyl)-carbodiimide)
EMA	European Medicines Agency
EMT	Epithelial-mesenchymal transition
EpCAM	Epithelial cell adhesion molecule
EPR effect	Enhanced permeability and retention effect
ER	Estrogen receptor
ESF	European Science Foundation
FDA	Food and Drug Administration
HDI	Human development index
HER2	Human epidermal growth factor receptor 2

HNSCC	Head and neck squamous cell carcinoma
HR	Hormone receptors
HSC	Hematopoietic stem cells
IARC	International Agency for Research on Cancer
IDC	Invasive ductal carcinoma
ILC	Invasive lobular carcinomas
KRAS	Kirsten rat sarcoma viral
LL	Liquid lipids
LSC	Leukemia stem cells
LT	Leukotrienes
mBC	Metastatic breast cancer
mCRC	Metastatic colorectal cancer
Md	Mean diameter
MDR channels	Multidrug resistant channels
MET	Mesenchymal-epithelial transition
MFD	Maximum feasible dose
MNPs	Magnetic nanoparticles
MPS	Mononuclear phagocyte system
MRP	multidrug resistance-associated proteins
MSI	Microsatellite instability
MSNs	Mesoporous silica nanoparticles
Msr1	Macrophage scavenger receptor 1
Nano-DDS	Nano-sized drug delivery systems
NCLs	Nanostructured lipid carriers
NCS	Niclosamide
NNI	National nanotechnology initiative
NP	Nanoparticles
NSCLC	Non-small cell lung cancer
PdI	Polydispersity index
PEG	Polyethylene glycol
PEI	Polyethyleneimine
PEO	Poly(ethylene oxide)
P-gp	P-glycoprotein
PM	Polymeric micelles
PMN	Pre-metastatic niches
PNP	Polymeric nanoparticles

PPO	Poly(propylene oxide)
PR	Progesterone receptor
PTX	Paclitaxel
QDs	Quantum dots
q-PCR	quantitative polymerase chain reaction
RES	Reticuloendothelial system
SCID	Severe combined immune-deficient
siRNA	small interfering RNA
SL	Solid lipids
SLNs	Solid lipid nanoparticles
SLs	Stealth liposomes
SMC2	Structural maintenance of chromosomes 2
SoC	Standard-of-care
TAMs	Tumor-associated macrophages
TCGA	The Cancer Genome Atlas
TEM	Transmission electron microscopy
TF	Transcription factors
TGF- β	Transforming growth factor β
TIC	Tumor-initiating cells
TME	Tumor microenvironment
TNBC	Triple negative breast cancer
WHO	World Health Organization

List of figures and tables

Figures

Figure 1. Cancer statistics in worldwide population.

Figure 2. Hallmarks of cancer.

Figure 3. Metastatic cascade.

Figure 4. CSC hallmarks.

Figure 5. Different therapeutic strategies in cancer treatment.

Figure 6. Breast cancer overview.

Figure 7. Colon cancer overview.

Figure 8. Historical timeline.

Figure 9. Tunable physicochemical properties of nano-DDS.

Figure 10. Different types of NP.

Figure 11. Schematic representation of PM production.

Tables

Table 1. Examples of different cancer therapeutic approaches targeting the CSC fraction.

Table 2. Examples of clinically approved nanomedicines for cancer treatment in Europe and United States.

Table 3. Examples of PM approved or in clinical trials for cancer treatment.

Table 4. Different inhibition strategies: summary of advantages and drawbacks of different therapeutic approaches for cancer treatment.

Introduction

1. Cancer statistics and facts

According to World Health Organization (WHO), cancer is defined as “a generic term that involves a large group of diseases, all of them characterized by the rapid creation of abnormal cells that growth beyond their usual boundaries, which can invade adjoining parts of the body and spread to other distant organs” (1).

Nowadays, cancer is the second leading cause of death globally after cardiovascular diseases. It accounts for an estimated of 9.9 million deaths and 19 million new cancer cases in 2020, being expected to increase to almost 30 million new cancer cases annually by 2040 (Figure 1) (1-3). Statistically, it is estimated that 1 in 8 men and 1 in 10 women will develop an oncological disease during their lifetimes, thus being considered a public health priority (3, 4). Moreover, taking into account the high cost of cancer care, it is urgent to find new efficient anti-cancer therapies. Breast, colorectal, lung, cervix uteri and thyroid cancers are the most common types of cancer in women, while lung, prostate, colorectal, stomach and liver cancers are the most common among men (3). Regarding worldwide population, although breast cancer is the most prevalent, rising to 2.26 million new cases in 2020 and becoming the cancer type with higher incidence in both sexes; lung cancer still remains the deadliest, accounting for nearly 1.8 million deaths in 2020 (Figure 1) (3).

Currently, the most challenging issues regarding cancer treatment are related to tumor resistance and the metastasis process (2, 5). Cancer development is a complex interaction between environmental and genetic factors, where only about 5-10% of all cancers are associated with inherited mutations (3). Thus, the vast majority of cancers arise from the negative impact of environmental agents such as tobacco and alcohol consumption, radiation exposure, infectious agents, air pollution, obesity, unbalanced diet, sedentary and stressed lifestyle (3, 6, 7). Interestingly, some risk factors, including infections and obesity/diet, change remarkably based on the human development index (HDI) and, therefore, according to geographical region. Cancers caused by infections such as stomach cancer, cervical cancer and liver cancer are highly prevalent in low HDI countries or underdeveloped regions, whereas high or very high-HDI countries have reduced infection-related cancers due to the better control of its eradication (8). Conversely, high and very high-HDI countries or developed regions present higher rates of cancers that have been related to sedentary behaviors and unhealthy lifestyles, including breast cancer, lung cancer, colorectal cancer, prostate cancer and thyroid

cancer. However, although between 30-50% of these lifestyle-related cancers could be easily prevented, they are continuously growing and have become the leading cause of cancer's mortality in these developed-regions (1, 3).

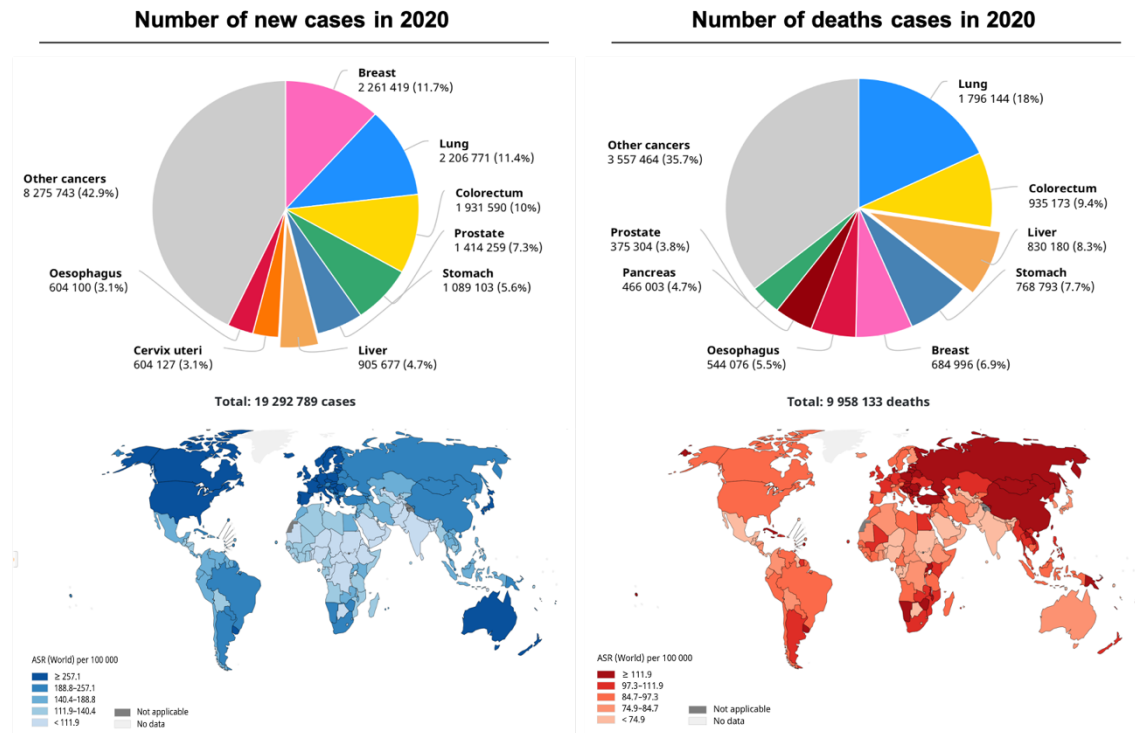


Figure 1. Cancer statistics in worldwide population. Number of new cases and deaths in 2020, both sexes, all ages. Estimated age-standardized incidence (blue) and mortality (red) rates for all cancers, both sexes, all ages. Data source: GLOBOCAN 2020 (9).

1.1. The complexity of cancer disease

Cancer development is a stepwise and dynamic process, where tumor cells progressively accumulate genetic and epigenetic alterations, activate oncogenes or inactivate tumor suppressor genes, thus evolving the primary tumor through different stages (10).

In this regard, Hanahan and Weinberg reported several biological features acquired by malignant cells that allow their uncontrolled growth, survival, and metastatic spread to distant organs (11, 12). Originally, the multistep development of carcinogenesis lays on six original hallmarks, including: i) proliferative signaling activation; ii) growth suppressors inhibition; iii) invasion and metastasis initiation; iv) replicative immortality; v) angiogenesis stimulation; and vi) resistance to cell death (11). Then, two new enabling

factors were also considered as essential for carcinogenesis development, namely vii) the genomic instability and the consequent formation of random mutations; and viii) the tumor-promoting inflammation. In addition, two emerging hallmarks have also been considered as crucial steps for the evolution of cancer, including ix) immune destruction prevention and x) deregulation of cellular energetics (Figure 2) (12). Furthermore, it has also been described that other components, such as aging or environmental factors, together with epigenetic mechanisms contribute to the modification of each individual hallmark by indirectly altering the two enabling characteristics (13, 14).

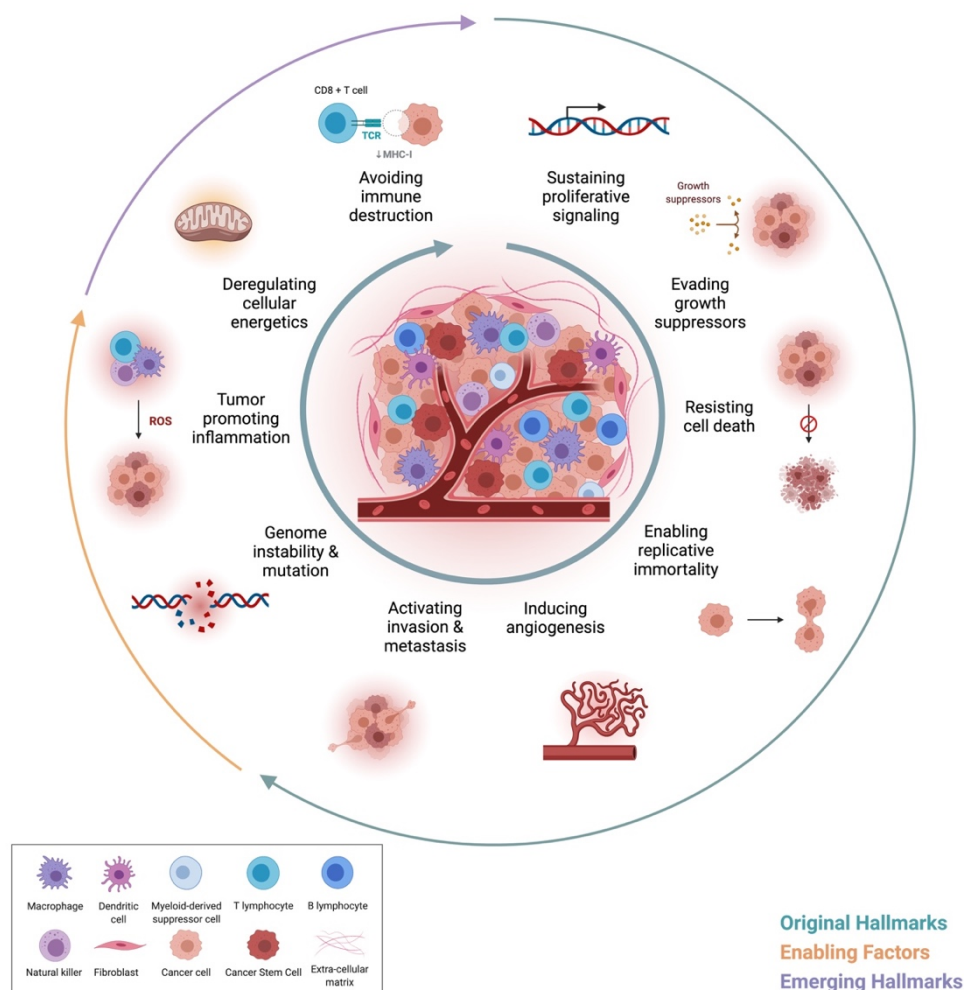


Figure 2. Hallmarks of cancer. Ten main biological acquired capabilities during the multistep development of human tumors. Defined by Hanahan and Weinberg, these hallmarks traits represent the driving forces of neoplastic transformation. Adapted from (12).

Metastasis represents the main cause of therapeutic failure and cancer-related death (15). More specifically, metastatic colonization is a multistep process that can be subdivided into two major phases: i) the cellular migration from primary tumors to distant

tissues and organs; and ii) the acclimatization of these malignant cells to foreign microenvironments, as well as the escape from immune system in order to achieve a successful establishment at a secondary site (Figure 3) (16).

Further, in the first step of the process, tumor evolution begins with local invasions, where epithelial cells lose their polarity and their cell-to-cell contacts, starting to detach from the extracellular matrix (ECM) while altering their cell-to-ECM adhesion. Then, malignant cells infiltrate nearby blood and lymphatic vessels, circulate through them, extravasate, and eventually reach new remote sites (15, 16). In that sense, the epithelial-mesenchymal transition (EMT) plays a leading role conferring these new biological capabilities to the primary tumor, enhancing its invasiveness and migratory potential (17-19). Although originally essential during embryonic development and adult tissue regeneration, EMT is also activated under pathological conditions, being a key process for the progression of most tumors, since about 90% of them are epithelial in nature (carcinomas) (18, 20, 21). At the molecular level, the EMT process is a reversible phenotypic change that is characterized by the downregulation or loss of epithelial markers, including E-cadherin, cytokeratin and laminins, among others; as well as the upregulation of mesenchymal markers, such as N-cadherin, vimentin and fibronectin (22, 23). Of note, while E-cadherin is an important molecule in maintaining adherent junctions and cellular quiescence between epithelial sheets; mesenchymal markers increase cell motility, cellular migration capacity, and resistance to apoptosis, thus promoting tumor malignancy (12, 24). Several molecular pathways are involved in the EMT phenomenon, including transforming growth factor β (TGF- β)/SMAD pathway (25), WNT/ β -catenin signaling (26), ECM-integrin signaling cascade (27), Hedgehog and Notch signaling pathways (28), among others (29). Furthermore, these pathways induce the EMT program by upregulating specific transcription factors (TF), such as Snail1/Snail, Snail2/Slug, Twist, and ZEB1, which maintain the acquired mesenchymal phenotype (30, 31).

In the second step of the metastasis process, malignant cells must adapt and establish themselves in the new microenvironment to successfully form small colonies of cancer cells or micrometastases. Finally, these lesions grow and evolve into macroscopic tumors or macrometastases, achieving the so-called colonization (12, 32). Noteworthy, in order to properly develop secondary tumor colonies, EMT has to be reversed when circulating tumor cells (CTC) find their new target organ, returning the cells to their initial epithelial phenotype through the inverse process known as mesenchymal-epithelial transition (MET) (33, 34). Thus, while the EMT process is related to the early steps of

metastatic development, MET is necessary to perpetuate the new tumor masses growth at distant locations, both processes being essential at different points in this sequential transition (15, 35).

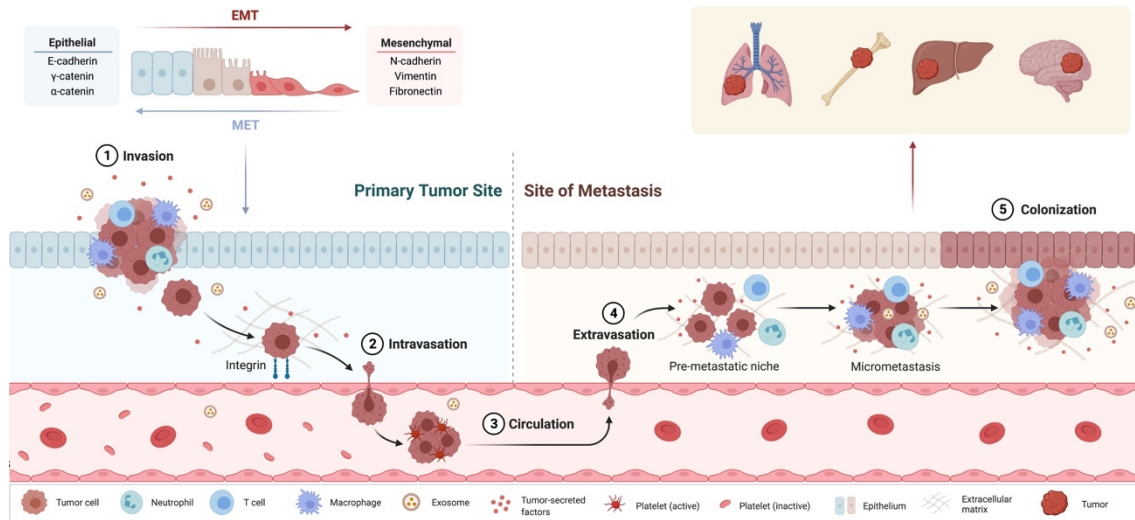


Figure 3. Metastatic cascade. Schematic representation of the multistep process of metastatic development. Five key steps allow the progression from the primary tumor to the site of metastasis, including: invasion, intravasation, circulation, extravasation, and colonization. EMT plays a leading role conferring new biological capabilities to the primary tumor, promoting its invasiveness and migratory potential. MET occurs when CTC arrive to the new target organ in order to achieve a successful establishment in foreign microenvironments and perpetuate the growth of new tumor masses (15). CTC: circulating tumor cells; EMT: epithelial-mesenchymal transition; MET: mesenchymal-epithelial transition.

1.1.1. The crucial role of tumor microenvironment

The tumor microenvironment (TME) is an important regulator of the EMT/MET phenotypic plasticity of cancer cells, tumor proliferation, invasion and colonization and, therefore, a crucial player in ensuring cancer progression as well as a subsequent metastatic expansion (36, 37). In fact, it has been widely studied that even before metastatic spread, the primary tumor actively preconditions specific distant sites by creating host microenvironments, the so-called pre-metastatic niches (PMN), aiming to successfully receive and accommodate the arriving CTC (Figure 3) (15, 38). Among the different steps conforming the niche development, ECM remodeling, vascular leakage, and immunosuppression stand out (38). Importantly, clinical data have shown that metastasis is a non-random process, since different types of cancer tend to metastasize to target organs, which is known as “metastatic organotropism” (39, 40). For instance,

breast cancer strongly confirms the “seed and soil” hypothesis postulated by Steven Paget in 1889, being observed organ-specific metastasis in bone, lung, liver and brain (40, 41).

Being considered one of the main causes of tumor heterogeneity, TME is composed of cancerous cells closely connected to the non-malignant part of the tumor, the tumor stroma, which actively modulates tumor cells and provide them nutrients while maintaining their survival (42, 43). The non-cancerous components include inflammatory and immune cells such as macrophages, neutrophils, eosinophils, mast cells, lymphocytes, natural killer, dendritic cells, and monocytes among others; as well as structural elements, like ECM, fibroblasts, endothelial cells, adipocytes, vessels, nerves and lymph nodes (42, 44). In addition, TME also comprises soluble tumor-secreted factors (e.g., enzymes, cytokines, chemokines, growth factors, miRNAs, and extracellular vesicles), which enable the communication between cancer and stromal cells, while inducing the PMN development (38, 44).

As a result, tumor-secreted factors are capable of transforming the aforementioned cell populations to a more malignant phenotype, mainly fibroblasts and macrophages subpopulations to cancer-associated fibroblasts (CAFs) and tumor-associated macrophages (TAMs), respectively. In particular, TGF- β is a potent inducer that allows the transformation of stromal fibroblasts into CAFs, which represent one of the main cell subpopulations within TME (45, 46). Once activated, CAFs increase their expression of growth factors, chemokines, cytokines, matrix proteins, as well as their proteolytic enzymes secretion, among others; thus, modifying the ECM structure and composition while promoting tumor invasive potential and cancer cell migration (47). In turn, CAFs release increased levels of TGF- β , which have been shown to induce EMT in different cancer types (48, 49). Conversely, TAMs are polarized macrophages that acquire a M2-like phenotype, which present tumorigenic and anti-inflammatory features. Moreover, TAMs contribute to immunosuppression, promoting cancer development and metastasis by suppressing the T-cell-mediated anti-tumor immune response and secreting high levels of anti-inflammatory cytokines such as IL-10 and TGF- β (50-52). Additionally, high levels of TAMs infiltration have been related to tumor initiation, angiogenesis, tumor progression, and chemotherapeutic resistance, being closely associated with poor clinical outcomes as patients are less responsive to treatment (53, 54).

Regarding the cell-to-cell communication, other TME important modulators are exosomes, nano-sized membrane vesicles (30-150 nm) derived from endocytic

compartments that are secreted by different cell types (55, 56). Thus, being intracellular messengers, their main function is to transfer different sorts of cargos from their cell of origin, including nucleic acids, proteins and lipids, not only facilitating the intracellular exchange of information between tumor and stromal cells, but also preconditioning the tumor niche while modulating the target organ for future metastases (56-58). Namely, exosomes are key players during the process of developing organ-specific metastases, driving cell organotropism (59).

Importantly, TME is highly variable among patients and tumor types, being also altered during the development of the disease (60). Therefore, in order to develop new targeted therapeutic strategies, tumors cannot be taken as a single mass, otherwise they must be treated as a complex and evolving network. In this regard, cancer complexity is also caused by the intratumoral heterogeneity. Specifically, growing tumors are composed of diverse cell subpopulations with different phenotypes and proliferative abilities (61, 62). Among them, cancer stem cells (CSC) stand out for exhibiting high tumorigenic potential and tumor repopulation capacities, being intrinsically resistant to most therapies (63).

2. Cancer Stem Cells

CSC represent a minority subpopulation of undifferentiated tumor cells within the entire heterogeneous tumor mass that can vary from 0.1 to 30% depending on the type and cancer stage (64-66). Lately, their crucial role in tumor initiation, relapse and metastatic spread has been highlighted, which is why they are also accurately named “tumor-initiating cells” (TIC). Being designated as the driving force of tumorigenesis, CSC are also able to avoid several cell regulatory mechanisms, rendering them insensitive to conventional anti-cancer therapies, antimitotic agents or radiation (63, 67). All these features lead to the development of highly aggressive metastases, being CSC considered the main cause of cancer mortality.

2.1. Cancer stem cells models

Before the CSC discovery, it was thought that all cells conforming the tumor mass had similar features, equal tumorigenic potential, and that tumor propagation was possible through a progressive accumulation of somatic cell mutations (68). Proposed by Peter Norwell in 1976, this theory known as the clonal evolution model postulates that this accumulation of mutations in single clones produces dominant clone populations, whose

expansion depends on the natural selection process, leading the tumor to a more aggressive phenotype (69-71).

Afterwards, CSC were first identified, isolated and characterized in acute myeloid leukemia (AML) patients (72). Specifically, the study performed by Bonnet and Dick in 1997 demonstrated that AML stem cells, with CD34⁺/CD38⁻ stem-like phenotype, were capable of generating AML in severe combined immune-deficient (SCID) mice as well as maintaining tumor progression (73). Thus, these data were the first evidence supporting the idea that tumors are hierarchically organized, being the hierarchic cancer model of tumorigenesis and cancer propagation then reported. In particular, the hierarchical model, also known as CSC theory, postulates that tissues are perfectly organized with the specific CSC subset at the top of the linear hierarchical chain. Accordingly, CSC subpopulation represents an essential component within the whole tumor mass, being considered the unique driver of tumor formation, chemoresistance gain, and metastatic dissemination, thus harboring the ability to self-renew, differentiate, and proliferate (74, 75). Moreover, CSC are also responsible for tumor recurrence and relapse due to the unlimited self-renewal capacity of their own population. Further, they exhibit the ability to differentiate into “bulk” tumor cells or non-CSC, generating the entire neoplasm, contrariwise to normal cells, whose propagation finish by clonal exhaustion (62, 76).

Since its first discovery in leukemia (73), the presence of CSC have been identified in both solid and non-solid tumors such as brain (77), breast (78), colon (79), gastric (80), head and neck (81), liver (82), lung (83), melanoma (84), ovarian (85), pancreas (86), prostate (87), among others. In this regard, different cell markers are used to characterize and isolate CSC subpopulations, including CD24, CD29, CD34, CD44, CD54, CD90, CD117, CD133, CXCR4, ALDH, EpCAM, among others (88-90). In fact, some of them are specific for a certain cancerous tissue, whereas others are commonly expressed by different types of cancer (89).

Even though their origin is still unclear, CSC are considered key players in tumor heterogeneity and chemoresistance. Therefore, intending to explain tumor heterogeneity development, two theoretical models have been proposed (65, 91). According to the clonal evolution model, the increase in tumor heterogeneity is given by the genetic and epigenetic alterations of the tumor cells, which allow the neoplasia to evolve through clonal selection advantages (70). Conversely, based on the hierarchical cancer model, CSC are the unique drivers of tumor formation that can differentiate into non-CSC, being

the sole progenitors of de-differentiated cells and, thus, conferring heterogeneity within the tumor (92). Although explaining the gain of heterogeneity differently, both models are not mutually exclusive, being interrelated processes where tumors combine some of their biological features (76, 91).

In this regard, an alternative model has to be considered since it has been seen that CSC do not exist as an isolated and static population within the tumor. Indeed, there is a dynamic equilibrium among tumor cell subpopulations, where not only CSC are capable of differentiating into “bulk” tumor cells, but also CSC phenotype can be achieved by the de-differentiation of non-CSC. This process, called reversion, takes place to ensure tumor progression, thus enabling the interconversion between CSC and differentiated bulk tumor cells (76, 93). Therefore, a new insight has emerged to understand tumor structure and reconstitution after treatment, which is known as the interconversion cancer model (76, 94). Specifically, this model suggests that under certain tumor cell intrinsic factors, as well as extrinsic microenvironmental stimuli, cancer cells can enter or exit from the stem-state in a bidirectional switching, thus harboring all cell subpopulations tumor-initiation capabilities (62). Furthermore, the heterogeneous tumor senses when a specific cancer cell subpopulation is depleted after therapy, being able to replace it in order to maintain the intratumoral equilibrium (62). Of note, both TME and exosomes are key factors regulating this stable and controlled but dynamic equilibrium, guaranteeing always the CSC survival (55, 95).

2.2. Cancer stem cells properties

Like adult and embryonic stem cells, CSC exhibit distinctive and essential stemness properties, including tumor initiation and multilineage differentiation capacities, unlimited self-renewal abilities, as well as long-term repopulation potential (74, 96, 97). Of note, all these features confer CSC an uncontrolled propagation capacity within the tumor, endowing them not only the ability to generate but also to perpetuate the neoplasia by maintain their undifferentiated state. Owing their anchored-independent growth capacity, CSC are able to survive in tridimensional tumorspheres, which increase their potential to invade and migrate by acquiring mesenchymal features, intravasating into the blood stream, and finally colonizing distant tissues (62). For all these reasons, CSC are considered essential for tumor initiation, progression, and further metastatic process, thus being highly tumorigenic (Figure 4).

Differing from normal stem cells or differentiated tumor cells, CSC exhibit specific traits and deregulations which contribute to their aggressive behavior. In this regard, Notch, Wnt/ β -Catenin and Hedgehog pathways stand out as the main CSC signaling routes involved in self-renewal, differentiation and survival (74, 98). Interestingly, these molecular pathways also modulate the EMT process, which confer cells a more aggressive mesenchymal phenotype, enhancing their invasion capacity and dissemination ability to distant healthy organs (21, 99). In fact, although traditionally studied independently, accumulating evidence suggests high parallelism between EMT activation and CSC formation (99, 100). Thus, it has been demonstrated that EMT induction is relevant to not only the acquisition but also the maintenance of cells with stem properties (101, 102). Specifically, several studies show an increase in CSC signature during EMT processes in many carcinomas such as pancreatic, hepatocellular, breast and colorectal (103, 104). Of note, the maintenance of stemness properties, as well as the regulation of EMT/MET and CSC plasticity are orchestrated by cell-intrinsic factors (e.g., mutations, epigenetic modifications or transcription factors) and cell-extrinsic factors such as TME and their tumor niche secreted molecules (75, 95, 105).

Furthermore, CSC are intrinsically insensitive to most conventional chemotherapies, antimitotic agents and/or radiation, which are completely valid therapeutic options for differentiated bulk tumor cells (63). Thanks to their particular phenotype, CSC harbor an aggressive behavior by containing multiple mechanisms to protect themselves from cytotoxic drugs and, therefore, perpetuate the tumoral spread, showing resistance to different types of stress (88). In particular, CSC are resistant to apoptosis due to their high expression levels of anti-apoptotic proteins (106), while harboring a high DNA repair response, as well as different mechanisms to avoid DNA damage-programmed cell death (107, 108). Consequently, these resistance mechanisms protect CSC from radio and chemotherapy-mediated apoptosis, conferring them additional protection and contributes to their therapeutic resistance (89). Besides, CSC overexpress a remarkable number of multidrug resistant (MDR) channels on the cell membrane, including ATP-dependent drug efflux transporters like P-glycoprotein (P-gp), the multidrug resistance-associated proteins (MRP), and ATP-binding cassette (ABC) transporters (e.g., ABCG2, ABCG1, ABCB1, MDR1, among others), which are able to pump-out chemotherapeutics from their cytoplasm (109, 110). Therefore, the intracellular drug accumulation is significantly decreased, being one of the most important limitations regarding drug efficacy (62, 111). In addition, a great number of detoxifying enzymes such as aldehyde dehydrogenase 1A1 (ALDH1A1) and bleomycin hydrolase (BLMH) are also expressed, providing CSC with further protection against anti-cancer therapies (90). Thereby,

prolonged exposure to anti-cancer drugs promotes elevated expression levels of efflux pumps and detoxifying enzymes, which leads to chemoresistance and correlates with a worse prognosis in cancer patients (112).

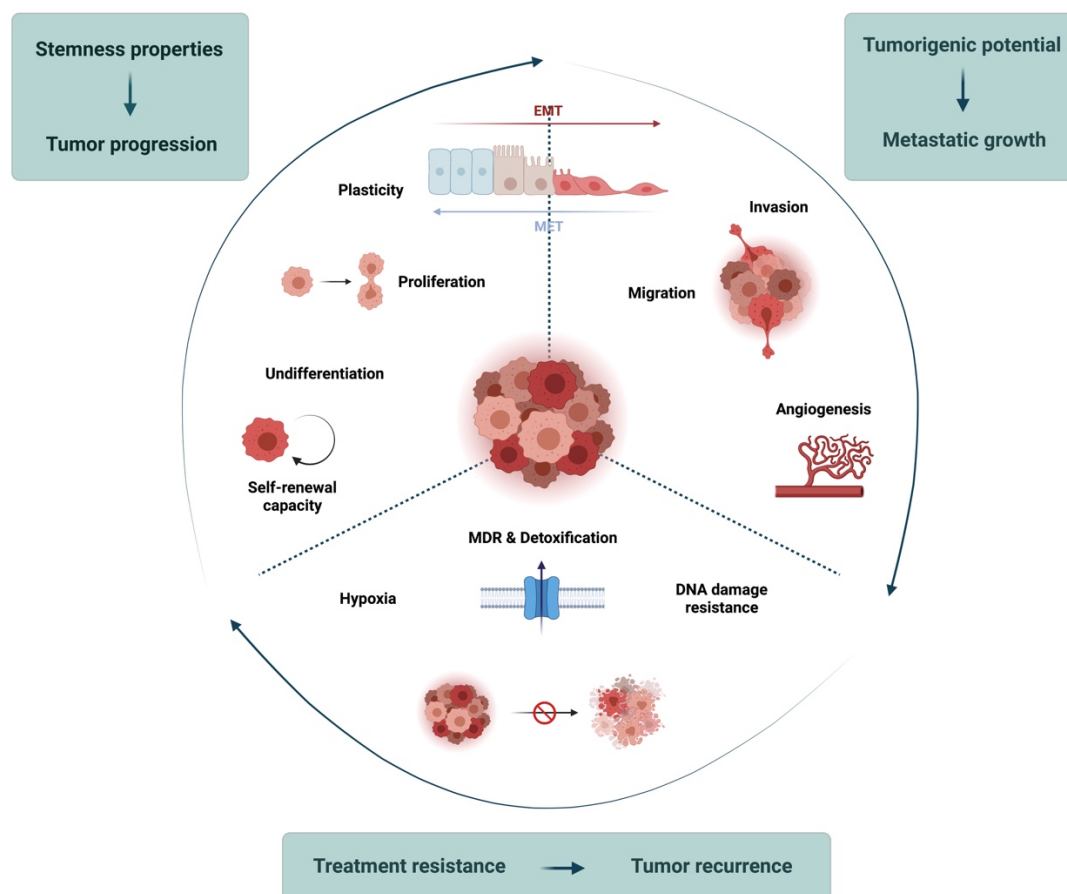


Figure 4. CSC hallmarks. Exhibiting unique features, CSC have been designated as the driving force of tumorigenesis for their key role in tumor progression, metastatic spread, and treatment resistance.

Furthermore, hypoxia is a key factor in maintaining stemness properties and overexpressing genes that promote CSC drug resistance capacity, being thus a hallmark of TME that has also been associated with poor prognosis (113, 114). Specifically, experimental data have shown that the hypoxic condition stimulates the de-differentiation process, contributing to tumor malignancy (115). Moreover, CSC are capable of inducing quiescence under hypoxic conditions and proliferate afterwards, once the stress state has been overcome (116, 117). In this regard, CSC present two distinct phenotypes, proliferative and quiescent, being the latest a reversible state in which cells do not divide or cells endow low proliferation rates, harboring the ability to return to the proliferative mode (118). Noteworthy, the presence of CSC with quiescent phenotype, also known as dormancy state, represents an important drawback which has been highly related to

therapy failure and tumor recurrence. In fact, a wide range of chemotherapeutics only target highly proliferating cells, whereas their effect is reduced in dormant or slow-dividing cancer cells, thus being quiescent CSC not only resistant to conventional cytotoxic drugs but also capable of metastasize to distant organs (89, 119).

2.3. CSC role and impact in cancer disease treatment

Despite advances in cancer treatment, most therapies still fail in achieving the complete cure, without long-term desired results and disease relapse once it is overcome. Therefore, conventional cancer treatments appear to be effective at reducing tumor mass by only eliminating bulk or differentiated tumor cells, while being ineffective against CSC subpopulation (100). Hence, CSC are not only able to evade treatment, but also to promote cell resistance and, eventually, regenerate the tumor (Figure 5a). In this regard, the remaining CSC may suppose a problem since only few of them are enough for tumor re-growth *in vivo* (62, 120). In addition, the percentage of CSC within the tumor often increases after traditional anti-cancer therapies, leading to cancer recurrence with increased malignancy, aggressiveness, and faster spreading metastasis, which are unresponsive to treatment although having achieved an early therapeutic success in controlling neoplastic disease (62, 121, 122). Furthermore, a higher amount of CSC has also been observed in patients with recurrent resistant tumors, which correlates with a worse prognosis and an increased metastasis risk (123-125). Thereby, according to the interconversion cancer model and the CSC's involvement in cancer treatment, the development of new therapies specifically targeting CSC fraction as well as their implementation in the clinical practice are required in order to completely eradicate cancer and prevent disease relapse (89, 126). Moreover, the selection of specific candidates for CSC targeting and elimination will improve the efficiency and specificity of the new therapeutic strategies under development.

2.4. CSC-specific targeting strategies

The main objective of CSC-specific therapeutic strategies is to achieve the potential to remove residual disease while hindering its relapse after therapy. Nowadays, there is an increasing interest and intensive research in this field, with multiple anti-CSC drugs in *in vivo* pre-clinical stages and also in early phases of clinical trials, showing positive anti-metastatic effects (Table 1). Notably, the ability to effectively target the CSC subset will be the key factor regarding their clinical success (127).

Table 1. Examples of different cancer therapeutic approaches targeting the CSC fraction (99).

Therapeutic target	Therapeutic approach	Cancer type	Development stage	References
AKT2	siRNA	Breast cancer	Preclinical (<i>in vivo</i>)	(128)
Bmi-1	Nigericin	Nasopharyngeal carcinoma	Preclinical (<i>in vivo</i>)	(129)
Bmi-1	shRNA	Nasopharyngeal carcinoma	Preclinical (<i>in vivo</i>)	(130)
Hedgehog signaling	Cyclopamine	Glioblastoma	Preclinical (<i>in vivo</i>)	(131)
IAP family	AT-406, SM-164, and TRAIL	Nasopharyngeal carcinoma	Preclinical (<i>in vivo</i>)	(132)
JAK 1/2	Ruxolitinib	Ovarian cancer	Preclinical (<i>in vivo</i>)	(133)
Krüppel-like factor 5	Metformin	TNBC	Preclinical (<i>in vivo</i>)	(134)
mTOR	Rapamycin	Neuroblastoma	Preclinical (<i>in vivo</i>)	(135)
NADH dehydrogenase	DECA-14	Neuroblastoma	Preclinical (<i>in vivo</i>)	(135)
Nestin	shRNA	Glioblastoma Lung carcinoma Pancreatic cancer	Preclinical (<i>in vivo</i>)	(136-138)
Nestin	siRNA	Pancreatic cancer	Preclinical (<i>in vivo</i>)	(139)
PI3K-AKT; ERK1/2 pathways	LY294002; U0126	Breast cancer	Preclinical (<i>in vitro</i>)	(140)
STAT3	LLL12; shRNA	Breast cancer	Preclinical (<i>in vivo</i>)	(141)
STAT3	BB1608	Various cancers	Preclinical (<i>in vivo</i>)	(142)
STAT3	Salinomycin	Breast cancer	Preclinical (<i>in vitro</i>)	(143)
STAT3 pathway	Oncostatin M	Hepatocellular carcinoma	Preclinical (<i>in vivo</i>)	(144)
WNT pathway	Nigericin	Lung cancer	Preclinical (<i>in vitro</i>)	(145)
ZEB1	shRNA	Pancreatic cancer	Preclinical (<i>in vivo</i>)	(146)
ALOX5	Zileuton	Leukemia	Clinical (phase I)	*NCT02047149 *NCT01130688
AKT	MK2206	Breast cancer	Clinical (phase II)	*NCT01277757
Hedgehog	GDC-0449	Ovarian cancer	Clinical (phase II)	*NCT00739661

p53 mutant cells	Metformin	Ovarian cancer FTPPC, Pancreatic cancer	Clinical (phase II)	*NCT01579812 *NCT02978547
PI3K, mTORC1/2	VS-5584	Solid tumors	Clinical (phase I)	*NCT01991938
STAT3	OPB-31121	Solid tumors	Clinical (phase I)	*NCT00955812

*ClinicalTrials.gov identifier. HNSCC: head and neck squamous cell carcinoma; FTPPC: fallopian tube, primary peritoneal cancer; TNBC: triple negative breast cancer.

Different approaches have been developed and are currently being explored to specifically target CSC subpopulation in cancer therapy, including: i) targeting specific cell surface CSC biomarkers, such as CD34, CD44, CD90, CD133, CD117, and EpCAM, among others; ii) targeting specific CSC signaling pathways or proteins related to CSC survival and proliferation, like PI3K-AKT, JAK/STAT, NF- κ B signaling or ALOX5 and SMC2 proteins, as well as pathways linked to their self-renewal and pluripotency, such as Notch pathway, WNT pathway, and Hedgehog signaling; iii) microRNA-based therapeutics; iv) targeting CSC microenvironment or niche components, such as chemokine receptors, TGF- β ; v) using immunotherapy for CSC targeting; vi) targeting CSC metabolism; vii) reversing the EMT process; and viii) inhibiting specific molecules, such as ALDH1A1 or PTEN (89, 126, 127, 147).

2.5. Combination therapy – the real solution for cancer treatment?

Although CSC specific eradication is crucial and a promising strategy, their elimination without killing non-CSC may not result in the complete cancer cure, since there is constant need for the presence of CSC within the tumor. Therefore, after CSC removal, differentiated bulk tumor cells revert into CSC thanks to their high plasticity and dynamic phenotype, ensuring tumor survival and propagation after therapy (Figure 5b) (62, 99). As aforementioned, it should be noted that tumors are evolving entities, where the amount of CSC within them seems to be constant in order to maintain a specific equilibrium between CSC and non-CSC subpopulations (99). Indeed, this tumor plasticity and CSC dynamic phenotype represent a huge challenge when developing cancer therapies. Consequently, aiming to achieve the complete tumor elimination, the combination of two types of active compounds, which simultaneously eradicate both bulk or differentiated cancer cells and CSC fraction is of utmost importance. In this scenario, new therapeutic strategies based on combined therapy represent the ideal treatment in order to not only remove the problematic CSC subpopulation but also hamper the non-

CSC reversion and, eventually, avoid future cancer relapses caused by the interconversion between both subpopulations (Figure 5c).

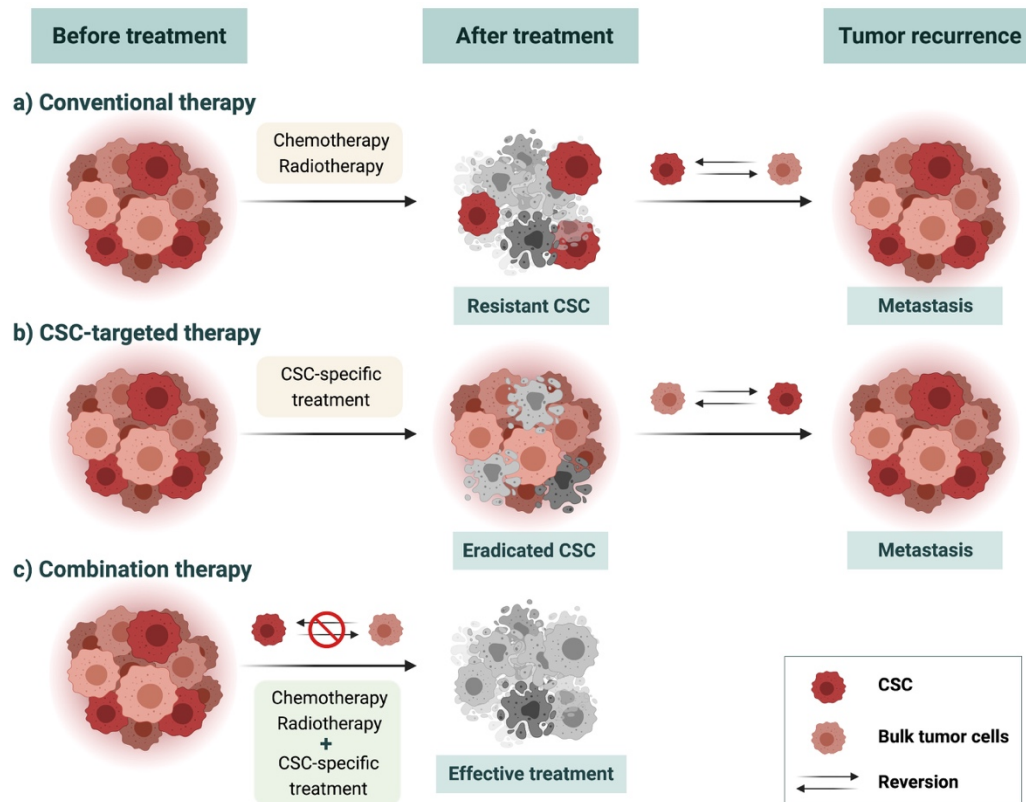


Figure 5. Different therapeutic strategies in cancer treatment. Since eliminated CSC are constantly replaced by new cells with stemness phenotype through a process of de-differentiation of bulk tumor cells, combination therapy is the proper treatment option for tumor remission. **a)** Conventional therapies are only active eradicating bulk tumor cells. Resistant CSC remain in treated tumors, promoting tumor recurrence and aggressive metastasis. **b)** Following the interconversion model, after CSC-targeted elimination, bulk tumor cells can acquire stemness characteristics through a complex process called reversion. Therefore, even after their specific eradication, restored CSC induce tumor recurrence. **c)** Combination therapy enables the possibility to simultaneously eradicate both CSC fraction and bulk tumor cells, while avoiding their interconversion capacity.

3. Breast and colorectal cancers

3.1. Breast cancer

Breast cancer (BC) is the most frequent neoplasm in women and, currently, the most common cancer worldwide in terms of incidence with an estimated 2.26 million new cases in 2020. Specifically, 1 in 8 females is expected to develop the disease in their lifetime (3).

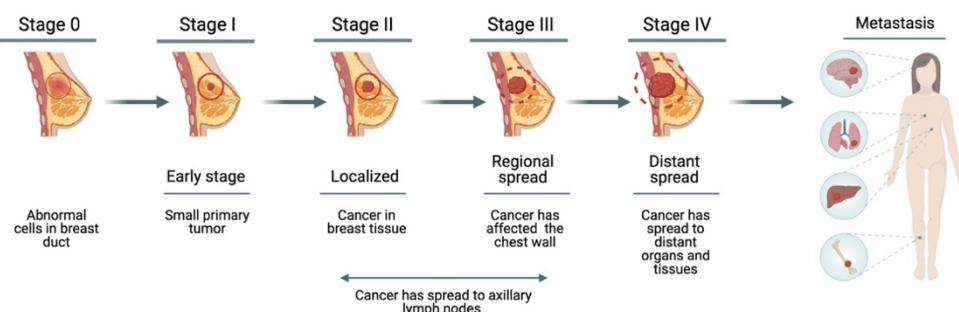
Although being referred as a single disease, BC is a heterogeneous malignancy at the molecular level, which includes several subtypes with different morphological features, biological behaviors, as well as distinct prognosis and clinical response to the treatment (148-150). While early BC (stages I and II) is regarded curable, advanced or metastatic BC (stage IV) is still considered an incurable disease, with no treatment options currently available to patients (149, 151). In terms of tumor structural and morphological heterogeneity, invasive ductal carcinoma (IDC) is the most common type of BC, accounting for about 70% of all cases, followed by invasive lobular carcinomas (ILC), which represent around 15-20%, being the two main subtypes of all breast cancers (152).

According to their histopathological features and the presence of specific markers, breast tumors have been classified in several subtypes depending on the presence or absence of hormone receptors (HR+/HR-): estrogen receptor (ER) and/or progesterone receptor (PR); and overexpression of human epidermal growth factor receptor 2 (HER2) (153). In fact, ER, PR and HER2 are the three tumor biomarkers routinely tested in BC for diagnosis, treatment selection and prognosis (148, 149). Thus, the combination of these markers allows their classification into different subsets: ER+ (ER+/HER2-), HER2+ (ER-/HER2+), triple positive (ER+/PR+/HER2+) and, triple negative (ER-/PR-/HER2-) (150, 153).

Further, accounting for about 70% of all breast carcinomas, hormone-positive BC is characterized by ER and/ or PR overexpression, being associated with the most favorable prognosis compared to other subtypes due to its slow growth (148, 153, 154). In addition, these tumors respond to anti-estrogen hormonal therapy, such as ER antagonists and aromatase inhibitors, which are therapeutic strategies targeting ER-dependent signaling pathways (151). Conversely, HER2-enriched tumors represent the 10-20% of BC patients and are associated with an aggressive phenotype and poor prognosis (148, 155). Nevertheless, HER2 positive tumors are responsive to HER2-

targeted therapy, anti-HER2 monoclonal antibodies such as TrastuzumabTM, reverting much of their expected outcome (156).

STAGES OF BREAST CANCER



FIVE MAIN INTRINSIC SUBTYPES OF BREAST CANCER

Molecular subtypes	Luminal A	Normal-like	Luminal B	HER2-Enriched	Basal-like /TNBC
Prevalence	~ 40 %	~ 2-8 %	~ 20 %	~ 10-15 %	~ 15-20 %
Molecular signature	HR + (ER + and/or PR +) HER2 -	HR + (ER + and/or PR +) HER2 -	HR + (ER + and/or PR +) HER2 + / -	HR - (ER - / PR -) HER2 +	HR - (ER - / PR -) HER2 -
Receptor expression	HR Expression		HER2 Expression		
Proliferation					
Histologic grade (level of cell differentiation)	Low grade (grade I)		High grade (grade III)		
Recurrence					
Prognosis	Best ← Worst				
Treatment options	Hormonal targeted therapy (Tamoxifen)		Targeted therapy (Trastuzumab)		Chemotherapy

Figure 6. Breast cancer overview. Breast cancer progression and main intrinsic molecular subtypes. Prevalence, molecular signature, proliferation, recurrence, prognosis and treatment options (149, 151).

Finally, tumors phenotypically characterized by the lack of both ER and PR expression and the absence of HER2 overexpression represent the triple-negative breast cancer (TNBC) molecular subtype (157, 158). Being the only subgroup lacking targeted therapeutic options, TNBC present the worst prognosis of all BC patients due to its aggressive behavior and metastatic nature, harboring the ability to develop early visceral

metastases rather than local recurrences (148, 159). TNBC is mainly seen in young women and is more common among African-American ethnicity, accounting for approximately 15-20% of all BC malignancies (160). Moreover, women with TNBC are usually diagnosed at a later stage (III or IV), which is why they no longer respond to conventional therapies. In addition, TNBC has often, but not exclusively, a basal-like phenotype and is a highly heterogenic BC subset (161-163). In spite of sharing the triple-negative phenotype, Lehmann, *et al.* (2011) have described six different molecular TNBC subtypes with distinct response to therapy as well as clinical outcomes (164, 165). Thus, due to the intrinsic complexity of TNBC, specific molecular-based therapies will be required for each subtype in order to obtain better treatment responses (161).

Of note, BC is a clear example of how a molecular subclassification has significantly improved the patient outcomes as well as their quality of life, being able to properly select the specific therapeutic strategy in each particular case. In this regard, Perou, *et al.* (2000), based on gene expression patterns using DNA microarrays, described different molecular subtypes with complementary information to conventional classification (166, 167). Therefore, the main intrinsic subtypes are: i) Luminal A; ii) Normal-like; iii) Luminal B; iv) HER2-enriched; and v) Basal-like/TNBC. As shown in Figure 6, these molecular subtypes are associated with different prognoses, treatment options, as well as relapse probability and expected overall survival (168, 169).

3.2. Colorectal Cancer

Colorectal cancer (CRC) is the third most common cancer in men and the second in women worldwide, accounting for an estimated 1.93 million new cases in 2020 and being the second leading cause of cancer mortality (3, 170, 171). More specifically, 71% of all the CRC cases are in the colon while 29% correspond to the rectum (172).

Nowadays, effective diagnoses, screening methodologies, such as colonoscopy, as well as prevention strategies are available in developed countries, which has reduced mortality from CRC in this target population (3, 172). However, incidence rates in these areas are still about five times higher compared to the African, Asian and South American regions (3). In this regard, CRC is highly related to sedentary lifestyle and diet of western countries, being thus a largely preventable disease with healthy dietary and physical activity patterns (173, 174). Furthermore, environmental and/or genetic factors also increase the chance of developing CRC (172, 175). Despite the effort to have an early detection, 25% of CRC patients exhibit metastasis at the time of diagnosis, and around

half of the treated patients will develop distant metastases, mainly in the liver and lungs (176, 177). In fact, although clinical advances have improved the overall outcome, the 5-year survival rate is about 90% for localized disease, meanwhile it still remains low for metastatic CRC (mCRC), around 14% (171).

As many solid tumors, CRC is a heterogeneous disease conformed by distinct subtypes that display specific genetic features with different prognosis and response to treatment (175, 178, 179). Specifically, around 75% of all CRC cases occur sporadically with no family history involved in the pathogenesis or apparent genetic predisposition (180, 181). Conversely, about 15-20% of patients present a positive family history of the disease, while 5-10% of all cases are hereditary and patients exhibit inherent germline mutations (182, 183). In all cases, CRC is characterized by being a sequenced carcinogenesis process, where the disease evolves through several stages, from a benign dysplastic adenoma (Stage 0) to a malignant metastatic carcinoma (stage IV). In particular, CRC pathogenesis arises as a result of the sequential acquisition of genetic mutations and epigenetic alterations by healthy epithelium (175, 184). Thus, the progressive accumulation of these modifications leads not only the onset, but also the progression of adenomas to invasive carcinomas and, finally, to metastatic colorectal tumors, a process that requires between 10 and 15 years on average (Figure 7) (185, 186).

Such malignant colorectal transformations can be developed through two different molecular pathways: i) the conventional adenoma-carcinoma pathway; and ii) the alternative or serrated pathway, each subtype being characterized by specific alterations and, therefore, exhibiting distinct phenotypes (175, 184, 187). Namely, the classic adenoma-carcinoma sequence is a staggered mutational pathway subdivided into two possible mechanisms of tumorigenesis: i) chromosomal instability (CIN); and ii) microsatellite instability (MSI) (188, 189). While CIN is found in 85% of sporadic CRC and is associated with the Adenomatous polyposis coli (APC) tumor suppressor gene loss of function, followed by the activation of Kirsten rat sarcoma viral (KRAS) proto-oncogene mutations (180, 188); MSI accounts for around 15% of CRC and is related to Wnt signaling alterations followed by serine/threonine-protein kinase B-Raf (BRAF) mutations (190, 191). Moreover, MSI has also been detected in the serrated pathway (187, 192). In contrast, the alternative serrated pathway displays a subset of polyps, the so-called sessile serrated polyps, as precursor lesions of cancer development (193, 194). At the molecular level, BRAF mutations are highly common in CRC caused by serrated lesions. Furthermore, there are also two different mechanisms that evolve serrated polyps in CRC: i) MSI; and ii) excessive aberrant CpG island DNA methylation

phenotype (CIMP) (187, 195). In fact, CIMP has been regarded for being the main mechanism implicated in the serrated pathway, harboring this phenotype around 20-30% of all CRC (187, 196).

According to the CRC subtyping consortium, distinct molecular subtypes have been defined with different clinical outcomes, namely CMS1 (MSI immune), CMS2 (canonical), CMS3 (metabolic) and CMS4 (mesenchymal) (197-199).

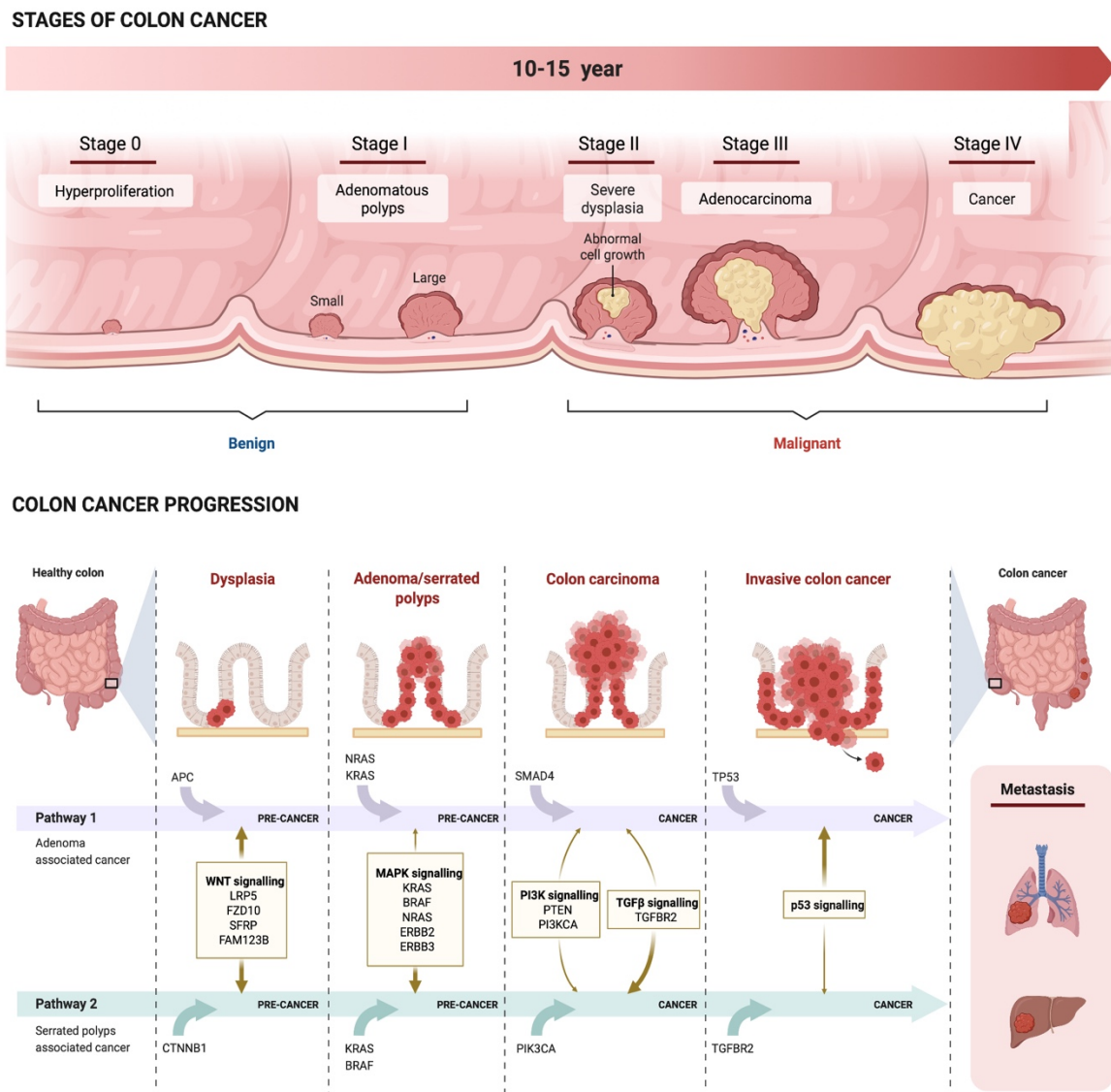


Figure 7. Colorectal cancer overview. Stages and progression of CRC. The sequential mutational process development from benign dysplastic adenoma to invasive colon cancer (175, 187).

3.3. Unmet needs in current cancer treatment

Nowadays, cancer treatment is based on a combination of surgery, radiation and/or systemic therapy, including chemotherapy, immunotherapy, hormone therapy and targeted therapy (200).

In order to determine the best therapy for BC patients, it is critical to identify its molecular subtype by biochemical or genomic approaches (148). Thus, luminal-like and HER2-enriched subtypes are treated quite effectively with hormonal and HER2-directed therapies, Tamoxifen (Nolvadex®) and Trastuzumab (Herceptin®), respectively (149, 151). In contrast, being phenotypically characterized by the lack of the aforementioned receptors, TNBC is a molecular subtype with no specific approved therapies available, which restricts its treatment options to ineffective conventional chemotherapies (151). Among them, anthracyclines, such as Doxorubicin (Adriamycin®, Rubex®), and taxanes, such as Paclitaxel (Taxol®) and nab-paclitaxel (Abraxane®), are the most common drugs for advanced breast cancer used clinically (201, 202). Regarding CRC patients, the routinely employed procedure includes surgical removal followed by the administration of chemotherapy. In this sense, first-line chemotherapy treatment comprises intravenous administration of 5-Fluorouracil (5-FU) and the oral administration of capecitabine (Xeloda®) (203). Both in combination with oxaliplatin (Eloxatin®) and irinotecan (Camptosar®) significantly improve their treatment efficacy (204). Thus, the main doublets used in first-line treatment are FOLFOX (5-FU plus oxaliplatin), FOLFIRI (5-FU plus irinotecan), XELOX (capecitabine plus oxaliplatin), and XELIRI (capecitabine plus irinotecan) (203). Additionally, Cetuximab (Erbix®) and Bevacizumab (Avastin®), monoclonal antibodies to block EGFR and VEGF respectively, are also used in clinical settings (205).

Although more effective therapies that have improved the overall survival are now reaching the market, many patients still fail therapy and present dismal prognosis. Of note, diagnoses at advanced stages of the disease are related to the presence of aggressive metastases, which do not respond to current therapeutic strategies due to their intrinsic and acquired drug resistance (206, 207). Furthermore, these conventional therapies still present some important drawbacks concerning treatment-associated toxicity, since the anti-cancer agent is indiscriminately delivered. Consequently, there is a high systemic toxicity associated with undesired side effects in healthy tissues and systems such as the renal, hepatic, gastrointestinal, pulmonary, cardiac, hematologic and nervous (208).

Therefore, the development of new, more personalized and efficient targeted therapeutic strategies is completely required to improve current outcomes since advanced cancer cure still remains as an important challenge, being considered a strong clinical unmet need. In this regard, nanotechnology offers a great opportunity to achieve this objective by overcoming some of the limitations related to current therapies.

4. Nanotechnology and nanomedicine in cancer field

The history of nanotechnology as well as the concept behind nanoscience began with the conference entitled “There’s Plenty of Room at the Bottom” given by the physicist Nobel Prize laureate Richard Feynman at an annual American Physical Society meeting in 1959 (209). In this lecture, he described for the first time the possibility of manipulating matter at the atomic level, thus opening a new field of research that later inspired many scientists. For all these reasons, Feynman is considered the father of nanotechnology (210). Later on, in 1974, the term “nanotechnology” was firstly coined by Norio Taniguchi, postulating that “nanotechnology mainly consists of the processing of separation, consolidation, and deformation of materials by one atom or one molecule” (211). Finally, the concept of nanotechnology became more popular and widespread when, in 1986, the first book on nanotechnology entitled “Engines of Creation: The Coming Era of Nanotechnology”, was published by K. Eric Drexler (212). From then until today, the nanotechnology field has been constantly growing and evolving, being one of the most revolutionary and promising new technologies of the 21st century (210).

In this regard, the National Nanotechnology Initiative (NNI) defined nanotechnology as “a science, engineering, and technology conducted at the nanoscale (1 to 100 nm), where unique phenomena enable novel applications in a wide range of fields, from chemistry, physics and biology, to medicine, engineering and electronics” (213). Of note, nano-sized particles show unique features compared to their large-sized scale material due to their structural conformation. While in conventional materials most of the atoms are part of their bulk, on the nanometer scale, the surface area to volume ratio is increased, exhibiting many of their atoms available on the particle surface (214). Thus, nanoparticles (NP) behave differently at physical (structural, mechanical, optical, magnetic, and electrical), chemical, and biological levels (210, 215).

Taking advantage of nanomaterials distinctive properties, NP are currently being used in almost all areas of knowledge, with potential new applications in different fields, such

as electronics, energy, environment, textile industry, food industry, biology, and medicine, among others. In particular, the application of nanotechnology in the medical field is called nanomedicine (216, 217). According to the European Science Foundation (ESF), nanomedicine is defined as “the science and technology of diagnosing, treating and preventing diseases and traumatic injuries, of relieving pain, and of preserving and improving human health, using molecular tools and molecular knowledge of the human body” (218, 219). Over the past few decades, the nanomedicine field has undergone a remarkable growth, emerging as a new independent field of health and life science (Figure 8) (217, 220). In fact, around 250 nanoproducts have been commercialized or are being evaluated in clinical trials, thus confirming their high potential in the biomedical field (221, 222).

Due to their unique properties, nanomedicines are being applied in several areas of the healthcare field, including diagnostics, molecular imaging and contrast agents, biomaterials and sensors, regenerative medicine and tissue engineering, as well as drug and gene delivery systems (217, 222). Specifically, three-quarters of the nanopharmaceuticals in clinical development are for oncological indications, as reported in the European Pharmaceutical Review 2020 (223). Of note, nanomedicine has made important contributions to oncology, being a promising tool for the challenging development of cancer therapy (224). Namely, since DOXIL[®] commercialization, the first FDA-approved nanodrug based on PEGylated liposomes in 1995 (225), several nanomedicines for oncological indications have reached the patients, being available for clinical use (Table 2).

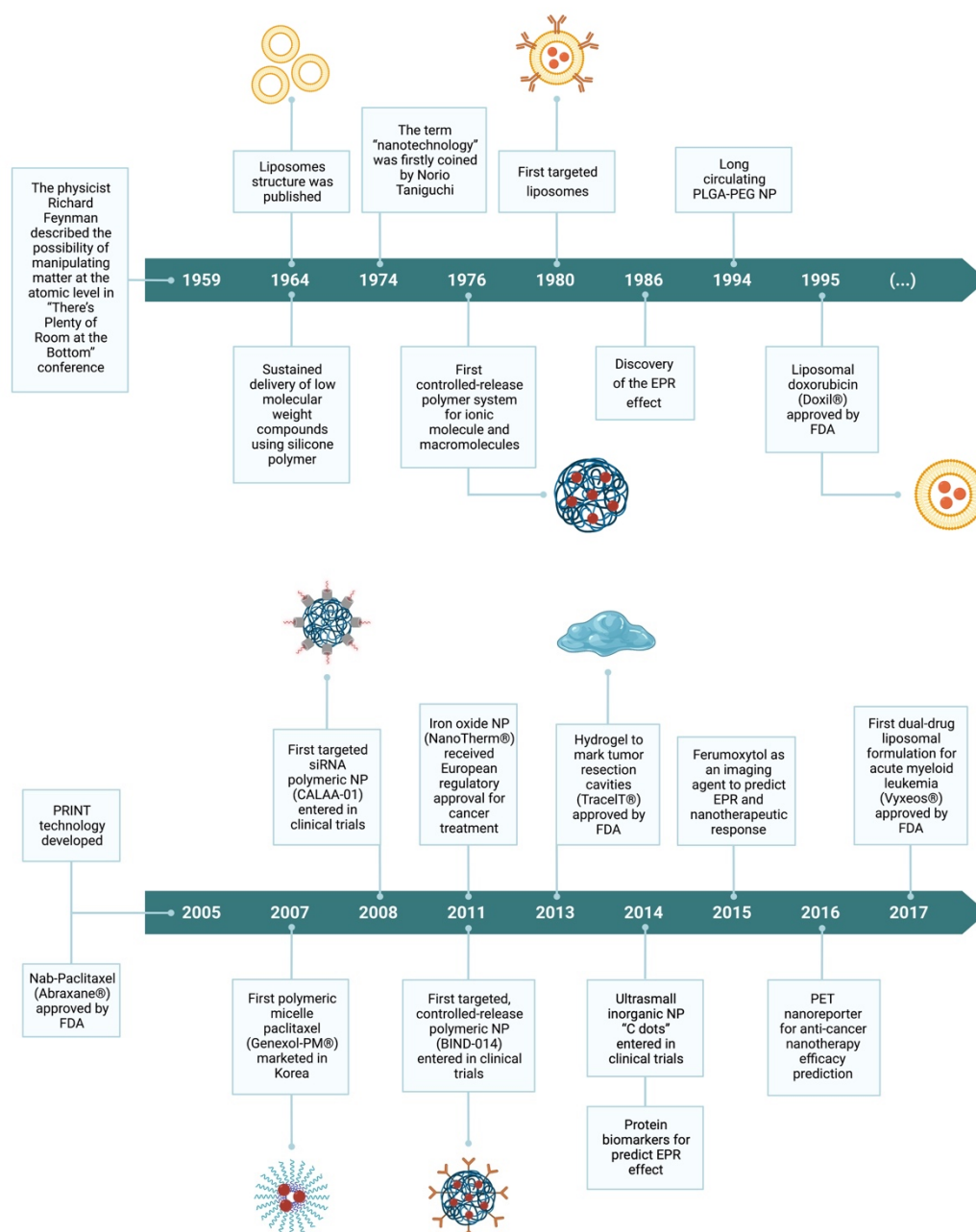


Figure 8. Historical timeline. Overview of the main advances in cancer nanomedicine field. Adapted from (224, 226).

4.1. Advantages of using nano-DDS for cancer treatment

As formerly mentioned, conventional cancer therapies are intrinsically related to several undesired side effects caused by the lack of drug specificity to the tumor site and the consequent affectation of healthy tissues and organs. Furthermore, these types of compounds present dose-limiting issues due to their low solubility and poor penetration

capacity, which leads to suboptimal therapeutic indexes (227, 228). Therefore, in cancer medicine, nano-sized drug delivery systems (nano-DDS) have the potential to overcome most of these drawbacks by improving the therapeutic index of the conventional drugs.

Interestingly, most nanomedicines passively accumulate in tumoral tissues due to the enhanced permeability and retention (EPR) effect, caused by the characteristic leaky vasculature of tumors and surrounding inflamed tissues (229, 230). This effect is based on tumor tendency to rapidly grow and expand creating new blood vessels to receive more oxygen, nutrients, and other growth factors from the blood stream through a biological process called angiogenesis, which increases the permeability of the intratumoral vasculature (231). Owing to this fast-growing tumor vasculature, newly formed blood vessels exhibit unhealthy and irregular endothelium, composed of wide fenestrations larger than 100 nm, like small pores (229). Furthermore, tumor tissues are also characterized by the lack of effective lymphatic drainage, that along with the fenestrated endothelium, lead not only to the prolonged accumulation of nano-DDS but also their preferred retention within the tumor over healthy tissues and, consequently, minimize adverse systemic side effects while increasing the anti-cancer drug efficacy (232, 233). Thereby, taking advantage of NP's small size, as well as the inherent tumor features, it is possible to selectively deliver cytotoxic drugs to the malignant region through a passive mechanism, strategy known as passive targeting.

Once administered, NP must overcome different biological barriers to achieve proper biodistribution patterns and be able to carry out their therapeutic action. In this regard, the physicochemical properties of NP are of utmost importance to successfully fulfill their systemic circulation, transport from the blood vessels to the tissues, accumulation in target cells and, finally, reach their cellular uptake (234). In practice, to effectively take advantage of the EPR effect and obtain a desired biodistribution, the size of developed NP is one of the most important parameters to be considered. Namely, the optimal particle size ranges from 10 nm to 100 nm since particles smaller than 10 nm are cleared from the blood stream by renal filtration before their action, whereas those higher than 100 nm are accumulated in different organs and, finally, uptaken and removed by reticuloendothelial system (RES) or mononuclear phagocyte system (MPS) (234, 235). Specifically, NP tend to accumulate in liver and spleen due to their vascular fenestrations which are around 200-500 nm, or within the pulmonary capillaries, which have a diameter of few micrometers (236). Of note, the EPR effect is a phenomenon highly dependent on tumor vascularization. In this regard, Cabral, *et al.* (2011), have demonstrated how NP of different sizes, from 30 nm to 100 nm can accumulate within highly permeable

tumors, whereas only small-sized NP (30 nm) are able to penetrate in poorly permeable tumors, such as pancreatic adenocarcinoma (237).

Besides, larger particles in size also increase their outer contact area and are more quickly recognized by the complement system due to their higher protein adsorption onto their surface. Therefore, after being intravenously injected, NP interacts with plasma proteins, where the protein corona effect may be observed (238). In this sense, stealth properties play an important role in prolonging their blood circulation half-life and, thus being the NP surface another critical parameter to be cogitated in their design. Noteworthy, adequate stealth properties mask NP from the biological environment, avoiding plasma protein interactions, cellular adhesion or NP opsonization, which could lead to early recognition, sequestration and clearance by RES or MPS (234).

Importantly, the surface charge of NP is also a key parameter to take into account, since the protein corona phenomenon has been mainly seen in hydrophobic and positively charged NP, in addition to showing higher toxicities such as platelet aggregation or hemolysis (239, 240). Hence, aiming to minimize undesired interactions with serum proteins, as well as their accumulation in organs, the ideal nanocarrier should be hydrophilic and neutral or slightly negatively charged (234). This effect can be achieved through surface decoration with hydrophilic polymeric coating, such as polyethylene glycol (PEG) or amphiphilic copolymers (241, 242). Among them, PEG is the most widely used biocompatible polymer for steric stabilization in clinical practice (243). Of note, PEG shielding confers a dense protective layer onto the NP's surface that impairs the absorption of opsonin proteins, increases drug hydrophilicity, as well as the nanocarrier's hydrodynamic size. This, consequently, decreases their renal filtration while reducing their interactions with the RES and, thus, significantly enhances the NP's stability and blood circulation half-life (244). Noteworthy, PEG chains improve the nano-DDS performance, being especially important for *in vivo* applications since blood vessels and cells present negatively charged surfaces, which is even more accentuated in tumor cells (245). In fact, NP's surface charge can be used to passively direct them towards the tumor, since they have a tendency to accumulate there by electrostatic affinity. In this context, usually positively charged NP are associated with higher rates of non-specific internalization by tumor cells compared to normal endothelial vasculature (246).

In this regard, apart from being slightly negatively charged, TME exhibits intrinsic features that may favor the passive targeting of NP. Specifically, the reduced tumor drainage limits the availability of oxygen and nutrients, which is supplied with glycolysis

and an altered metabolism, generating a surrounding acidic environment (247). Consequently, these physiological differences between healthy and tumor tissues have recently been used to develop stimulus-responsive or “smart” nano-DDS (248). These intelligent nanocarriers are based on controlled drug release mechanisms at the tumor site in response to a specific external or internal stimulus. Of note, controlled external stimuli, including temperature, light, ultrasounds, radiation, and magnetic or electric fields, can be applied locally to the nanosystem once at the tumor area, reducing normal tissue damage (249). Conversely, internal stimuli provided by the tumor biology such as changes in pH compared to normal tissues (6.7 vs 7.4 respectively), redox potential, enzyme expression or higher tumor temperature are the most commonly used in preclinical studies (249). Interestingly, an innovative application is site-specific charge conversion, where the NP superficial charge is switched as response to environmental stimuli, such as pH. Thus, this enables prolonged circulation times after intravenous administration, and increased cellular uptake once NP reach the tumor site, which are achieved with neutral/slightly negative charges or positively charged surfaces, respectively (234, 250). For example, Yuan, et al. (2012) have designed zwitterionic NP with a switchable charge based on environmental stimuli, which released the anionic component from their surface after extravasation into TME with lower pH values. Consequently, the positive surface charge of NP was exposed and facilitated their penetration into tumor cells, with improved *in vivo* responses (251).

In addition, the shape and geometry of NP is also important regarding the biodistribution pattern, being the spherical particles the preferred ones since they present fluid dynamics in blood vessels while reducing their adhesion to endothelium (252). Therefore, along with size, NP shape is a critical parameter that affects their *in vivo* fate.

Overall, an ideal nano-DDS for cancer treatment should be: i) biocompatible and biodegradable; ii) non-immunogenic; iii) exhibit stealth properties to circumvent the immunological recognition and achieve longer circulation times; iv) avoid premature drug release and degradation before reach the target area; v) promote a controlled release pattern at the desired site; and vi) be easily functionalized to promote an active targeting (255, 256). Depending on their final target, NP can be loaded with different payloads, including molecular drugs, cytotoxic compounds, imaging agents, nucleic acids, proteins, among others (257, 258).

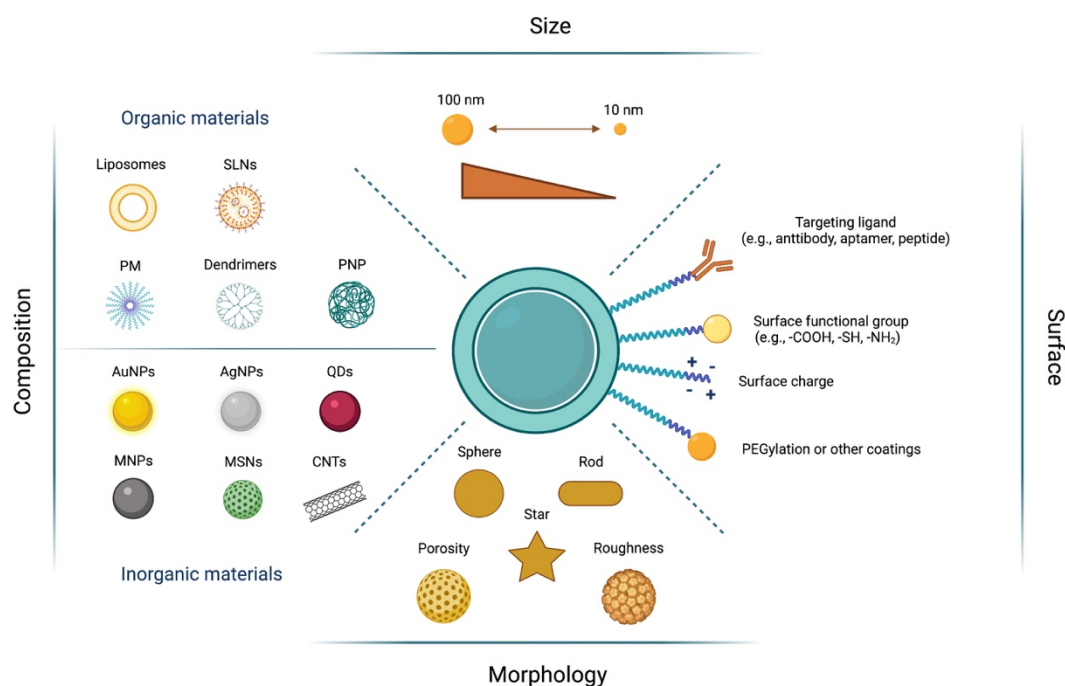


Figure 9. Tunable physicochemical properties of nano-DDS. A summary of nano-DDS explored for cancer treatment and their possible modifications. Adapted from (253, 254). AgNPs: silver nanoparticles; AuNPs: gold nanoparticles; CNTs: carbon nanotubes; MNPs: magnetic nanoparticles; MSNs: mesoporous silica nanoparticles; PM: polymeric micelles; PNP: polymeric nanoparticles; QDs: quantum dots; SLNs: solid lipid nanoparticles.

4.1.1. Passive vs. active targeting

Although the EPR effect is widely important in the nanomedicine field, its benefits are closely linked to the specific characteristics of each tumor, such as its vasculature as well as the irregular size of its fenestrations (229). In this context, passive targeting presents important limitations, including non-uniform distribution and inefficient drug diffusion into tumor cells, thus being EPR effect a highly heterogeneous phenomenon that varies significantly among patients (259, 260). For this reason, active targeting has become a widely researched strategy in cancer therapy, aiming to achieve directionality towards a desired target area.

While passive targeting uses and depends on the pathophysiological properties of tumor tissue, active targeting is able to direct nano-DDS by conjugating different moieties onto the NP surface that recognize and specifically bind to biomarkers or receptors overexpressed by diseased target cells (261, 262). Thereby, different targeting ligands have been tested for surface decoration, including monoclonal antibodies, antibodies

fragments, peptides, aptamers, vitamins, carbohydrates or sugars among others (262). In this regard, active targeting reduces off-target interactions and allows better control of the nano-DDS biodistribution, thus increasing their specificity as well as their uptake through endocytosis process and, subsequent intracellular drug release. Consequently, higher intracellular drug concentration is achieved, which overall improve its therapeutic efficacy. Nowadays, the discovery of new and suitable targeting moieties has become a priority and a promising alternative to EPR or the passive targeting strategy to further improve the efficiency of currently available cancer nanomedicines (262, 263).

4.2. Advantages of using nano-DDS for specific targeting against CSC

One of the main advantages regarding the use of NP is that due to their cellular uptake via endocytosis, the membrane diffusion and drug expulsion through MDR channels is avoided. In fact, regarding CSC intrinsic treatment resistance, nanomedicine field offers an unparalleled platform to specifically deliver anti-CSC therapies taking advantage of the nano-DDS inherent features (62, 264). Moreover, these nanomedicines are able to incorporate drugs or biotherapeutic products targeting key molecular processes in CSC survival and self-renewal. On the other side, since nanomedicines are often able to evade MDR channels skipping the highly expressed CSC pump-out machinery, higher amount of anti-CSC agents can be accumulated in the perinuclear region (62). In this regard, Karandish, *et al.* (2018) have demonstrated a decreased expression of NOTCH-1 and NANOG cancer stemness markers after the treatment with napabucasin loaded into stimuli-responsive iRGD-targeted polymersomes. Their results also showed how napabucasin encapsulated polymersomes significantly reduced cell viability in both pancreatic and prostate CSC, reinforcing their potential against cancer stemness (265). Additionally, Li, *et al.* (2019) have encapsulated the CGX1321 inhibitor into liposomes to reduce its associated undesired side effects. Namely, CGX1321 is currently being evaluated in clinical trials (phase I, NCT02675946), exhibiting potential to effectively block Wnt ligand synthesis. CGX1321-loaded liposomes interfered with the aberrant Wnt signaling form CSC and significantly inhibited tumor growth in LoVo xenograft and GA007 patient derived xenograft (PDX) models. Their results showed focused effects on LGR5+ CSC, without being significantly cytotoxic to other cells (266).

Importantly, it has been shown that reduced drug resistance and better therapeutic outcomes are achieved by combination therapy, where synergistic effects are observed. Therefore, the combination of specific anti-CSC inhibitors together with conventional anti-cancer drugs within the same nanoplatform represents the solution to

simultaneously eradicate the entire tumor mass and be able to obtain better clinical results (267). Recently, co-delivery nano-DDS for combination therapy are being developed and investigated. For instance, Ren, *et al.* (2016), designed a co-delivery system for simultaneously eliminate CSC and non-CSC. Specifically, they have produced PAMAM modified hollow gold nanoparticles (HGNPs) loaded with miR-21 inhibitor and DOX, D-P-HGNPS/21i system. The sequential release of both agents using D-P-HGNPS/21i significantly improved cytotoxicity compared to free Dox and simple co-administration therapy in breast cancer cell lines. Furthermore, a potent inhibition in tumor growth was also observed after D-P-HGNPS/21i treatment compared to the simple co-administration therapy in a subcutaneous MDA-MB-231 tumor model in nude mice. Thus, they have demonstrated that specific miR-21 inhibition is critical to improve the drug sensitivity and impair the CSC malignancy upon the sequential therapy (268). In addition, Zhao, *et al.* (2016) have developed an elastin-like polypeptide (iTEP)-conjugated NP to co-deliver salinomycin (Sali) and paclitaxel (PTX), iTEP-Sali-ABA NP and PTX NP. Their combination therapy suppressed the primary tumor growth and decreased subsequent metastasis compared to iTEP-Sali-ABA NP alone in subcutaneous BC *in vivo* model (269).

4.3. Different types of nanoparticles

Nowadays, there are a large variety of nano-DDS whose fate and therapeutic outcome can be modified by altering their chemical composition (organic or inorganic), physical characteristics, dimensions, morphology, surface properties and functionalization, as shown in Figure 9 (241, 254, 270). Organic-based nanocarriers, including lipid, polymeric, and protein-based nanoformulations, have been widely investigated and used for drug and gene delivery applications as well as imaging agents (256, 271). Meanwhile, inorganic-based systems have intrinsic ability for imaging, diagnostic and sensing applications due to their unique physicochemical properties (272, 273). Among them stand out carbon-based nanocarriers, metal-based nanoformulations, such as gold and silver NP, quantum dots, mesoporous silica NP, and magnetic nanocarriers. Each type of nanoplatform presents unique strengths and drawbacks, which are compiled in Figure 10.

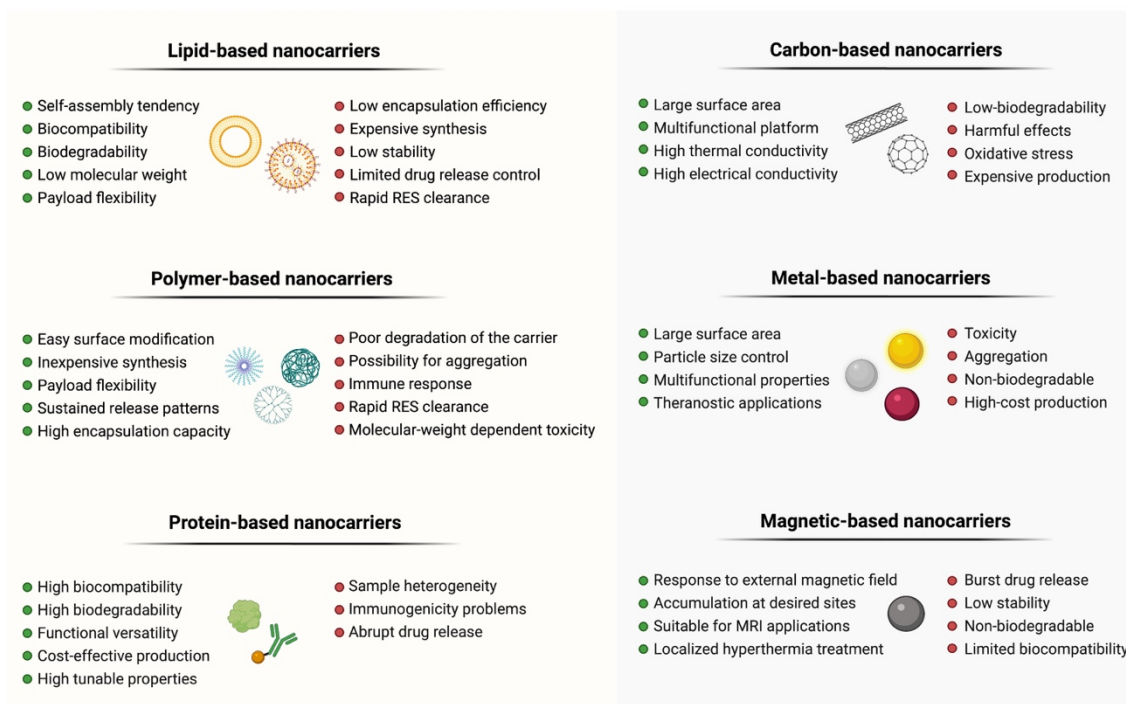


Figure 10. Different types of NP. Summary of the main advantages and drawbacks of NP used for drug delivery applications. MRI: magnetic resonance imaging; RES: reticuloendothelial system.

4.3.1. Lipid-based nanoformulations

There are different types of lipid-based nanoformulations such as liposomal systems, solid lipid nanoparticles (SLNs), and nanostructured lipid carriers (NCLs), among others; most of them showing spherical structure with an internal aqueous cavity and at least one surrounding lipid bilayer.

4.3.1.1. Liposomes

Liposomes are self-assembled colloidal spherical vesicles constituted by a lipid bilayer membrane of amphiphilic phospholipids and cholesterol which surround an interior aqueous space (274). Owing to their lipid structure and polar nature, hydrophilic compounds can be encapsulated within the liposome liquid core, whereas hydrophobic therapeutics are retained by affinity in their lipid bilayer (275, 276). Noteworthy, liposomal structure shares morphological similarities with cellular membranes, which provide them easier cellular uptake and thus higher therapeutic activity (275). Furthermore, neutral conventional liposomes surface can be coated with PEG chains in order to enhance their blood circulation time. These PEG-coated liposomes are also known as stealth

liposomes (SLs) (242). Of note, both neutral conventional and PEGylated liposomes can be produced with either natural or synthetic phospholipids that confer them biocompatible and biodegradable properties while reducing possible toxicity or antigenic reactions. Moreover, several physicochemical parameters can be controlled by mixing different fatty acids chain lengths, as well as different head groups in order to modulate their interactions with the environment (277). Therefore, exhibiting several advantageous characteristics, liposomes have been extensively investigated for more than 50 years. In fact, liposomes are the most common type of FDA-approved nano-DDS for cancer treatment, being Doxil® the first nanomedicine that reach the market in 1995 for the treatment of HIV-related Kaposi's sarcoma, ovarian cancer and multiple myeloma (278, 279).

Nonetheless, liposomal-based formulations present some limitations including low encapsulation capacity, burst drug release profiles, phospholipid oxidation or degradation, poor stability, and difficulties in industrial reproducibility (274). As a result, different types of lipid-based nanocarriers, such as SLNs and NCLs, have been developed to overcome these drawbacks.

4.3.1.2. Solid Lipid Nanoparticles

SLNs are colloidal carriers composed of solid-lipid core at physiological temperature, surrounded and stabilized by surfactants for their emulsification (280). SLNs have emerged as a promising alternative aiming to overcome the limitations presented by traditional carriers, including liposomes and polymeric nanoparticles (280). In fact, being more stable than liposomes, SLNs provide prolonged and controlled drug release, thus improving its overall therapeutic efficacy. Besides, SLNs are versatile nanocarriers that allow both lipophilic and hydrophilic compounds loading, which show lower toxicities since they can be produced without using organic solvents (280). Importantly, in order to obtain high quality SLNs formulations, as well as suitable drug release patterns, its lipid matrix crystal structure is a crucial feature, which depends on the selection and proportion of the lipids and surfactant components conforming the particles (280, 281).

Nevertheless, SLNs have also presented some limitations in drug loading and encapsulation capacity. Since they are compactly packed solid lipid matrix, the available space for drug encapsulation is limited, thus resulting in low drug loading efficiency (282). Furthermore, this problem increases the possibility of drug expulsion from the

formulation due to polymorphic transitions produced during storage (280). Accordingly, in order to overcome these limitations, Müller, *et al.* (2011) developed nanostructured lipid carriers (NLCs), which incorporate liquid lipids (LL) into the previous formulations (283).

4.3.1.3. Nanostructured Lipid Carriers

NLCs are nano-DDS composed of both liquid and solid lipids (LL and SL, respectively) as a core matrix, which overcome the aforementioned limitations, and are considered the second generation of SLNs (280, 284). The introduction of the LL into the solid matrix is the key point that allows significantly improve their properties compared to SLNs (284). Specifically, NLCs have a non-ideal crystalline structure, which not only avoid drug expulsion triggered by polymorphic transitions, but also improve their physical stability (280, 284). In addition, the incorporation of LL into the crystalline solid matrix generates an amorphous core structure with substantial imperfections, which provides more space for drug accommodation and, consequently, increases its drug loading capacity (280, 284). According to their composition, NLCs can be classified into different subtypes, all of them generally requiring the nanoemulsification of a lipophilic phase, composed of a mixture of SL and LL, and further stabilization with surfactant solutions (285).

4.3.2. Polymer-based nanoformulations

Polymer-based nanocarriers are widely used for drug and gene delivery applications due to their biocompatibility and biodegradability, with specific physicochemical features that can be modified by varying the type and nature of polymer (natural or synthetic), as well as its chain length. They can be presented in different structures: i) polymeric micelles, characterized by their amphiphilic core-shell structure; ii) dendrimers, hyperbranched macromolecules; and iii) polymeric nanoparticles, constituted by nanocapsules or nanospheres, among others (286).

4.3.2.1. Polymeric Micelles

Polymeric micelles (PM) are self-assembled nano-constructs composed of amphiphilic block copolymers (ABC) that spontaneously form spheroidal core-shell structures in aqueous environments (287-289). Structurally, ABC are heterogeneous polymers composed of at least two regions of distinct chemical nature, hydrophilic and

hydrophobic, which are organized in blocks. Changing the chain length of the different blocks or the polymer type it is possible to modulate the final polymer properties (288, 290). Of note, ABC stand out for their biocompatibility, biodegradability, water solubility and low immunogenicity, making them suitable for human administration (291, 292). Several factors such as hydrophobic chain size, amphiphiles concentration, temperature, and solvent type affect the micelle formation. Another important parameter is the so-called critical micellar concentration (CMC), which corresponds to the minimum polymer concentration where the micelles remain self-assembled (293, 294). Therefore, at lower concentrations, amphiphilic molecules exist separately, whereas spontaneous supramolecular aggregates are formed when CMC is reached due to the saturation of the solution (295). Accordingly, PM are stable when the concentration of polymeric chains is higher than CMC, being CMC value the most important parameter regarding micelles thermodynamic stability (295, 296).

PM are versatile nanocarriers used to deliver a wide variety of payloads, including hydrophobic small molecules, peptides, proteins, small interfering RNA (siRNA), and DNA, among others (287, 297). In fact, nano-sized micelles are able to accommodate high payload, allow more controlled drug release patterns, as well as improved stability compared to liposomes, which together with an outstanding biocompatibility improve system biosafety (298, 299). In addition, different types of polymers are used for micelles production, including amphiphilic diblock copolymers (polystyrene and PEG), triblock copolymers (Pluronics®), graft copolymers (chitosan), and ionic copolymers (poly(ethylene glycol)-poly(ϵ -caprolactone)-g-polyethyleneimine) (295). Among them, Pluronics® stand out for their unique properties, being Pluronic®-based PM a suitable nanoplatform for the delivery of different therapeutic agents.

In particular, Pluronics®, also known as poloxamers, are synthetic triblock copolymers of poly(ethylene oxide) (PEO) and poly(propylene oxide) (PPO) arranged in an A-B-A structure, namely PEO-PPO-PEO, available in different PEO/PPO ratios and molecular weights (300, 301). Due to their amphiphilic nature, above CMC, Pluronics® self-assemble into micelles in aqueous media, ranging from 10 to 100 nm. In these core-shell nanoparticulate structures, PPO constitutes the hydrophobic core while PEO chains form hydrophilic outer shell, providing stealth properties to the system, which in turn improve particle stability and increase half-life blood stream circulation (287, 300, 301).

Moreover, increases in both temperature and poloxamer concentration promote polymer gelation, being a thermo-reversible process characterized by the sol-to-gel transition

temperature (302, 303). At high temperatures, poloxamer copolymer molecules aggregate into micelles through the dehydration of hydrophobic PPO blocks, leading to the PM formation. Subsequently, increasing their hydrophobicity and insolubility, poloxamers start the gelling process (303, 304). Due to their versatility, innocuous nature, and feasibility of modulating their properties, poloxamers have been used in a wide range of biomedical applications, including tissue engineering, bone regeneration, wound healing, as well as nano-DDS (305-307).

Among the wide variety of Pluronics®, Pluronic® F127 (PEO₁₀₀-PPO₆₅-PEO₁₀₀), also known as poloxamer 407, is an FDA-approved biodegradable polymer that has gained special interest due to their potential in the nanomedicine field (306, 308). In preclinical studies, Pluronic® F127-based PM are being assessed as versatile nanocarriers to deliver a wide range of payloads. Regarding gene delivery strategies, Rafael, *et al.* (2018) have demonstrated that the presence of Pluronic® F127 in their PEI-siRNA-Pluronic® PM-based systems improves the transfection efficiency of PEI-siRNA polyplexes and reduces PEI-associated cytotoxicity. Consequently, the results showed a significant reduction in invasion and colony formation capabilities of breast cancer cells, after the inhibition of different genes of interest through siRNA technology (128, 309).

Interestingly, Kabanov, *et al.* (2008) have discovered that poloxamers reduce the MDR capacity of cancer cells by interfering with the function of efflux transporters, such as P-gp or multidrug resistance proteins, inducing ATP depletion, as well as increasing pro-apoptotic signaling, among other mechanisms (301, 310). In this sense, Pluronic® F127 can act as a biological response modifier by sensitizing CSC and, subsequently, reducing cancer recurrence. For instance, Xu, *et al.* (2020) have produced doxorubicin hybrid micelles based on Pluronics® F127 and P123 for efficiently overcome MDR in breast cancer. Their results showed increased drug accumulation at tumor sites and high efficacy in *in vivo* breast cancer models, with 78.2% inhibition of tumor growth (311). Further, Russo, *et al.* (2016) have demonstrated the ability of Niclosamide (NCS) loaded in biotin-targeted Pluronic® P123/F127 mixed micelles to overcome MDR in multidrug resistant NSCLC. Their results showed significant cytotoxicity of NCS-loaded biotin-targeted micelles in A549 lung cell line, resistant to cisplatin, 5-FU and docetaxel; being the treated cells unable to proliferate (312).

Importantly, thanks to their structural versatility, Pluronic® F127-based PM also allow the co-delivery of different therapeutic agents, providing the possibility of performing a

combined therapy. In this regard, Kelishady, *et al.* (2015) were able to co-load PTX and lapatinib (LPT) in Pluronic® F127-based PM to be delivered simultaneously against metastatic BC. Their results showed a sustained release pattern *in vitro* and a significant reduction in terms of proliferation in the resistant T-47D cell line after PTX-LPT-loaded PM compared to the binary free mixture (313). Further, positive effects after the co-delivery of miR-345 and gemcitabine (GEM) for pancreatic cancer treatment were obtained by Uz, *et al.* (2019). They presented a novel multifunctional polymeric dual delivery nanoscale device (DDND) using Pluronic® F127 to encapsulate GEM, and the pH responsive cationic polymer (poly(2-diethylaminoethyl methacrylate)) (PDEAEM) to efficiently release the miR-345 in the cytoplasm, facilitating its endosomal escape. Specifically, PDEAEM electrostatically complexed the miR-345 and, subsequently, self-assembles with GEM encapsulated into Pluronic® F127, enabling its co-delivery. Their results showed an efficient reduction in terms of cell viability in Capan-1 and CD18/HPAF pancreatic cells lines after DDND co-loaded with GEM and miR-345 treatment compared to GEM or miR-345 alone. Furthermore, the combination therapy was able to significantly inhibit tumor growth, accompanied by a significant reduction in metastasis compared to individual treatments in orthotopic pancreatic cancer *in vivo* model (314).

4.3.2.2. Dendrimers

Dendrimers are unique multi-branched polymeric nanocarriers that are synthesized from a central core molecule by controlled and repeated polymeric reactions, leading to their complex three-dimensional architecture (315, 316). Dendrimers are highly monodispersed, homogeneous and symmetric structures surrounded by surfaces containing multifunctional peripheral groups that allow the easy modification of their surface (315).

Regarding their structure, dendrimers are composed of three different components: i) the core; ii) the branches; and iii) the terminal groups linked to the ramifications (315). The core is formed by a central atom or group of atoms, where the branches of the so-called “dendrons” begin to grow through repeated covalent chemical reactions. Therefore, during the synthesis process, each successive reaction generates a layer labeled as dendrimer generation (G). Namely, they are classified as low- and high-generation dendrimers according to their G, $G < 4$ and $G \geq 4$ respectively, being the dendrimer core designated as generation zero or G0 (317). Eventually, terminal groups are attached to their outer branches as “capping agents”, thus ending the chemical chain reaction (315). These end-groups can be easily functionalized not only to modify the

physicochemical properties of dendrimers, but also to bind different ligands as targeting moieties and perform active targeting (318, 319).

Unlike the self-assembly method used in the aforementioned PM production, dendrimers are obtained by specific synthesis methods, which allow the control of various parameters throughout the process (316). During their synthesis, polymer arrangement generates internal cavities which are used to accommodate different types of therapeutic molecules, thus increasing either their solubility and stability (315, 316). However, although showing unique properties and advantageous points over other types of NP, there are also some drawbacks that can hinder their clinical application. Due to the complexity of dendrimers, their production requires specialized workforce and presents high manufacturing costs (315, 320). Furthermore, dendrimers have amine groups, positively charged groups, which increase their cytotoxicity (321). To overcome this effect, dendrimers can be modified by adding PEG chains or fatty acids onto their surfaces (320, 322).

4.3.2.3. Polymeric Nanoparticles

Polymeric nanoparticles (PNP) are defined as biodegradable solid colloidal systems build with both natural and synthetic polymers leading to spherical nano-sized vehicles (323). Thanks to their high versatility, several types of cargos can be delivered, where therapeutic molecules are either encapsulated, physically entrapped, dissolved, adsorbed, and/or conjugated into or onto the resulting polymeric matrix (324). Depending on their production method, as well as the composition of the organic phase, PNP present different morphological structures (323, 325). Namely, two main polymeric particles can be prepared: i) nanocapsules, also known as reservoir system; and ii) nanospheres, recognized as matrix system (323). Thereby, nanocapsules consist of a core-shell structure where the therapeutic agent is dissolved into an oily or aqueous cavity, surrounded by a polymeric shell, that enable controlled drug release pattern (323, 325, 326). Conversely, in nanospheres, the active compound is uniformly dispersed throughout the polymeric matrix or adsorbed onto their surface, conforming a polymeric network (323).

Of note, PNP stand out for their controlled and sustained drug release, the ability to protect the loaded therapeutic molecule from the external environment, the improvement of cargo bioavailability, the enhancement of the therapeutic index, as well as the possibility of combining both therapy and imaging techniques, the so-called theranostics

(327-329). In addition, they also exhibit high drug payload and controllable physicochemical properties. Nevertheless, particle aggregation, as well as polymer chemical instability are the main limitations regarding PNP industrial applications, showing poor long-term stability (323, 330).

4.3.3. Protein-based nanoformulations

Proteins can be defined as natural synthetic polymers, biopolymers, which are considered excellent raw materials that present interesting features for nano-DDS development (331). Like polymers, proteins are constructed by molecular subunits, known as amino acids, linked through covalent peptide bonds. Protein-based NP are suitable and versatile platforms for several purposes due to their intrinsic properties such as biodegradability, biocompatibility, and bioavailability, as well as allowing the accommodation of a wide range of active compounds (332, 333). Regarding their source, proteins can be subclassified into animal or vegetal origin, where gelatin, serum albumin, collagen, keratin, elastin, silk fibroin and milk proteins are the most widely used animal proteins, while legumin, prolamins such as corn zein and wheat gliadin, soy proteins and lectins are the most common of plant origin (332, 334). Importantly, since they are obtained from sustained and renewable sources, protein-based NP are cheaper than synthetic polymer-based ones, while being easy to produce and scale-up (335, 336). Besides, they are also decomposable and metabolizable into harmless peptides through digestive enzymes, thus being less cytotoxic than synthetic polymers (332). Owing to the multiple functional groups comprised in the primary structure of the protein, the possibilities of modifying the resulting nanocarrier are higher compared to other biomaterials, thus highlighting for their tunable properties (337). Namely, the NP internal cavity can be modified to achieve different types of interactions with the loaded therapeutic agent. On the other side, the presence of surface functional groups, such as carboxylic and amino groups, offer the opportunity to decorate their surfaces, leading to the development of active targeting through specific ligands conjugation onto their surfaces (332).

Nonetheless, they also present some limitations related to their heterogeneity and NP size distribution, which lead to batch-to-batch variation and may produce allergenic problems (338). Furthermore, hydrophilic protein-based NP show abrupt drug release patterns in aqueous environments. In this sense, recombinant protein technology and chemical crosslinkers are being used in the produced formulations in order to overcome these drawbacks (332).

4.4. Nanopharmaceuticals for cancer treatment

Over the past few decades, nanomedicine has emerged as a new field of health and life science, with a major impact on human health (217). Although still being in an early stage, the nanopharmaceutical market is continually expanding and is expected to continue growing with the development of new and innovative products (221). In fact, these types of formulations have evolved from being simple new therapeutic hypothesis to being real products available on the market. In 2016, according to BBC Research, the global nanomedical market was valued at \$134.4 billion, and is projected to grow to \$293.1 billion by 2022 (339). Noteworthy, nanopharmaceuticals have made important contributions in the treatment of various diseases, especially in the field of oncology where it appears as a promising tool for the challenging development of cancer therapy (224).

Nowadays, several nanopharmaceuticals for cancer treatment are available on the market and used in clinical settings (Table 2). They are mainly based on the reformulation of small-molecule drugs in order to improve their pharmacokinetic profiles and reduce undesired side effects to, finally, enhance their therapeutic efficacy. Therefore, representing the first-generation nanopharmaceuticals, the majority of approved nanomedicines depend on passive targeting provided by the EPR effect (262, 340). However, the future of nanomedicine is focused on active targeting strategies in order to improve their specificity and cellular uptake once at the tumor site. In this sense, our proposed nanosystem offers the possibility to perform active targeting, which has been shown to have positive results in *in vivo* colon cancer models (341).

Table 2. Examples of clinically approved nanomedicines for cancer treatment in Europe and United States (221, 222, 256, 278).

Trade Name	Formulation	Active compound	Cancer type	Company	Approval year
Lipid-based nanoformulations					
Doxil / Caelyx	PEGylated Liposomal Doxorubicin	Doxorubicin	HIV-related Kaposi's sarcoma, Ovarian cancer, Breast cancer, Multiple myeloma	Janssen	1995 (FDA) 1996 (EMA)

Trade Name	Formulation	Active compound	Cancer type	Company	Approval year
Lipid-based nanoformulations					
DaunoXome	Liposomal Daunorubicin	Daunorubicin citrate	HIV-related Kaposi's sarcoma	Galen	1996 (FDA)
DepoCyt	Liposomal Cytarabine	Cytarabine	Lymphoma, Leukemia, Meningeal Neoplasms	Enzon Pharmaceuticals	1999 (FDA) 2001 (EMA)
Myocet	Liposomal Doxorubicin	Doxorubicin	Breast cancer	Teva	2000 (EMA)
Mepact	Liposomal Mifamurtide	Mifamurtide	Osteosarcoma	Takeda Pharmaceutical	2009 (EMA)
Marqibo	Liposomal Vincristine	Vincristine sulfate	Acute lymphoblastic leukemia	Talon Therapeutics	2012 (FDA)
Onivyde	PEGylated Liposomal Irinotecan	Irinotecan	Metastatic pancreatic cancer	Merrimack Pharmaceuticals	2015 (FDA) 2016 (EMA)
Vyxeos	Dual Liposomal Cytarabine and Daunorubicin	Cytarabine and Daunorubicin (5:1 molar ratio)	Acute myeloid leukemia	Jazz Pharmaceuticals	2017 (FDA) 2018 (EMA)
Polymer-based nanoformulations					
Eligard	Leuprolide acetate and polymer [PLGH (poly (dl-lactide-coglycolide))]	Leuprolide acetate	Prostate cancer	Tolmar Pharmaceuticals	2004 (FDA)
Apealea	Paclitaxel Micellar	Paclitaxel	Ovarian cancer	Oasmia Pharmaceutical	2018 (EMA)
Protein-based nanoformulations					
Oncaspar	PEGylated L-Asparaginase	Pegaspargase	Acute lymphoblastic leukemia, Chronic myelogenous leukemia	Enzon Pharmaceuticals	1994 (FDA) 2016 (EMA)
Ontak	Recombinant diphtheria toxin protein conjugated to IL-2	Denileukin diftitox	Cutaneous T-cell lymphoma	Eisai Pharmaceuticals	1999 (FDA)
Abraxane	Human Serum Albumin-bound Paclitaxel nanoparticles (nab-PTX)	Paclitaxel	Breast cancer, NSCLC, Pancreatic cancer	Celgene	2005 (FDA) 2008 (EMA)
Sylatron	PEGylated interferon alfa-2b	Interferon alfa-2b	Melanoma	Merck & Co.	2011 (FDA)

Metal-based nanoformulations					
NanoTherm	Iron Oxide Nanoparticles	Aminosilane	Brain tumors	MagForce	2011 (EMA)
Hensify	Crystalline Hafnium oxide nanoparticles	Electron production through external radiation	Soft tissue sarcoma	Nanobiotix	2019 (EMA)

EMA: European Medicines Agency; FDA: Food and Drug Administration; NSCLC: Non-small cell lung cancer; PEG: Polyethylene glycol; PTX: Paclitaxel.

Specifically, PM have been widely used for drug delivery applications in the oncology field due to their excellent physicochemical properties, allowing the solubilization and administration of several types of payloads. Noteworthy, several drug-loaded PM are currently under clinical evaluation for cancer treatment with promising anti-cancer activity (Table 3). In fact, Genexol-PM® and Nanoxel® M are PM-based formulations that are approved in South Korea and commercialized by Samyang Biopharmaceuticals Corporation (342). In particular, Genexol® was the first micellar formulation to be approved for human use in 2007 for the treatment of breast, non-small cell lung cancers (NSCLC) and ovarian cancers. It consists of 20-50 nm PTX loaded-PM of block copolymer methoxy poly(ethylene glycol)-*b*-poly(D,L-lactide) (mPEG-*b*-PDLLA). Being a Cremophor EL-free formulation, Genexol-PM® allows PTX solubilization with limited hypersensitivity-related reactions, improving its safety compared to Taxol® (343). Further, Genexol-PM® is currently in clinical evaluation in the USA and EU under the trade name of Cynviloq™ (344, 345). Furthermore, Nanoxel® M is a docetaxel (DTX)-loaded mPEG-*b*-PDLLA PM, which was developed using the same PM-based formulation as Genexol-PM®. In this case, micelles are used to solubilize DTX removing the excipient Tween 80 and, thus, find an alternative for Taxotere®, the conventional DTX formulation (346). It was approved by South Korean regulatory agencies in 2012 for the treatment of breast, NSCLC, esophageal, ovarian, head and neck, gastric and prostate cancers; and it is currently in clinical trials for the treatment of head and neck squamous cell carcinoma (HNSCC) and non-muscle-invasive bladder cancer (342).

On the other side, the first anti-cancer micellar formulation to reach clinical trials in 1999 was SP1049C, composed of a mixture of Pluronics®, namely L61 and F127 (1:8 weight ratio) (300, 347). Specifically, SP1049C is a doxorubicin-loaded PM developed by Supratek Pharma Inc, which obtained two orphan drug designations by FDA for the treatment of adenocarcinoma of the esophagus and gastric cancer (347, 348).

Table 3. Examples of PM approved or in clinical trials for cancer treatment (298, 349).

Product name	Polymer	Active compound	Cancer type	Clinical phase	Reference/ Trial code
Genexol-PM®	mPEG- <i>b</i> -PDLLA	Paclitaxel	Breast cancer NSCLC Ovarian cancer	Approved in Korea (2007)	(344, 345)
		Paclitaxel	Breast cancer	Phase III	*NCT00876486
		Paclitaxel	NSCLC	Phase II	*NCT01023347
		Paclitaxel	Pancreatic cancer	Phase II	*NCT00111904
		Paclitaxel	Ovarian cancer	Phase I	*NCT00877253
Nanoxel® M	mPEG- <i>b</i> -PDLLA	Docetaxel	Advanced solid tumors	Approved in Korea (2012)	(342, 346)
		Docetaxel	HNSCC	Phase II	*NCT02639858
NK105	mPEG- <i>b</i> -modified P(Asp)	Paclitaxel	Advanced or recurrent breast cancer	Phase III	*NCT01644890
NC-6004 Nanoplatin®	PEG- <i>b</i> -P(Glu)	Cisplatin / Gemcitabine	Pancreatic	Phase III	*NCT02043288
		Cisplatin / Gemcitabine	Solid tumors	Phase I/II	*NCT02240238
		Cisplatin / 5-FU / Cetuximab	HNSCC	Phase I/II	*NCT03109158
SP1049C	Pluronic® L61 and F127	Doxorubicin	Advanced adenocarcinoma	Phase III	(347, 348)
NK012	PEG- <i>b</i> -P(Glu) covalent drug-copolymer conjugate	SN-38	TNBC	Phase II	*NCT00951054
		SN-38	Small Cell Lung Cancer	Phase II	*NCT00951613
		SN-38 / 5-FU	Metastatic CRC Advanced solid tumors	Phase I	*NCT01238939
CPC634 CriPec®	PEG- <i>b</i> -P(HPMAm-Lac _n) covalent drug copolymer conjugate	Docetaxel	Ovarian cancer	Phase II	*NCT03742713
NK911	PEG- <i>b</i> -P(Asp) covalent drug-copolymer conjugate	Doxorubicin	Solid tumors	Phase I	(350)

NC-4016	PEG- <i>b</i> -P(Glu) coordination complex	Oxaliplatin	Advanced solid tumors and lymphoma	Phase I	*NCT03168035
---------	--	-------------	------------------------------------	---------	--------------

*ClinicalTrials.gov identifier. 5-FU: 5-Fluorouracil; CRC: colorectal cancer; HNSCC: head and neck squamous cell carcinoma; HPMA: poly[N-(2-hydroxypropyl) methacrylamide]; mPEG-*b*-PDLLA: methoxy poly(ethylene glycol)-*b*-poly(D,L-lactide); NSCLC: non-small cell lung cancer; P(Asp): poly(aspartic acid); P(Glu): poly(glutamic acid); PEG: polyethylene glycol; TNBC: Triple negative breast cancer.

5. Different proposed nanotechnology-mediated strategies targeting CSC fraction

Nanotechnology-mediated therapeutic strategies have emerged as promising options to overcome the aforementioned drawbacks related to currently available cancer therapies. In this project, two therapeutic strategies have been designed to eradicate CSC fraction by specifically targeting signaling pathways related to CSC survival and proliferation, namely, i) the pharmacological approach, and ii) the biotherapeutic approach. To this purpose, we have taken advantage of the properties provided by nanomedicine, using Pluronic® F127-based PM as nano-DDS. Specifically, the proposed nanocarriers will lead their loading molecules towards CSC, after passively accumulate within the tumor fenestrations. We then hypothesized the consequent decrease of tumor growth and metastatic spread. Moreover, Pluronic® F127-based PM can be used as a multifunctional nanoplatform to co-deliver different compounds in order to simultaneously eliminate both populations, CSC and bulk tumor cells, while hampering their interconversion ability.

Therefore, the pharmacological approach is based on the arachidonate 5-lipoxygenase (ALOX5) enzyme blocking through its chemical inhibitor, Zileuton™. Due to its hydrophobicity, Zileuton™ will be encapsulated within the inner core of Pluronic® F127-based PM. On the other side, in the biotherapeutic approach, the structural maintenance of chromosomes 2 (SMC2) protein will be specifically blocked through antibodies anti-SMC2 (Ab-SMC2). In order to avoid enzymatic degradation and enable the extracellular membrane crossing, Ab-SMC2 will be conjugated with PM using two different approaches: i) encapsulation by affinity into the PM hydrophilic shell (PM:SMC2), and ii) covalent conjugation between the -COOH terminals of the PM and the -NH₂ groups of the Ab-SMC2 (PM-CON:SMC2). Furthermore, to evaluate the effects of the combination

therapy, PTX and 5-FU chemotherapeutics will also be entrapped into the hydrophobic PM region of the decorated Ab-SMC2 micelles.

For that, Pluronic® F127-based PM will be produced using the thin-film hydration technique, as explained in detail in the materials and methods of the results section, and showed in Figure 11.

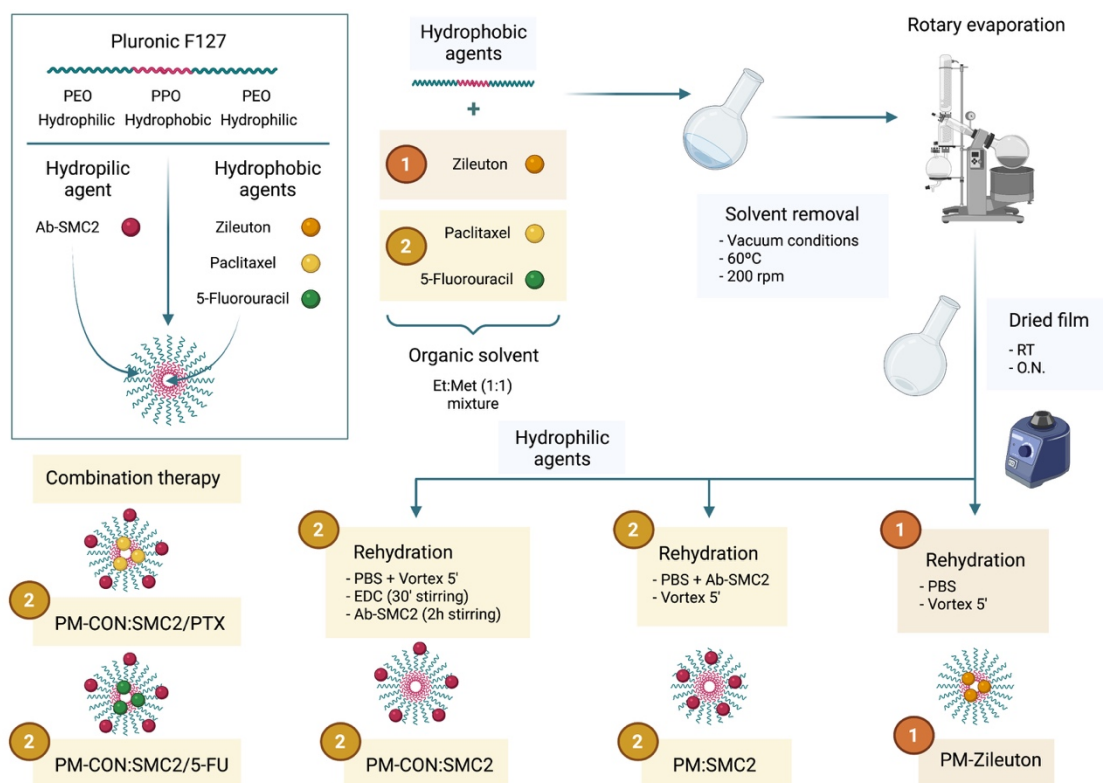


Figure 11. Schematic representation of PM production. (1) Pharmacological approach; (2) Biotherapeutic approach alone and in combination with standard of care drugs. 5-FU: 5-Fluorouracil; Ab-SMC2: antibodies anti-SMC2; EDC: (1-ethyl- 3-(3-dimethylaminopropyl)-carbodiimide); O.N.: overnight; PEO: poly(ethylene oxide); PM: polymeric micelles; PPO: poly(propylene oxide); PTX: paclitaxel; RT: room temperature.

5.1. Targeting CSC: *in vitro* and *in vivo* fluorescent models

In order to validate our nano-DDS we will use fluorescent CSC models, in which CSC can be assessed separately. To precisely evaluate the therapeutic effect of proposed treatment on CSC subpopulation, these cells have to be previously separated from the whole tumor mass, non-CSC or bulk tumor cells. Thus, a CSC *in vitro* model was developed and used in our laboratory, which enable the identification and isolation of

CSC, using a tdTomato reporter vector (351). In this system, tdTomato protein, a fluorescent reporter close to the near infrared region, is expressed under the control of ALDH1A1 promoter, a CSC-specific marker (351, 352). Consequently, just cells expressing the CSC-specific marker are detected by red fluorescence (tdTomato⁺ cells), while the non-CSC are not fluorescent in cell culture (tdTomato⁻ cells). Therefore, this strategy allows to identify and isolate CSC, but also to biological monitor the presence of CSC *in situ*; before, during and after the treatment.

Objectives

Since CSC survival after treatment seems to be the leading cause of cancer recurrence, therapeutic resistance, and metastatic aggressiveness, new and more efficient strategies that specifically target the CSC fraction are of utmost importance.

Therefore, the main aim of this project is to develop two new anti-CSC therapeutic strategies to eradicate the challenging CSC subpopulation within the tumor in order to prevent the metastatic spread and the tumor re-growth. Specifically, this work is mainly focused on the design, production, characterization and functional validation of Pluronic® F127-based PM, used as a multifunctional nanoplatform that allows the loading of different specific compounds for the CSC inhibition, such as hydrophobic drugs and macromolecules. Aiming to achieve this general purpose, specific objectives have been addressed, which are listed below:

1. To validate specific and suitable CSC targets for the design of a novel therapeutic strategy. For this purpose, the inhibition of chosen targets will be assessed in CSC isolated from breast and colon cancer cell lines.
2. To design, produce and physicochemically characterize Pluronic® F127-based PM.
3. To evaluate the proposed formulation regarding cytotoxicity and cellular internalization profiles using *in vitro* models.
4. To functionally validate the proposed formulation in both adherent and low attachment conditions in relation to free compounds treatment *in vitro*, as well as to compare the efficacy of the proposed anti-CSC therapeutic strategy with current standards of care used in the clinic for the cancer treatment.
5. To assess the synergistic effect of combined therapy, simultaneously addressed to the CSC fraction and the differentiated bulk tumor cells *in vitro*.
6. To evaluate the toxicity and accumulation of Pluronic® F127-based PM to guarantee an efficient and safe transport of the cargo *in vivo*.
7. To assess the therapeutic efficacy of the presented formulation in appropriate tumor-bearing mice disease models.

Results

Article 1

ZileutonTM loaded in polymer micelles effectively reduce breast cancer circulating tumor cells and intratumoral cancer stem cells

Sara Montero^{a,c,1}, Petra Gener^{a,*,1}, Helena Xandri-Monje^a, Zamira V. Díaz-Riascos^{a,b}, Diana Rafael^{a,c}, Fernanda Andrade^{a,d,e}, Francesc Martínez-Trucharte^a, Patricia González^{a,c}, Joanquin Seras-Franzoso^a, Albert Manzano^a, Diego Arango^f, Joan Sayós^{c,g}, Ibane Abasolo^{a,b,c,*}, Simo Schwartz Jr^{a,c,*}.

^a Drug Delivery and Targeting Group, Molecular Biology and Biochemistry Research Center for Nanomedicine (CIBBIM-Nanomedicine), Vall d'Hebron Institut de Recerca, Universitat Autònoma de Barcelona, Barcelona, Spain.

^b Functional Validation and Preclinical Research (FVPR), CIBBIM-Nanomedicine, Vall d'Hebron Institut de Recerca, Universitat Autònoma de Barcelona, Barcelona, Spain.

^c Networking Research Center for Bioengineering, Biomaterials, and Nanomedicine (CIBERE-BBN), Instituto de Salud Carlos III, Zaragoza, Spain.

^d i3S – Instituto de Investigação e Inovação em Saúde, Universidade do Porto, Porto, Portugal.

^e INEB – Instituto Nacional de Engenharia Biomédica, Universidade do Porto, Porto, Portugal.

^f Biomedical Research in Digestive Tract Tumors, CIBBIM-Nanomedicine, Vall d'Hebron Institut de Recerca, Universitat Autònoma de Barcelona, Barcelona, Spain.

^g Immune Regulation and Immunotherapy, CIBBIM-Nanomedicine, Vall d'Hebron Institut de Recerca, Universitat Autònoma de Barcelona, Barcelona, Spain.

¹ These authors contributed equally

Nanomedicine: Nanotechnology, Biology, and Medicine. 2020;24:102106.

DOI:10.1016/j.nano.2019.102106; PMID: 31666201.

IF 2020: 6.458; Quartile: Q1.

Breast cancer (BC) has been the most common cancer worldwide in terms of incidence in 2020, being metastatic BC (mBC) still an incurable disease. In this regard, the aggressiveness of recurrent cancer is related to the presence of surviving cancer stem cells (CSC) within the tumor, which promote tumor relapse despite having achieved an early therapeutic success. Apart from being ineffective eradicating CSC, conventional chemotherapy not only produces high systemic toxicity, but also presents dose-limiting issues that hinder reaching clinically desired efficacy. In this context, nano-sized drug delivery systems (nano-DDS) offer the great opportunity to develop an effective therapy specifically targeting the CSC subpopulation.

In this work, we have proposed a new anti-CSC strategy to eradicate the challenging fraction of CSC in advanced BC. Therefore, we have identified and functionally validated arachidonate 5-lipoxygenase (Alox5) as an essential gene for CSC survival in different breast CSC fluorescent models by high throughput screening, which has been considered a promising candidate to block specific CSC pathways while overcoming the progressive gain of chemo-resistance related to this cell subpopulation. Once ALOX5 was selected as a suitable target for breast CSC elimination, ZileutonTM, an FDA-approved ALOX5 iron-chelator chemical inhibitor already on the market for the treatment of asthma, has been validated as a suitable drug for the development of a new therapeutic strategy targeting CSC subset. After being encapsulated within the hydrophobic core of Pluronic® F127-based polymeric micelles (PM), ZileutonTM therapeutic potential was subsequently demonstrated both *in vitro* and *in vivo* breast CSC fluorescent models. Specifically, it has been shown how ZileutonTM loaded into Pluronic® F127-based PM core effectively reduces CSC content within treated primary tumors in both *in vivo* orthotopic BC models. Noteworthy, in the highly aggressive triple negative breast cancer (TNBC) metastatic MDA-MB-231 *in vivo* model, CSC reduction was conveyed with the circulating tumor cells (CTC) eradication in the blood stream after PM-ZileutonTM treatment. Furthermore, CTC blockade was also accompanied by a significant decrease in lung metastasis, thus diminishing their characteristic metastatic potential.

Keywords: Arachidonate 5-lipoxygenase (ALOX5), Cancer stem cells (CSC), Pluronic® F127-based polymeric micelles (PM), ZileutonTM, Circulating tumor cells (CTC).



ELSEVIER



BASIC SCIENCE

Nanomedicine: Nanotechnology, Biology, and Medicine
24 (2020) 102106



Original Article

nanomedjournal.com

ZileutonTM loaded in polymer micelles effectively reduce breast cancer circulating tumor cells and intratumoral cancer stem cells

Petra Gener, PhD^{a,*},¹, Sara Montero^{a,c,1}, Helena Xandri-Monje^a,
Zamira V. Díaz-Riascos, PhD^{a,b}, Diana Rafael, PhD^{a,c}, Fernanda Andrade, PhD^{a,d,e},
Francesc Martínez-Trucharte^a, Patricia González^{a,c}, Joaquin Seras-Franzoso, PhD^a,
Albert Manzano^a, Diego Arango, PhD^f, Joan Sayós, PhD^{c,g}, Ibane Abasolo, PhD^{a,b,c,*},
Simo Schwartz JrMD, PhD^{a,c,*}

^aDrug Delivery and Targeting Group, Molecular Biology and Biochemistry Research Centre for Nanomedicine (CIBBIM-Nanomedicine), Vall d'Hebron Institut de Recerca, Universitat Autònoma de Barcelona, Barcelona, Spain

^bFunctional Validation & Preclinical Research (FVPR), CIBBIM-Nanomedicine, Vall d'Hebron Institut de Recerca, Universitat Autònoma de Barcelona, Barcelona, Spain

^cNetworking Research Centre for Bioengineering, Biomaterials, and Nanomedicine (CIBER-BBN), Instituto de Salud Carlos III, Zaragoza, Spain

^di3S - Instituto de Investigação e Inovação em Saúde, Universidade do Porto, Porto, Portugal

^eINEB - Instituto Nacional de Engenharia Biomédica, Universidade do Porto, Porto, Portugal

^fBiomedical Research in Digestive Tract Tumors, CIBBIM-Nanomedicine, Vall d'Hebron Institut de Recerca, Universitat Autònoma de Barcelona, Barcelona, Spain

^gImmune Regulation and Immunotherapy, CIBBIM-Nanomedicine, Vall d'Hebron Institut de Recerca, Universitat Autònoma de Barcelona, Barcelona, Spain

Revised 28 August 2019

Abstract

Tumor recurrence, metastatic spread and progressive gain of chemo-resistance of advanced cancers are sustained by the presence of cancer stem cells (CSCs) within the tumor. Targeted therapies with the aim to eradicate these cells are thus highly regarded. However, often the use of new anti-cancer therapies is hampered by pharmacokinetic demands. Drug delivery through nanoparticles has great potential to increase efficacy and reduce toxicity and adverse effects. However, its production has to be based on intelligent design. Likewise, we developed polymeric nanoparticles loaded with ZileutonTM, a potent inhibitor of cancer stem cells (CSCs), which was chosen based on high throughput screening. Its great potential for CSCs treatment was subsequently demonstrated in *in vitro* and in *in vivo* CSC fluorescent models. Encapsulated ZileutonTM reduces amount of CSCs within the tumor and effectively blocks the circulating tumor cells (CTCs) in the blood stream and metastatic spread.

© 2019 The Authors. Published by Elsevier Inc. This is an open access article under the CC BY-NC-ND license (<http://creativecommons.org/licenses/by-nc-nd/4.0/>).

Key words: Cancer stem cells (CSC); Circulating tumor cells (CTC); Nanomedicine; Polymeric micelles; ZileutonTM

Despite the latest progress in early diagnosis and more effective treatments, advanced breast cancer is still an

incurable disease.^{1,2} Particularly aggressive is the Triple Negative Breast Cancer (TNBC), which does not respond to current hormonal therapy and medicines targeting HER2 receptors, because of the absence of estrogen-, progesterone-, and Her2- surface receptors in tumor cells. It has been suggested that tumor progression and dissemination are mediated by the presence of specific Cancer Stem Cells (CSCs) subpopulations within the tumor. CSCs are also thought to be responsible for cancer relapse and of being intrinsically resistant to most current treatments. Accordingly, CSCs are thus responsible for many therapeutic failures.³⁻⁵ Unfortunately, there are no effective treatments yet targeting CSCs and their metastatic spread to distal organs.

Statement of funding

The authors declare no potential conflicts of interest

*Corresponding authors at: Drug Delivery and Targeting Group, Molecular Biology and Biochemistry Research Centre for Nanomedicine (CIBBIM-Nanomedicine), Vall d'Hebron Institut de Recerca, Universitat Autònoma de Barcelona, Barcelona, Spain.

E-mail addresses: petra.gener@vhir.org (P. Gener), ibane.abasolo@vhir.org (I. Abasolo), simo.schwartz@vhir.org (S. Schwartz).

¹ These authors contributed equally.

<https://doi.org/10.1016/j.nano.2019.102106>

1549-9634/© 2019 The Authors. Published by Elsevier Inc. This is an open access article under the CC BY-NC-ND license 4.0

Please cite this article as: Gener P, et al, ZileutonTM loaded in polymer micelles effectively reduce breast cancer circulating tumor cells and intratumoral cancer stem cells. *Nanomedicine: NBM* 2020;24:102106, <https://doi.org/10.1016/j.nano.2019.102106>

Therefore, in order to increase patient survival, it has become essential to develop new therapeutic strategies against CSC to successfully eradicate advanced cancer and prevent metastasis.

Unfortunately, many prospective drugs do not have sufficient solubility or adequate pharmacokinetics to reach good efficacy and toxicity profiles for clinical use. In this context, specific nano-sized drug delivery systems (nano-DDS) offer the possibility of converting agents with low therapeutic profile into forthcoming clinical drug candidates. Further, nano-encapsulation facilitates the administration of hydrophobic agents while protecting them during circulation, lowering the undesired side effects associated with a systemic, non-controlled distribution of the drug. Nanomedicines can also evade Multi Drug Resistant mechanisms (*i.e.*, MDR channels) and increase drug's intracellular accumulation, improving the efficacy of the treatment.^{4,6,7}

We have used two recently characterized fluorescent breast CSC models to identify by high throughput screening potential therapeutic target candidates in CSCs.^{8,9} These models express tdTomato (red fluorescence) under the control of the CSC specific promoter, ALDH1A1. Thus, tdTomato fluorescence is detected exclusively in the CSC subpopulation, while differentiated cancer cells (non-CSCs) do not express the fluorescent marker. This system allows not only to segregate CSCs from non-CSCs subpopulations, but also to monitor the biological performance of CSCs *in situ*; before, during and after treatment.^{8–11} Our data revealed arachidonate 5-lipoxygenase (5-LO) gene (Alox5) as a potential therapeutic candidate in breast CSCs. Recently, ALOX5 was also identified as a critical regulator of CSCs from Chronic Myeloid Leukemia (CML).¹² Moreover, we have recently demonstrated that siRNA inhibition of Alox5 is able to downregulate the expression of the gene *in vitro* and also of decreasing invasion and malignant transformation of breast CSCs.¹³

ZileutonTM is a specific marketed drug inhibitor of ALOX5, approved by the FDA as an anti-leukotriene oral drug for the treatment of asthma.^{14,15} Its potential use as anticancer drug has been recently addressed in clinical trials. Thus, no safety issues related to oral administration of ZileutonTM were reported in a clinical trial (Safety; phase I) in combination with Dasatinib (Sprycel®) (NCT02047149) and with Imatinib Mesylate (Gleevec) (NCT01130688) respectively, in patients with CML. Unfortunately, additional randomized phase-II trials to study the efficacy of oral ZileutonTM in cancer patients in combination with *Standard-of-Care* treatments have not yield positive results, so far (ClinicalTrials.gov). Most likely, the need of an intravenous administration, the high hydrophobicity of the drug and its high IC₅₀, hamper its potential clinical use in the oncology field. Here, we report on the anticancer and anti-metastatic effects of new ZileutonTM-loaded polymeric micelles, using *in vivo* breast CSCs models. Our data show significant intratumoral reduction of CSCs *in vivo*, and also a strong reduction of circulating cancer cells and CSCs in the blood in these models.

Methods

Microarray performance and validation

In total 8 RNA samples, comparing 2 technical replicates of tdTomato positive (tdTomato⁺) and tdTomato negative (tdTomato[−]) samples (corresponding to CSC and non-CSC) sorted from two different cell lines (MCF7-ALDH1A1:tdTomato, MDA-MB-231-ALDH1A1:tdTomato) (details in supplementary data) were analyzed by microarray. For this, 100 ng of total RNA was labeled using LowInputQuick Amp Labeling kit v6.5 (Agilent 5190-2305) following manufacturer instructions. The labeled cRNA was hybridized to the Agilent SurePrint G3 Human gene expression 8×60K microarray (ID039494) according to the manufacturer's protocol. The arrays were scanned on an Agilent G2565CA microarray scanner at 100% PMT and 3 μm resolution. Raw data were taken from the Feature Extraction output files and were corrected for background noise using the normexp method.¹⁶ To assure comparability across samples we used quantile normalization.¹⁷ Differential expression analysis was carried out in noncontrol probes with an empirical Bayes approach on linear models (limma), applying a paired test.¹⁸ Results were corrected for multiple testing according to the False Discovery Rate (FDR) method.¹⁹ Obtained results were confirmed by qPCR and flow cytometry (details in supplementary data). Clinical and expression data of ALOX5 were obtained from The Cancer Genome Atlas (TCGA) for breast invasive cancer collection, in order to correlate these two features. Also, expression microarray data from the same portal were used to evaluate ALOX5 overexpression with ovarian serous cystadenocarcinoma, lung adenocarcinoma and colon adenocarcinoma.

In vitro functional validation of free and encapsulated ZileutonTM

To validate efficacy of ZileutonTM *in vitro*, we performed i.) Cell viability assay ii.) CSC resistance assay, and iii.) Cell Transformation Assay (Anchorage-Independent Growth Assay) (experimental details are in supplementary data).

Production and physicochemical characterization of PMs for ZileutonTM delivery

PMs were prepared using the thin-film hydration technique and characterized them by Dynamic Light Scattering (DLS) (Malvern Instruments), Transmission Electron Microscopy (TEM) and Cryo-Transmission Electron Microscopy (Cryo-TEM) (details in supplementary data).

Furthermore; i.) Entrapment efficiency ii.) PMs stability, and iii.) PMs internalization were evaluated (details in supplementary data).

In vivo preclinical validation of PM-ZileutonTM

Animal care was handled in accordance with the Guide for the Care and Use of Laboratory Animals of the Vall d'Hebron University Hospital Animal Facility, and the Animal Experimentation Ethical Committee at the institution approved the experimental procedures. All the *in vivo* studies were performed by the ICTS "NANBIOSIS" of CIBER-BBN's *In Vivo*

Experimental Platform of the Functional Validation & Preclinical Research (FVPR) area (CIBBIM-Nanomedicine, Barcelona, Spain).

Orthotopic breast cancer models

MCF-7 and MDA-MB-231 breast cancer cells were orthotopically inoculated into mammary fat pad (i.m.f.p) as previously described.^{8,9,20,21} In detail, MDA-MB-231 cells and MCF-7 cells suspended with Matrigel (1:1) (BD Bioscience, Bedford, MA, USA) were respectively implanted into the right abdominal mammary fat pad (i.m.f.p.) of NOD-SCID mice (Supplementary data). MCF-7 tumor bearing mice were also subcutaneously injected with estrogen pellets (17 β -Estradiol, 0.36 mg/pellet, 90 days release; Innovative Research of America, Sarasota FL, USA). Further, 3 days before i.m.f.p. inoculation their drinking water was supplemented with Baytril (Enrofloxacin) 0.08 mg/mL as a preventive measure to minimize the side effects from estradiol. Tumor growth was monitored twice a week by conventional caliper measurements ($D \times d^2/2$, where D is the major diameter and d the minor diameter).

Toxicity

Female athymic mice were treated intravenously (i.v.) with 1.5, 5 and 15 mg/kg ($n = 5$ /dose) 3 times per week during 3 weeks. Body weight changes and animal welfare were monitored along the assay. Animals were euthanized 1 h after the last administration and blood and tissue samples collected after gross necropsy.

Biodistribution

Ten mice were administered with a unique dose of PMs labeled with fluorescent dye DiR at 0.8 mg DiR/kg by i.v. administration route. Eight of these mice had i.m.f.p. MDA-MB-231 tumors and 2 mice without tumor were also included in the assay as a control to set the autofluorescence of the tissue. At 24, 44 and 72 h administration, tumor-accumulation and whole-body biodistribution were measured non-invasively by DiR fluorescence imaging (FLI) from the ventral and dorsal mouse views, using the IVIS Spectrum (Perkin Elmer) imaging system analyzed using Living Image® 4.5.2 software (PerkinElmer). In addition, at 72 h post administration end time point, plasma, tissue and tumor samples were collected, weighed and processed for *ex vivo* imaging. The fluorescence signal in *ex vivo* images was quantified in Radiant Efficiency units and referred to the tissue weight following procedures previously described.^{8,20,21}

Efficacy

In order to test the effects of PM-Zileuton™ in the tumor growth and in the CSC population, orthotopic breast cancer models were generated using freshly sorted tdTomato+ cells (0.6×10^6 cells / mouse for the MCF-7 cell line and 0.1×10^6 cells/animal for the MDA-MB-231 cell line). Animals were then treated with i.v. administration of PM-Zileuton™ (15 mg/kg), 3 times per week during 3 weeks. One day (MDA-MB-231) or 7 days (MCF-7) after the last administration animals were euthanized and blood and tumor samples were collected for the analysis of CSC content. To measure the extent of lung metastasis *ex vivo* bioluminescent imaging (BLI) was also performed using the IVIS Spectrum after administering

150 mg/kg of luciferin to mice. Immediately after necropsy, lung tissues were placed individually into separate wells containing 300 μ g/mL of D-luciferin, and imaged and quantified using Living Image® 4.5.2 software.²¹ Determination of circulating tumor cells in the blood stream and the content of tdTomato+ cells within the tumor was performed by flow cytometry (details in supplementary data). For this all injected cells expressed GFP under CMV promotor. We analyzed all alive cells (Dapi⁻) that emitted green fluorescence and quantified the ones which were also tdTomato⁺ as CSC.

Results:

ALOX5 is a breast CSC specific therapeutic target candidate

In order to design an effective anti-cancer therapy, we analyzed transcriptome of CSCs sorted from two different CSC fluorescent models; MDA-MB-231-ALDH1A1:tdTomato, a basal-like breast cancer cell line highly aggressive and chemo-resistant, and MCF7-ALDH1A1:tdTomato, a luminal breast cancer cell line. Correlation-based clustering analysis of microarray data revealed substantial disparity due to epithelial (MCF7) and mesenchymal (MDA-MB-231) characteristics of respective cell lines (Figure S1). Several mesenchymal markers (e.g. *VIM*, *CD44*, *SERPINE1/2*, *ESAM*) were clearly over-expressed in MDA-MB-231 cells and under-expressed in MCF7 cells. Contrarily, epithelial markers (e.g. *CD24*, *KRT6B*, *KRT8*, *KRT18*, *CDH1*) were over-expressed in MCF7 cells and under-represented in MDA-MB-231 cells²⁵ (Figure S1). These pronounced differences between cell line characteristics, partly concealed the expected differences in reported CSC markers (e.g. *KLF5*, *DUSP6*, *ITGB2*, *ALDH1A1*, *SOX9/2*, *NOTCH2/4*, *MUC16*, *GRHL2*) comparing CSCs with non-CSCs¹ (Figure S1). Nonetheless, we identified 75 up-regulated genes ($FC > 2$) and 58 down-regulated genes ($FC < 0.5$) in CSCs segregated from both, MCF7 and MDA MB 231 cell lines. Several candidates were chosen for further confirmation based on the uniformity of these increased levels found in CSCs in all related samples and/or their relationship with CSC biology (Figure 1, A).

In MDA-MB-231 CSCs, we confirmed increased mRNA expression of; *ALOX5* (Arachidonate 5-Lipoxygenase), *CMKLR1* (Chemokine like receptor 1), *BST2* (Bone Marrow Stromal Cell Antigen 2), *SNAIL1* (Snail family zinc finger 1). In MCF7 CSCs, we confirmed increased expression of; *TGFB2* (Transforming Growth Factor β 2), *ALOX5*, *SPARC* (Secreted Protein, Acidic, Cysteine-Rich), *PTPRE* (Protein Tyrosine Phosphatase, Receptor type, E), *EGR4* (Early Growth Response 4), and *SNAIL2*. Contrary to the microarray analysis, validation through q-PCR did not prove any significant difference between CSC and nonCSC regarding *BST2* and *LIPA* in MCF7, and *EGR4*, *PTPRE*, *LIPA*, *TGFB2* and *SNAIL2* genes in MDA-MB-231 (Figure 1, B).

Only *ALOX5* was significantly overexpressed in both, MDA-MB-231 and MCF7 CSCs. Moreover, *in silico* analysis of data from 590 patients with invasive breast cancer, revealed over-expression of *ALOX5* mRNA ($FC > 2$) in 83.6% of total cases (Figure 1, C). However, no significant correlation with known

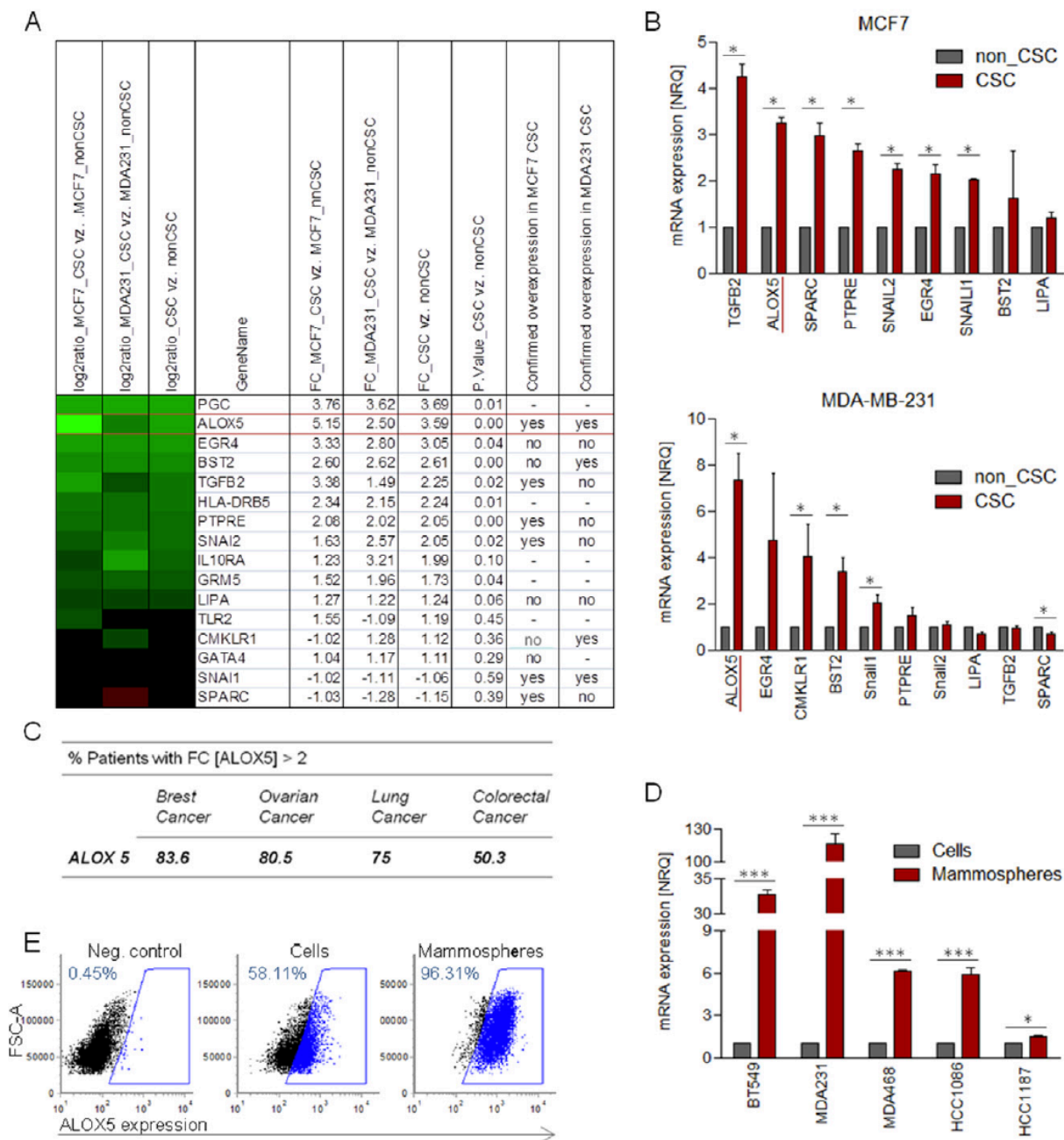


Figure 1. High-throughput microarray data from breast cancer cell lines. (A) Expression microarray analysis showing selected candidates for further validation by qPCR. FC = fold-change. P value >0.05 shown in light red, P value <0.05 shown in light green. (B) Relative expression levels of selected candidates in CSC in MCF-7 and MDA-MB-231 cell lines. Significant results with P value >0.05 are marked with *. Alox5 gene is upregulated in both cell lines. (C) ALOX5 expression levels for Breast Cancer, Ovarian Cancer, Lung Cancer and Colorectal Cancer according to *The Cancer Genome Atlas* (TCGA). (D) Alox5 expression in CSCs in breast cancer cell lines. In order to obtain a CSCs enriched population, cells were grown as mammospheres in low attachment conditions without FBS. (E) Increased expression of ALOX5 protein level was confirmed in MDA-MB-231 mammospheres. Significant results with P value ≤ 0.001 are marked with ***.

clinical pathological features of the patients was found (data not shown). Interestingly, clinical data also revealed over-expression of ALOX5 mRNA in 80% of patients with ovarian cancer, 75% of patients with lung cancer and in 50% of patients with

colorectal cancer. Increased ALOX5 mRNA expression was further confirmed in a battery of triple negative breast cancer cell lines (TNBC), BT549, MDA-MB-231, MDA-MB-468, HCC1086, HCC1187, comparing normal cell culture conditions

(growing in attachment and with complete medium) with CSC culture conditions (growing in non-attachment and in serum depleted medium as mammospheres) (Figure 1, D). Moreover, the increase of ALOX5 protein level was confirmed in MDA-MB-231 CSC culture (Figure 1, E). Therefore, we have further explored ALOX5 prospects as therapeutic target candidate to develop anti-CSCs therapy.¹³

Significant antitumoral efficacy of Zileuton™ against CSCs mammospheres

To validate the antitumoral effects against CSCs of inhibiting ALOX5 we investigated the efficacy of a selective, FDA approved ALOX5 inhibitor, Zileuton™. First, we determined the half inhibitory concentration (IC₅₀) of Zileuton™ in MDA-MB-231 and MCF7 breast cancer cell lines. As expected, Zileuton™ was more effective against MCF7 than in more resistant and aggressive MDA-MB-231 cell line. Of note IC₅₀ [MCF7] = 292 μM, IC₅₀ [MDA-MB-231] = 461 μM (Figure S2). After, we determined the IC₅₀ of Zileuton™ using pure tdTomato⁺ CSCs subpopulation sorted from both cell lines. The IC₅₀ was determined in two different cell culture conditions. On the one hand, in attachment conditions as normal cell culture conditions and on the other, in low attachment conditions as optimal conditions for CSCs culture. Interestingly, we observed increased efficacy of Zileuton™ in CSCs from both cell lines when CSCs were cultured in low attachment conditions; (IC₅₀ [MCF7] = 29.4 μM, IC₅₀ [MDA-MB-231] = 619 μM) compared to normal attachment culture (IC₅₀ [MCF7] = 499 μM, IC₅₀ [MDA-MB-231] = 852 μM) (Figure 2, A). Of note, we could also determine that ALOX5 expression is increased when CSCs are cultured as mammospheres (Figure 1, D, E).

Furthermore, Zileuton™ efficiently inhibited cellular growth in soft agar (transformation assay), which is a hallmark of CSCs, in a concentration dependent manner (Figure 2, B). Moreover, in order to compare the effect of Zileuton™, with Paclitaxel (PTX) and Abraxane™ (ABX), both drugs currently used in the clinics,^{22,23} we evaluated the relative abundance of CSCs before and after treatment, respectively. However, in order to mimic chemotherapeutic cycles in a similar way than used as standard-of-care, CSC *in vitro* models were treated with Zileuton™, PTX and ABX for 72 h, and then cells left to recover in medium without drugs during 48 additional hours. Even though in all cases similar efficacy was reached, the relative abundance of tdTomato⁺ CSCs increased significantly after PTX and ABX treatment while remarkably, this was not observed after Zileuton™ treatment, particularly in the resistant line, MDA-MB-231 (Figure 2, C).

Production and physico-chemical characterization of pluronic-F127 polymeric micelles loaded with Zileuton™

Zileuton™ is a highly hydrophobic compound that cannot be administrated i.v. to reach the required therapeutic effect. Because of this, we encapsulated Zileuton™ in the inner core of polymeric micelles formed by amphiphilic polymer Pluronic® F127, by thin-film hydration technique.^{24–26} The micelles obtained (PM-Zileuton™) showed a mean diameter of 25 nm, with a low polydispersity index (≤ 0.2) (Figure 3, A). These data

were confirmed by TEM and Cryo-TEM images, where it was possible to observe micelles of small size in the region of 25 nm with spherical morphology (Figure 3, B). DLS measurements performed one and two months after the preparation of the polymeric micelles confirmed their high stability at room temperature, since their physico-chemical features did not change over time (Figure S3, A). In addition, we tested the stability of PM-Zileuton™ in bovine serum. Accordingly, no aggregates appeared during 24 h in medium with FBS (50%) (Figure S3, B). Further, we could also establish 0.075 μM Zileuton™ stock as maximal encapsulatable dose, with up to 96% of encapsulation efficacy. These results were confirmed by UPLC. Of note, it was impossible to further increase the concentration of encapsulated Zileuton™, because at higher concentration Zileuton™ precipitated and formed crystals during the rehydration step.

Moreover, with the perspective to allow future clinical studies, we also demonstrated stability and efficacy of lyophilized PM-Zileuton™. Accordingly, no significant differences regarding size and *in vitro* efficacy were observed after the lyophilization and rehydration processes (Figure 3, C).

Finally, internalization studies were also performed. Fluorescently tagged PMs were internalized as early as one minute after its addition to cell culture in both cell lines (results of MCF7 cell line not shown). After 10 min all cells have internalized the tagged micelles and the intracellular amount of them followed to increase afterwards, as it was perceived by a constant increase of the fluorescence intensity (Figure 4, A). Interestingly, no significant differences regarding PMs internalization were observed between the subpopulations of CSCs and non-CSCs, respectively (Figure 4, A). By confocal microscopy, we observed lysosomal co-location of PMs tagged with 5-DTAF after 1 h and also 24 h after internalization (Figure 4, B).

Strong inhibition of CSCs by PM-Zileuton™ in *in vitro* and *in vivo* breast CSC models

Once polymeric micelles were produced and characterized, its functional validation was assessed. First, a biodistribution study was performed with DiR labeled PM™ in tumor bearing mice. *In vivo* fluorescent imaging (FLI) clearly showed that micelles tend to accumulate in the tumor area (mammary gland in the left caudal area). Fluorescent signal was also observed in the abdominal area, corresponding to the liver. *Ex vivo* imaging and quantification of the fluorescent signal were performed 24 and 72 h post-injection showing the kinetics of the micelles biodistribution and excretion (Figure 5). Data revealed that micelles were being accumulated in the tumor with a relative accumulation of 9.11% \pm 2.68% of total FLI signal per gram of tissue at 24 h that was kept practically invariable at 72 h post-administration (8.21% \pm 0.83% FLI/g). Liver and spleen also retained the micelles in levels comparable to those in the tumor. On the other hand, fluorescent signals in plasma, kidneys, lungs and muscle showed clearly descended between 24 and 72 h, indicating that micelles were cleared out by these organs.

Second, *in vitro* and *in vivo* efficacy was tested. Accordingly, the IC₅₀ of Zileuton™ was significantly decreased after its encapsulation into PMs (IC₅₀ [PM-Zileuton™] = 304 μM). Of

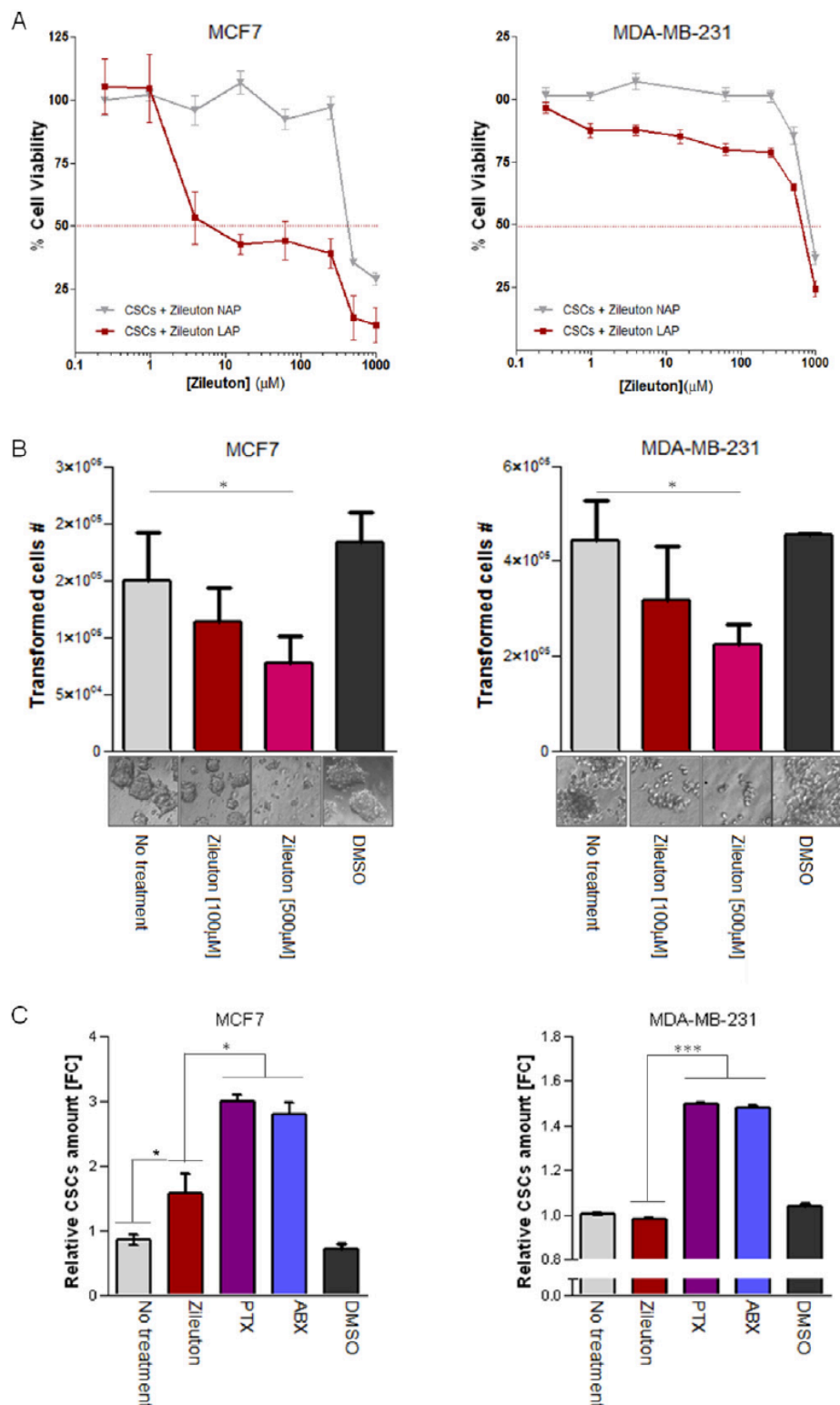


Figure 2. *In vitro* cell viability and transformation capacity of breast cancer cell lines and CSCs treated with ZileutonTM. (A) Cell viability (MTT) assay for MCF7 and MDA-MB-231 CSCs treated with ZileutonTM. Cells were grown in normal condition (NAP: normal attachment plates) and as mammospheres (LAP: low attachment plates). IC₅₀ corresponds to the half maximal inhibitory concentration and is indicated by a discontinuous red line. Cells without treatment represent 100% of viability. (B) Transformation capacity (anchorage independent growth) of MCF-7 and MDA-MB-231 CSCs treated with ZileutonTM. (C) Content of CSCs (tdTomato+) after treatment with ZileutonTM and ABX / PTX was quantified by flow cytometry in MCF-7 and MDA-MB-231 cell lines.

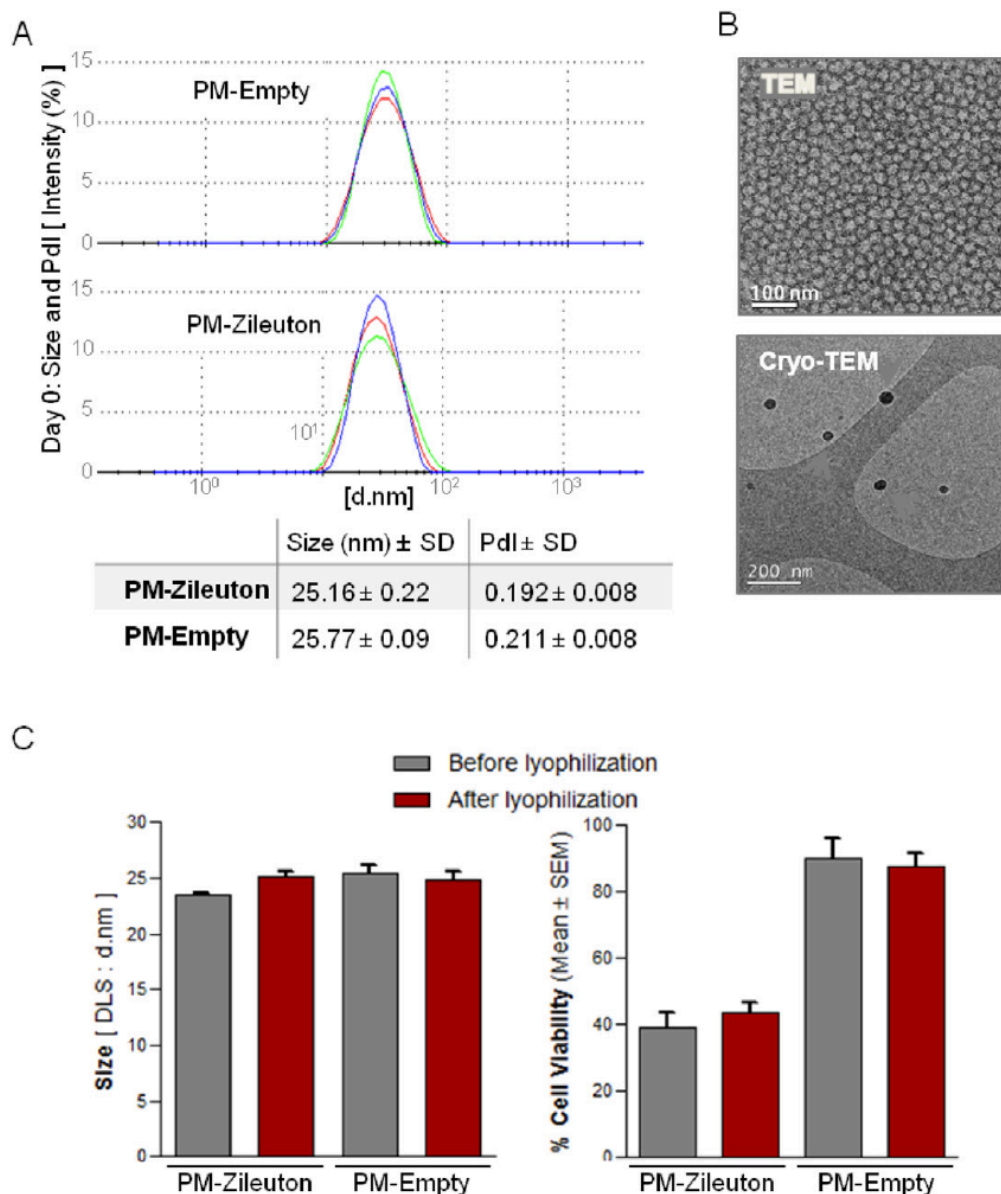


Figure 3. Physico-chemical characterization and cell internalization of PM-Zileuton™.(A) DLS size distributions by intensity with Z-average and Pdl values of Polymeric micelles loaded with Zileuton™, and unloaded nanoconjugates. (B) Electron microscopy images; TEM technique / Cryo-TEM of polymeric micelles loaded with Zileuton™. (C) Mean diameters (nm) of PM-Zileuton™ and unloaded micelles, measured by DLS before and after lyophilization and MDA-MB-231 CSCs viability, measured before and after lyophilization.

note, unloaded polymeric micelles did not show any substantial toxicity (Figure 6, A). Further, the transformation capacity of the cells was significantly decreased by PM-Zileuton™ when compared to free Zileuton™ (Figure 6, B). Moreover, because CSCs growing as tumorspheres in low attachment are highly resistant to common treatment (PTX, ABX), we wondered if PM-Zileuton™ would be effective in these conditions. Remarkably, PM-Zileuton™ were able to reduce the viability of CSCs in low attachment conditions, while no effect was seen for PTX and ABX in these conditions (Figure 6, C). Moreover, we have compared the viability of CSCs in normal growth condition or in

low attachment (mammospheres) after Zileuton™ treatment in combination with Abraxane or Paclitaxel. Even though no synergistic or additive effect was observed in combinatory treatment, Zileuton™ PMs significantly compromised the viability of MDA-MB-231 CSCs in all tested conditions (Figure S4).

Next, to determine possible *in vivo* adverse side effects, maximal feasible dose (MFD = 15 mg/kg) of PM-Zileuton™ was intravenously (i.v.) administrated into athymic mice. We did not observe significant loss of weight of the animals or any alterations in their overall well-being. Also, no macroscopic

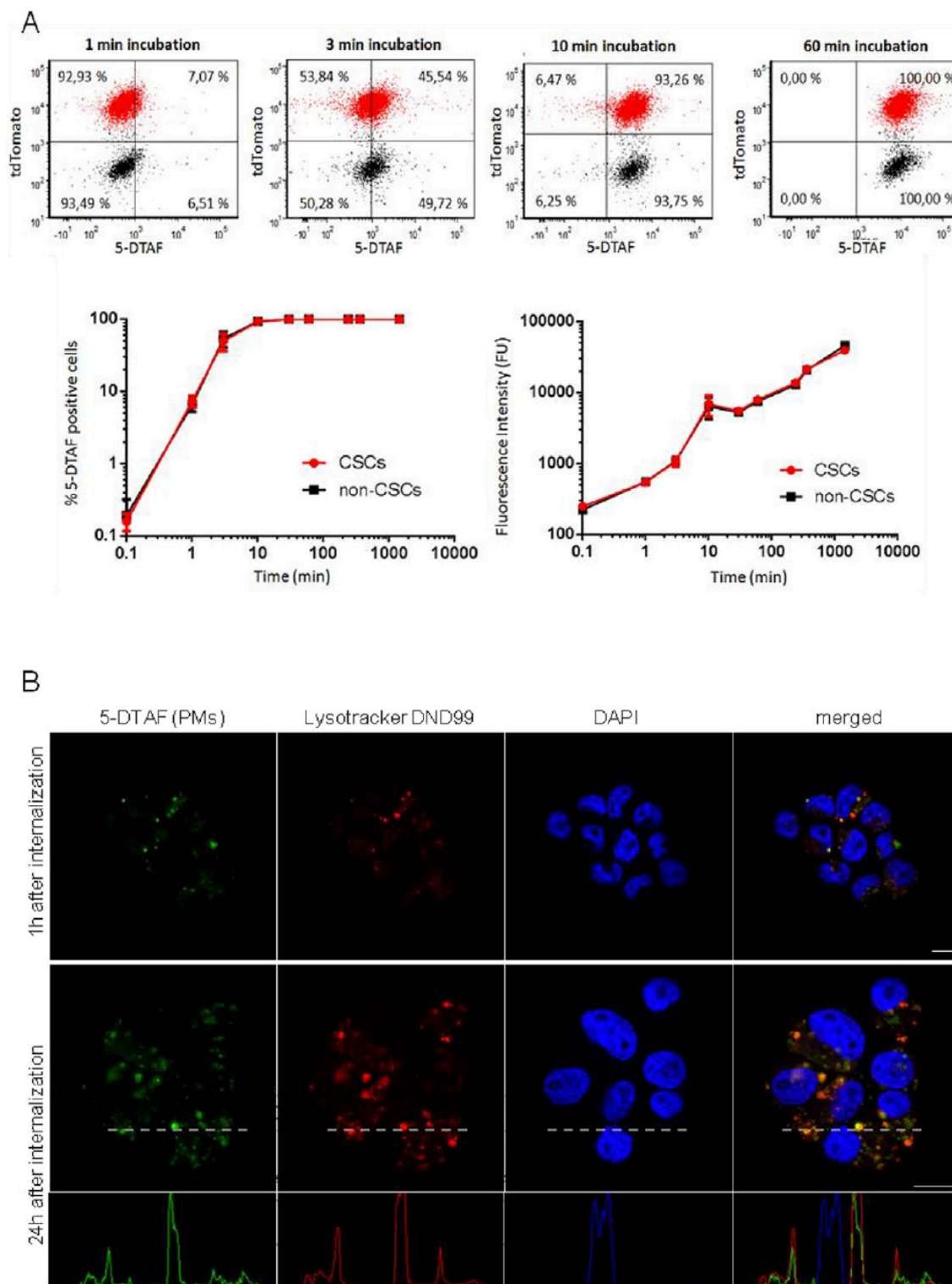


Figure 4. Internalization of PM-Zileuton™ in breast cancer cells. (A) Over time course quantification of CSCs (tdTomato+; red) and non-CSCs (tdTomato-; black) cellular uptake of fluorescently tagged PMs (PM-DTAF), reported as percentage of DTAF positive cells and relative increase of fluorescence intensity over time. For each sample, at least 10,000 individual cells were collected and the mean fluorescence intensity was evaluated. (B) The internalization of PM-Zileuton™ in breast MDA-MB-231 cancer cells was also observed by confocal microscopy 1 h and 24 h after internalization. Micelles were labeled with 5-DTAF (green fluorescence), lysosomes were labeled with Lysotracker DND99 (in red) and DAPI was used to visualize nuclei (in blue). The co-location of micelles and lysosomes was confirmed by fluorescence intensity plots over the illustrated dot line (24 h).

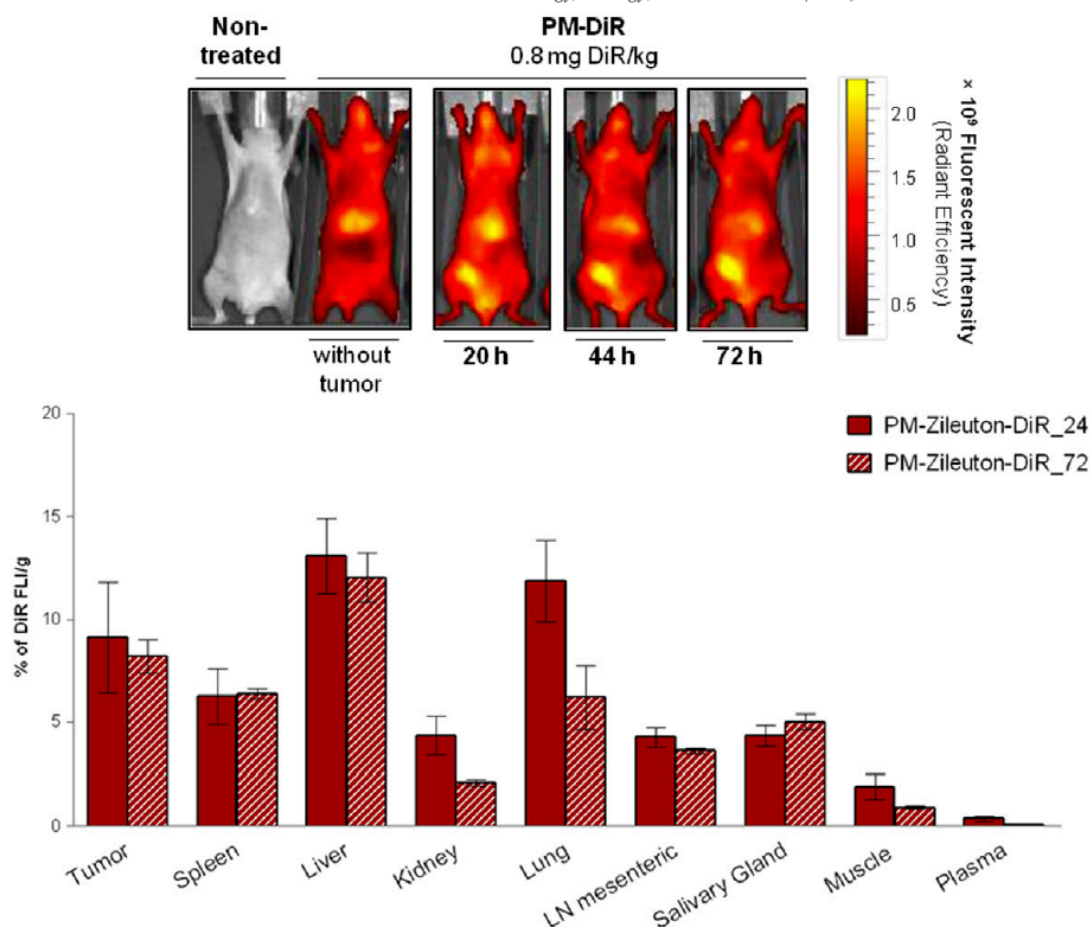


Figure 5. *In vivo* biodistribution of PM in mice with breast cancer orthotopic tumors. *In vivo* and *ex vivo* BLI of intravenously administered DiR labeled PMTM in athymic mice revealed that PM tended to accumulate in tumor tissues, being the clearance rate of nanoparticles in tumor lower than for other tissues. Fluorescent signal was observed the tumor and in the abdominal area, corresponding to the liver. *Ex vivo* imaging and quantification of the fluorescent signal were performed 24 and 72 h post-injection showing the kinetics of the micelles biodistribution and excretion.

alterations were found by gross necropsy and further histological evaluation (Figure S5).

Finally, we performed *in vivo* efficacy studies using orthotopic breast cancer models. For this, CSCs sorted from the MCF7 luminal breast cancer cell line and from the highly aggressive MDA-MB-231 basal-like breast cancer cell line were used. Cells were injected into mammary fat pad to ensure high CSCs content in the growing tumors. Remarkably though, PM-ZileutonTM significantly reduced almost by two-fold the content of CSCs in the treated tumors compared to non-treated animals, in both orthotopic models (Figure 7, A). CSCs decrease from 58% \pm 9% in vehicle-treated MDA-MB-231 tumors to 37.2% \pm 4.7% in PM-ZileutonTM treated ones, and from 33.43% \pm 3.18% to 17.98% \pm 6.25% in MCF-7 models, respectively. CSCs reduction was conveyed with the eradication of circulating tumor cells (CTC) after PM-ZileutonTM treatment in a metastatic MDA-MB-231 *in vivo* model (Figure 7, B). No CTC was detected in MCF7 *in vivo* model in any case (data not shown). As expected, reduction of CTC in MDA-MB-231 model was

accompanied by a significant reduction of metastasis detected by BLI (Figure 7, C). In contrast, we have not observed differences in tumor growth comparing group of animals treated with vehicle or PM-ZileutonTM (Figure S6).

Discussion

To identify CSC specific targets, in order to design effective anti-CSCs treatment, we performed high throughput screening of breast cancer CSCs. Our microarray results confirm that CSCs derived from luminal MCF7 epithelial cell type are related to the Epithelial to Mesenchymal Transition (EMT) phenotype as it was previously suggested.²⁷ We identified several EMT genes (TGFB2, SNAI2 and SPARC) upregulated in CSCs isolated from MCF7 cell line. Contrarily, these genes were not up-regulated in MDA-MB-231 luminal cell line, most likely, because of the high basal expression of EMT genes in this cell line. In this context, overall data suggest that the EMT pathway

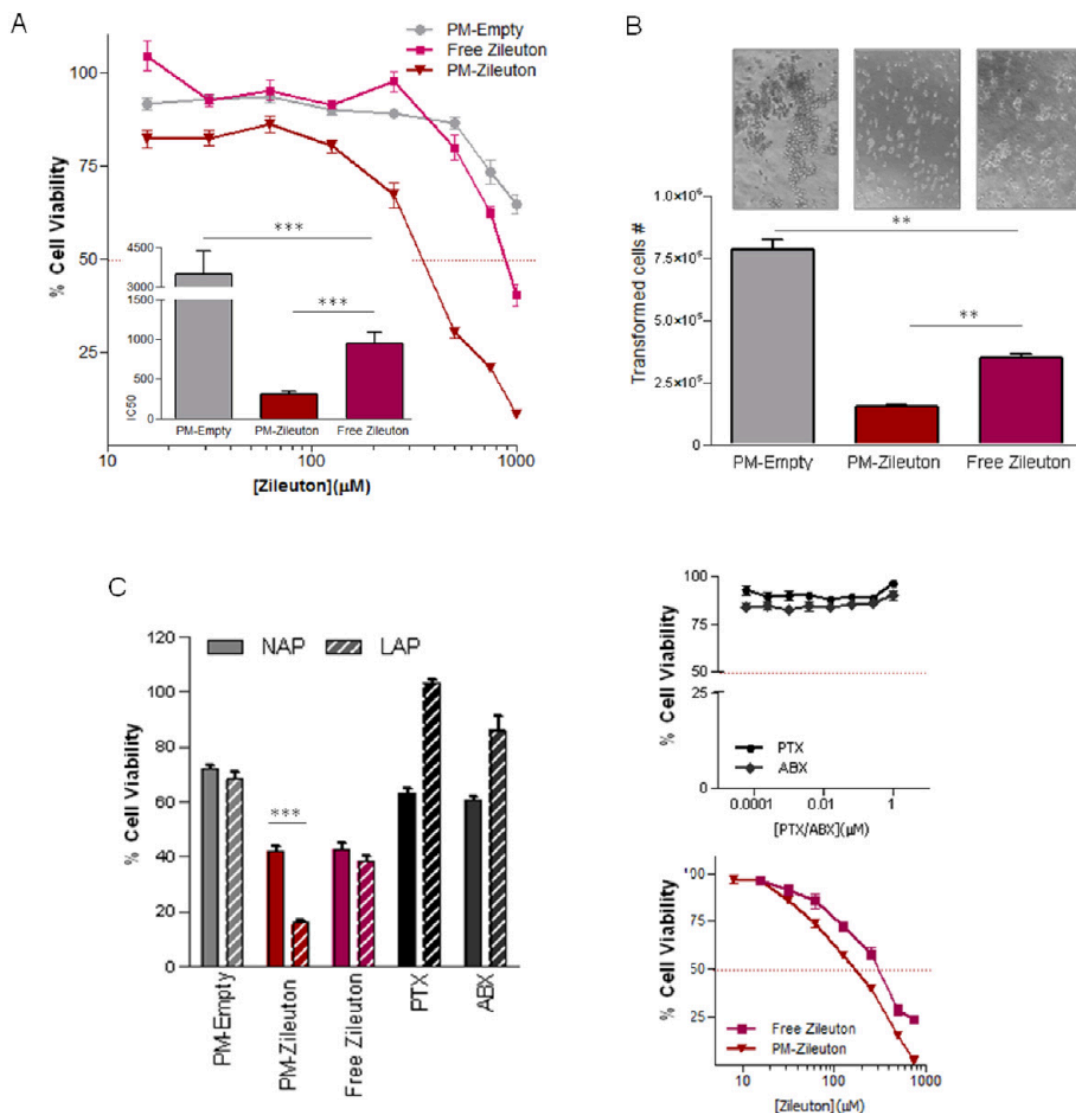


Figure 6. *In vitro* cell viability of breast cancer cell lines treated with PM-ZileutonTM. (A) Cell viability of MDA-MB-231 cell line treated with ZileutonTM and PM-ZileutonTM and with corresponding mass of empty nanoparticles has been determined. IC₅₀ corresponds to the half maximal inhibitory concentration and is indicated by a discontinuous red line. Cells without treatment represent 100% of viability. (B) Cell transformation assay of MDA-MB-231 treated with ZileutonTM and PM-ZileutonTM has been determined. (C) Cells were grown in normal condition (NAP: normal attachment plates) and as mammospheres (LAP: low attachment plates) and treated with ZileutonTM and PM-ZileutonTM, PTX or ABX. IC₅₀ corresponds to the half maximal inhibitory concentration and is indicated by a discontinuous red line. Cells without treatment represent 100% of viability.

may serve for effective targeting of CSCs derived from luminal breast tumors.^{10,27,28} Future high throughput screening might reveal additional CSCs target candidates, because the disparity between the two analyzed cell lines can veil some less pronounced differences in gene expression when comparing CSCs *versus* non-CSCs. Nonetheless, we have found and corroborated ALOX5 overexpression in CSC subpopulations from these two highly distinctive breast cancer cell lines.

It has been reported that Alox5 deficiency resulted in a significant reduction of Leukemic Stem Cells (LSCs) in bone marrow, and thus largely prolonged survival of CML mice.²⁹

Importantly, there was no significant influence of Alox5 deficiency on normal hematopoietic stem cells (HSCs) or on the induction of lymphoid leukemia by BCR-ABL.¹² Besides, ALOX5 is largely known as an oncogene in solid tumors, *e.g.* prostate cancer and pancreas cancer.^{30–32} On the molecular level, the inhibition of Alox5 was linked to upregulation of the tumor suppressor gene, Msr1, and consequent regulation of PI3K-AKT-GSK-3 β and β -Catenin pathways (19). In this study we have further confirmed ALOX5 overexpression in a large battery of TNBC breast cancer cell lines cultured as mammospheres, in order to mimic CSCs growth. Further, clinical data confirmed its

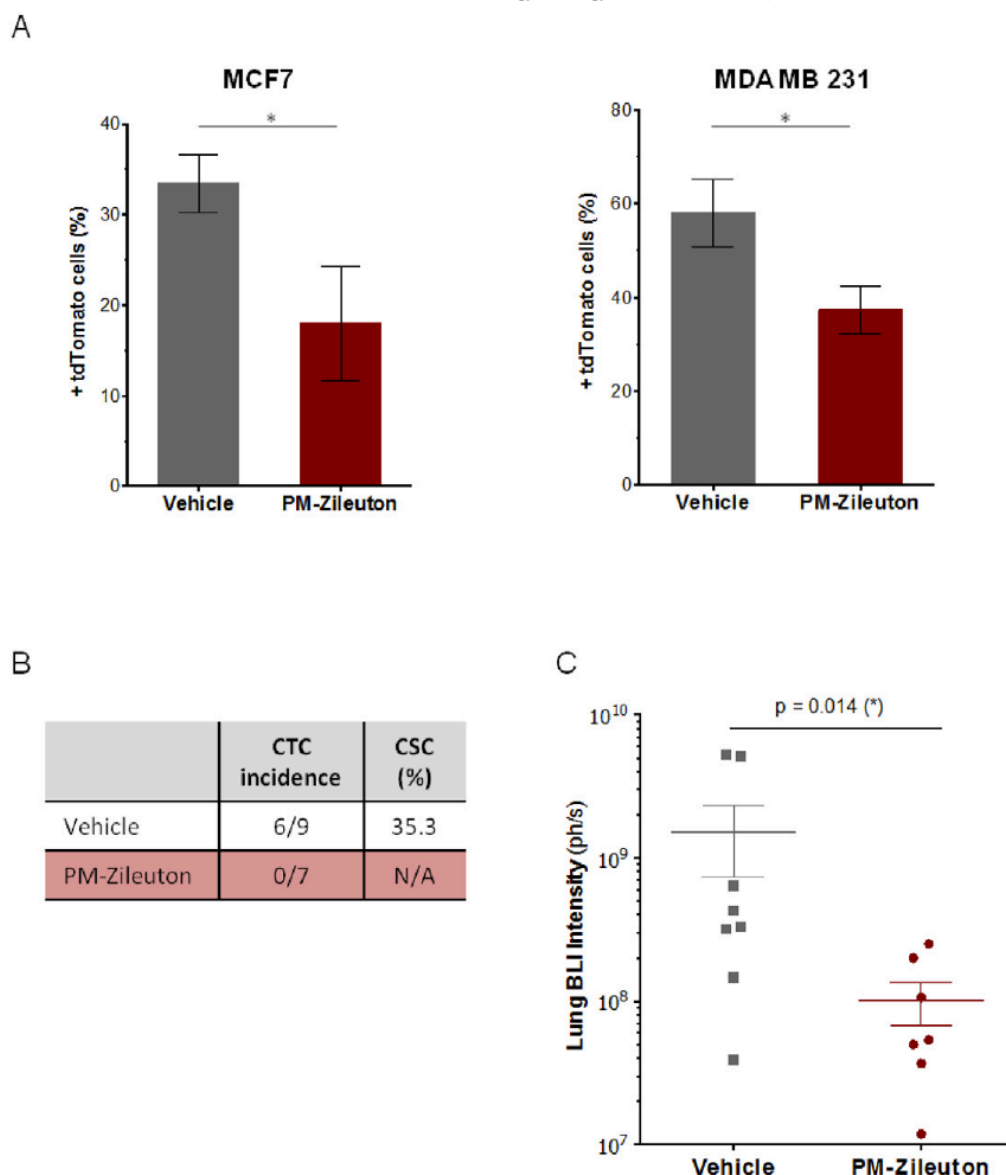


Figure 7. Effects of PM-Zileuton™ on CSC and CTC *in vivo*. Orthotopic breast cancer models were generated using tdTomato+ MDA-MB-231 cells. A posteriori, animals were then treated with i.v. administration of PM-Zileuton™ (15 mg/kg), 3 times per week during 3 weeks and blood and tumor samples were collected for the analysis of CSC content. Also lung metastasis *ex vivo* bioluminescent imaging (BLI) was performed using the IVIS Spectrum after administering 150 mg/kg of luciferin to mice. (A) *In vivo* effects of PM-Zileuton™ in CSC content in mice tumors; (B) *In vivo* effects of PM-Zileuton™ in CTC and CSC in the blood stream in tumor bearing mice; (C) *In vivo* effects of PM-Zileuton™ in lung metastasis.

overexpression in 86% of human breast tumors even though its overexpression was not significantly confined to any clinical feature, or any specific cancer stage. Our data suggest a potential role of Alox5 in CSC homeostasis in tumorigenesis.

Fortunately, Zileuton™, a specific inhibitor of ALOX5, is approved by the FDA for treating asthma.^{14,15} Studies with Zileuton™ as anti-cancer agent are undergoing. Zileuton™ (Zyflo®) is in clinical trial (phase 1) in combination with Dasatinib (Sprycel®) (NCT02047149) and with Imatinib Mesylate (Gleevec) (NCT01130688), respectively, in patients with CML. Zileuton™ (Zyflo®) is also being investigated for lung cancer chemoprevention

(currently in phase 2), with the aim to prevent lung cancer in patients with bronchial dysplasia (NCT00056004).

We have confirmed the effectiveness of its inhibition against CSCs population in various *in vitro* assays. Interestingly, Zileuton™ shows much better IC₅₀ score in low attachment conditions, where just CSCs can proliferate because of their capacity to survive in non-adherent conditions, a clear feature of stemness. Of note, ALOX5 expression is also significantly increased during these conditions. This might suggest a potential functional role of Alox5 in non-attached cells where its inhibition causes greater effect in CSC than in normal adherent culture

conditions. This further confirms the feasibility of targeting CSCs by using Zileuton™. In agreement to this, we also confirmed the anti-CSCs effects of Zileuton™ by using transformation assays in soft agar, one of the hallmarks of CSCs.

Nonetheless, Zileuton™ efficacy dose is considerably high in terms of future clinical use. Moreover, because of its highly hydrophobicity, Zileuton™ also needs to be solubilized for i.v. administration. Here, we used versatile amphiphilic polymer, Pluronic® F127 to encapsulate Zileuton™. It is an FDA approved biodegradable polymer with known characteristics and proved advantages for synthesis of drug delivery systems, and its usefulness has been demonstrated previously in various drug delivery systems.^{10,11,24}

We employed a thin-film hydration technique to synthesize polymeric micelles with Zileuton™ encapsulated in their hydrophobic inner core. Importantly, due to their stability and the possibility of lyophilization, PM-Zileuton™ are easily scalable for future Good Manufacturing Practice (GMP) production in order to facilitate posterior translation and clinical implementation.

Furthermore, we do not observe any toxicity *in vivo* when using the maximal feasible dose (MFD) (15 kg/mg). This dose was calculated based on maximal encapsulation dose and volume that can be injected per mice. The biodistribution assay performed with DiR labeled PM in tumor bearing mice shows very good accumulation of PM within the tumor. On the other hand, fluorescent signals in plasma, kidneys, lungs and muscle clearly diminish between 24 and 72 h, indicating that micelles are cleared out from these organs.

As expected, CSCs population is significantly decreased in both CSCs orthotopic models after PM-Zileuton™ treatment and importantly, in the highly metastatic MDA-MB-231 cell line we observe a complete eradication of CTCs in the blood stream. Because CTCs and particularly, the fraction of CSCs within them are thought to be responsible for metastatic spread, we hypothesized an effect of PM-Zileuton™ treatment on tumor dissemination. Our data confirms that metastatic foci from MDA-MB-231 in our orthotopic *in vivo* model are significantly smaller after PM-Zileuton™ treatment suggesting a clear potential use of PM-Zileuton™ as anti-metastatic agent. This further suggests that PM-Zileuton™ could show synergistic efficacy in combination with current cytotoxic treatments, which might be highly relevant to improve current *Standard-of-Care* therapies. Of note, therapies seeking for the elimination of CSCs in order to prevent tumor growth and the appearance of metastases have an important limitation. Eliminated CSCs are constantly replaced by new cells with stemness phenotype by a process of de-differentiation (so call reversion) of non-CSC in order to ensure tumor survival and propagation after treatment. As a result, CSCs specific treatments have just limited clinical success, so far. We thus propose to evaluate the combination of PM-Zileuton™ and *Standard-of-Care* treatments (*i.e.*, Abraxane™ (Nab-PTX) nanoparticles), used in the clinical setting. This cocktail may represent an ideal option to abrogate tumor and metastatic growth, along with avoiding CSC reversion.

Appendix A. Supplementary data

Supplementary data to this article can be found online at <https://doi.org/10.1016/j.nano.2019.102106>.

References

- Li R, Zhang K, Siegal GP, Wei S. Clinicopathological factors associated with survival in patients with breast cancer brain metastasis. *Hum Pathol* 2017 Jun;64:53–60.
- Shen T, Gao C, Zhang K, Siegal GP, Wei S. Prognostic outcomes in advanced breast cancer: the metastasis-free interval is important. *Hum Pathol* 2017 Dec;70:70–6.
- Lee G, Hall RR, Ahmed AU. Cancer stem cells: cellular plasticity, niche, and its Clinical Relevance *J Stem Cell Res Ther* 2016 Oct;6(10).
- Gener P, Rafael DF, Fernandez Y, Ortega JS, Arango D, Abasolo I, et al. Cancer stem cells and personalized cancer nanomedicine. *Nanomedicine (Lond)* 11: 307–320.
- Dean M, Fojo T, Bates S. Tumour stem cells and drug resistance. *Nat Rev Cancer* 5: 275–284.
- Shen S, Xia JX, Wang J. Nanomedicine-mediated cancer stem cell therapy. *Biomaterials* 74: 1–18.
- Vinogradov S, Wei X. Cancer stem cells and drug resistance: the potential of nanomedicine. *Nanomedicine (Lond)* 7: 597–615.
- Gener P, Gouveia LP, Sabat GR, Sousa Rafael DF, Fort NB, et al. Fluorescent CSC models evidence that targeted nanomedicines improve treatment sensitivity of breast and colon cancer stem cells. *Nanomedicine* 2015 Nov;11(8):1883–92.
- Gener P, Rafael D, Seras-Franzoso J, Perez A, Pindado LA, Casas G, et al. Pivotal role of AKT2 during dynamic phenotypic change of breast cancer stem cells. *Cancers (Basel)* 2019 Jul 26;11(8), <https://doi.org/10.3390/cancers11081058> (pii: E1058).
- Rafael D, Martínez F, Andrade F, Seras-Franzoso J, García-Aranda N, Gener P, et al. Efficient EGFR mediated siRNA delivery to breast cancer cells by cetuximab functionalized Pluronic® F127/Gelatin. *Chem Eng J* 2018;340:81–93.
- Rafael D, Gener P, Andrade F, Seras-Franzoso J, Montero S, Fernandez Y, et al. AKT2 siRNA delivery with amphiphilic-based polymeric micelles show efficacy against cancer stem cells. *Drug Deliv* 2018 Nov;25(1):961–72.
- Chen Y, Li DF, Li S, Chen Y, Hu YF, Zhang HF, et al. The Alox5 gene is a novel therapeutic target in cancer stem cells of chronic myeloid leukemia. *Cell Cycle* 2009 Nov 1;8(21):3488–92.
- Rafael D, Andrade F, Montero S, Gener P, Seras-Franzoso J, Martínez F, et al. Rational design of a siRNA delivery system: ALOX5 and cancer stem cells as therapeutic targets. *Prec Nanomed* 2: 86–105.
- Carter GW, Young PR FAU, Albert DH FAU, Bouska JF, Dyer RF, Bell RL et al. 5-lipoxygenase inhibitory activity of zileuton. *J Pharmacol Exp Ther* 1991 Mar;256(3):929–37.
- Poff CD, Balazy M. Drugs that target lipoxygenases and leukotrienes as emerging therapies for asthma and cancer. *Curr Drug Targets Inflamm Allergy* 2004 Mar;3(1):19–33.
- Ritchie ME, Silver JF, Oshlack AF, Holmes MF, Diyagama DF, Holloway AF, et al. A comparison of background correction methods for two-colour microarrays. *Bioinformatics* 2007 Oct 15;23(20):2700–7.
- Parrish RS, Spencer HJ. Effect of normalization on significance testing for oligonucleotide microarrays. *J Biopharm Stat* 2004 Aug;14(3):575–89.
- Smyth GK. Linear models and empirical bayes methods for assessing differential expression in microarray experiments. *Stat Appl Genet Mol Biol* 2004;3(5523):5541.
- Liang K. False discovery rate estimation for large-scale homogeneous discrete p-values. *Biometrics* 2016 Jun;72(2):639–48.

20. Chen Y, Sullivan C, Peng C, Shan Y, Hu Y, Li D, et al. A tumor suppressor function of the Msr1 gene in leukemia stem cells of chronic myeloid leukemia. *Blood* 2011 Jul 14;118(2):390-400.
21. Mendez O, Peg VA, Salvans C, Pujals M, Fernandez Y, Abasolo I, et al. Extracellular HMGA1 promotes tumor invasion and metastasis in triple-negative breast cancer. *Clin Cancer Res* 2018 Dec 15;24(24):6367-82.
22. Zong Y, Wu J, Shen K. Nanoparticle albumin-bound paclitaxel as neoadjuvant chemotherapy of breast cancer: a systematic review and meta-analysis. *Oncotarget* 2017 Mar 7;8(10):17360–17372 doi: 10.18632/oncotarget.14477 -17372.
23. Schettini F, Giuliano M, De PS, Arpino G. Nab-paclitaxel for the treatment of triple-negative breast cancer: rationale. *clinical data and future perspectives Cancer Treat Rev* 2016 Nov;50:129-41.
24. Andrade F, Fonte P, Costa A, Reis CC, Nunes R, Almeida A, et al. Pharmacological and toxicological assessment of innovative self-assembled polymeric micelles as powders for insulin pulmonary delivery. *Nanomedicine (Lond)* 2016 Sep;11(17):2305-17.
25. Andrade F, Fonte P, Oliva M, Videira M, Ferreira D, Sarmiento B. Solid state formulations composed by amphiphilic polymers for delivery of proteins: characterization and stability. *Int J Pharm* 2015;486(1–2):195-206.
26. Andrade F, das NJ, Gener P, – Schwartz S Jr, Ferreira D, Oliva M, Sarmiento B. Biological assessment of self-assembled polymeric micelles for pulmonary administration of insulin. *Nanomedicine* 2015 Oct;11(7):1621-31.
27. Gener P, Seras-Franzoso J, Gonzales Callego P, Andrade F, Rafael D, et al. Dynamism, sensitivity, and consequences of mesenchymal and stem-like phenotype of cancer cells. *Stem Cells International* 2018 Oct 10;4516:4524.
28. Rafael D, Doktorovova S, Florindo H, Gener P, Abasolo I, Schwartz Jr S, et al. EMT blockage strategies: targeting Akt dependent mechanisms for breast cancer metastatic behaviour modulation. *Curr Gene Ther* 2015;15(3):300-12.
29. Chen Y, Hu Y, Zhang H, Peng C, Li S. Loss of the Alox5 gene impairs leukemia stem cells and prevents chronic myeloid leukemia. *Nat Genet* 41: 783–792.
30. Sarveswaran S, Chakraborty D, Chitale D, Sears R, Ghosh J. Inhibition of 5-lipoxygenase selectively triggers disruption of c-Myc signaling in prostate cancer cells. *J Biol Chem* 2015 Feb 20;290(8):4994-5006.
31. Sarveswaran S, Thamilselvan VF, Brodie CF, Ghosh J. Inhibition of 5-lipoxygenase triggers apoptosis in prostate cancer cells via down-regulation of protein kinase C-epsilon. *Biochim Biophys Acta* 2011 Dec;1813(12):2108-17.
32. Zhou GX, Ding XL, Wu SB, Zhang HF, Cao W, Qu LS, et al. Inhibition of 5-lipoxygenase triggers apoptosis in pancreatic cancer cells. *Oncol Rep* 2015 Feb;33(2):661-8.

Supplementary information:

Supplementary information about material and methods:

Cell lines and culture conditions

Breast cancer MDA-MB-231 and MCF7 cell lines were obtained from American Type Culture Collection (ATCC). Cells were cultured in RPMI medium (ThermoFisher Scientific) supplemented with 10% of Fetal Bovine Serum (FBS) (Lonza), 1% of antibiotic-antimitotic mixture, 1% of Non-Essential Amino Acids (NEAA) and 1% of sodium pyruvate (ThermoFisher Scientific). In addition, 5 mg/ml of blasticidin (ThermoFisher Scientific) was used for selection.

Both cell lines were also cultured in low attachment conditions, as mammospheres, in serum-free media. This medium consisted of RPMI (1640) supplemented with 30% of glucose (Sigma), 1% L-GlutaMAX (Sigma), 1% penicillin-streptomycin (ThermoFisher Scientific), 100 mg/ml Heparin (Sigma), 2 g/l of Bovine Serum Albumin (BSA) (Sigma-Aldrich), 20 µg/ml of human recombinant EGF (Sigma-Aldrich), 10 µg/ml of human recombinant bFGF (BD Bioscience) and 10% of Hormone Mix (Glucocorticoids, Putrescine, Apo-transferrin, Insulin, Selenium, Progesterone). Cells cultured were seeded in Ultra-Low attachment surface plates (Corning).

Quantitative (qPCR)

The cDNA reverse transcription product was amplified with specific primers, which were tested for specificity and efficacy (Table S1) using SYBR Green method (ThermoFisher Scientific). β -ACTIN together with GAPDH were used as endogenous controls. Relative normalized quantities (NRQ) of mRNA expression were calculated by the comparative Ct method ($2^{-\Delta\Delta Ct}$) using qBase software (353). At least three biological replicates, each involving at least two technical replicates were involved in final results expressed as the mean \pm SEM. Some of the original candidates could not be validated by QPCR because their primers didn't conquer the validation test. This was the case for PGC (Progastricsin (Pepsinogen C)), HLA-DRB5 (Major Histocompatibility Complex, Class II, DR Beta 5), IL10RA (Interleukin 10 Receptor, alpha), GRM5 (Glutamate Receptor, metabotropic 5), TLR2 (Toll-like Receptor 2) and GATA4 (GATA binding protein 4).

ALOX5 protein detection by flow cytometry

ALOX5 protein expression was quantified by flow cytometry using Fortessa instrument (BD Biosciences). Equal amount of MDA-MB-231 cells grown in the attachment or as mammospheres was trypsinised, centrifuged (1,200 rpm, 5 min, 4°C) and fixed in 100 µl of 2 % formaldehyde for 10 min at room temperature. The pellet was washed with PBS-BSA. Cells were then resuspended in 75 µl of blocking solution (Human Ig 200 µg/mL PBS) for 15 min at room temperature. 1/50 dilution of 5-LO (33) (Santa cruz Biotechnology, sc-136195) antibody were added. 45 min after incubation at 4°C out from light. Samples incubated only with secondary antibody were used as negative control. For each sample, at least 10000 individual cells were collected and the mean fluorescence intensity was evaluated.

Production and physicochemical characterization of PMs for Zileuton delivery

First, amphiphilic polymer, Pluronic® F127 was diluted in an ethanol:methanol (1:1) mixture and ZileutonTM was added. Then, the solvent was removed under vacuum in a rotary evaporator (bath temperature 60°C, 200 rpm). The resulting thin-film was rehydrated with PBS and vortexed during 5 minutes at full speed. The obtained product was filtered through a 0.22µm syringe filter to sterilize the final formulation. PMs' mean hydrodynamic diameter and polydispersity index (Pdi) were measured by Dynamic Light Scattering (Malvern Instruments). All samples were diluted 1:5 in PBS, pH 7.4, in order to obtain an adequate nanoparticle concentration. Data reported from each type of formulation are mean values, which were measured at least in triplicate.

The morphology of PMs was observed by Transmission Electron Microscopy (TEM) and Cryo-Transmission Electron Microscopy (Cryo-TEM). For TEM, a drop of sample was placed on a carbon 400-mesh copper grid, treated with uranyl acetate and then assessed in a JEM-1400 Electron Microscope (JEOL Ltd., Tokyo, Japan) with an applied voltage of 120kV. For Cryo-TE, a drop of the sample was deposited onto the grid. Subsequently, the aqueous suspension of PMs was immediately vitrified by rapid immersion in liquid ethane. Images were obtained using a Jeol JEM 2011 cryo-electron microscope operating at 200kV, under low-dose conditions and using different defocus degrees (500-900 nm) in order to obtain an adequate phase contrast.

Cell viability assay: In order to analyze the cytotoxic effect of ZileutonTM we calculated the half maximal inhibitory concentration (IC₅₀) and viability curves. Serial dilutions of ZileutonTM (free and encapsulated) were added to cells growing in adhesion or as

mammospheres for 24-72h, depending on experiment requirements. A corresponding mass of empty nanoparticles has been used as negative control in each assay. In addition, combinatory treatment; ZileutonTM (free and encapsulated) with 0.1 μ M Paclitaxel and 0.1 μ M Abraxane for MDA-MB-231 has been applied. Viable cells were identified by using 3-(4,5-dimethylthiazol-2-yl)-2,5-diphenyltetrazolium bromide (MTT) or PrestoBlue (ThermoFisher Scientific), and respective absorbance acquired. At least 6 technical and 3 biological replicates were used.

Cancer stem cells resistance assay: In order to assess the therapeutic effect of ZileutonTM, Paclitaxel and Abraxane[®] (Nab-PTX), different amount of cells were seeded (1.10^5 cells for the controls and 3.10^5 cells for treated ones) and left 24h to allow adhesion. Cells were treated with the concentration corresponding to the IC₅₀ of the respective drugs (500/300 μ M Zileuton, 1/0.1 μ M Paclitaxel and 1/0.1 μ M Abraxane for MDA-MB-231 / MCF7 cells, respectively) for 72h. Afterwards, cells were let to recover in drug free complete medium for 48h. We evaluated the relative abundance of CSCs before and after the treatment by flow cytometry, using Fortessa (BD Bioscience). Cell viability and cell proliferation were controlled along the experiment in order to ensure the equal therapeutic effect of the tested drugs. For each replicate, at least 10.000 individual cells were collected and the mean fluorescence intensity was evaluated.

Cell Transformation Assay (Anchorage-Independent Growth Assay): Anchorage independent growth of breast cancer cell lines was assessed by CytoSelectTM Cell Transformation Assay Kit (Cell Biolabs). A semisolid agar media was prepared according to the manufacturer instructions prior addition of the proper inhibitor to each well; assessing each sample in triplicate. After 6-8 days of incubation, colonies were observed under optical microscopy and viable transformed cells were counted using trypan blue.

Entrapment efficiency determination: PMs loading ZileutonTM were filtered through centrifugation for 10 minutes at 12000 rpm using Nanosep 100k devices (Pall Corporation). The amount of free drug (unloaded drug) was determined from the obtained filtrate with a Waters Acquity Ultra Performance Liquid Chromatography (UPLC) coupled with a Waters Xevo TQ MS triple quadrupole mass spectrometer. Separation was achieved on an Acquity UPLC HSS C18 column (2.1 \times 100 mm, 1.8 μ m particle size). A gradient elution program was conducted for chromatographic separation with mobile phase A (0.1% Formic Acid in Acetonitrile) and mobile phase B (0.1% Formic Acid in water) as follows: 0–2 min (30% A–70% B), 2–3 min (95% A–5% B), 3.0–3.5 min

(30% A–70% B), and 3.5–4.5 min (30% A–70% B). The flow rate was 0.300 mL/min. The overall run time was 4.5 min. The autosampler was at room temperature. The injection volume of sample was 5 μ L. The mass spectrometer was operated using an electrospray source in positive mode. The ZileutonTM MRM transition was m/z 237 \rightarrow 127.9. The system control and data analysis were carried out using MassLynx software (Version 4.1) and processed using TargetLynxTM program.

PMs stability

Three independent assays regarding PM stability were performed: a) storage stability, b) serum stability and c) post-lyophilization stability.

a) PMs were stored at room-temperature for 30 and 60 days and the size analyzed by DLS.

b) In order to study the stability of formulations in the presence of serum and predict their aggregation pattern *in vivo*, medium containing a concentration of 50% FBS to simulate blood conditions, was prepared and incubated with the micelles. Samples were collected at different time-points (0, 4, 6, 12 and 24 hours) and measured by DLS.

c) After production, PMs were lyophilized in a Virtis BenchTop Freeze Dryer (SP Scientific, USA) in order to study their efficacy after this process. Briefly, PMs were produced with 5% of mannitol as a cryoprotectant and immediately frozen in liquid nitrogen. Then, the primary drying was set overnight at room temperature and under vacuum conditions (40 μ bar). Finally, obtained powder was rehydrated in sterile water to obtain the PMs formulation.

Internalization Assay: To assess the internalization behavior of PMs in MDA-MB-231 cell line, a fluorescent tag (5-DTAF) was conjugated with the amphiphilic polymer as previously reported [9,10]. Briefly, 2×10^5 cells / 100 μ L were seeded in complete RPMI medium in 96-well plates and left to attach for 24h. Micelles were added to cells at different time points: 1, 3, 10, 30 minutes and, 1, 4, 6 and 24 hours. Then, cells were washed with 1x PBS, trypsinized and resuspended in PBS-FBS (10%) with DAPI (1 μ g/ml), used for vital staining. Only cells alive (DAPI negative cells) were admitted for the analysis, while cell debris or possible aggregates were removed by forward and side scatter gating. The plate was read using the cytometer Fortessa (BD Biosciences) and data was analyzed with FCS Express 4 Flow Research Edition software (De Novo Software).

Animals

Female immunodeficient athymic (Hsd:Athymic Nude-Foxn1, Envigo, Spain) and NOD-SCID (NOD.CB17-Prkdcscid/J, Charles River Laboratories, Spain or NOD.CB-17-Prkdcscid/Rj from Janvier Laboratories Le Genest-Saint-Isle, France) mice were kept in pathogen-free conditions and used at 7 weeks of age. Animal care was handled in accordance with the Guide for the Care and Use of Laboratory Animals of the Vall d'Hebron University Hospital Animal Facility, and the Animal Experimentation Ethical Committee at the institution approved the experimental procedures. All the *in vivo* studies were performed by the ICTS "NANBIOSIS" of CIBER-BBN's *In Vivo* Experimental Platform of the Functional Validation & Preclinical Research (FVPR) area (CIBBIM-Nanomedicine, Barcelona, Spain).

Quantification of CSCs and CTCs present in tumor and blood samples

At the end point of *in vivo* experiments, tumors were excised, weighted, and divided into several fragments for FACS analyses. Tumor tissue was digested using cocktail of Collagenase I and DNase 1 and homogenized to single cell suspension. In addition, blood samples were drawn from each animal by cardiac puncture. Whole blood was transferred directly into commercial EDTA containing tubes and processed immediately to isolate circulating tumor cells (CTC). Briefly, blood samples were subjected to several cycles of hemolysis using mixture of 90% of 16 M NH₄Cl and 10% of 0.17 M Tris (pH 7.65) and centrifuged. White blood cell pellets and disintegrated tumor tissue were resuspended in phosphate buffered saline (PBS; Lonza, Porriño, Spain), supplemented with 10% Fetal Bovine Serum (FBS). DAPI (1 µg/mL, Life Technologies) was used for vital staining (Life Technologies). Cells were examined for tdTomato and DAPI expression in a by flow cytometry (Fortessa, BD Biosciences, CA, USA). Data were analyzed with FCS Express 4 Flow Research Edition software (De Novo Software,).

Statistical analysis

All data are represented as the mean value \pm SEM, standard error of the mean. Unpaired Student's t-test was used to determine p-values. Differences were regarded as statistically significant when p-value was smaller than 0.05 (*), 0.01 (**) and 0.001 (***). All the analyses and graphs were performed using GraphPad Prism 6 software.

Table S1: List of primers used for qPCR

Name	Sequence (5' to 3')	Name	Sequence (5' to 3')
ALOX5 F01	AGAACCTGGCCAACAAGATTGT	LIPA F01	CCTCATGGGAGGAAGAACCA
ALOX5 R01	TCTGGTGGACGTGGAAGTCA	LIPA R01	CCACACGTCAAAACCAGCAT
BST2 F01	AAGGGCTTTCAGGATGTGGA	IL10RA F01	CCTCTGGAGAAGTGGGAGAGTTC
BST2 R01	CGCGTCCTGAAGCTTATGGT	IL10RA R01	GGACAAAGGCAAAGAAGATGATG
CMKLR1 F01	GGAGCCTGTGATTGGCAGAA	HLA-DRB1 F01	GAGTACTGGAACAGCCAGAAGGA
CMKLR1 R01	CAGCCAATCAGTCCCTGTACAC	HLA-DRB1 R01	GGGCTGGGTCTTTGAAGGAT
EPHA4 F01	ACCTGTGACCGAGGCTTTTTTC	PTPRE F01	GTCAGCACCAGCGACAAGAA
EPHA4 R01	GCGGCCACCTGTATTCTGA	PTPRE R01	TCGTCGGCGGATCTGATAC
TLR2 F01	GATGCCTGGCCCTCTCTACA	TGFB2 F01	CGTCTCAGCAATGGAGAAGAATG
TLR2 R01	CTGACAAGTTTCAGGCATAGAATGA	TGFB2 R01	CGCTGGGTTGGAGATGTAAAA
GATA4 F01	CCGACACCCCAATCTCGATA	SNAI2 F01	GGCTGGCCAAACATAAGCA
GATA4 R01	ATGCCGTTTCATCTTGTGGTAGA	SNAI2 R01	GCTTCTCCCCCGTGTGAGT
GRM5 F01	GTTTCCACAGGAGAACAGCAAAT	SNAI1 F01	ATGCCGCGCTCTTTCCT
GRM5 R01	CAGAGGGACATCTGCATGTTGT	SNAI1 R01	GCTGGAAGGTAACTCTGGATTAGA
GRM5 F02	ACTCTCCAGGAAGGTATGAAATAATGA	SPARC F01	TCGGGCCTTGCAAATACATC
GRM5 R02	ATTTTAAATTCTCCATTGTCCCACT	SPARC R01	GGTGACCAGGACGTTCTTGAG
EGR4 F01	CCTGGAGCAGGCGACTTCT	GAPDH F	ACCCACTCCTCCACCTTTGAC
EGR4 R01	AGGAAGCAGGAGTCGGCTAAG	GAPDH R	CATACCAGGAAATGAGCTTGACAA
PGC F01	CTCTTCCTCTGTGGCCAGTTG	ACT 01F	CATCCACGAAACTACCTTCAACTCC
PGC R01	CAGCAAGCCCTTCTCCTTCA	ACT 01R	GAGCCGCCGATCCACAC
PGC F02	CCCAGCAGTACATGAGTGCTCTT		
PGC R02	GGCAGATTCTGAATGCTGTTACA		

Figure S1: Sample clustering of CSC from breast cancer cell lines

(A) Correlation-based clustering of samples using 25623 probes with SD/mean > 0,5;
 (B) Expression microarray analysis comparing mesenchymal, epithelial and stemness genes expression.

Log2[nt_MDA231_CSC 01]	Log2[nt_MDA231_CSC 02]	Log2[nt_MCF7_CSC 01]	Log2[nt_MCF7_CSC 02]	Log2[nt_MDA231_nonCSC 01]	Log2[nt_MDA231_nonCSC 02]	Log2[nt_MCF7_nonCSC 01]	Log2[nt_MCF7_nonCSC 02]	log2ratio_CSC vz. nonCSC	log2ratio_MDA231 vz. MCF7	GeneName	FC_CSC vz. nonCSC	P.Value_CSC vz. nonCSC	FC_MDA231 vz. MCF7	P.Value_MDA231 vz. MCF7	
										CD24	-1.11	0.86	-30.10	0.00	Mesenchymal markers
										KRT6B	-1.80	0.13	-4.66	0.01	
										KRT8	-1.26	0.42	-4.80	0.00	
										KRT18	-1.10	0.82	-10.14	0.00	
										CDH1	-1.05	0.96	-803.06	0.00	
										VIM	-1.06	0.96	1324.89	0.00	
										CD44	-1.22	0.33	2.81	0.00	CSC markers
										SERPINE	1.05	0.91	9.11	0.00	
										ESAM	-1.01	0.97	12.94	0.00	
										SERPINE	-1.05	0.93	22.90	0.00	
										KLF5	1.20	0.08	1.12	0.56	
										DUSP6	1.20	0.79	56.58	0.00	
										ITGB2	1.60	0.16	5.78	0.00	CSC markers
										ALDH1A1	-1.09	0.28	-1.06	0.65	
										SOX9	1.22	0.30	1.95	0.02	
										NOTCH2	1.03	0.78	1.85	0.00	
										NOTCH4	1.80	0.32	1.58	0.60	
										MUC16	1.26	0.22	-1.30	0.39	
										SOX2	1.25	0.56	-7.65	0.00	CSC markers
										GRHL2	1.98	0.24	-9.15	0.01	

Figure S2: *In vitro* cell viability of breast cancer cell lines treated with Zileuton™

Cell viability (MTT) assay for MCF-7 and MDA-MB-231 “bulk” cells treated with Zileuton™. IC₅₀ corresponds to the half maximal inhibitory concentration and is indicated by a discontinuous red line.

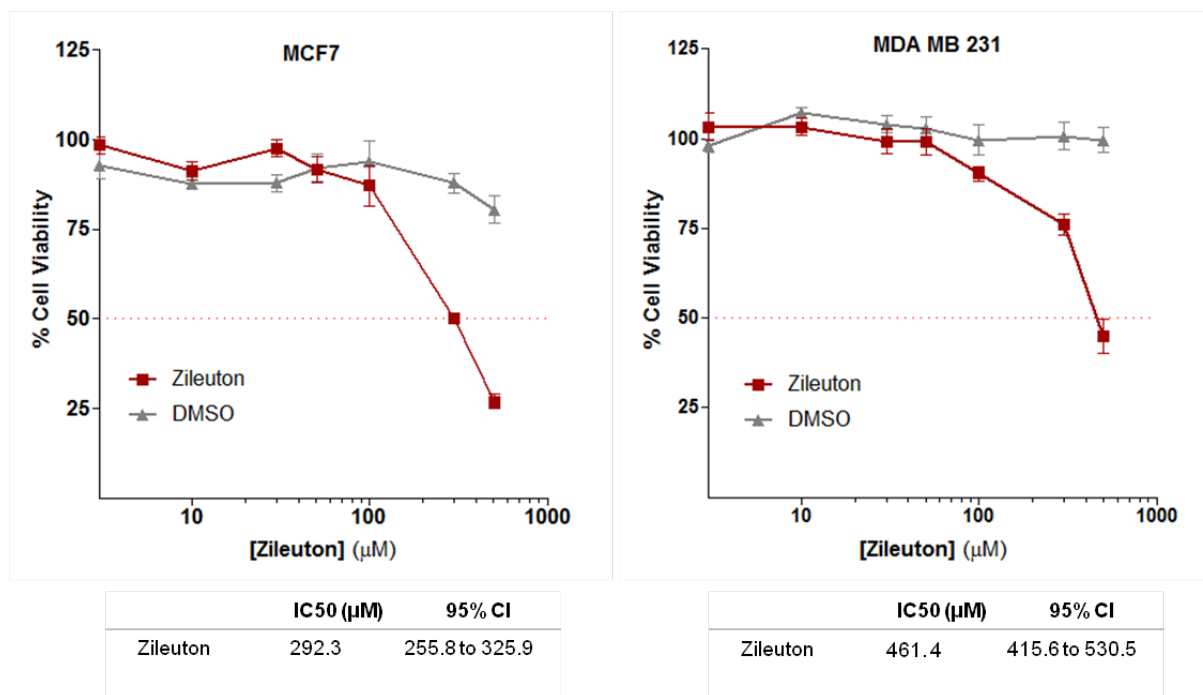
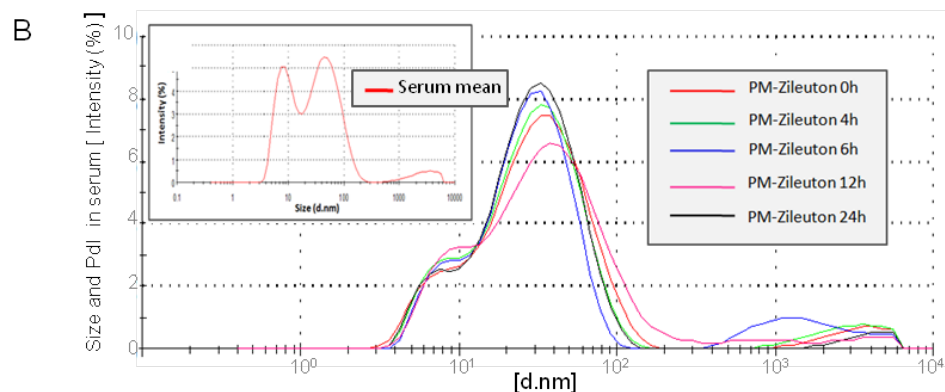
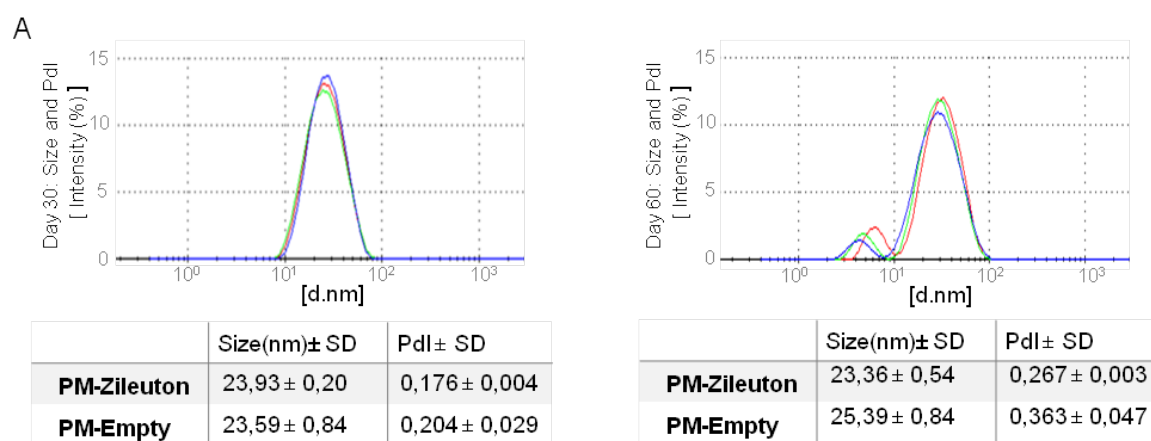


Figure S3: Stability of polymeric micelles

(A) Stability over time: DLS size distributions by intensity with Z-average and Pdl values of micelles stored in PBS solution at room temperature during one month and two months. **(B)** Stability in serum: PMs were mixed (1:1) with medium-FBS 50% and incubated up to 24 h. All solutions were diluted 1:5, with sterile water, before each DLS measurement. (Small peak = nanoparticles < 20nm; medium peak = nanoparticles 20-100nm; big peak = nanoparticles > 100nm).



Sample	Z-Average	Pdl	small peak		medium peak		big peak	
(mean, n=3)	d.nm		d.nm	%	d.nm	%	d.nm	%
Serum only	19,31	0,481	9,88	38	55,66	57,3	2917	4,8
PM Zil. 0 h	23,43	0,410	N/A	N/A	35,3	94,6	3331	5,4
PM Zil. 4 h	22,78	0,399	N/A	N/A	32,22	93,3	3120	6,7
PM Zil. 6 h	23,29	0,429	N/A	N/A	29,14	88,2	1913	11,8
PM Zil. 12 h	24,4	0,449	N/A	N/A	43,78	94,9	3531	2,6
PM Zil. 24 h	21,9	0,387	6,732	11	34,66	86	3932	2,9

Figure S4: Assessment of synergic effect

Results of cell viability assay after 48h of combined treatment. MDA-MB-231 CSCs (tdTomato+ cells) were grown in both low attachment conditions (LAP) and normal attachment conditions (NAP). Cells without treatment represented 100% of viability. **(A)** Zileuton™ **(B)** Zileuton™ combined with Paclitaxel; **(C)** Zileuton™ combined with Abraxane. Significant results with p-value ≤ 0.001 are marked with ***.

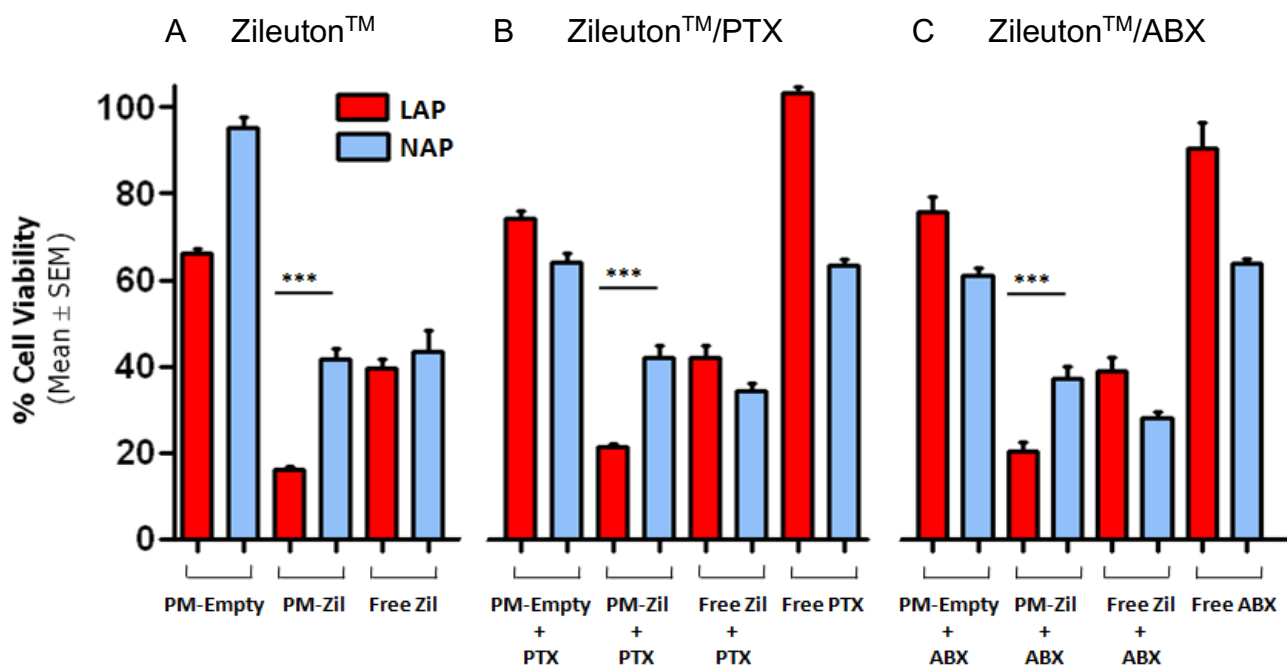


Figure S5: Body weight monitoring during treatment

The graph presents the body weight variation of animals up to 19 days post-injection (tail vein) of vehicle (PBS) and PM-Zileuton™ (15 mg/kg). Arrows in the figure are showing the different time-points of injection.

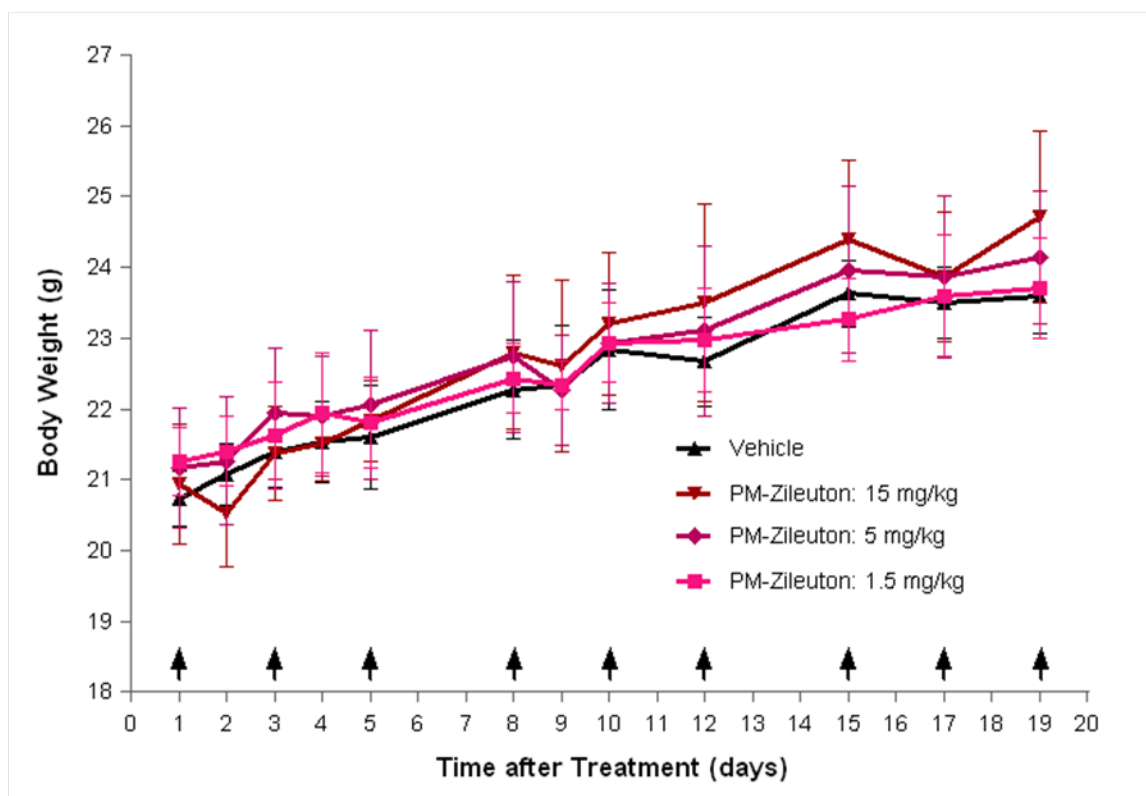
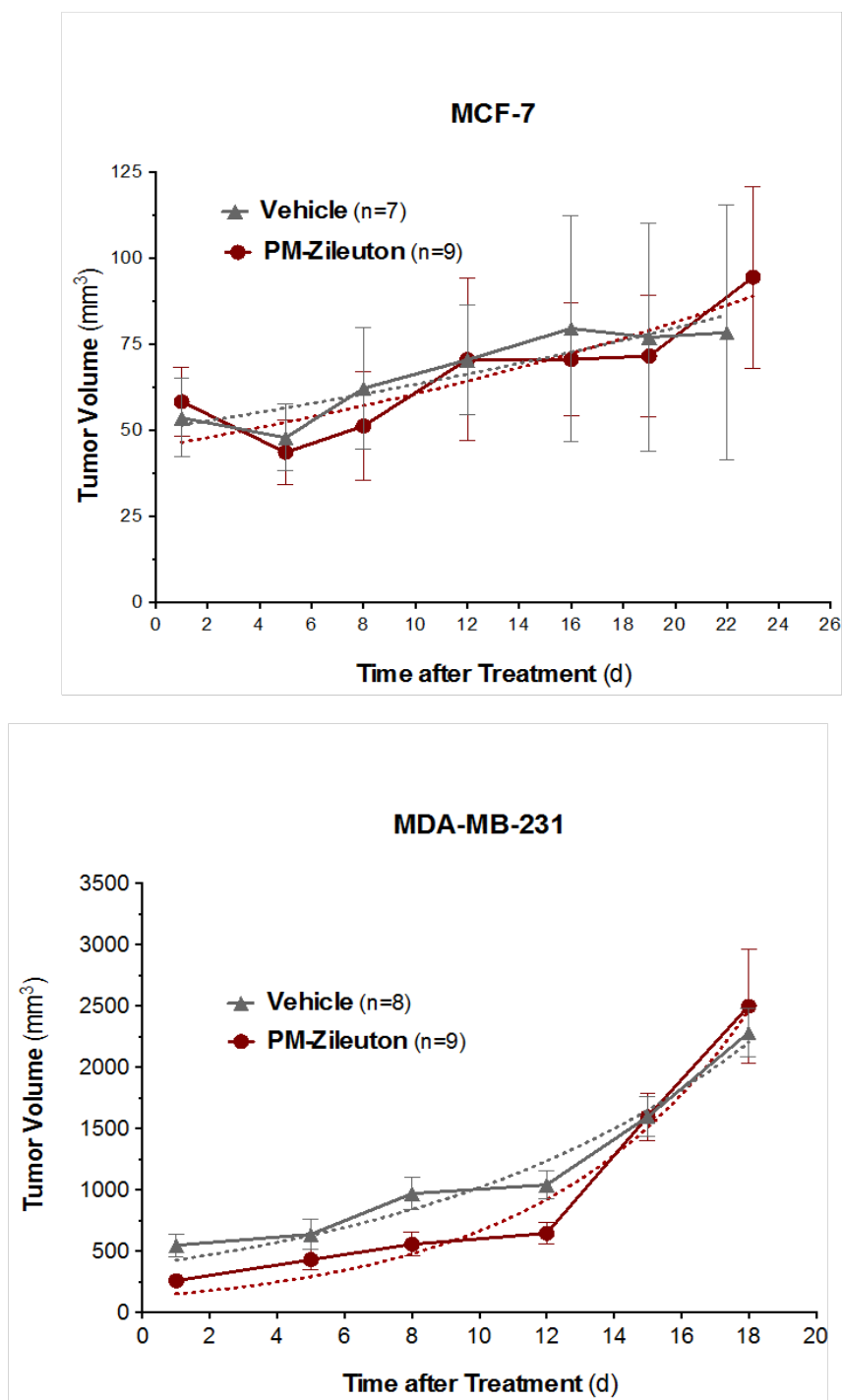


Figure S6: In vivo tumor growth

Orthotopic breast cancer models were generated using freshly sorted tdTomato+ cells (0.6x 10⁶ cells / mouse for the MCF-7 cell line and 0.1x 10⁶ cells/animal for the MDA-MB-231 cell line). Posteriori, animals were then treated with i.v. administration of PM-ZileutonTM (15 mg/kg), or vehicle (PBS) 3 times per week during 3 weeks and subsequent tumor growth has been monitored.



Article 2

Intracellular Delivery of Anti-SMC2 Antibodies against Cancer Stem Cells

Sara Montero^{1,2,†}, Joaquin Seras-Franzoso^{1,†}, Fernanda Andrade^{1,3,4}, Francesc Martinez-Trucharte¹, Mireia Vilar-Hernández¹, Manuel Quesada¹, Helena Xandri¹, Diego Arango⁵, Ibane Abasolo^{1,2,6,*}, Diana Rafael^{1,2,*} and Simo Schwartz, Jr.^{1,2,*}

¹ Drug Delivery and Targeting Group, Molecular Biology and Biochemistry Research Center for Nanomedicine (CIBBIM-Nanomedicine), Vall d'Hebron Institut de Recerca, Universitat Autònoma de Barcelona, 08035 Barcelona, Spain.

² Networking Research Center for Bioengineering, Biomaterials, and Nanomedicine (CIBERE-BBN), Instituto de Salud Carlos III, 28029 Madrid, Spain.

³ i3S – Instituto de Investigação e Inovação em Saúde, Universidade do Porto, Rua Alfredo Allen 208, 4200-180 Porto, Portugal.

⁴ INEB – Instituto Nacional de Engenharia Biomédica, Universidade do Porto, Rua Alfredo Allen 208, 4200-180 Porto, Portugal.

⁵ Biomedical Research in Digestive Tract Tumors, CIBBIM-Nanomedicine, Vall d'Hebron Institut de Recerca, Universitat Autònoma de Barcelona, 08035 Barcelona, Spain.

⁶ Functional Validation and Preclinical Research, Molecular Biology and Biochemistry Research Center for Nanomedicine (CIBBIM-Nanomedicine), Vall d'Hebron Institut de Recerca, Universitat Autònoma de Barcelona, 08035 Barcelona, Spain.

[†] These authors contributed equally to this work.

Pharmaceutics. 2020;12(2):185.

DOI: 10.3390/pharmaceutics12020185; PMID: 32098204.

IF 2020: 6.321; Quartile: Q1.






Even though therapeutic strategies specifically directed against the cancer stem cells (CSC) fraction are completely required to overcome tumor resistance and recurrence, the unique elimination of CSC do not represent the complete cancer cure, as few surviving CSC are able to regenerate the tumor. In this regard, combination therapies that simultaneously target not only CSC subpopulation but also differentiated tumor cells are needed. Importantly, there are a wide range of intracellular targets that lack small drugs for their inhibition, the so-called undruggable targets. In this context, the intracellular delivery of antibodies is gaining special interest in nanomedical field, since they are able to reach a large number of molecules that currently have no available inhibitors. In particular, previous results from our laboratory group showed the structural maintenance of chromosomes 2 (SMC2) protein importance in tumor survival and cancer cell malignancy, being until now an undruggable target without any chemical inhibitor currently available for this protein. Therefore, we opted to block the cytosolic SMC2 protein through intracellular delivery of specific antibodies against SMC2 protein, anti-SMC2 antibodies (Ab-SMC2).

In this work, we have proposed a combined therapy aiming to eliminate the entire tumor mass, using the SMC2 protein as a target for CSC eradication, whereas Standard-of-Care (SoC) drugs for cancer treatment will be responsible for killing bulk or differentiated tumor cells. In particular, Ab-SMC2 have been encapsulated in the hydrophilic shell of Pluronic® F127-based polymeric micelles (PM) in order to protect their integrity as well as improve their cellular internalization, while SoC drugs have been entrapped into the hydrophobic core of the resulting PM. Thus, micelles loaded with Ab-SMC2 significantly increase their therapeutic effect in terms of cell viability and hinder the tumorspheres formation, meanwhile neither the micelles nor Ab-SMC2 alone showed any efficacy. Furthermore, a combinatorial effect has also been assessed by combining Ab-SMC2-containing micelles with Paclitaxel (PTX) and 5-Fluorouracil (5-FU). Herein, strong inhibition of tumorspheres formation, CSC-like *in vitro* cultures, was observed after combined treatment compared to free SoC drugs or Ab-SMC2 treatment. Therefore, the presented system offers the possibility of simultaneously eliminating both tumor subpopulations, CSC and bulk tumor cells, potentially improving its performance.

Keywords: Structural maintenance of chromosomes 2 (SMC2) protein, Cancer stem cells (CSC), Pluronic® F127-based polymeric micelles (PM), Intracellular delivery of antibodies, Combined therapy.

Article

Intracellular Delivery of Anti-SMC2 Antibodies against Cancer Stem Cells

Sara Montero ^{1,2,†}, Joaquin Seras-Franzoso ^{1,†}, Fernanda Andrade ^{1,3,4} ,
 Francesc Martinez-Trucharte ¹, Mireia Vilar-Hernández ¹ , Manuel Quesada ¹, Helena Xandri ¹,
 Diego Arango ^{5,6} , Ibane Abasolo ^{1,2,7,*}, Diana Rafael ^{1,2,*}  and Simo Schwartz, Jr. ^{1,2,*} 

¹ Drug Delivery and Targeting Group, Molecular Biology and Biochemistry Research Centre for Nanomedicine (CIBBIM-Nanomedicine), Vall d'Hebron Institut de Recerca, Universitat Autònoma de Barcelona, 08035 Barcelona, Spain; sara.montero@vhir.org (S.M.); joaquin.seras@vhir.org (J.S.-F.); fernanda.silva@vhir.org (F.A.); francesc.martinez@vhir.org (F.M.-T.); mireia.vilar@alumni.vhir.org (M.V.-H.); mbenque@correo.ugr.es (M.Q.); helena.xandri@alumni.vhir.org (H.X.)

² Networking Research Centre for Bioengineering, Biomaterials, and Nanomedicine (CIBER-BBN), Instituto de Salud Carlos III, 28029 Madrid, Spain

³ i3S—Instituto de Investigação e Inovação em Saúde, Universidade do Porto, Rua Alfredo Allen 208, 4200-180 Porto, Portugal

⁴ INEB—Instituto Nacional de Engenharia Biomédica, Universidade do Porto, Rua Alfredo Allen 208, 4200-180 Porto, Portugal

⁵ Biomedical Research in Digestive Tract Tumors, CIBBIM-Nanomedicine, Vall d'Hebron Institut de Recerca, Universitat Autònoma de Barcelona, 08035 Barcelona, Spain; diego.arango@vhir.org

⁶ Immune Regulation and Immunotherapy, CIBBIM-Nanomedicine, Vall d'Hebron Institut de Recerca, Universitat Autònoma de Barcelona, 08035 Barcelona, Spain

⁷ Functional Validation and Preclinical Research, Molecular Biology and Biochemistry Research Centre for Nanomedicine (CIBBIM-Nanomedicine), Vall d'Hebron Institut de Recerca, Universitat Autònoma de Barcelona, 08035 Barcelona, Spain

* Correspondence: ibane.abasolo@vhir.org (I.A.); diana.fernandes_de_so@vhir.org (D.R.); simo.schwartz@vhir.org (S.S.J.); Tel.: +34-934893375 (I.A.); +34-934894056 (D.R.); +34-934894055 (S.S.J.)

† These authors contributed equally to this work.

Received: 10 February 2020; Accepted: 20 February 2020; Published: 21 February 2020



Abstract: Structural maintenance of chromosomes protein 2 (SMC2) is a central component of the condensin complex involved in DNA supercoiling, an essential process for embryonic stem cell survival. SMC2 over-expression has been related with tumorigenesis and cancer malignancy and its inhibition is regarded as a potential therapeutic strategy even though no drugs are currently available. Here, we propose to inhibit SMC2 by intracellular delivery of specific antibodies against the SMC2 protein. This strategy aims to reduce cancer malignancy by targeting cancer stem cells (CSC), the tumoral subpopulation responsible of tumor recurrence and metastasis. In order to prevent degradation and improve cellular internalization, anti-SMC2 antibodies (Ab-SMC2) were delivered by polymeric micelles (PM) based on Pluronic® F127 amphiphilic polymers. Importantly, scaffolding the Ab-SMC2 onto nanoparticles allowed its cellular internalization and highly increased its efficacy in terms of cytotoxicity and inhibition of tumorsphere formation in MDA-MB-231 and HCT116 breast and colon cancer cell lines, respectively. Moreover, in the case of the HCT116 cell line G1, cell-cycle arrest was also observed. In contrast, no effects from free Ab-SMC2 were detected in any case. Further, combination therapy of anti-SMC2 micelles with paclitaxel (PTX) and 5-Fluorouracil (5-FU) was also explored. For this, PTX and 5-FU were respectively loaded into an anti-SMC2 decorated PM. The efficacy of both encapsulated drugs was higher than their free forms in both the HCT116 and MDA-MB-231 cell lines. Remarkably, micelles loaded with Ab-SMC2 and PTX showed the highest efficacy in terms of inhibition of tumorsphere formation in HCT116 cells. Accordingly, our data clearly suggest an effective intracellular release of antibodies targeting SMC2 in these cell models and, further, strong cytotoxicity against CSC, alone and in combined treatments with Standard-of-Care drugs.

Keywords: SMC2; condensin complexes; nanomedicine; polymeric micelles; cancer stem cells; 5-FU; PTX; breast cancer; colon cancer; antibody intracellular delivery

1. Introduction

Protein therapy has emerged as a promising therapeutic alternative due to its high specificity and reduced off-target effects [1]. Among protein-based therapies, the use of antibodies have been largely explored and numerous treatments are currently available for a broad spectrum of clinical indications, from transplant rejection to cancer [2]. One of the most interesting features of antibody-based therapies is their potential to reach a wide range of targets, including those that are usually unattainable by other strategies (i.e., undruggable targets). However, because most antibodies are unable to easily cross the extracellular membrane, their applications are often limited to extracellular targets [3,4]. In the last years, several research groups have explored the use of antibodies against intracellular targets. Straightforward techniques for antibody delivery, such as microinjection, electroporation and antibody modification with cell penetration peptides (CPPs), have been tested. Unfortunately, even though experimentally effective *in vitro*, they have not been efficiently translated to *in vivo* models or into clinical applications [5,6]. In addition, although different nanoparticles, mainly metallic and lipidic, have been developed for intracellular delivery of antibodies, only few of them showed efficient intracellular delivery [7,8]. The current drawbacks are related with limited cargo for hydrophilic substances, un-adequate endosomal escape, *in vivo* instability and a short half-life circulation time. Thus, intracellular delivery of antibodies is still a considerable challenge [9,10].

On the other hand, although extensively investigated and besides constant development of new therapies, cancer often remains as an incurable disease. Insights into cancer physiology have shown the complexity of cancer regulatory networks in which a large variety of different cell types are involved and largely interconnected to determine disease progression. In this regard, particular attention should be addressed to metastatic spreading, resistance to treatment and tumor recurrence. These features are related with the presence of a cancer cell subpopulation known as cancer stem cells (CSC). CSC display stemness properties, such as self-renewal, quiescence and the capability to remain in an undifferentiated state [11,12]. Besides, CSC have been shown to exhibit high expression levels of drug efflux transporters and unregulated DNA repair machinery, conferring them drug resistance potential. In this context, CSC have become a highly appealing target in order to improve current anti-cancer therapies [13,14]. Although the number of new drugs with therapeutic potential against CSC is rising and several products are already in clinical trials, there is still strong need to broaden the catalogue of therapeutic options.

In this sense, the Structural Maintenance of Chromosomes 2 (SMC2) protein could be a good therapeutic target candidate. SMC2 forms part of the condensin complex that has a central role in many aspects of chromosome biology, including the segregation of sister chromatids and compaction of chromosomes during cell division, as well as the regulation of gene expression during the interphase [15–18]. Importantly, SMC2 protein has been mostly located at the cell cytoplasm during cell interphase with only a minor amount remaining associated to chromatin in the nucleus. The condensin complex is formed by five subunits and requires the initial arrangement of a SMC2/SMC4 heterodimer. The condensin complex is completed by the union of a subcomplex, formed by the three non-SMC subunits (Cnd1, Cnd2 and Cnd3), to the heterodimer of SMC2/SMC4 [15–17]. Of note, SMC2 has been found to be over-expressed in a significant number of patients with colorectal cancer, gastric cancer, lymphoma and some types of neuroblastoma [19,20], and has been suggested as a risk biomarker in pancreatic cancers [21]. Moreover, when SMC2 expression was knocked down it drastically reduced tumor growth in colorectal cancer mice models [18]. This data and the central role of the condensin complex in cell division suggested that an effective inhibition of the activity of this complex would

prevent cancer cells from dividing. Under this premise, directing SMC2-targeted inhibitory molecules into the cell cytoplasm should ensure SMC2 protein blockade and serve as a novel therapeutic strategy.

Hereby we propose a polymeric micelle delivery system (PM) based on amphiphilic polymers, namely the Pluronic® F127 as a nanoplatform to cluster the antibodies directed against the SMC2 protein. Because of its small size, biocompatibility, stealth properties and amphiphilic nature, this is an ideal system to overcome major drawbacks related to intracellular delivery of antibodies. Furthermore, poloxamer polymers like Pluronic® F127 have shown to interfere with the function of P-glycoprotein, being therefore helpful to further overcome drug resistance and reduce cancer recurrence [22–24]. Moreover, taking advantage of the plasticity provided by amphiphilic PM we have also explored potential combinatorial therapeutic strategies with 5-FU and PTX, drugs commonly used in colon and breast cancer, respectively.

2. Materials and Methods

2.1. Cell Lines and Culture Conditions

The HCT116 (ATCC® CCL-247™) colon cancer cell line, MDA-MB-231 (ATCC® HTB-26™) breast cancer cell line and PANC-1 (ATCC® CRL-1469™) pancreas cancer cell line were obtained from American Type Culture Collection (ATCC®, LGC Standards, Barcelona, Spain). Cells were cultured in RPMI medium (ThermoFisher Scientific, Madrid, Spain) supplemented with 10% Fetal Bovine Serum (FBS) (ThermoFisher Scientific, Madrid, Spain), a 1% penicillin–streptomycin mixture (ThermoFisher Scientific, Madrid, Spain), 1% L-glutamine (Lonza, Basel, Switzerland) and 1% Non-Essential Amino Acids (NEAA) (ThermoFisher Scientific, Madrid, Spain). All cell lines were maintained at 37 °C under a 5% CO₂-saturated atmosphere. The medium was changed every two days, and upon sub-confluence, cells were harvested from plates with 0.25% trypsin-EDTA and subcultured (ThermoFisher Scientific, Madrid, Spain).

Cells were also cultured in low attachment conditions as tumorspheres in serum-free media and seeded in ultra-low attachment surface plates (Corning Life Sciences, Chorges, France). The medium for breast and pancreas sphere growth was supplemented with glucose, 60 mg/mL (Merck Life Science S.L.U., Madrid, Spain), as well as 10 µL/mL L-Glutamax (Merck Life Science S.L.U., Madrid, Spain), 10 µL/mL antibiotic–antimitotic mixture (Merck Life Science S.L.U., Madrid, Spain), 4 µg/mL heparin (Merck Life Science S.L.U., Madrid, Spain), 2 mg/mL BSA (Merck Life Science S.L.U., Madrid, Spain), 0.02 µg/mL of human recombinant EGF (Merck Life Science S.L.U., Madrid, Spain), 0.01 µg/mL of human recombinant bFGF (ThermoFisher Scientific, Madrid, Spain) and 10% of Hormone Mix: 10 µg/mL putrescin, 20 µM progesterone (both from Merck Life Science S.L.U., Madrid, Spain), 0.1 mg/mL apo-transferrin, 25 µg/mL insulin and 30 µM selen (ThermoFisher Scientific, Madrid, Spain). Tumorspheres from the HCT116 cell line were also cultured in serum-free media supplemented with a 1% antibiotic–antimitotic mixture, 10 ng/mL of human recombinant EGF, 20 ng/mL of human recombinant bFGF and 10 ng/mL of LIF Recombinant Human Protein (ThermoFisher Scientific, Madrid, Spain).

2.2. Phase Contrast Microscopy

The morphology and structure of adherent cells and spheres were routinely assessed by phase contrast microscopy imaging after treatment with the distinct compounds. Images were acquired at 10× amplification using a Nikon Eclipse TS100 (Nikon Instruments Europe BV, Amsterdam, Netherlands) inverted microscope and further edited with ImageJ 1.49v software.

2.3. Cell Transfection with siRNA

2.3.1. Gene Expression Determination

10⁵ cells were seeded in 6-well plates and transfected with SMC2-siRNA (SI02654260, Qiagen, Hilden, Germany) using Lipofectamine® 2000 (ThermoFisher Scientific, Madrid, Spain) according to the manufacturer's instructions. A nonspecific sequence was used as the control (siControl). The culture medium was changed 6 h after transfection and cells harvested after 72 h of incubation. Samples were further processed for RNA extraction as detailed below in Section 2.4.

2.3.2. Cell Growth Assay

After cell transfection, cells were washed in PBS and harvested by trypsin digestion following standard procedures. Cells were counted in a Countess™ II (ThermoFisher Scientific, Madrid, Spain).

2.3.3. Sphere Formation Assay

SMC2 knock-down was performed following a 2-times siRNA shot strategy in order to guarantee an efficient gene expression inhibition along the assay. Briefly, a first treatment with SMC2-siRNA using Lipofectamine® 2000 (ThermoFisher Scientific, Madrid, Spain) was performed as described above. After 72 h an identical SMC-siRNA shot was performed. After 6 h upon the second siRNA transfection, cells were harvested and washed 3 times in serum free media. Then, 1000 cells were seeded in ultra-low attachment 96-well plates, adding sphere growth media for assessing sphere formation (as described in the cell viability assay Section 2.10.1).

2.4. RNA Extraction and Real-Time Quantitative Reverse Transcription Polymerase Chain Reaction (qRT-PCR)

Total RNA was extracted from cells using RNeasy Micro Kit (Qiagen, Hilden, Germany), and the obtained RNA was reverse transcribed with a High Capacity cDNA Reverse Transcription Kit (Applied Biosystems, Madrid, Spain), according to the manufacturer's instructions. The cDNA reverse transcription product was amplified with specific primers for SMC2 (hSMC2 F: 5' AAT GAG CTG CCG GCT CTA GA 3'; hSMC2 R: 5' TTG TTG CTT GTG ATA TGA GCT TTG 3'); GAPDH (hGAPDH F: 5' ACC CAC TCC TCC ACC TTT GAC; hGAPDH R: 5' CAT ACC AGG AAA TGA GCT TGA CAA 3') and Actin (hActin F: 5' CAT CCA CGA AAC TAC CTT CAA CTC C 3'; hActin R: 5' GAG CCG CCG ATC CAC AC 3') by qPCR using SYBR Green (ThermoFisher Scientific, Madrid, Spain) to fluorescently label double stranded DNA. The reaction was performed on a 7500 Real time PCR system (Applied Biosystems, Madrid, Spain). At least three biological replicates, each comprising two technical replicates, were performed. Relative normalized quantities (NRQ) of mRNA expression were calculated using the comparative Ct method ($2^{-\Delta\Delta Ct}$) with two reference genes (hGAPDH and hActin) used as endogenous controls through Qbase™ software v3.2.

2.5. Protein Extraction and Western Blotting

Cell pellets were lysed with the Cell Lytic M reagent (Merck Life Science S.L.U., Madrid, Spain) containing a protease inhibitor cocktail (Roche cOmplete™, Merck Life Science S.L.U., Madrid, Spain). Proteins in the crude lysates were quantified using the Pierce™ BCA protein quantification kit (ThermoFisher Scientific, Madrid, Spain) following the manufacturer's instructions. A total of 20 µg of whole-cell lysates were separated by SDS-PAGE and transferred onto PVDF membranes. Blots were probed using primary antibodies anti-SMC2 (Merck Life Science S.L.U., Madrid, Spain) and β-Tubulin (Invitrogen, ThermoFisher Scientific, Madrid, Spain). Proteins were detected using HRP-conjugated secondary antibodies (Dako, Palex Medical SA, Barcelona, Spain) and developed after appropriate incubation in an Immobilon® Western reagent (Merck Life Science S.L.U., Madrid, Spain) using an Odyssey FC imaging system (LI-COR Biotechnology GmbH, Bad Homburg, Germany) for chemiluminescence detection.

2.6. Production of Polymeric Micelles

Pluronic® F127 was kindly provided by BASF (Ludwigshafen, Germany). PM were prepared using the thin-film hydration technique [22]. Pluronic® F127 carboxylation was performed as previously reported [25]. Briefly, F127 and F127:COOH polymers were individually weighed in an 8:2 (*w/w*) ratio and dissolved in a mixture of methanol:ethanol (1:1) (Merck Life Science S.L.U., Madrid, Spain). For the formation of loaded micelles, the drug, 5-FU or PTX (both from Merck Life Science S.L.U., Madrid, Spain) were added to the organic solution at the desired concentration. Then, the solvent was removed under vacuum in a rotary evaporator (bath temperature 60 °C, 200 rpm), and the resulting film left to dry overnight at room temperature to eliminate any remaining solvent. The film was then hydrated with PBS and vortexed for 5 min at full speed. For the PM encapsulating SMC2 antibodies (PM:SMC2), the antibody (Anti-SMC2/hCAP-E Antibody, Merck Life Science S.L.U., Madrid, Spain) was added at the aqueous phase during the rehydration step. For PM functionalized with SMC2 antibodies (PM-CON:SMC2), an adequate amount of EDC (polymer:EDC ratio 1:1.5) (Merck Life Science S.L.U., Madrid, Spain) was incubated with the formulation during 30 min at RT. Afterwards, the SMC2 antibody solution was added and incubated under stirring during 2 h at RT. Samples were freeze-dried for long-term storage using a VirTisBenchTop Freeze-Dryer (SP Scientific, Ipswich, UK) when required.

2.7. Physicochemical Characterization of the Polymeric Micelles

2.7.1. Zeta Potential Measurements

Zeta potential was assessed by laser Doppler microelectrophoresis using a NanoZS (Malvern Instruments, Malvern, UK) with an angle of 173°. Samples were diluted 1:5 in Milli-Q® water (18.2 MΩ·cm at 25 °C) in order to obtain an adequate nanoparticle concentration. Data obtained from each formulation were represented as mean values and measured at least in triplicate.

2.7.2. Transmission Electron Microscopy (TEM)

Particle shape and morphology were observed by TEM, using a JEM-1400 Electron Microscope (JEOL Ltd., Croissy-sur-Seine, France) with an applied voltage of 120 kV. For that, a drop of sample (previously diluted 1:20 in Milli-Q® water) was placed on a carbon 400-mesh copper grid, the liquid excess removed, and the sample contrasted with uranyl acetate before visualization. Image J 1.49v software was used to process information and determine diameter measures ($n > 200$) from TEM images, while histogram plots from nanoparticles size distribution were generated by GraphPad Prism 6. The dispersion index (*d*) was determined by Equation (1).

$$\text{Standard Deviation (SD)/Particle Size Arithmetic Mean} \quad (1)$$

2.7.3. Loading/Association Efficiency Determination

The efficacy of SMC2 loading in the case of PM:SMC2 and association efficiency in the case of PM-CON:SMC2 was assessed by BCA protein assay. Briefly, the amount of free SMC2 antibody in the aqueous phase of the PM was separated by centrifugation with filtration (10,000 *g*, 10 min at RT) using 300k membrane centrifugal devices (Nanosep® Centrifugal Devices, Pall España, Madrid, Spain). Then, the protein level was measured from the flow using a Pierce™ BCA protein assay kit (ThermoFisher Scientific, Madrid, Spain). The Loading/Association efficiency percentage was determined according to Equation (2):

$$\frac{\text{Total amount of SMC2 (unfiltered PM)} - \text{free SMC2 in filtrate}}{\text{Total amount of SMC2 (unfiltered PM)}} \times 100 \quad (2)$$

2.7.4. Fourier-Transform Infrared Spectroscopy (FTIR)

The conjugation of the SMC2 antibody at the PM surface was also confirmed by FTIR analysis. FTIR was carried out using a spectrometer Perkin-Elmer Spectrum One (energy range: 450–4000 cm^{-1}) equipped with a Universal Attenuated Total Reflectance Accessory (U-ATR, Perkin-Elmer, Madrid, Spain). Prior to analysis, samples were freeze-dried using a VirTisBenchTop Freeze-Dryer (SP Scientific, Ipswich, UK).

2.8. Micelles Internalization: Flow Cytometry and Confocal Microscopy

Cell internalization of the different formulations was assessed in HCT116 and MDA-MB-231 using 5-DTAF (Merck Life Science S.L.U., Madrid, Spain) fluorescently labeled PM [25,26].

2.8.1. Flow Cytometry

Briefly, 20,000 cells were seeded in complete RPMI medium in 96-well plates and left to attach for 24 h. PM were added to cells (10 mg/mL) and incubated for 15, 30, 60, 180, 360 and 1440 min, respectively. Then, cells were washed with 1× PBS, trypsinized and neutralized with PBS supplemented with 10% FBS and 1 $\mu\text{g/mL}$ DAPI (Merck Life Science S.L.U., Madrid, Spain) used for vital staining. The plate was read in a cytometer Fortessa (BD Biosciences, Madrid, Spain) and data was analyzed with FCS Express 4 Flow Research Edition software (De Novo Software, Los Angeles, USA, Version 4). Three biological replicated were performed for each condition and only DAPI negative cells were admitted for the analysis, while cell debris or possible aggregates were removed by forward and side scatter gating. For each sample, at least 10,000 individual cells were collected, and the percentage of fluorescent cells evaluated.

2.8.2. Confocal Microscopy

A total of 50,000 cells were seeded in complete RPMI medium in 8-well chambered coverglass (ThermoFisher Scientific, Madrid, Spain) and incubated overnight at 37 °C and 5% CO_2 to allow cell adhesion. Cells were incubated with 5-DTAF-fluorescently labelled PM (10 mg/mL) for 6 h. Lysosomes were stained with 1 μM LysoTracker[®] Red DND-99 (ThermoFisher Scientific Madrid, Spain) for 30 min at 37 °C while the cell membrane was stained with 5 $\mu\text{g/mL}$ CellMask[™] (Invitrogen, ThermoFisher Scientific, Madrid, Spain) for 15 min at 37 °C. Subsequently, cells were fixed in 4% PFA (Merck Life Science S.L.U., Madrid, Spain) at 4 °C for 20 min followed by nuclei staining with DAPI (1 $\mu\text{g/mL}$) for 5 min at RT in the dark. Cells were viewed under a Spectral Confocal Microscope MFV1000 Olympus (Olympus Iberia, S.A.U., L'Hospitalet de Llobregat, Spain). The 561 nm excitation wavelength of the green laser (10 mW) was used for selective detection of the red fluorochromes (LysoTracker[®] Red and CellMask[™]). The 488 nm excitation wavelength of Argon multiline laser (40 mW) was used for selective detection of the green fluorochrome (5-DTAF). The nuclear staining DAPI was excited at 405 nm with a violet laser (6 mW). Minimal single optical sections were collected for each fluorochrome sequentially. Images were merged and analyzed with Image J 1.49v software.

2.9. Cell Cycle Assay by Flow Cytometry

A flow cytometric analysis of cell cycle with propidium iodide DNA staining was carried out. Briefly, 40,000 cells of HCT116 cells and 30,000 cells of MDA-MB-231 cells were seeded in 24-well plates and left to adhere during 24 h at 37 °C and a 5% CO_2 -saturated atmosphere. Then, cells were treated and incubated with empty PM (control PM) (5 mg/mL) and PM-CON:SMC2 (5 mg/mL polymer and 32.9 $\mu\text{g/mL}$ of SMC2 antibody) for 48 h. Untreated cells were used as the negative control. Afterwards, cells were harvested, centrifuged (8000 rpm, 5 min at 4 °C) and fixed in cold 70% ethanol for 30 min at 4 °C. After centrifugation, cells were washed two times with PBS and the cell pellets resuspended in 250 μL of the staining solution containing 100 $\mu\text{g/mL}$ of ribonuclease PureLink[™] RNase A (ThermoFisher

Scientific, Madrid, Spain) and 50 µg/mL of propidium iodide (Merck Life Science S.L.U., Madrid, Spain) in order to ensure that only DNA, not RNA, was stained.

Cell cycle evaluation was performed using an FACS Calibur (BD Biosciences, Madrid, Spain) flow cytometer and the resulting histograms analysed with FCS Express 4 Flow Research Edition software (De Novo Software, Version 4). Three biological replicates were performed and at least 5000 individual cells were collected for the analysis once debris were removed by forward and side scatter gating. The multicycle option in autofit mode was performed in order to automatically quantify the percentage of cells in each cell cycle phase. By this method a Gaussian curve was fitted to each phase allowing the precise determination of the area under the curve. In addition, the G2/G1 ratio was also represented, scoring around 2 in all the cases, in compliance with the accepted quality standards for cell-cycle assays.

2.10. Tumor Cell Viability Assays

2.10.1. Viability Assay in Adherent Cell Cultures

3000 cells of the HCT116 cell line and 5000 cells of the MDA-MB-231 cell line were seeded in 96-well plates and incubated overnight to allow adhesion. Then, cells were treated and incubated during 72 h with crescent concentrations of the different formulations (PM, PM:SMC2 and PM-CON:SMC2) at 5 mg/mL of polymer and 32.9 µg/mL of SMC2 antibody. To determine the cytotoxicity of free 5-FU and free PTX (Merck Life Science S.L.U., Madrid, Spain), cells were incubated during 48 h with a range concentration of 5-FU and PTX of 384.40 µM to 0.023 µM and 1 µM to 0.0078 µM, respectively. Complete medium was used as negative control and 10% DMSO as positive control of toxicity. Cell viability was measured using the 3-(4,5-dimethylthiazol-2-yl)-2,5-diphenyltetrazolium bromide (MTT) reagent (Merck Life Science S.L.U., Madrid, Spain). The absorbance of each well was read on an absorbance microplate reader ELx800 (BioTek, Colmar, France), at 590 and 630 nm for 5-FU and PTX, respectively. The half-maximal inhibitory concentration (IC₅₀) was determined by nonlinear regression of the concentration-effect curve fit using Prism 6.02 software (GraphPad Software, Inc.).

2.10.2. Tumorsphere Viability Assays

Studies were performed using ultra-low attachment surface plates (Corning Life Sciences, Chorges, France). Cells were cultured in serum free media supplemented differently for HCT116 colon cell line and MDA-MB-231 breast cancer cell line, as mentioned above. HCT116, MDA-MB-231 and Panc-1 cells were transfected with siRNA anti-SMC2, as previously described. A total of 1000 cells were seeded and cultured for 6 days in ultra-low attachment plates.

For PM and drug efficacy assays, 1000 cells from the HCT116 cell line and 2000 cells from the MDA-MB-231 cell line were seeded in 96-well ultra-low attachment plates in serum-free media, supplemented as described above. After overnight incubation, cells were treated with different PM formulations (PM, PM-CON:SMC2, PM/5-FU, PM-PTX, PM-CON:SMC2/5-FU, PM-CON:SMC2/PTX) (1 mg/mL of polymer), the free drugs (5-FU, 3.84 µM and PTX, 0.1 µM) and free SMC2 antibody (6.58 µg/mL) for 7 days. The IC₅₀ of the free tested drugs were also determined in low attachment conditions. Cells were treated with serial 1:2 dilutions of 5-FU (from 768.80 µM to 0.047 µM) and PTX (from 10 µM to 0.078 µM) for 7 days. Free serum medium was used as negative control and 10% DMSO as positive control of toxicity. In all cases, sphere formation was monitored with a Nikon Eclipse TS100 inverted microscope (Nikon Instruments Europe BV, Amsterdam, Netherlands) and quantified by Presto Blue® Reagent assay (ThermoFisher Scientifics, Madrid, Spain). The absorbance of each well was read on a Multiskan™ FC Microplate Photometer (ThermoFisher Scientific, Madrid, Spain), at 570 and 620 nm, and the data were processed by GraphPad Prism 6 software.

2.11. Statistical Analysis

At least three batches of each PM were produced and characterized. The results were expressed as the mean ± standard deviation. For biological studies, at least 3 replicates, each involving at least

two technical replicates, were involved in the final results expressed as the mean \pm standard deviation. Statistical analysis was performed in GraphPad Prism 6 software using a non-parametric Dunn test for multiple comparisons and Mann–Whitney U test for simple comparisons. Differences were regarded as statistically significant when the p -value was smaller than 0.05.

3. Results

3.1. SMC2 Silencing Causes Strong Reduction of Tumorsphere Formation in Cancer Cells

SMC2 siRNA efficiently reduces the expression of the gene at mRNA and protein level in the three different cell lines. Namely, colorectal cancer cell line HCT116, triple negative breast cancer cell line MDA-MB-231 and pancreatic cancer cell line PANC-1 (Figure 1a,b and Figure S1a,b). Interestingly, the effect of SMC2 silencing resulted in a clear decrease in cell viability in HCT116, whereas only a trend to reduce the number of cells was observed for MDA-MB-231 (Figure 1c); no difference could be detected in other tumor types tested as in the case of PANC-1 (Figure S1c). Importantly, when cells were serum deprived and forced to grow in absence of cell-surface contacts, a remarkable decrease of tumorspheres proliferation was observed in all cell lines treated with SMC2 siRNA (Figure 1d and Figure S1d). Of note, as previously reported by our group and others [27,28], cells growing as spheres display CSC-like features (i.e., HCT116 cell line; Figure S2).

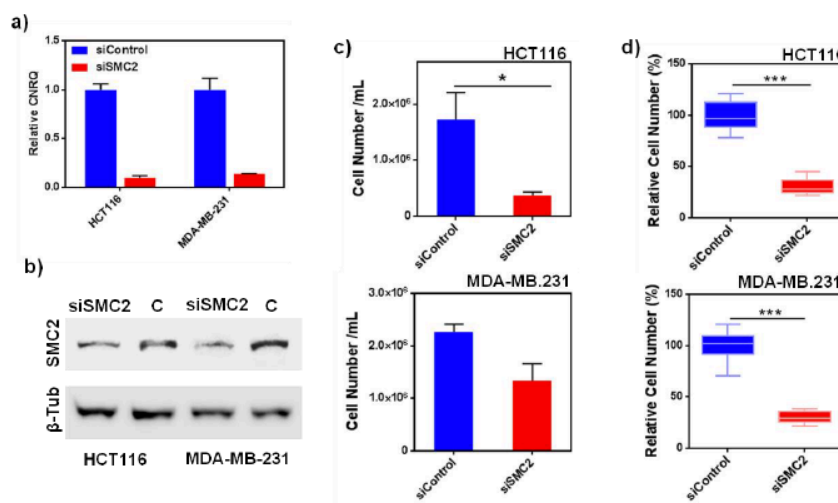


Figure 1. SMC2 siRNA inhibition. (a) Relative mRNA levels after SMC2 silencing for HCT116 and MDA-MB231 cell lines (siSMC2). Fold change is represented with respect to mRNA levels obtained from non-relevant siRNA-treated cells (siControl); (b) SMC2 and beta tubulin proteins detected by Western blot after SMC2 silencing (siSMC2) and compared to non-relevant siRNA-treated cells C; (c) cell viability assay for HCT116 and MDA-MB-231 adherent cells after treatment with siRNA against SMC2 (siSMC2) and with a scrambled control siRNA (siControl); and (d) cell viability assay for HCT116 and MDA-MB-231 growing in non-adherent conditions as tumorspheres, after treatment with siRNA against SMC2 (siSMC2) and with a scramble control siRNA (siControl). * $p < 0.05$, *** $p < 0.001$.

3.2. Physicochemical Characterization of Polymeric Micelles with Conjugated or Encapsulated SMC2 Antibodies

In order to develop a drug delivery system able to target SMC2 protein intracellularly, anti-SMC2 antibodies (Ab-SMC2) were successfully conjugated onto PM using two different approaches: (1) encapsulation by affinity into the PM hydrophilic shell (PM:SMC2) and (2) by covalent conjugation between the $-COOH$ terminals of the PM and the $-NH_2$ groups present in Ab-SMC2 (PM-CON:SMC2). Particles TEM analysis revealed spherical morphologies in all cases and displayed rather homogenous populations in size (Figure 2b). The PM obtained by the first approach presented a mean diameter of

35.99 ± 0.39 nm with a dispersity index of 0.16, and a slightly negative superficial charge measured by NanoZS (Figure 2c). The micelles produced according to the second approach presented a mean diameter of $(35.04 \pm 0.42$ nm), a d value of 0.18 and are faintly negatively charged (Figure 2c).

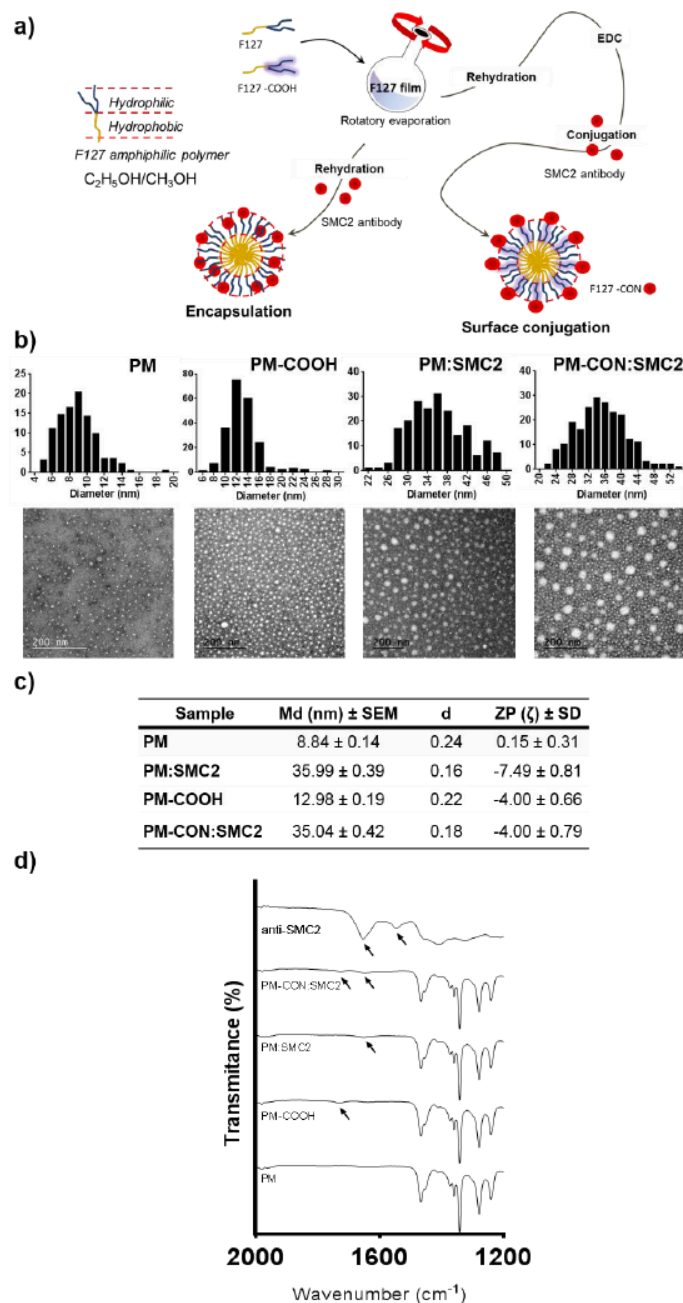


Figure 2. PM-Ab-SMC2 characterization. (a) Schematic representation of the two strategies employed for PM synthesis loaded with anti SMC2 antibody, namely encapsulation and surface conjugation. (b) TEM micrographs of the four distinct PM formulations. The panels above the micrographs correspond to the size distribution of the particles obtained by TEM image analysis. Scale bar represents 200 nm. (c) Summary table of mean diameter (Md), Dispersity Index (d), Zeta Potential (ZP) and (d) FTIR spectra, displaying the appearance of a peak at 1646 cm^{-1} and corresponding to amide I bond formation.

Regarding the antibody loading/association efficiency, it was determined by the measurement of free antibody in the micelle's supernatant after 300 KDa filtration. PM:SMC2 presented an SMC2 loading efficiency of $68.02\% \pm 1.01\%$ and PM-CON:SMC2 showed an association efficiency of $61.49\% \pm 3.11\%$. Moreover, the loading/association of Ab-SMC2 at the micelles surface were confirmed by FTIR (Figure 2d). Regarding FTIR analysis, control PM-COOH showed a peak at 1727 cm^{-1} corresponding to the $\text{C}=\text{O}$ stretching of the COOH groups of the carboxylated Pluronic® F127. As expected, this peak is absent in control PM composed only by unmodified Pluronic® F127 [25]. Ab-SMC2 showed a peak at 1654 cm^{-1} corresponding to the $\text{C}=\text{O}$ stretching vibrations of the peptide bond of the amide I and also a peak at 1545 cm^{-1} related to the N-H bending vibration/ C-N stretching vibration of the amide II [29].

In the case of PM:SMC2, it was possible to observe a small shift of the peak corresponding to the amide I of Ab-SMC2 from 1654 to 1648 cm^{-1} , possibly due to non-covalent interactions/hydrogen bonding between the protein and the Pluronic® F127 [30]. In the case of PM-CON:SMC2, a small shift together with an increase in the intensity of the peak of the amide I (1646 cm^{-1}) were detected, probably due to the conjugation of the NH_2 of Ab-SMC2 with the COOH from carboxylated Pluronic® F127 and the formation of new bonds. A small peak shift (1726 cm^{-1}) accompanied by a drop of intensity of the COOH peak also suggested a reduction of the availability of these free groups due to conjugation with NH_2 . Altogether, these results suggest a covalent conjugation of Ab-SMC2 to the surface of the PM. In order to better confirm the peaks, PM-CON:SMC2 were produced with 100% of carboxylated Pluronic® F127 (Figure S3). A peak at 1728 cm^{-1} , corresponding to the $\text{C}=\text{O}$ stretching of the COOH groups, and a peak at 1653 cm^{-1} , corresponding to the $\text{C}=\text{O}$ stretching vibrations of the peptide bond of the amide I, were observed. The lower shift of the amide I peak could be a result of the absence of the OH groups from the unmodified Pluronic® F127 and, consequently, lower hydrogen bonding interactions.

3.3. In Vitro Efficacy of PM-SMC2 and PM-CON:SMC2 in Adherent Cultures

Cell viability assays were performed in HCT116 colon and MDA-MB-231 breast cancer cells. PM-SMC2 and PM-CON:SMC2 formulations were compared with the free SMC2 antibody and control PM. As expected, control PM and the free antibody did not show cell cytotoxicity at the maximum tested dose, namely $32.9\text{ }\mu\text{g/mL}$ for Ab-SMC2 and 5 mg/mL for Pluronic® 127 (Figure 3a,b). On the other hand, the two formulations presented a significant cytotoxic effect in both cell lines at 72 h of incubation (Figure 3b). Nonetheless, PM-CON:SMC2 displayed a slight advantage in terms of effectiveness comparing to PM:SMC2. Thus, we decided to continue with the conjugated formulation of Ab-SMC2.

Further, we analyzed whether PM-CON:SMC2 might also cause changes in cell morphology and cell distribution in HCT116 and MDA-MB-231 models. Our data show a dramatic change in cell morphology in HCT116 cells. Cells treated with PM-CON:SMC2 showed a highly stretched shape and formed significantly less cell clusters than free Ab-SMC2 and empty PM (control PM). For fibroblast-shaped MDA-MB-231 cultures, cells treated with PM-CON:SMC2 displayed similar morphology and distribution than controls. Interestingly, a significant number of vacuoles were observed in samples incubated with PM-CON:SMC2 whereas no such structures were detected with free Ab-SMC2 and control PM (Figure 3a). These results show a biological activity of Ab-SMC2 when administered in PM that is not observed when PM are not employed.

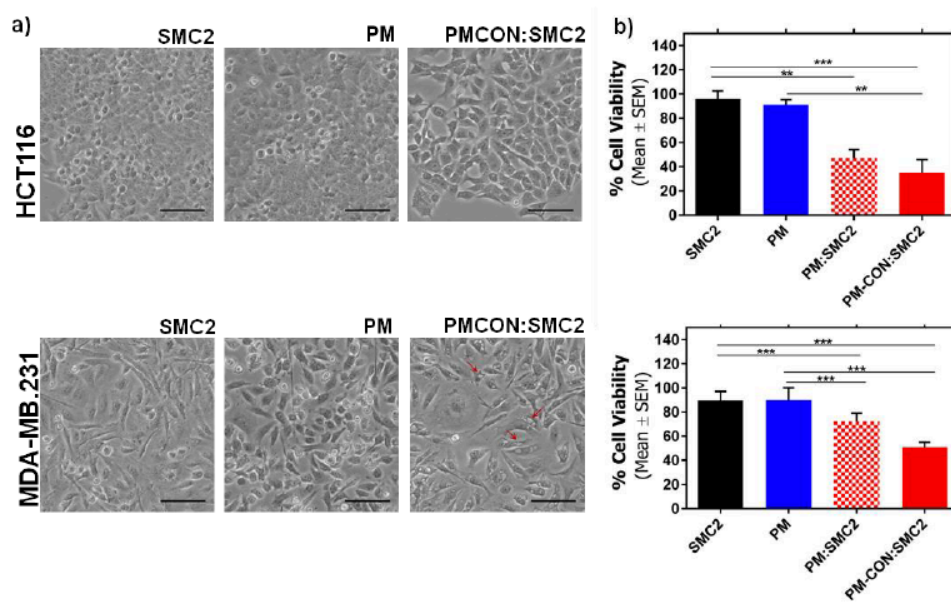


Figure 3. In vitro efficacy of Ab-SMC2 in tumor cell lines. (a) Phase contrast images of HCT116 (above panel) and MDA-MB-231 (below) after 48 h incubation with free SMC2 antibody, control PM and PM-CON:SMC2. Red arrows point at vacuoles appeared after PM-CON:SMC2 treatment. Scale bar correspond to 100 μ m; (b) cell viability representation of HCT116 (above panel) and MDA-MB-231 (below) after 72 h of incubation with anti SMC2 antibody, control PM, PM:SMC2 and PM-CON:SMC2. The concentrations of the antibody and Pluronic® 127 were 32.9 μ g/mL and 5 mg/mL, respectively. These concentrations were also maintained in both formulations: PM:SMC2 and PM-CON:SMC2. ** $p < 0.01$, *** $p < 0.001$.

3.4. PM-CON:SMC2 Micelles Show Faster Cellular Uptake than Control PM

Cellular internalization and intracellular localization assessment of PM decorated with Ab-SMC2 were carried out at several time-points by flow cytometry. Accordingly, 5-DTAF fluorescently labeled PM-CON:SMC2 were incubated with HCT116 and MDA-MB-231 cells. Figure 4a shows that the conjugated nanoparticle (PM-CON:SMC2) presented a faster uptake profile than PM in both cell lines. Further, we could also observe that the MDA-MB-231 cell line exhibited faster uptake profiles than HCT116 cells, which indicates that internalization efficiency is largely dependent on the cell type.

Fluorescently labelled PM were also employed for confocal analysis, after 6 h of incubation with HCT116 and MDA-MB-231 cells. Acidic vesicles were labelled with Lysotracker® Red to discriminate whether particles ended up into the lysosomes or were able to escape, at least partially, from the endosomal compartments. For all the tested formulations, we observed yellow dots corresponding to the merge of the green signal provided by DTAF and the red signal produced by the Lysotracker® labelling late endosomes, lysosomes and other membrane structures with an acidic pH (Figure 4b). These results indicate that at least part of the formulated PM was endocytosed and finally processed in the lysosomes. Nevertheless, because an effective blockage of SMC2 will require a cytosolic delivery of Ab-SMC2, we also measured the green fluorescence intensity at the cytoplasm of the HCT116 and MDA-MB-231 cells after their incubation with PM-CON:SMC2. For this, we used cell mask membrane staining and DAPI nucleus labelling to define a region of interest, namely the cellular cytosol. Excluding from the analysis bright green dots as PM accumulation within endosomal vesicles, we could detect an increase of green fluorescence in the cell cytoplasm of cells treated with PM-CON:SMC2, suggesting that this formulation was able to reach the cell cytoplasm (Figure 4c).

3.5. G1/S Cell Cycle Arrest Induced by PM-CON:SMC2

Finally, to further validate these results, we performed cell cycle assays in HCT116 and MDA-MB-231 cells treated with PM and PM-CON:SMC2. Of note, an effective targeting of intracellular SMC2 should have an impact in the cell cycle and reduce the number of cells into G2/M phase. As it can be observed in Figure 4d, HCT116 cells treated with PM-CON:SMC2 displayed a markedly higher percentage of cells in G1 in comparison to untreated cells and cells incubated with PM as controls. In addition, the percentage of cells in G2/M was also reduced in the PM-CON:SMC2-treated samples. For MDA-MB-231 the response pattern was similar when comparing untreated and PM-CON:SMC2-treated cells, exhibiting even higher differences regarding the decrease of G2/M percentage. Unexpectedly, control PM also showed an impact in cell-cycle arrest at G1 in this cell line (see Figure S3 for cell-cycle curve fitting examples).

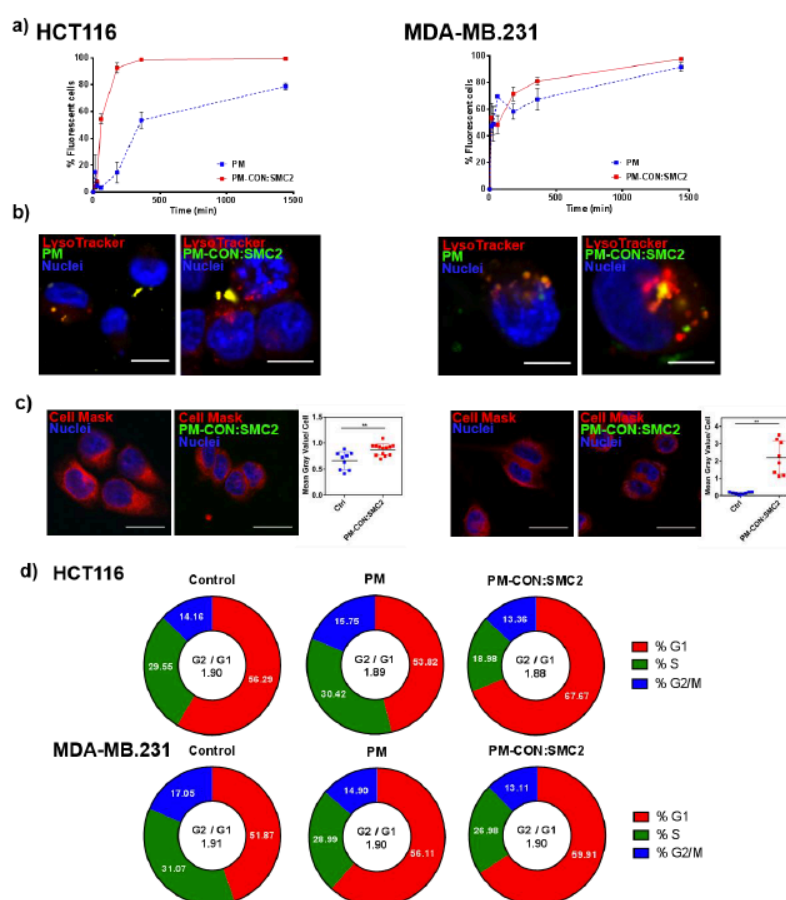
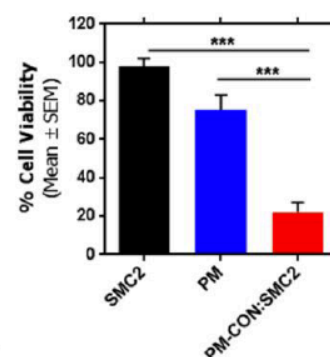
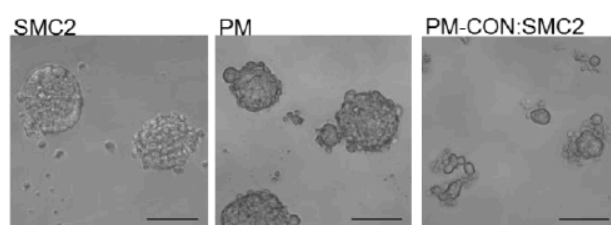


Figure 4. PM-CON:SMC2 uptake and intracellular fate. (a) Flow cytometry graphs displaying the percentage of fluorescent cells after HCT116 and MDA-MB-231 cell incubation with 5 mg/mL PM, PM:SMC2 and PM-CON:SMC2. (b) Confocal images showing either PM or PM-CON:SMC2 in green, acidic vesicles in red and nuclei in blue for HCT116 and MDA-MB-231 cells after 6 h incubation with 5 mg/mL PM. Scale bar represent 10 μ m. (c) Confocal images displaying PM-CON:SMC2 in green, plasma membrane in red and nuclei in blue, for HCT116 and MDA-MB-231 cells after 6 h incubation with 5 mg/mL PM. Scale bar represent 20 μ m. Side panels, graphical representations of green fluorescence measures in the cytoplasm. (d) Diagrams of cell cycle assay performed for HCT116 and MDA-MB-231 cells after 48 h of incubation with 5 mg/mL PM, PM-CON:SMC2 (32.9 μ g/mL of antibody) and their respective untreated control. Percentages of cells at distinct cell cycle phases: G1, S and G2/M are displayed. The G2/G1 ratio is shown inside the circle. ** $p < 0.01$.

3.6. Strong Anti-CSC Efficacy of PM-CON:SMC2 in Comparison with Free Ab-SMC2

CSC growing under serum starvation conditions and in independent cell anchorage were employed. Tumorsphere formation assays were performed using HCT116 and MDA-MB-231 cancer cells treated with PM-CON:SMC2, Ab-SMC2 and control PM. As expected, free Ab-SMC2 did not produce any cytotoxic effect in sphere formation in any of the tested cell lines. Remarkably, strong cytotoxicity was observed when cells were treated with PM-CON:SMC2 for both cell lines, while control PM showed a slight decrease on the capacity of cells to produce tumorspheres. Furthermore, a deeper analysis of the structure of the tumorspheres showed that in PM-CON:SMC2 treated cells spheres shrank and displayed looser conformations, confirming the effects of PM-CON:SMC2 over CSC. These results suggest that SMC2 blockage is crucial in order to eliminate CSC. Moreover, these data confirm the intracellular delivery of Ab-SMC2 through PM also in a tumorsphere model (Figure 5).

a) HCT116



b) MDA-MB.231

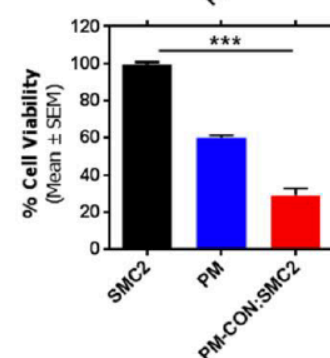
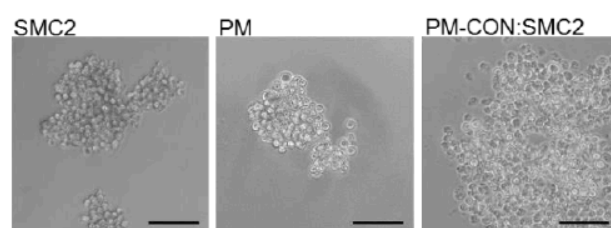


Figure 5. PM-CON:SMC2 in vitro efficacy in CSC. Left panels, microscopy images of HCT116 (a) and MDA-MB-231 (b) tumorspheres after treatment with Ab-SMC2 (6.58 µg/mL), control PM (1 mg/mL of Pluronic® 127) and PM-CON:SMC2 (6.58 µg/mL of antibody and 1 mg/mL of Pluronic® 127). Scale bar correspond to 100 µm. Right panels represent cell viability assays in HCT116 and MDA-MB-231 spheres growing for 7 days in non-adherent conditions. *** $p < 0.001$.

3.7. PM-CON:SMC2/5-FU and PM-CON:SMC2/PTX Combined Effect

In the clinical setting, PTX and 5-FU are often used in combined chemotherapeutic regimens against breast and colon cancer, respectively. Because a combination of different chemo-therapeutic drugs is commonly endured to improve clinical outcomes, we tested the cytotoxic activity of PM-CON:SMC2 loaded with either PTX or 5-FU anti-tumor drugs for combined treatments. For this, we took advantage of the amphiphilic nature of Pluronic® 127. Thus, while Ab-SMC2 remained conjugated onto the PM surface, we were able to encapsulate these drugs into the hydrophobic core of the resulting PM. Interestingly, when looking respectively at the efficacy of 5-FU and PTX as free drugs in regular cell cultures of HCT116 and MDA-MB-231 in comparison to cells growing as tumorspheres

(non-attachment), we observed that both drugs were significantly more active against adherent cells than against tumorspheres (Figure 6a). Tumorsphere resistance was noticeable for 5-FU in HCT116 at concentrations up to 1 μ M. In the case of MDA-MB-231, tumorspheres showed resistance to PTX at all tested concentrations, including the highest one (10 μ M) (Figure 6a, right panel). These results are in accordance to the CSC-like phenotype associated with tumorsphere growth and more specifically to the described drug resistance capacity of CSC.

Because eradicating CSC in tumors is becoming a great challenge for designing new treatments, we focused in the potential synergism of delivering Ab-SMC2 together with either PTX or 5-FU against tumor cells in non-adherent conditions. In this regard, the efficacies of 5-FU and PTX were tested at concentrations of 48 μ M of 5-FU and 1 μ M of PTX in HCT116 and MDA-MB-231 cells in adherence, respectively, during 48 h of incubation with either the free drugs or the drugs encapsulated in PM (PM/5-FU or PM/PTX). In both cell lines, PM-CON:SMC2 did not show cytotoxic activity at 48 h.

Despite drug efficacy that was observed, no significant differences were detected between free and encapsulated drugs, with or without Ab-SMC2 in both cell lines cultured in adherent conditions. On the other hand, when treatments were applied against tumorsphere formation, remarkable cytotoxic activity was detected with PM-CON:SMC2 in both cell lines. Interestingly, significant stronger activities were also detected for 5-FU and PTX when encapsulated alone or in combination with SMC2, compared to free drugs (Figure 6c). In fact, no efficacy was detected for PTX in MDA-MB-231 (Figure 6c, right panel). These results indicate that encapsulation of 5-FU and PTX into PM improves their performance, in particular when added to CSC-like cells. Of note, the combination of a classical chemotherapeutic agent with Ab-SMC2 was non-deleterious for both encapsulated 5-FU and PTX formulations offering the possibility of eliminating both subpopulations simultaneously, CSC and “bulk” or differentiated cancer cells.

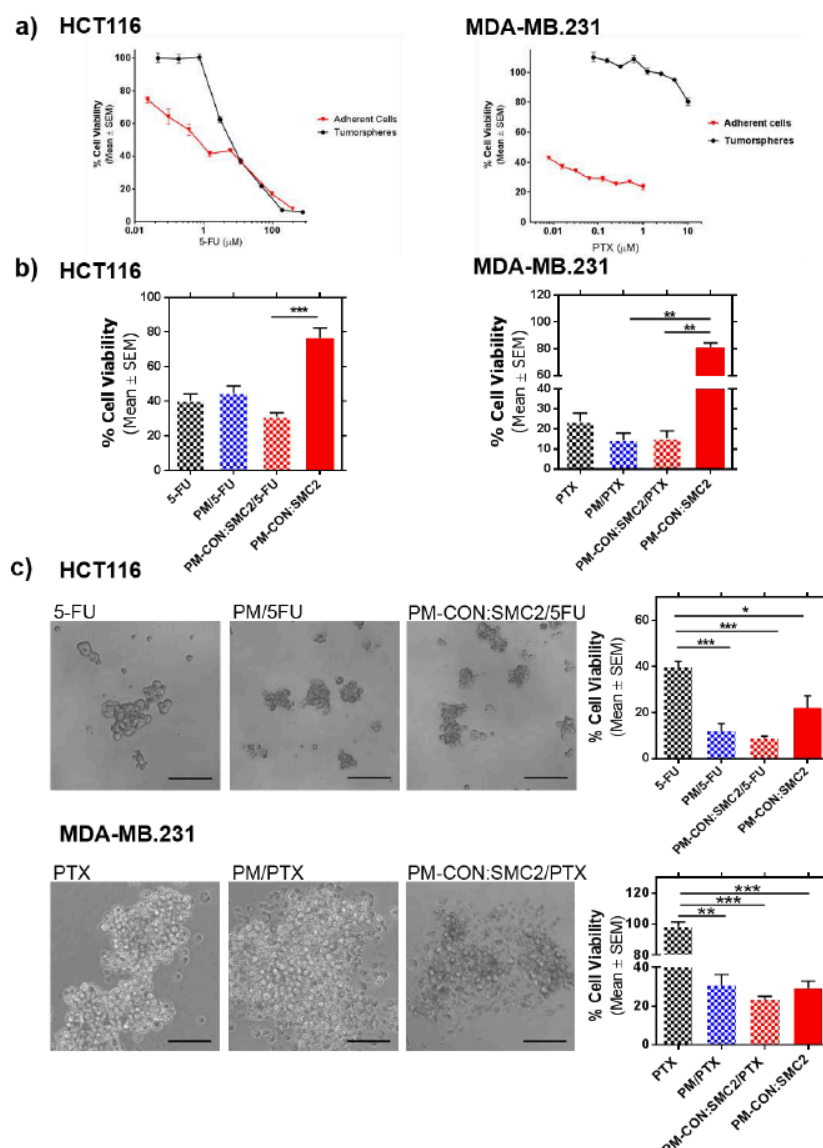


Figure 6. PM-Ab-SMC2/Drug combination. (a) Cell viability curves of HCT116 and MDA-MB-231 cells cultured in adherent culture or as tumorspheres after the incubation of increasing concentrations of 5-FU for HCT116 (from 0.023 μM to 384.40 μM for adherent conditions and from 0.047 μM to 768.86 μM for low-attachment conditions) and PTX for MDA-MB-231 cells (from 0.0078 μM to 1 μM for adherent growing cells and from 0.078 μM to 10 μM for tumorspheres). (b) Efficacy on adherent cells of the free drug (48 μM of 5-FU and 1 μM of PTX), encapsulated drug into PM (0.625 mg/mL for HCT116 and 5 mg/mL for MDA-MB-231 of polymer) and encapsulated drug into PM-CON:SMC2 (4.11 $\mu\text{g/mL}$ for HCT116 and 32.9 $\mu\text{g/mL}$ for MDA-MB-231 of Ab-SMC2). (c) Left panels, microscopy images of HCT116 and MDA-MB-231 spheres after treatment with the free drug (3.84 μM of 5-FU and 0.1 μM of PTX), PM/Drug (1 mg/mL of polymer) and PM-CON:SMC2/Drug (6.58 $\mu\text{g/mL}$ of anti SMC2 antibody). Scale bar correspond to 100 μm . Right panels, sphere formation assay of HCT116 and MDA-MB-231 cells after treatment with the free drug, PM/Drug and PM-CON:SMC2/Drug. * $p < 0.05$, ** $p < 0.01$, *** $p < 0.001$.

4. Discussion

SMC2 forms part of the condensin I and II complexes, thus being a crucial player in several cellular biological processes related to mitotic and meiotic chromosome condensation and rigidity, interphase

ribosomal DNA compaction, as well as removal of cohesion during mitosis and meiosis [15–17]. Moreover, SMC2 overexpression and mutations in some of the condensing subunits had been reported in cancer genomes, suggesting that functional alterations affecting condensin complexes are common in tumorigenesis [19,20]. Given the essential role of SMC2 in the survival of embryonic stem cells, it is reasonable to speculate that SMC2 could play an important function also in the homeostasis of tumoral CSC. This is a relevant issue since finding an efficient target against this subpopulation is of major importance in order to avoid cancer resistance and tumor recurrence [11,13]. Ideally, a therapy should be able to eradicate not only the primary tumor but also CSC that often survive after most conventional treatments. In order to investigate CSC response to new therapeutic strategies, several methods have been described to generate CSC models in vitro [31]. A simple and rapid approach is based on culturing tumor cell lines in non-adherent conditions, exploiting CSC ability to form pseudo-spherical colonies. This method was firstly reported in 1992 by Reynolds and colleagues [32] and lately improved by Tatianna Herheliuk et al., in 2019 [33], among others.

Aiming to validate SMC2 as a CSC target, SMC2 was silenced in different cancer cell lines (HT116, MDA-MB-231 and PANC-1, from colorectal, breast and pancreatic origin) using RNA interference technology. Its effect was assessed in terms of cell viability and colony formation impairment. As predicted, the silencing of SMC2 was able to reduce cell viability in adherent conditions and the formation of spheres for HCT116 cells in non-adherent cultures. In the case of MDA-MB-231 and PANC-1 the effect of SMC2 silencing was only observed in low attachment conditions. This result revealed that SMC2 could be an important target within stem cell subpopulations (Figure 1 and Figure S1). After SMC2 validation as a promising target, different therapeutic silencing strategies were considered. SMC2 silencing by siRNA arose as the most straightforward approach since a previous report by our group showed effective in vivo tumor growth inhibition after ex vivo silencing of the SMC2 gene in tumor cells [18]. However, unforeseen challenges related with siRNA stability and the need to reach high doses to render biological efficacy after i.v. administration, prompted us to choose an alternative strategy [34]. Thus, we attempted to block SMC2 activity by specific interaction with an antibody against the protein. In order to protect the antibody integrity and improve its intracellular delivery, Ab-SMC2 was conjugated with Pluronic® F127-based PM. The use of nanocarriers allows (i) the systemic delivery of high amount of Ab, (ii) to decrease off-target related toxicity in other organs, (iii) to protect the cargo from enzymatic degradation, and (iv) the sustained release of the Ab alone or in combination with other chemo-therapeutic compounds [9]. In the last years, several formulations have been developed for the intracellular release of antibodies. One of them consists of cationic lipid-based carriers, which are also employed for siRNA delivery, as proven by Courtete et al. (2007) [35]. Nonetheless, even though some of these formulations are reaching clinical trials, strong concerns about their reported toxicity are delaying its entrance into the clinical practice. Moreover, inorganic and viral carriers have also been developed but with the same toxicity and immunogenicity concerns that reduce their clinical expectations. Some polymeric-based nanoparticles also has been developed for intracellular delivery such as the polymersomes described by Canton et al. (2013) and Tian et al. (2014) [36,37], or the self-assembling pyridylthiourea modified polyethylenimine nanoparticles designed by Postupalenko et al. (2014) [8]. Although great efforts have been invested until today, the proposed formulations still present important limitations, such as (i) difficult and expensive production methods, (ii) high mean diameter and immunogenicity issues, (iii) lack of endosomal escape capacity, and (iv) toxicity, among others [9]. In this regard, the proposed delivery system solves some of these drawbacks. Accordingly, they are biocompatible and non-immunogenic, present a small size, and can be produced in compliance to a simple and easily scalable production method. In previous studies, we have demonstrated that these PM can be repeatedly administered in vivo without causing toxicities and can accumulate into tumors upon i.v. administration [38]. Furthermore, our PM were previously used to efficiently conjugate Cetuximab, showing an effective active targeting against the epidermal growth factor receptor (EGFR) in overexpressing breast cancer cells [25].

In the present work, we focused into the intracellular delivery of Ab-SMC2 to silence the activity of SMC2 in CSC. For that, Ab-SMC2 was conjugated to PM through two different approaches. The first one consisted in the encapsulation of the antibody into the micelles hydrophilic shield (PM:SMC2). The second one was based on the covalent bonding of the amine groups of the antibody with the carboxylic terminals of the modified polymer (PM-CON:SMC2). As expected, the formulations with Ab-SMC2 presented larger mean diameter. The conjugation was also confirmed by the FTIR where was possible to see the appearance of a peak at 1646 cm^{-1} (Figure 2 and Figure S3). Since the two encapsulation techniques presented adequate physicochemical features and similar association efficiency, both formulations were tested for cell toxicity in HCT116 and MDA-MB-231 colon and breast cancer cells, to evaluate whether the level of exposure to Ab-SMC2 might affect its *in vitro* efficacy. As expected, control PM and free antibody did not show cell toxicity in any tested cell lines. However, when conjugated, Ab-SMC2 showed higher efficacy in terms of cell toxicity and impairment of colony formation, suggesting specific positive activity against CSC. In addition, the way Ab-SMC2 was loaded into the PM might affect the efficacy of the formulation, since a slight higher effect was displayed by cells treated with PM-CON:SMC2 in comparison with the ones treated with PM:SMC2 in both tested cell lines (Figure 3). These results and the fact that the covalent conjugation of Ab-SMC2 would be more stable and controlled, made us select PM-CON:SMC2 for further studies. Moreover, the differential effect observed between free antibody and the one conjugated onto PM was clear when analyzing the morphology of treated cells. Thus, it was possible to detect strong morphologic changes in HCT116 cells and the formation of vacuoles in MDA-MB-231 after treatment with PM-CON:SMC2. In contrast, no changes were detected when cells were treated with free antibody or non-conjugated PM. These data indicate that PM-CON:SMC2 were exerting a specific cytotoxic action visibly affecting cellular structures. This was also in accordance with the results seen in the viability assays.

Additionally, in terms of internalization, PM-CON:SMC2 demonstrated to have a faster uptake when compared with the control PM, probably due to its more negatively charged particle surface and Van der Waals interactions between the functional groups of the particle and the cellular membrane. Confocal microscopy images revealed the co-localization of fluorescently labeled PM with endocytic vesicles, suggesting that PM formulations could enter into the cells via endocytosis, at least partially. Other cellular entry routes cannot be discarded, nonetheless. One of the most critical steps regarding the intracellular delivery of antibodies is the need of their endosomal escape. The antibody must be released to the cytosol before reaching the lysosomes, otherwise it might be degraded inside these vehicles. By analyzing the levels of green fluorescence in the whole cytoplasm, it was possible to conclude that a substantial part of Ab-SMC2 PM was able to escape the endosomes and reach the cytoplasm, where the Ab-SMC2 exert its activity. Importantly, these results strongly support the *in vitro* efficacy outcomes in terms of cell toxicity and colony formation. In order to confirm the biological action of PM-CON:SMC2 inhibiting the SMC2 protein, a cell-cycle assay was performed. Of note, the condensin complex is mostly found in the cell cytoplasm in interphase while during mitosis is found associated to chromatin. Therefore, in order to effectively block SMC2 dimerization and the activity of the condensin complex, the antibody must reach the cell cytosol. Our results demonstrate that at least in the case of HCT116 cells a significant arrest of cell cycle in G1 was driven by the incubation with PM-CON:SMC2, reinforcing our previous results showing a decrease in cell viability. These also suggest the capacity of our system to deliver the antibody to the cell cytoplasm. This pattern, however, was not clear for MDA-MB-231 cells. The effect of the SMC2 inhibition in adherent cultures was restricted to the CSC-like subpopulation in this cell line (Figure 1).

Finally, we further investigated the potential use of PM-CON:SMC2 as adjuvant treatment with Standard-of-Care (SoC) drugs. 5-FU and PTX are the SoC therapy for colon and breast cancer, respectively. Therefore, 5-FU and PTX were loaded into the hydrophobic core of PM-CON:SMC2. In a previous study, we showed that Zileuton™, a drug with reported efficacy in breast CSC, presented higher efficacy when encapsulated in similar micelles than its free form [38]. In agreement with this, both 5-FU and PTX also presented higher efficacy in terms of inhibition of colony formation when

encapsulated into PM-CON:SMC2. Interestingly, both 5-FU and PTX showed increased efficacy when encapsulated into PM, particularly regarding tumorsphere formation. This was remarkable in the case of the MDA-MB-231 cell line, known for its high resistance to most treatments. In this case, no efficacy was detected with free PTX (Figure 6c). Although, we could not detect a clear additive efficacy when treating cells with PM-CON:SMC2 loaded with the respective chemotherapeutic drugs, a significant effect was observed in CSC-like in vitro models in comparison with SoC. Our results suggest that the combination of drugs and Ab-SMC2 delivery might cooperate in the eradication not only of bulk tumor cells but also of cells with stemness properties.

5. Conclusions

SMC2 block emerges as a promise strategy to complement the current therapies based on chemotherapeutic drugs, intending not only to attack bulk tumor cells but also the remaining CSC. The intracellular delivery of antibodies is still considered a challenge; thus, the discovery of a delivery system with this capacity is of major importance. When conjugated with PM, the Ab-SMC2 is able to reach the cytoplasm, block SMC2 action and obtain a significant impairment in the viability of CSC enriched cultures from colon and breast origin. Moreover, PM were adapted for the combinatory delivery of conventional chemotherapeutic agents and potentially improved their performance. Altogether, the present results suggest that the proposed nanosystem gathers ideal features to ensure the intracellular delivery of Ab-SMC2 into cancer cells. More importantly, it is possible to conclude that by combining PM, drugs and Ab-SMC2, we can make an important contribution, not only to the treatment of the primary tumor, but also in the eradication of the CSC population responsible for tumor recurrence and the metastatic spread of the disease.

Supplementary Materials: The following are available online at <http://www.mdpi.com/1999-4923/12/2/185/s1>, Figure S1. SMC2 therapeutic target validation, Figure S2. Stemness gene expression of HCT116 growing in adherent cell cultures or as tumorspheres, Figure S3. FTIR spectra for PM-CON:SMC2 at 100% –COOH, Figure S4. Examples Cell cycle curves fitting.

Author Contributions: S.M., J.S.-F., D.R.: Conceptualization, methodology, formal analysis, data curation, investigation, validation, writing—original draft preparation, writing—review and editing; F.A., F.M.-T., M.V.-H., H.X., M.Q.: methodology, formal analysis, data curation and writing—review and editing; S.S.J., I.A., D.A.: Writing—review and editing, resources, project coordination, administration and funding acquisition. All authors have read and agreed to the published version of the manuscript.

Funding: This research was partially funded by the Networking Research Centre for Bioengineering, Biomaterials and Nanomedicine (CIBER-BBN), Instituto de Salud Carlos III. FA was supported by a post-doctoral grant from Fundação para a Ciência e a Tecnologia (FCT), Portugal. JSF was supported by a post-doctoral grant from Asociación Española Contra el Cáncer (AECC), Spain. FMT was supported by a pre-doctoral grant from Plan Estratégico de Investigación e Innovación en Salud (PERIS), Agència de Qualitat i Avaluació Sanitàries de Catalunya (AQuAS), Spain.

Acknowledgments: We are indebted to the Characterization of Soft-Materials Services at Institut de Ciència de Materials de Barcelona (ICMAB-CSIC), the “Servei d’Alta Tecnologia” at Vall Hebron Research Institute (VHIR) and the “Servei de Microscopia” at the Autonomous University of Barcelona (UAB).

Conflicts of Interest: The authors declare no conflict of interest. A patent on the use of SMC2 as biomarker of colorectal cancer was issued by S.S.J. in 2006.

References

1. Yin, L.; Yuvienco, C.; Montclare, J.K. Protein based therapeutic delivery agents: Contemporary developments and challenges. *Biomaterials* **2017**, *134*, 91–116. [\[CrossRef\]](#)
2. Brekke, O.H.; Sandlie, I. Therapeutic antibodies for human diseases at the dawn of the twenty-first century. *Nat. Rev. Drug Discov.* **2003**, *2*, 52–62. [\[CrossRef\]](#)
3. Scott, A.M.; Wolchok, J.D.; Old, L.J. Antibody therapy of cancer. *Nat. Rev. Cancer* **2012**, *12*, 278–287. [\[CrossRef\]](#)
4. Carter, P.J.; Lazar, G.A. Next generation antibody drugs: Pursuit of the ‘high-hanging fruit’. *Nat. Rev. Drug Discov.* **2018**, *17*, 197–223. [\[CrossRef\]](#)

5. Dixon, C.R.; Platani, M.; Makarov, A.A.; Schirmer, E.C. Microinjection of Antibodies Targeting the Lamin A/C Histone-Binding Site Blocks Mitotic Entry and Reveals Separate Chromatin Interactions with HP1, CenpB and PML. *Cells* **2017**, *6*, 9. [[CrossRef](#)]
6. Heller, L.C.; Heller, R. Electroporation gene therapy preclinical and clinical trials for melanoma. *Curr. Gene Ther.* **2010**, *10*, 312–317. [[CrossRef](#)] [[PubMed](#)]
7. Kumar, S.; Aaron, J.; Sokolov, K. Directional conjugation of antibodies to nanoparticles for synthesis of multiplexed optical contrast agents with both delivery and targeting moieties. *Nat. Protoc.* **2008**, *3*, 314–320. [[CrossRef](#)] [[PubMed](#)]
8. Postupalenko, V.; Sibler, A.P.; Desplancq, D.; Nomine, Y.; Spehner, D.; Schultz, P.; Weiss, E.; Zuber, G. Intracellular delivery of functionally active proteins using self-assembling pyridylthiourea-polyethylenimine. *J. Control. Release* **2014**, *178*, 86–94. [[CrossRef](#)] [[PubMed](#)]
9. Slastnikova, T.A.; Ulasov, A.V.; Rosenkranz, A.A.; Sobolev, A.S. Targeted Intracellular Delivery of Antibodies: The State of the Art. *Front. Pharmacol.* **2018**, *9*, 1208. [[CrossRef](#)]
10. Trenevskaya, I.; Li, D.; Banham, A.H. Therapeutic Antibodies against Intracellular Tumor Antigens. *Front. Immunol.* **2017**, *8*, 1001. [[CrossRef](#)]
11. Gener, P.; Rafael, D.F.; Fernandez, Y.; Ortega, J.S.; Arango, D.; Abasolo, I.; Videira, M.; Schwartz, S., Jr. Cancer stem cells and personalized cancer nanomedicine. *Nanomedicine* **2016**, *11*, 307–320. [[CrossRef](#)] [[PubMed](#)]
12. Asghari, F.; Khademi, R.; Ranjbar, F.E.; Malekshahi, Z.V.; Majidi, R.F. Application of Nanotechnology in Targeting of Cancer Stem Cells: A Review. *Int. J. Stem Cells* **2019**, *12*, 227–239. [[CrossRef](#)] [[PubMed](#)]
13. Gener, P.; Rafael, D.; Schwartz, S.; Andrade, F. The Emerging Role of Nanomedicine in the Advances of Oncological Treatment. In *Nanoparticles in the Life Sciences and Biomedicine*, 1st ed.; Reis, S., Ed.; Pan Stanford Publishing Pte Ltd.: New York, NY, USA, 2018; pp. 269–310.
14. Annett, S.; Robson, T. Targeting cancer stem cells in the clinic: Current status and perspectives. *Pharmacol. Ther.* **2018**, *187*, 13–30. [[CrossRef](#)] [[PubMed](#)]
15. Losada, A.; Hirano, T. Dynamic molecular linkers of the genome: The first decade of SMC proteins. *Genes Dev.* **2005**, *19*, 1269–1287. [[CrossRef](#)] [[PubMed](#)]
16. Belmont, A.S. Mitotic chromosome structure and condensation. *Curr. Opin. Cell Biol.* **2006**, *18*, 632–638. [[CrossRef](#)] [[PubMed](#)]
17. Fazio, T.G.; Panning, B. Condensin complexes regulate mitotic progression and interphase chromatin structure in embryonic stem cells. *J. Cell Biol.* **2010**, *188*, 491–503. [[CrossRef](#)]
18. Davalos, V.; Suarez-Lopez, L.; Castano, J.; Messent, A.; Abasolo, I.; Fernandez, Y.; Guerra-Moreno, A.; Espin, E.; Armengol, M.; Musulen, E.; et al. Human SMC2 protein, a core subunit of human condensin complex, is a novel transcriptional target of the WNT signaling pathway and a new therapeutic target. *J. Biol. Chem.* **2012**, *287*, 43472–43481. [[CrossRef](#)]
19. Ham, M.F.; Takakuwa, T.; Rahadiani, N.; Tresnasari, K.; Nakajima, H.; Aozasa, K. Condensin mutations and abnormal chromosomal structures in pyothorax-associated lymphoma. *Cancer Sci.* **2007**, *98*, 1041–1047. [[CrossRef](#)]
20. Strunnikov, A.V. One-hit wonders of genomic instability. *Cell Div.* **2010**, *5*, 15. [[CrossRef](#)]
21. Zhong, J.; Jermusyk, A.; Wu, L.; Hoskins, J.W.; Collins, I.; Mocci, E.; Zhang, M.; Song, L.; Chung, C.C.; Zhang, T.; et al. A Transcriptome-Wide Association Study (TWAS) Identifies Novel Candidate Susceptibility Genes for Pancreatic Cancer. *J. Natl. Cancer Inst.* **2020**. [[CrossRef](#)]
22. Andrade, F.; Fonte, P.; Costa, A.; Reis, C.C.; Nunes, R.; Almeida, A.; Ferreira, D.; Oliva, M.; Sarmiento, B. Pharmacological and toxicological assessment of innovative self-assembled polymeric micelles as powders for insulin pulmonary delivery. *Nanomedicine* **2016**, *11*, 2305–2317. [[CrossRef](#)] [[PubMed](#)]
23. Andrade, F.; das Neves, J.; Gener, P.; Schwartz, S., Jr.; Ferreira, D.; Oliva, M.; Sarmiento, B. Biological assessment of self-assembled polymeric micelles for pulmonary administration of insulin. *Nanomed. Nanotechnol. Biol. Med.* **2015**, *11*, 1621–1631. [[CrossRef](#)] [[PubMed](#)]
24. Andrade, F.; Almeida, A.; Rafael, D.; Schwartz, S., Jr.; Sarmiento, B. Micellar-Based Nanoparticles for Cancer Therapy and Bioimaging. In *Nanooncology*; Gonçalves, G., Tobias, G., Eds.; Springer International Publishing: Basel, Switzerland, 2018.
25. Rafael, D.; Martínez, F.; Andrade, F.; Seras-Franzoso, J.; Garcia-Aranda, N.; Gener, P.; Sayós, J.; Arango, D.; Abasolo, I.; Schwartz, S. Efficient EGFR mediated siRNA delivery to breast cancer cells by Cetuximab functionalized Pluronic®F127/Gelatin. *Chem. Eng. J.* **2018**, *340*, 81–93. [[CrossRef](#)]

26. Rafael, D.; Gener, P.; Andrade, F.; Seras-Franzoso, J.; Montero, S.; Fernández, Y.; Hidalgo, M.; Arango, D.; Sayós, J.; Florindo, H.F.; et al. AKT2 siRNA delivery with amphiphilic-based polymeric micelles show efficacy against cancer stem cells. *Drug Deliv.* **2018**, *25*, 961–972. [[CrossRef](#)]
27. Ayinde, O.; Wang, Z.; Pinton, G.; Moro, L.; Griffin, M. Transglutaminase 2 maintains a colorectal cancer stem phenotype by regulating epithelial-mesenchymal transition. *Oncotarget* **2019**, *10*, 4556–4569.
28. Botchkina, I.L.; Rowe, R.A.; Rivadeneira, D.E.; Karpeh, M.S., Jr.; Crawford, H.; Dufour, A.; Ju, J.; Wang, Y.; Leyfman, Y.; Botchkina, G.I. Phenotypic subpopulations of metastatic colon cancer stem cells: Genomic analysis. *Cancer Genom. Proteom.* **2009**, *6*, 19–29.
29. Barth, A. Infrared spectroscopy of proteins. *Biochim. Biophys. Acta* **2007**, *1767*, 1073–1101. [[CrossRef](#)]
30. Ryu, I.S.; Liu, X.; Jin, Y.; Sun, J.; Lee, Y.J. Stoichiometric analysis of competing intermolecular hydrogen bonds using infrared spectroscopy. *RSC Adv.* **2018**, *8*, 23481–23488. [[CrossRef](#)]
31. Gener, P.; Gouveia, L.P.; Sabat, G.R.; de Sousa Rafael, D.F.; Fort, N.B.; Arranja, A.; Fernandez, Y.; Prieto, R.M.; Ortega, J.S.; Arango, D.; et al. Fluorescent CSC models evidence that targeted nanomedicines improve treatment sensitivity of breast and colon cancer stem cells. *Nanomedicine* **2015**, *11*, 1883–1892. [[CrossRef](#)]
32. Reynolds, B.A.; Weiss, S. Generation of neurons and astrocytes from isolated cells of the adult mammalian central nervous system. *Science* **1992**, *255*, 1707–1710. [[CrossRef](#)]
33. Herheliuk, T.; Perepelytsina, O.; Ugnivenko, A.; Ostapchenko, L.; Sydorenko, M. Investigation of multicellular tumor spheroids enriched for a cancer stem cell phenotype. *Stem Cell Investig.* **2019**, *6*, 21. [[CrossRef](#)] [[PubMed](#)]
34. Shajari, N.; Mansoori, B.; Davudian, S.; Mohammadi, A.; Baradaran, B. Overcoming the Challenges of siRNA Delivery: Nanoparticle Strategies. *Curr. Drug Deliv.* **2017**, *14*, 36–46. [[CrossRef](#)] [[PubMed](#)]
35. Courtete, J.; Sibler, A.P.; Zeder-Lutz, G.; Dalkara, D.; Oulad-Abdelghani, M.; Zuber, G.; Weiss, E. Suppression of cervical carcinoma cell growth by intracytoplasmic codelivery of anti-oncoprotein E6 antibody and small interfering RNA. *Mol. Cancer Ther.* **2007**, *6*, 1728–1735. [[CrossRef](#)] [[PubMed](#)]
36. Canton, I.; Battaglia, G. Polymersomes-mediated delivery of fluorescent probes for targeted and long-term imaging in live cell microscopy. *Methods Mol. Biol.* **2013**, *991*, 343–351.
37. Tian, X.; Nyberg, S.; Sharp, P.S.; Madsen, J.; Daneshpour, N.; Armes, S.P.; Berwick, J.; Azzouz, M.; Shaw, P.; Abbott, N.J.; et al. LRP-1-mediated intracellular antibody delivery to the Central Nervous System. *Sci. Rep.* **2015**, *5*, 11990. [[CrossRef](#)]
38. Gener, P.; Montero, S.; Xandri-Monje, H.; Diaz-Riascos, Z.V.; Rafael, D.; Andrade, F.; Martinez-Trucharte, F.; Gonzalez, P.; Seras-Franzoso, J.; Manzano, A.; et al. Zileuton loaded in polymer micelles effectively reduce breast cancer circulating tumor cells and intratumoral cancer stem cells. *Nanomedicine* **2019**, *24*, 102106. [[CrossRef](#)]



© 2020 by the authors. Licensee MDPI, Basel, Switzerland. This article is an open access article distributed under the terms and conditions of the Creative Commons Attribution (CC BY) license (<http://creativecommons.org/licenses/by/4.0/>).

Supplementary Materials: Intracellular Delivery of Anti-SMC2 antibodies Against Cancer Stem Cells

Sara Montero, Joaquin Seras-Franzoso, Fernanda Andrade, Francesc Martinez-Trucharte, Mireia Vilar-Hernández, Manuel Quesada, Helena Xandri, Diego Arango, Ibane Abasolo, Diana Rafael and Simó Schwartz Jr.

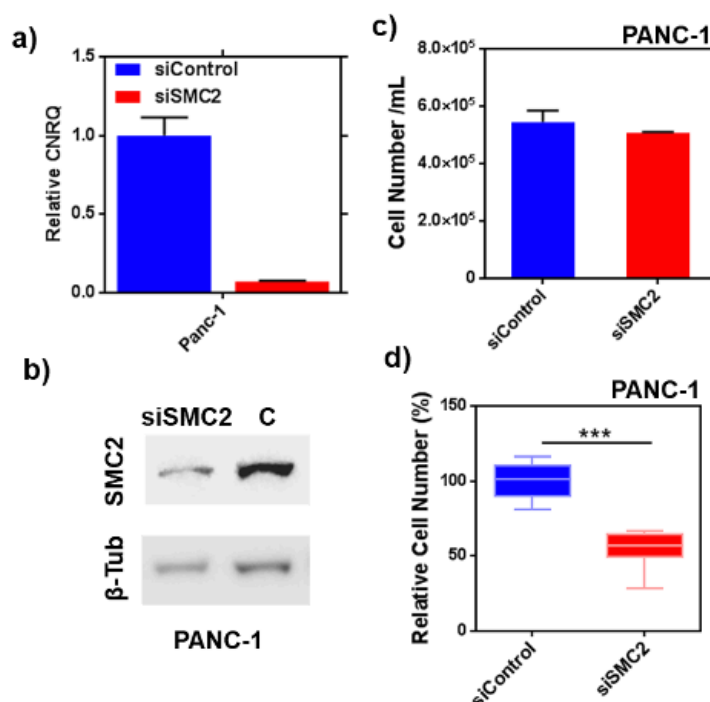


Figure S1. SMC2 therapeutic target validation. a) Relative mRNA levels after SMC2 silencing for PANC-1 pancreatic cancer cell line (siSMC2). Fold change was represented with respect to mRNA levels obtained from non-specific siRNA sequence treated cells (siControl); b) SMC2 and beta-tubulin proteins detected by western blot after SMC2 silencing compared to siControl treated cells (C); c) Cell viability assay for PANC-1 adherent cells after treatment with siSMC2 and siControl; d) Relative cell number percentage for PANC-1 cells growing in non-adherent conditions treated with siSMC2 and siControl.

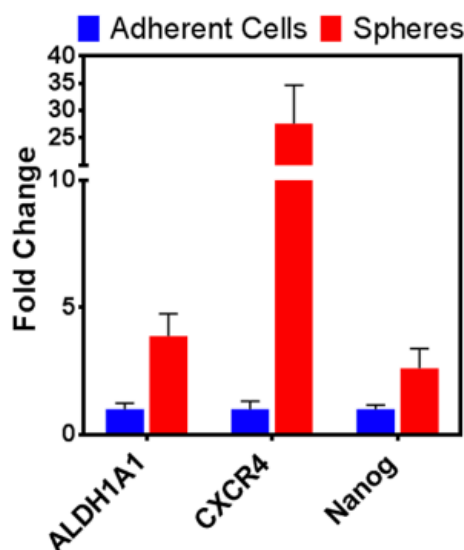


Figure S2. Stemness gene expression of HCT116 cell line growing in adherent cell culture or as tumorspheres (non-attachment). Fold change in gene expression for cells growing as tumorspheres (red bars) are represented with respect to mRNA levels obtained for adherent cells (blue bars). Stemness genes in colon cancer: ALDH1A1, CXCR4 and Nanog were analyzed using GAPDH and β -Actin as housekeeping references.

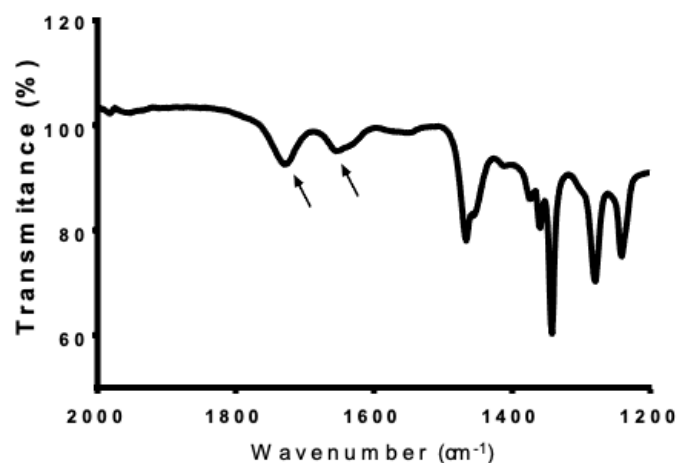
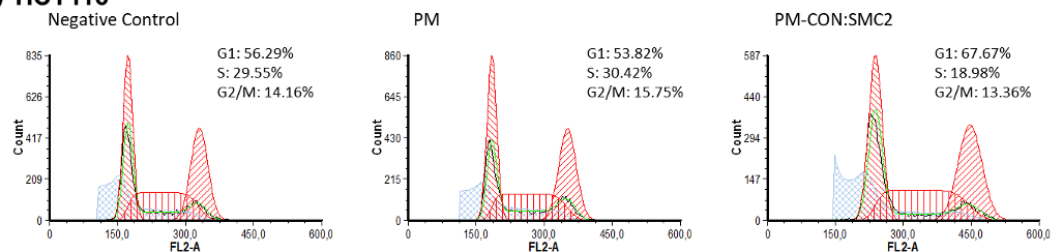
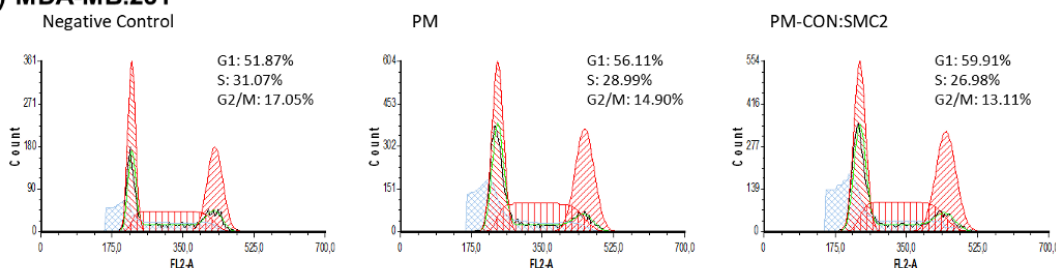


Figure S3: FTIR spectra for PM-CON:SMC2 at 100% -COOH. A peak displayed at 1728 cm^{-1} correspond to the -C=O stretching of the -COOH groups and a peak at 1653 cm^{-1} correspond to the C=O stretching vibrations of the peptide bond of the amide I.

a) HCT116

HCT116	% G1 ± SD	% S ± SD	% G2/M ± SD	G2 / G1
Control	56.291 ± 2.382	29.546 ± 1.205	14.163 ± 1.223	1.900 ± 0.010
PM	53.824 ± 8.322	30.422 ± 7.600	15.754 ± 3.031	1.890 ± 0.031
PM-CON:SMC2	67.667 ± 1.562	18.975 ± 1.212	13.358 ± 0.364	1.876 ± 0.005

b) MDA-MB.231

MDA-MB.231	% G1 ± SD	% S ± SD	% G2/M ± SD	G2 / G1
Control	51.866 ± 7.764	31.086 ± 5.203	17.047 ± 3.049	1.910 ± 0.009
PM	56.111 ± 7.065	28.995 ± 6.389	14.895 ± 0.984	1.902 ± 0.005
PM-CON:SMC2	59.913 ± 6.950	26.977 ± 6.519	13.110 ± 0.459	1.900 ± 0.011

Figure S4: Representative cell cycle analysis of HCT116 colon cell line (a) and MDA-MB-231 breast cell line (b). Plots of cell cycle fitting curves distribution. Below, quantification of the percentage of cells at distinct cell cycle phases: G1, S and G2/M. G2/G1 ratio was also determined.

Discussion

Cancer treatment still represents a clinical challenge with almost ten million deaths per year, being tumor resistance and recurrence two of the main causes of therapeutic failure. Patients suffering from resistant tumors are insensitive to available treatments, and most of them develop distant metastases over time, accounting for more than 90% of cancer-related deaths (15, 118, 354). A broad body of evidence places CSC as the main responsible for this progressive gain of chemo-resistance and the high aggressivity of the recurrent tumors. Taking this into consideration it is of utmost importance the complete eradication of CSC reservoirs to increase the success of the current therapies. In this context, the interest in CSC has been increasing in the last years, which originates an increase in the design of new therapies to specifically target this subpopulation.

Fortunately, the development and clinical implementation of different nanotechnology-based therapies have emerged as promising options to achieve more efficient and safer therapeutic strategies for a wide range of indication, especially focusing on cancer disease. In fact, oncology is one of the sectors that has benefited the most from the nanotechnology revolution, being the first covered therapeutic indication and representing around 37% of the global nanopharmaceutical market (221). In this regard, nano-DDS offer the possibility of converting low-profile therapeutic agents into future clinical drug candidates, thus increasing the therapeutic index of anti-cancer drugs. Among the different materials under investigation, lipids, polymers and proteins stand out, all of them seeking biocompatibility and biodegradability as the main objective in order to generate safe nanocarriers for their implementation in clinical practice. Specifically, PM have been successfully used for their multiple advantages, including: i) versatility to deliver a wide variety of payloads; ii) increased encapsulation capacity and cargo solubility; iii) precise control of physicochemical properties; iv) easy surface modification; v) enhanced cargo bioavailability; and vi) suitable biodistribution patterns, among others (293, 355). All these benefits have allowed the clinical implementation of PM-based nanosystems such as Genexol-PM® and Nanoxel® M (298).

Based on this background, our research group has developed efficient anti-CSC therapeutic strategies mainly focused on the inhibition of specific targets essential for CSC survival by using PM-based nano-DDS, namely Pluronic® F127-based PM.

1. CSC-specific therapeutic target candidates: study and target selection for the design of new nanomedicines against the CSC compartment

Owing to their unique characteristics and dynamic phenotype, CSC are insensitive to conventional therapies while maintaining metastatic spread and tumor relapse. In fact, tumor resistance and recurrence are the main challenge in clinical practice, with CSC being a key factor when improving current anti-cancer treatments (126, 356, 357). Lately, there has been an increase in the number of therapeutic approaches specifically targeting CSC-related pathways, being most of them in preclinical phases and a small percentage in clinical trials (99, 127, 147). However, there are still important handicaps related to the specificity of the recently developed anti-CSC products. Therefore, a proper target selection is of major importance to guarantee the specific target of CSC without damage the somatic stem cells or normal cells.

In this regard, high-throughput screening techniques have proven to be reliable approaches to find new therapeutic targets to design effective and specific treatments against CSC. For example, in the present work the transcriptome of CSC and non-CSC from two BC cell lines: i) MDA-MB-231, a basal-like BC cell line highly aggressive and chemo-resistant; and ii) MCF7, a luminal BC cell line, was analyzed and compared (**Article 1, Figure 1A**). Due to their differential nature and phenotype, the correlation-based clustering analysis of microarray data showed substantial disparity between both analyzed BC cell lines (**Article 1, Figure S1**). Nonetheless, using the microarray results as a cribbage step and further validation through quantitative polymerase chain reaction (q-PCR) of preselected candidates, Alox5 was the only gene significantly overexpressed in CSC subpopulations of these highly distinct BC cell lines (**Article 1, Figure 1A and 1B**). ALOX5 is an oxidative enzyme with a non-heme iron atom in its active site, which in humans is encoded by the Alox5 gene, a member of lipoxygenase gene family (358). It is involved in the regulation of inflammatory responses, degrading essential fatty acids into leukotrienes (LT), pro-inflammatory mediators implicated in many human chronic inflammatory diseases such as asthma, allergic diseases, as well as cancer (359, 360). In this sense, ALOX5 has a crucial role in cancer development, particularly in CSC malignancy, of several cancer types (361-364). Furthermore, clinical data from *The Cancer Genome Atlas* (TCGA) confirmed overexpression (FC > 2) of ALOX5 mRNA in 83.6% of invasive breast cancer patients, 80.5% of patients with ovarian cancer, 75% of patients with lung cancer and 50.3% of patients with colorectal cancer (**Article 1, Figure 1C**). On the molecular level, Chen Y, *et al.* (2011) described a non-canonical pathway regulated by ALOX5 which may explain its involvement in cancer development (365).

Thus, Alox5 inhibition leads to the upregulation of the tumor suppressor gene, macrophage scavenger receptor 1 (Msr1) and, consequently, to the inhibition of PI3K-AKT-GSK-3 β and β -Catenin pathways, both of them crucial signaling routes related to BC development, as well as CSC malignancy and proliferation (366-368). Moreover, in a similar screening, Alox5 gene has been identified as a critical regulator of leukemia stem cells (LSC) in chronic myeloid leukemia (CML), since ALOX5 enzyme deficiency resulted in a significant reduction of LSC in bone marrow and prevents the induction of CML in mice (361, 369, 370). Importantly, no significant influence of ALOX5 deficiency was observed on normal hematopoietic stem cells (HSC), providing the opportunity to only harm CSC without being toxic to somatic stem cells and, therefore, being a selective target for the CSC compartment (361, 370).

On the other side, previous studies by our laboratory group showed a strong inhibition of tumor growth in colorectal cancer mouse models when SMC2 expression was knocked down through *ex vivo* silencing of the SMC2 gene in tumor cells (371). In particular, SMC2 protein is a central component of the condensin I and II complexes which has a key role in many aspects of chromosome biology, including the regulation of gene expression during interphase, chromosomes condensation, and segregation of sister chromatids during cell division (372-374). Condensins are pentameric complexes that requires the initial arrangement of the core SMC2/SMC4 (hCAP-E/hCAP-C) heterodimer, and is completed by the union of three non-SMC subunits (Cnd1, Cnd2 and Cnd3) (375). Importantly, dysfunction or mutations in some human condensin subunits can cause defects in chromosome condensation and segregation, leading to chromosomal instability that has been reported in some cancer genomes (376). Indeed, SMC2 overexpression has been related to tumorigenesis and cancer malignancy, with SMC2 being involved in a significant number of patients with colorectal cancer, pancreatic cancer, gastric cancer, breast cancer, lymphoma and some types of neuroblastoma (371, 376-378). Furthermore, given its crucial function in embryonic stem cell survival, the SMC2 protein is likely to play an important role in tumor CSC homeostasis. Therefore, the blockage of SMC2 dimerization, as well as its condensin complex activity, has emerged as a promising strategy, where SMC2 could be a potential therapeutic target.

Aiming to validate ALOX5 and SMC2 as suitable CSC-specific targets and investigate their response to new therapeutic strategies, CSC subpopulation was isolated using an *in vitro* fluorescent model based on the tdTomato expression under the control of CSC-specific promoter, ALDH1A1 (351). In addition, their behavior was also assessed by

culturing tumor cells under stressful conditions, such as in low adherence and serum deprivation, where only CSC have the ability to survive forming spherical colonies or tumorspheres (379, 380). Of note, cells growing in these conditions display CSC-like features, which serve as a CSC *in vitro* growth model (**Article 2, Figure S2**) (351, 381). In this sense, reinforcing the idea that ALOX5 is specific for CSC subpopulation, its overexpression in mammospheres was confirmed in comparison with normal cancer cells at mRNA and protein expression levels (**Article 1, Figure 1D and Figure 1E**). Noteworthy, Alox5 overexpression was also corroborated in CSC from a battery of TNBC cell lines (**Article 1, Figure 1D**). This result is highly relevant since TNBC is the BC subtype with the worst prognosis, and the only subgroup that currently lacks targeted therapeutic options. Consequently, its treatment is based on ineffective chemotherapies that cause recurrence and, finally, aggressive and lethal metastasis (151). Taking all this into account, we have focused on the design of an anti-CSC strategy based on the inhibition of ALOX5. One of the used strategies consisted in the ALOX5 inhibition by gene silencing using small interfering RNA (siRNA) delivered by PEI-siRNA-Pluronic® nanosystems (309). This study demonstrated that Alox5 silencing caused a significant reduction in the invasion and colony formation capabilities of CSC subpopulation isolated from the MDA-MB-231 TNBC cell line (**Article 3, Figure 5D-F**). Being the invasive potential and cell neoplastic transformation two key hallmarks of the CSC aggressive behavior, the importance of ALOX5 involvement in CSC survival and its potential as a CSC-specific therapeutic target candidate, was again corroborated. The same siRNA technology was used to validate SMC2 as a suitable CSC-specific target. SMC2 silencing caused a reduction in cell viability and a significant impairment in colony formation in different tested cell lines. While the reduction of cell viability was only relevant in the case of HCT116 CRC cell line, the inhibition of colony formation was remarkable in all tested cell lines, namely HCT116 CRC cell line, MDA-MB-231 TNBC cell line, and PANC-1 pancreatic cancer cell line (**Article 2, Figure 1C, Figure 1D and Figure S1**). All these data, together with its central role in cell division, showed that an effective inhibition of the condensin complex activity would prevent cancer cells proliferation, especially in the CSC fraction.

In conclusion, both ALOX5 enzyme and SMC2 protein have demonstrated to meet the essential requirements to become promising CSC-specific therapeutic candidates for the development of novel and more efficient anti-CSC nanomedicines.

2. Different proposed strategies: specific inhibitors selection

Nowadays, there is a wide range of therapeutic options to inhibit specific molecules, block cancer-related proteins, or signaling networks involved in tumor incitation and proliferation. Regarding cancer treatment, small-molecule drugs, antibody-based therapeutics, and gene therapy are among the most common strategies. Their strengths and drawbacks are listed in Table 4.

Table 4: Different inhibition strategies: summary of advantages and drawbacks of different therapeutic approaches for cancer treatment.

Small-molecule drugs		Antibody-based therapeutics		Gene therapy	
Advantages	Drawbacks	Advantages	Drawbacks	Advantages	Drawbacks
Low-cost production	Difficult i.v. administration (Hydrophobic drugs)	Ability to reach undruggable targets	High-cost production	Ability to reach undruggable targets	High-cost production
Low MW	Systemic toxicity and undesired side effects	High specificity	<i>In vivo</i> instability	High specificity	Low stability
Ability to cross cell membranes	Not all targets are druggable	Reduced off-target effects	Immunogenicity related toxicity	Reduced off-target effects	Easy degradation
High stability		High interaction surfaces with targeted protein	Enzymatic degradation	Useful for any type of mutation	Loss of activity <i>in vivo</i>
			Poor intracellular penetration		Insufficient transfection efficiency

MW: molecular weight; *i.v.*: intravenous.

In this project, two different inhibitory strategies have been presented: i) pharmacological approach, and ii) biotherapeutic approach; both designed to eradicate CSC by specifically targeting key molecular pathways involved in CSC survival and proliferation.

For the pharmacological strategy, Zileuton™ has been selected as a specific iron-chelator ALOX5 inhibitor for being the only FDA-approved drug among several ALOX5

inhibitors that has already reached the market as an oral anti-leukotriene drug for the treatment of asthma (382-384). Furthermore, the potential use of ZileutonTM as an anti-cancer drug is currently undergoing clinical trials. Specifically, ZileutonTM (Zyflo®) is in phase I in combination with Imatinib Mesylate (Gleevec®) (NCT01130688) for first-line therapy in patients with CML, since LSC are not eradicated by Imatinib alone (370). In addition, no safety issues have been reported in phase I clinical trials of ZileutonTM (Zyflo®) in combination with Dasatinib (Sprycel®) (NCT02047149) in CML patients, also being in phase II clinical trials aiming to prevent lung cancer in patients with bronchial dysplasia (NCT00056004). Importantly, positive effects for cancer treatment of drugs previously approved for other indications have already been reported, thus facilitating their regulatory process. In fact, Corsello, *et al.* (2020) have tested the antitumor activity of 4518 non-oncology drugs in 578 human cancer cell lines. An unexpected number of drugs selectively inhibited subsets of cancer cell lines, finding that provides an excellent starting point for developing new oncological therapeutics based on drug repurpose and, eventually, enabling their clinical translation (385). In this regard, studies performed in our laboratory have demonstrated the potential of Niclosamide (NCS) in eradicating the CSC subpopulation (341). NCS is an FDA / EMA approved anti-helminthic drug that has shown anti-cancer activity by inhibiting crucial pathways related to proliferation, invasion, and migration, including the Wnt / β -catenin pathway (386, 387).

Nonetheless, ZileutonTM efficacy dose is considerably high regarding future clinical use in the oncology field, as it was designed to reduce the specific inflammation produced by asthma and not to cause cell death (**Article 1, Figure S2**). Additionally, its high hydrophobicity hinders its intravenous (i.v.) administration *in vivo*, requiring its solubilization. Thus, the use of nano-DDS for ZileutonTM delivery was assessed.

On the other side, although the SMC2 inhibition has been validated as a potential therapeutic strategy against CSC, no drugs are currently available for SMC2 protein, being considered an undruggable target. In this sense, different inhibitory therapeutic strategies were evaluated. Initially, SMC2 silencing by siRNA emerged as a possible option due to the positive results previously obtained by our laboratory group (371). However, the limitations associated with the low siRNA stability and its loss of activity *in vivo* after i.v. administration, led us to select an alternative strategy (388). Thus, we opted to block the SMC2 activity through the specific interaction with antibodies against the intracellular protein SMC2. Of note, one of the main advantages of using antibody-based therapies is their high potential to inhibit a wide range of targets, including those that remain unattainable by other strategies, such as SMC2. However, the condensin

complex is mostly located in the cell cytoplasm during interphase with only a minor amount remains associated to the chromatin in the nucleus, being apparently inaccessible to antibodies since they are unable to cross extracellular membranes (389, 390). Thereby, the use of nanoplateforms that allow the clustering of antibodies directed against the SMC2 protein will not only enable their cell penetration but will also protect their integrity by avoiding the cargo enzymatic degradation, which overall increases the intracellular delivery of antibodies.

Since most of the presented limitations presented in Table 4 can be solved using nano-DDS, both promising inhibitors have been encapsulated into the hydrophobic core or conjugated with Pluronic® F127-based PM, obtaining PM-Zileuton™ or PM-CON:SMC2, respectively.

3. The proposed nanosystem based on Pluronic® F127 gather the requirements for an efficient and safe transport of anti-cancer agents

The use of Pluronic® F127-based PM as nano-DDS allows not only to improve the biodistribution patterns of CSC-targeting agents, but also to increase their therapeutic efficacy, while reducing the undesired off-target side effects. In this project, we have produced and characterized Pluronic® F127-based self-assembly PM due to its biocompatibility and biodegradable nature, both essential properties to obtain successful nanomedicines. Specifically, Pluronic® F127 is an FDA-approved biocompatible and biodegradable triblock copolymer, which is composed of PEO-PPO-PEO and had shown to be useful in a wide range of biomedical applications, including nano-DDS synthesis (300, 306, 308). In fact, the first PM formulation for cancer treatment that entered in clinical trials was composed of Pluronic® block copolymers, namely SP1049C, which consists in doxorubicin solubilized in a mixture of Pluronic® F127 and Pluronic® L61 (347).

Our Pluronic® F127-based PM were produced using the thin-film hydration technique, a simple, economic, robust and reproducible production method. Furthermore, being easy to scale-up, thin-film hydration technique is already applied at industrial level. In fact, Genexol-PM® and Nanoxel® M, PM currently on the market, base their production method on this technique, thus making its future clinical implementation feasible (298). Particularly, the physicochemical characterization of the obtained nano-DDS demonstrates a spherical, neutral, small-sized, and monodisperse PM formulation (**Article 1, Figure 3A and Figure 3B; Article 2, Figure 2B and Figure 2C**). While the

small size (< 30 nm) and low polydispersity index (Pdl) values (≤ 0.2) of Pluronic® F127-based PM could be explained by their low CMC that give rise to compact micelles, their neutral surface charge at physiological pH is an intrinsic characteristic of poloxamers (391, 392). Note that when measuring mean diameter (Md) by transmission electron microscopy (TEM) image analysis, the obtained size is slightly smaller as a consequence of the vacuum atmosphere into the TEM column, situation in which PM are dry and do not show their real hydrodynamic radius (**Article 2, Figure 2B and Figure 2C**).

Furthermore, the produced formulation presented high stability at room temperature, maintaining its physicochemical properties over time, namely 30 and 60 days after its production (**Article 1, Figure S3, A**). Besides the large stability time in liquid form, the possibility to lyophilize these PM was studied in order to facilitate the long-term storage of the formulations. No significant differences were observed after the lyophilization and rehydration process in terms of mean hydrodynamic diameters and *in vitro* efficacy of both fresh and lyophilized samples (**Article 1, Figure 3C**). Altogether, the results showed a stable and reproducible formulation, parameters completely required to guarantee the nano-DDS safety and allow its subsequent clinical implementation.

Moreover, stability in serum was also confirmed since no aggregates appeared after 24h of incubation with bovine serum components (**Article 1, Figure S3, B**). Being a critical characteristic for drug delivery, the obtained stability suggested that PM may be suitable for *in vivo* applications, particularly for i.v. administration. The observed PM stability is due to the presence of external PEG regions of the Pluronic® F127 triblock copolymer, which act as a shell mask for the biological environment, known as stealth properties. These intrinsic features enhance particle stability and protect PM from protein opsonization, avoiding their premature removal before they reach their target sites. In addition, the small size of obtained micelles (< 30 nm) also helps to prevent their clearance by the RES, thus increasing their half-life in blood stream. Importantly, another benefit related to the PM small size is their ability to easily penetrate through the tumor fenestrations, even in poorly permeable tumors, passively accumulating in the lesion area due to the so-called EPR effect (237).

In order to verify that PM are able to enter in the cells of interest, internalization studies at different time-points were performed for each one of the prepared formulations. Therefore, the uptake profile of Pluronic® F127-based fluorescent-labelled PM was assessed quantitatively by flow cytometry (**Article 1, Figure 4A; Article 2, Figure 4A**) and qualitatively by confocal microscopy (**Article 1, Figure 4B; Article 2, Figure 4B and**

Figure 4C). Generally, the produced PM were completely internalized after few hours of incubation with cells (**Article 1, Figure 4; Article 2, Figure 4 A-C**). Moreover, yellow dots were observed due to the co-localization of the fluorescently labeled 5-DTAF-PM, in green, with the endocytic vesicles, in red (**Article 1, Figure 4B; Article 2, Figure 4B**), showing that at least part of PM were internalized via endocytosis. Importantly, since both selected targets, ALOX5 and SMC2, are intracellular proteins, it is necessary that ZilteutonTM and Ab-SMC2 reach the cytosol to perform their biological function. However, unlike small-molecule drugs that by their low molecular weight are able to easily cross cell membranes through passive diffusion, antibodies exhibit difficulties to achieve endosomal escape, being one of the most critical steps regarding the intracellular delivery of antibodies. In fact, antibody-based therapies are currently limited to extracellular targets due to the difficulties related to their internalization process (393, 394). Although several delivery approaches have been explored in the last years, there is still no efficient system for the intracellular delivery of antibodies (395, 396).

In this sense, poloxamers have shown the ability to interfere with cell membranes and decrease their microviscosity (290, 397), thus facilitating the Ab-SMC2 endosomal escape possibly via pore formation and membrane disruption. Consequently, aiming to confirm the intracellular delivery of Ab-SMC2, the green fluorescence in the whole cell cytoplasm was evaluated after incubation with Pluronic® F127-based PM-CON:SMC2 (**Article 2, Figure 4C**). The results showed a significant increase in fluorescence intensity, which indicates that a substantial part of Ab-SMC2 was able to escape the endosomes, avoiding their degradation by the lysosomes acidic pH. In addition, the intracellular delivery of Ab-SMC2 was also confirmed with the *in vitro* efficacy outcomes, results that are discussed in the following sections.

Noteworthy, problems related to toxicity are among the possible limitations when developing nano-DDS. In this context, the proposed system did not present significant toxicity both *in vitro* (**Article 1, Figure 6A and Figure 6B; Article 2, Figure 3 and Figure 5**) or *in vivo* (**Article 1, Figure 5 and Figure S5**), which is in accordance with the aforementioned Pluronic® F127 biocompatibility. Note that when tested in low-attachment conditions, empty PM are slightly toxic (**Article 1, Figure 6C; Article 2 Figure 5**). Nonetheless, since no adverse effects were observed in *in vivo* studies, the resulting toxicity has been attributed to the CSC-like model culture conditions, namely serum starvation and surface contacts absence. In fact, when treating cells once tumorspheres are completely formed, PM do not cause toxicity (data not shown). Importantly, PM can be repeatedly intravenously administrated *in vivo* without causing

undesired toxicity at the maximum feasible dose (MFD) of ZilutonTM (15 mg/kg, three times per week during three weeks), where no significant loss of weight or any alteration in mice overall well-being was detected (**Article 1, Figure S5**).

Another key factor to evaluate the nano-DDS safety and efficacy is its biodistribution pattern. Our results demonstrated that PM were able to reach and accumulate in the tumor area (mammary gland in the left caudal area) through passive targeting, with almost 10% of the injected dose detected 24 and 72 h post-administration (**Article 1, Figure 5**). This result is highly relevant since, for free drugs, the average rate of tumor accumulation is 0.1% of the total dose, thus corroborating the potential of Pluronic® F127-based PM in the oncological field (398). On the other side, nanomedicines tend to accumulate in different organs such as liver, lung, and spleen due to their vascular fenestrations and the presence of the RES. In this regard, the results showed an accumulation of 14% in liver, 13% in lung and 6% in spleen 24 h post-injection. However, fluorescent signals in plasma, kidney, lungs and muscle diminish between 24 and 72 h post-administration, indicating that micelles are cleared out from these organs (**Article 1, Figure 5**). Of note, similar biodistribution profiles were observed with NCS-loaded PM functionalized with Fab-CD44v6 in CRC models (341).

Additionally, another micellar formulation with similar physicochemical properties also produced in our laboratory, namely PEI-siRNA-Pluronic® F127-based PM, was used to assess its behavior in the blood stream (128). Thus, this formulation was able to extravasate from blood circulation to the tumor mass in an *in vivo* pancreatic cancer model, which is in accordance with our biodistribution obtained results. Of note, thanks to the obtained PM small size, around 25 nm, higher local accumulation in tumor lesions is promoted by the EPR effect, being reported the ability of 30 nm PM to penetrate poorly permeable tumors, including challenging pancreatic tumors (237).

Altogether, the proposed nano-DDS based on Pluronic® F127 amphiphilic triblock copolymer meets all the required physicochemical parameters for an efficient and safe transport, providing several benefits for the development of targeted therapeutic strategies against CSC fraction.

4. Pluronic® F127-based PM significantly increases its cargo therapeutic efficacy, particularly in the challenging fraction of CSC

Aiming to functionally validate the antitumor effects against CSC subpopulation *in vitro*, both selected CSC-specific targets were inhibited. Regarding the pharmacological approach, the specific FDA-approved iron-chelator ALOX5 inhibitor, Zileuton™, showed anti-CSC efficacy since its IC₅₀ score was significantly reduced when cells were grown under serum starvation and low attachment conditions, optimal environment for CSC culture (**Article 1, Figure 2A**). In fact, ALOX5 overexpression was also significantly increased in these conditions, which may explain its higher sensitivity to Zileuton™ treatment, thus confirming the feasibility of using this ALOX5 chemical inhibitor to specifically eradicate the CSC fraction (**Article 1, Figure 1D and Figure 1E**). Furthermore, the transformation capacity of CSC was significantly abolished by Zileuton™, in a concentration-dependent manner, also impairing the proper colony formation (**Article 1, Figure 2B**). Of note, this anchorage-independent growth ability is an important CSC hallmark involved in their malignancy, being low attachment condition not only a specific CSC growth model where normal cancer cells are not able to survive, but also serve as a model for CTC in the blood stream, which are destined to form metastases (399). Thus, an effective eradication of CSC in low adherence conditions is related to proper removal of metastatic founders *in vivo*. Importantly, similar effects were shown after the SMC2 silencing, where a significant decrease of tumorspheres proliferation was detected in all tested cell lines, CSC-like models (**Article 2, Figure 1D and Figure S1, D**). Therefore, ALOX5 and SMC2 involvement in CSC survival reinforce their suitability as specific targets to develop novel targeted therapeutic strategies against CSC subpopulations, which is crucial to overcome CSC resistance and is also in accordance with the current market trend. In fact, 18 of the 19 anti-cancer drugs approved by the FDA between 2012 and 2014 were already targeted drugs, which based their action mechanism on inhibiting specific cancer-related proteins or pathways, unlike the unspecific and toxic conventional chemotherapies (241).

Noteworthy, both proposed strategies showed higher therapeutic efficacy in terms of IC₅₀ and cell viability reduction, when the molecules were loaded into the hydrophobic core of PM or conjugated onto their hydrophilic shell, PM-Zileuton™ or PM-CON:SMC2, respectively (**Article 1, Figure 6A; Article 2, Figure 3**). Further, the transformation capacity of MDA-MB-231 cells was significantly decreased more than two-fold by PM-Zileuton™ compared to free Zileuton™ (**Article 1, Figure 6B**). Importantly, in the

particular case of PM-CON:SMC2 formulation, the conjugation of Ab-SMC2 permit the antibodies to have a biological effect, since the free antibody did not show capacity to cross cell membrane and exert its effect. Interestingly, when conjugated, Ab-SMC2 were able to change cell morphology in HCT116 cell line, showing a stretched shape and forming less clusters compared to free Ab-SMC2 (**Article 2, Figure 3A above panel**). For MDA-MB-231 cell line, an increased number of vacuoles were observed, whereas no such structures were detected after free Ab-SMC2 and control PM treatment (**Article 2, Figure 3A below panel**). In addition to exerting visible action modifying cellular structures, the biological action of PM-CON:SMC2 blocking cytosolic SMC2 protein was assessed through a cell cycle assay. A significant cell cycle arrest in G1 after PM-CON:SMC2 treatment reinforces the observed decreases in cell viability. Moreover, these results are in accordance with the green fluorescence observed by confocal microscopy in the cell cytoplasm, showing the capacity of the proposed system to deliver antibodies intracellularly (**Article 2, Figure 4C, Figure 4D and Figure S4**).

Additionally, the use of nano-DDS is of utmost importance when targeting the CSC subpopulation in order to circumvent CSC-related toxicity. In this regard, the obtained results demonstrate that anti-CSC efficacy have been displayed by both proposed Pluronic® F127-based PM formulations in tumorsphere models compared to adherent cell cultures, with higher efficacies achieved by the encapsulated option (**Article 1, Figure 6C; Article 2, Figure 5, Figure 6B and Figure 6C**). As a result, increased cell toxicity and impaired colony formation were observed, suggesting positive specific activity against the CSC subpopulation and confirming that the ALOX5 and SMC2 blockage using nano-DDS is crucial to eliminate these cancer-sustaining cells (**Article 1, Figure 6C; Article 2, Figure 5**). Similar results were also obtained with the same NCS-loaded functionalized Pluronic® F127-based PM for advanced CRC treatment (341). Furthermore, PM designed for gene delivery have also shown efficacy at eliminating the most resistant cancer cells in previous experiments using PEI-siRNA-Pluronic® F127-based PM (**Article 3, Figure 5D-F**) (128, 309).

In addition, the use of Pluronic® F127 as a nanoplatform for ZileutonTM and Ab-SMC2 delivery not only improve their therapeutic efficacy against CSC fraction, but also make their in vivo administration possible. Importantly, thanks to their structural versatility, PM also allow the co-loading of different therapeutic agents on the same nanoplatform, providing the possibility of performing a combined therapy (discussed in the following section).

5. Pluronic® F127-based PM proposed strategies are effective against CSC fraction when conventional treatments show resistance

Exhibiting high expression levels of drug efflux transporters and unregulated DNA repair machinery, CSC are intrinsically resistant to conventional anti-cancer treatments, therefore MDR-related problems still represent a great challenge in the clinical practice (63, 400). In particular, Paclitaxel (PTX) and 5-Fluorouracil (5-FU) are the standard of first-line treatment for BC and CRC, respectively (203, 401). These types of drugs are only effective eradicating differentiated tumor cells, while resistant CSC remain intact. In this regard, our results showed strong resistance when cells growing in tumorspheres, CSC-like models, were treated with PTX or 5-FU compared to their activity in cells growing in adherent cultures (**Article 1, Figure 6C; Article 2, Figure 6A**). Noteworthy, the effect of CSC-related resistance was remarkably observed in the highly aggressive MDA-MB-231 basal-like BC cell line, remaining its cell viability around 100% at the maximum tested doses, 1 μ M (**Article 1, Figure 6C**) or 10 μ M (**Article 2, Figure 6A**), in cells growing in serum-deprived medium and without surface contacts. Importantly, when common treatments currently used in clinical settings showed high resistance, both proposed anti-CSC strategies based on Pluronic® F127 PM were substantially effective in terms of cell viability reduction and colony formation impairment (**Article 1, Figure 6C and Figure S4; Article 2, Figure 6C**), result that is of utmost importance in the TNBC model since it currently lacks specific options available in clinical practice.

Indeed, PM based on Pluronic® block copolymers have the potential to improve the efficacy of the loaded agent by increasing its intracellular accumulation while circumventing MDR mechanisms and, finally, enhancing the overall treatment efficiency (62, 402). In this sense, Kabanov, *et al.* (2008) have discovered that poloxamers reduce the MDR capacity of cancer cells by interfering with the function of efflux transporters, inducing ATP depletion, as well as increasing pro-apoptotic signaling, among other mechanisms (301, 310). Thus, since CSC present most of the features of MDR cells, Pluronic® F127-based PM exhibit the capacity to improve the antitumor efficacy of both ZileutonTM and Ab-SMC2, especially in the CSC fraction, as shown in **Article 1, Figure 6B and Figure 6C; Article 2, Figure 5**. Of note, being helpful to overcome drug resistance, several Pluronic®-based PM encapsulating commonly used chemotherapeutics have been explored, where the cytotoxic activity of PTX was significantly increased in PTX-resistance models (403, 404). In fact, NK105 (phase III, NCT01644890) is a PTX-incorporating micellar NP formulation that is currently being tested in clinical trials for BC treatment (405), whereas Genexol-PM® is already

approved in Korea and is being evaluated in EU and USA as Cynviloq® for the treatment of breast, ovarian and non-small cell lung cancers (344, 345). Accordingly, regarding our results, when encapsulated in Pluronic® F127-based PM, PTX improves its performance showing increased efficacy compared to the free drug, especially in tumorsphere growth models, where no effect was detected for free PTX in MDA-MB-231 resistant cell line (**Article 2, Figure 6C**). Altogether, these results confirm the great potential of the proposed micelles to overcome CSC-related resistance and prevent future cancer relapses.

Furthermore, the presence of CSC represents an important challenge when developing new and more effective therapies since they are not only intrinsically resistant to traditional treatment strategies, but also their percentage within the tumor often increases after chemotherapy, being only small fraction of them enough to re-grow the entire tumor (62, 122). In this regard, we assessed the relative abundance of CSC subpopulation before and after treatment, aiming to mimic the chemotherapy cycles performed in clinical practice. Notably, while after conventional drugs treatment, PTX and Abraxane® (ABX), the CSC content was increased, Zileuton™ significantly abolished the relative increase of CSC, particularly in the resistant MDA-MB-231 BC cell line (**Article 1, Figure 2C**). ABX is an albumin-bound paclitaxel nanoparticle (nab-PTX) that has been approved by EMA for metastatic BC (mBC). Being a solvent-free formulation, nab-PTX permits higher administration doses with shorter infusion duration, thus increasing the drug concentration that reaches the tumor area (406). However, despite the promising clinical results treating the primary tumor, ABX did not show efficacy in terms of CSC eradication. In fact, it was demonstrated that CSC remain in the lesion after the first tumor treatment with ABX, which originates a secondary lesion with more aggressive phenotype (407). Taking all this into account it is possible to assume that the ideal anti-cancer therapy would consist in a combination of molecules able not only to treat the primary tumor, but also to eradicate the reminiscence CSC, thus avoiding the formation of a recurrent tumor.

In this context, we have also explored the combination therapy strategy, mixing our proposed anti-CSC therapeutic strategies with either PTX and ABX or 5-FU, standard of care (SoC) drugs commonly used in the clinical settings against breast and colorectal cancers, respectively. Regarding the pharmacological model, no additive effect was observed when comparing the cell viability of CSC growing in both adherent and low adherent conditions treated with PM-Zileuton™ alone or in combination with PTX or ABX (**Article 1, Figure S4**). Conversely, in the biotherapeutic model, taking the advantage

provided by the amphiphilic PM plasticity, the co-encapsulation of PTX or 5-FU into the hydrophobic core of PM-CON:SNC2 was assessed. Although no significant synergistic effect could be detected at tested concentrations, after combined treatment, a remarkable reduction in cell viability was observed in tumorsphere models compared to free SoC drugs (**Article 2, Figure 6C**). Therefore, it would be interesting to perform a study with different concentration ranges to find synergistic concentrations that improve the efficacy of the combined therapy.

Nevertheless, our results have shown the feasibility of the proposed nano-DDS of being able to co-delivery different types of therapeutic agents that cooperate to simultaneously eliminate both tumor cell subpopulations, CSC and differentiated cancer cells. Of note, this co-administration has emerged as a promising therapeutic option, as the unique eradication of differentiated tumor cells or CSC may not result in the complete cancer cure. Furthermore, since there is a constant need for the presence of CSC within the tumor, removed CSC are constantly replaced by new cells with stemness phenotype arising from a de-differentiation process or reversion of non-CSC, thus ensuring tumor survival and propagation after treatment. Therefore, the ideal option should be able to eradicate not only the primary tumor but also the metastatic disease caused by surviving CSC, as well as avoid interconversion from non-CSC to CSC; a challenging goal that can be achieved with the implementation of an efficient combination therapy (Figure 5, Introduction section).

6. ZileutonTM loaded in Pluronic® F127-based PM effectively reduces intratumoral CSC and CTC in *in vivo* BC models

The anti-CSC therapeutic potential of PM-ZileutonTM was also demonstrated in *in vivo* orthotopic breast CSC fluorescent models. For that purpose, all injected cells expressed GFP under CMV promotor to detect CTC in the blood stream and tdTomato under ALDH1A1 promotor to determine the CSC content within the tumor by flow cytometry, green and red fluorescence, respectively. Remarkably, PM-ZileutonTM significantly reduced the amount of intratumoral CSC compared to non-treated animals in both BC models, namely from 58.00% \pm 9.00% to 37.20% \pm 4.70% in MDA-MB-231, and from 33.43% \pm 3.18% to 17.98% \pm 6.25% in MCF7 (**Article 1, Figure 7A**). Nevertheless, no differences in primary tumor size were observed (**Article 1, Figure S6**), which is in accordance with the CSC amount present in the entire tumor mass. The number of CSC has been reported to vary between 0.1 to 30% depending on cancer type and stage (402). In this sense, since ZileutonTM specifically impairs the CSC survival by inhibition

of ALOX5 overexpression, it is not expected that cause direct effects on primary tumor growth. Consequently, the reduction of intratumoral CSC led to an effective eradication of CTC from the blood stream in the highly metastatic MDA-MB-231 BC model after PM-ZileutonTM treatment (**Article 1, Figure 7B**). Of note, the decrease in the number of CSC subsequently reduced their intravasation and invasion capacities, which was directly related to the abolition of CTC detected in blood. This is a promising result due to their involvement in the disease dissemination (408).

Therefore, taking into account the key role of CSC and CTC in metastatic spread, we hypothesized a positive effect on metastases reduction after PM-ZileutonTM treatment. In this regard, the presence of secondary lesions in the pulmonary area was examined since, following the organotropism concept, lungs have been described as one of the main affected organs in breast metastases (41). As expected, metastatic foci from TNBC *in vivo* model were significantly smaller in treated animals, thus being confirmed the potential of PM-ZileutonTM as anti-metastatic agent. Finally, in order to be able to perform a complete tumor eradication, the next step should be the combination therapy of our PM-ZileutonTM with conventional chemotherapies, therefore improving the SoC therapies currently available for the treatment of metastatic disease. The actual implementation of this kind of cocktail in clinical settings would improve the overall outcomes and bring new hopes in the treatment of this challenging disease.

Conclusions

The clinical implementation of anti-CSC therapies to overcome tumor drug resistance and improve the overall therapeutic efficacy of cancer treatment is of utmost importance. Therefore, two innovative anti-CSC therapeutic strategies for advanced cancer treatment based on nano-DDS have been developed, characterized and successfully tested. The reached objectives are described below:

1. ALOX5 enzyme and SMC2 protein were validated as promising CSC-specific targets, thus being suitable candidates for the development of new nanotechnology-mediated therapeutic strategies.
2. Two types of Pluronic® F127-based PM were developed, aiming to show two different inhibitory strategies for breast and colon cancer treatments, namely the pharmacological and the biotherapeutic approaches.
3. The proposed nanosystems met the essential requirements to allow safe transport and become an efficient anti-CSC therapy. Pluronic® F127-based PM formulation was stable, monodisperse, and lyophilizable, where no significant toxicity was observed both *in vitro* or *in vivo*. Furthermore, the biodistribution pattern of the micelles showed values around 10% of tumor accumulation.
4. Both produced formulations, PM-ZileutonTM and PM-CON:SMC2 were able to reach the cytoplasm and block their specific target, ALOX5 and SMC2, respectively. Increased therapeutic efficacy was shown in terms of cytotoxicity and impairment of colony formation compared to their free compounds.
5. Both PM-ZileutonTM and PM-CON:SMC2 formulations were effective overcoming CSC-related resistance compared to currently available SoC therapies, even in the highly aggressive MD-MB-231 TNBC cell line.
6. Combination therapy offers the possibility of eliminating both CSC and differentiated tumor cells subpopulations. In this regard, Pluronic® F127-based PM showed the feasibility of co-load small-molecule drugs, including PTX and 5-FU, into the hydrophobic core of decorated PM-CON:SMC2 micelles. Combined micelles significantly improve their performance in CSC-like models compared to conventional chemotherapeutic agents.

7. The administration and therapeutic efficacy evaluation of PM-ZileutonTM was possible in *in vivo* orthotopic BC models, showing its potential as anti-metastatic agent. Altogether, this type of treatment in combination with those that target differentiated tumor cells will prevent tumor recurrence and improve the therapeutic outcomes of patients with advanced cancer.

In fact, these types of combined nanomedicines would provide a potential option to improve the current treatment of metastatic disease and may represent the future of cancer treatment. Furthermore, the use of nano-DDS is a helpful tool for the design of new therapeutic strategies based on personalized medicine. In this regard, the current oncology market is moving from the first-generation of nanopharmaceuticals to the new generation of NP-based delivery systems, where biotherapeutics (e.g. antibodies, nucleic acids, and recombinant proteins, among others) are gaining more importance. Importantly, due to their unique specificity, they exhibit high therapeutic potential and offer promising opportunities, being able to target specific mutations.

In this context, our proposed nanoplatform enables the safe and efficient administration of this type of molecules alone or in combination with small-molecule drugs. Furthermore, Pluronic® F127-based PM are capable of being covalently functionalized with different types of moieties to perform active targeting. Therefore, by modifying the PM surface, we would expect to achieve enhanced specificity, higher cellular penetration once at the tumor site, as well as improved *in vivo* responses. Finally, proper optimization of targeted nano-DDS in order to obtain robust, reproducible and scalable nanosystems are some of the challenges of this second-generation NP-based delivery systems. Nevertheless, all these requirements are necessary to obtain approval from regulatory agencies and reach their actual clinical implementation. Despite the aforementioned difficulties, an increase in these next-generation products is expected in the following years, bringing new and more effective therapies to cancer patients.

References

1. World Health Organization. [online] WHO [Accessed 5th of May 2021] Available from: <http://www.who.int/cancer>.
2. Siegel RL, Miller KD, Jemal A. Cancer statistics, 2020. *CA Cancer J Clin*. 2020;70(1):7-30.
3. Christopher P. Wild EW, Bernard, Stewart. W. World cancer report: cancer research for cancer prevention 2020.
4. Bray F, Ferlay J, Soerjomataram I, Siegel RL, Torre LA, Jemal A. Global cancer statistics 2018: GLOBOCAN estimates of incidence and mortality worldwide for 36 cancers in 185 countries. *CA Cancer J Clin*. 2018;68(6):394-424.
5. Vasan N, Baselga J, Hyman DM. A view on drug resistance in cancer. *Nature*. 2019;575(7782):299-309.
6. Wu S, Zhu W, Thompson P, Hannun YA. Evaluating intrinsic and non-intrinsic cancer risk factors. *Nat Commun*. 2018;9(1):3490.
7. Anand P, Kunnumakkara AB, Kunnumakara AB, Sundaram C, Harikumar KB, Tharakan ST, et al. Cancer is a preventable disease that requires major lifestyle changes. *Pharm Res*. 2008;25(9):2097-116.
8. Bray F, Jemal A, Grey N, Ferlay J, Forman D. Global cancer transitions according to the Human Development Index (2008-2030): a population-based study. *Lancet Oncol*. 2012;13(8):790-801.
9. Estimated cancer incidence, mortality, and prevalence worldwide in 2020 WHO [online] WHO [Accessed 5th of September 2021] Available from: <https://gco.iarc.fr/today/home>.
10. Sadikovic B, Al-Romaih K, Squire JA, Zielenska M. Cause and consequences of genetic and epigenetic alterations in human cancer. *Curr Genomics*. 2008;9(6):394-408.
11. Hanahan D, Weinberg RA. The hallmarks of cancer. *Cell*. 2000;100(1):57-70.
12. Hanahan D, Weinberg RA. Hallmarks of cancer: the next generation. *Cell*. 2011;144(5):646-74.
13. Darwiche N. Epigenetic mechanisms and the hallmarks of cancer: an intimate affair. *Am J Cancer Res*. 2020;10(7):1954-78.
14. Timp W, Feinberg AP. Cancer as a dysregulated epigenome allowing cellular growth advantage at the expense of the host. *Nat Rev Cancer*. 2013;13(7):497-510.
15. Fares J, Fares MY, Khachfe HH, Salhab HA, Fares Y. Molecular principles of metastasis: a hallmark of cancer revisited. *Signal Transduct Target Ther*. 2020;5(1):28.
16. Massagué J, Obenauf AC. Metastatic colonization by circulating tumour cells. *Nature*. 2016;529(7586):298-306.
17. Kalluri R, Weinberg RA. The basics of epithelial-mesenchymal transition. *J Clin Invest*. 2009;119(6):1420-8.
18. Ribatti D, Tamma R, Annese T. Epithelial-Mesenchymal Transition in Cancer: A Historical Overview. *Transl Oncol*. 2020;13(6):100773.
19. Lamouille S, Xu J, Derynck R. Molecular mechanisms of epithelial-mesenchymal transition. *Nat Rev Mol Cell Biol*. 2014;15(3):178-96.
20. Thiery JP, Acloque H, Huang RY, Nieto MA. Epithelial-mesenchymal transitions in development and disease. *Cell*. 2009;139(5):871-90.
21. Zeisberg M, Neilson EG. Biomarkers for epithelial-mesenchymal transitions. *J Clin Invest*. 2009;119(6):1429-37.
22. Micalizzi DS, Farabaugh SM, Ford HL. Epithelial-mesenchymal transition in cancer: parallels between normal development and tumor progression. *J Mammary Gland Biol Neoplasia*. 2010;15(2):117-34.
23. Kalluri R. EMT: when epithelial cells decide to become mesenchymal-like cells. *J Clin Invest*. 2009;119(6):1417-9.
24. Niessen CM, Leckband D, Yap AS. Tissue organization by cadherin adhesion molecules: dynamic molecular and cellular mechanisms of morphogenetic regulation. *Physiol Rev*. 2011;91(2):691-731.

25. Xu J, Lamouille S, Derynck R. TGF-beta-induced epithelial to mesenchymal transition. *Cell Res.* 2009;19(2):156-72.
26. Kim WK, Kwon Y, Jang M, Park M, Kim J, Cho S, et al. β -catenin activation down-regulates cell-cell junction-related genes and induces epithelial-to-mesenchymal transition in colorectal cancers. *Sci Rep.* 2019;9(1):18440.
27. Keely PJ. Mechanisms by which the extracellular matrix and integrin signaling act to regulate the switch between tumor suppression and tumor promotion. *J Mammary Gland Biol Neoplasia.* 2011;16(3):205-19.
28. Kumar V, Vashishta M, Kong L, Wu X, Lu JJ, Guha C, et al. The Role of Notch, Hedgehog, and Wnt Signaling Pathways in the Resistance of Tumors to Anticancer Therapies. *Front Cell Dev Biol.* 2021;9:650772.
29. De Craene B, Berx G. Regulatory networks defining EMT during cancer initiation and progression. *Nat Rev Cancer.* 2013;13(2):97-110.
30. Puisieux A, Brabletz T, Caramel J. Oncogenic roles of EMT-inducing transcription factors. *Nat Cell Biol.* 2014;16(6):488-94.
31. Stemmler MP, Eccles RL, Brabletz S, Brabletz T. Non-redundant functions of EMT transcription factors. *Nat Cell Biol.* 2019;21(1):102-12.
32. Lambert AW, Pattabiraman DR, Weinberg RA. Emerging Biological Principles of Metastasis. *Cell.* 2017;168(4):670-91.
33. Jie XX, Zhang XY, Xu CJ. Epithelial-to-mesenchymal transition, circulating tumor cells and cancer metastasis: Mechanisms and clinical applications. *Oncotarget.* 2017;8(46):81558-71.
34. Thiery JP. Epithelial-mesenchymal transitions in tumour progression. *Nat Rev Cancer.* 2002;2(6):442-54.
35. Hugo H, Ackland ML, Blick T, Lawrence MG, Clements JA, Williams ED, et al. Epithelial--mesenchymal and mesenchymal--epithelial transitions in carcinoma progression. *J Cell Physiol.* 2007;213(2):374-83.
36. Gao D, Mittal V. Tumor microenvironment regulates epithelial-mesenchymal transitions in metastasis. *Expert Rev Anticancer Ther.* 2012;12(7):857-9.
37. Jin MZ, Jin WL. The updated landscape of tumor microenvironment and drug repurposing. *Signal Transduct Target Ther.* 2020;5(1):166.
38. Peinado H, Zhang H, Matei IR, Costa-Silva B, Hoshino A, Rodrigues G, et al. Pre-metastatic niches: organ-specific homes for metastases. *Nat Rev Cancer.* 2017;17(5):302-17.
39. Gao Y, Bado I, Wang H, Zhang W, Rosen JM, Zhang XH. Metastasis Organotropism: Redefining the Congenial Soil. *Dev Cell.* 2019;49(3):375-91.
40. Chen W, Hoffmann AD, Liu H, Liu X. Organotropism: new insights into molecular mechanisms of breast cancer metastasis. *NPJ Precis Oncol.* 2018;2(1):4.
41. Paget S. The distribution of secondary growths in cancer of the breast. *Lancet* 1889;133:571-3
42. Hass R, von der Ohe J, Ungefroren H. Impact of the Tumor Microenvironment on Tumor Heterogeneity and Consequences for Cancer Cell Plasticity and Stemness. *Cancers (Basel).* 2020;12(12).
43. Runa F, Hamalian S, Meade K, Shisgal P, Gray PC, Kelber JA. Tumor microenvironment heterogeneity: challenges and opportunities. *Curr Mol Biol Rep.* 2017;3(4):218-29.
44. Ribeiro Franco PI, Rodrigues AP, de Menezes LB, Pacheco Miguel M. Tumor microenvironment components: Allies of cancer progression. *Pathol Res Pract.* 2020;216(1):152729.
45. Kalluri R, Zeisberg M. Fibroblasts in cancer. *Nat Rev Cancer.* 2006;6(5):392-401.
46. Ping Q, Yan R, Cheng X, Wang W, Zhong Y, Hou Z, et al. Cancer-associated fibroblasts: overview, progress, challenges, and directions. *Cancer Gene Ther.* 2021;28(9):984-99.

47. Erdogan B, Webb DJ. Cancer-associated fibroblasts modulate growth factor signaling and extracellular matrix remodeling to regulate tumor metastasis. *Biochem Soc Trans.* 2017;45(1):229-36.
48. Yu Y, Xiao CH, Tan LD, Wang QS, Li XQ, Feng YM. Cancer-associated fibroblasts induce epithelial-mesenchymal transition of breast cancer cells through paracrine TGF- β signalling. *Br J Cancer.* 2014;110(3):724-32.
49. Zhuang J, Lu Q, Shen B, Huang X, Shen L, Zheng X, et al. TGF β 1 secreted by cancer-associated fibroblasts induces epithelial-mesenchymal transition of bladder cancer cells through lncRNA-ZEB2NAT. *Sci Rep.* 2015;5:11924.
50. Mantovani A, Marchesi F, Malesci A, Laghi L, Allavena P. Tumour-associated macrophages as treatment targets in oncology. *Nat Rev Clin Oncol.* 2017;14(7):399-416.
51. Xiang X, Wang J, Lu D, Xu X. Targeting tumor-associated macrophages to synergize tumor immunotherapy. *Signal Transduct Target Ther.* 2021;6(1):75.
52. Chanmee T, Ontong P, Konno K, Itano N. Tumor-associated macrophages as major players in the tumor microenvironment. *Cancers (Basel).* 2014;6(3):1670-90.
53. Chen Y, Song Y, Du W, Gong L, Chang H, Zou Z. Tumor-associated macrophages: an accomplice in solid tumor progression. *J Biomed Sci.* 2019;26(1):78.
54. Ruffell B, Coussens LM. Macrophages and therapeutic resistance in cancer. *Cancer Cell.* 2015;27(4):462-72.
55. Su C, Zhang J, Yarden Y, Fu L. The key roles of cancer stem cell-derived extracellular vesicles. *Signal Transduct Target Ther.* 2021;6(1):109.
56. Maia J, Caja S, Strano Moraes MC, Couto N, Costa-Silva B. Exosome-Based Cell-Cell Communication in the Tumor Microenvironment. *Front Cell Dev Biol.* 2018;6:18.
57. Tao SC, Guo SC. Role of extracellular vesicles in tumour microenvironment. *Cell Commun Signal.* 2020;18(1):163.
58. Kalluri R, LeBleu VS. The biology, function, and biomedical applications of exosomes. *Science.* 2020;367(6478).
59. Mo Z, Cheong JYA, Xiang L, Le MTN, Grimson A, Zhang DX. Extracellular vesicle-associated organotropic metastasis. *Cell Prolif.* 2021;54(1):e12948.
60. Klemm F, Joyce JA. Microenvironmental regulation of therapeutic response in cancer. *Trends Cell Biol.* 2015;25(4):198-213.
61. Marusyk A, Polyak K. Tumor heterogeneity: causes and consequences. *Biochim Biophys Acta.* 2010;1805(1):105-17.
62. Gener P, Rafael DF, Fernández Y, Ortega JS, Arango D, Abasolo I, et al. Cancer stem cells and personalized cancer nanomedicine. *Nanomedicine (Lond).* 2016;11(3):307-20.
63. Dean M, Fojo T, Bates S. Tumour stem cells and drug resistance. *Nat Rev Cancer.* 2005;5(4):275-84.
64. Vinogradova TV, Chernov IP, Monastyrskaya GS, Kondratyeva LG, Sverdlov ED. Cancer Stem Cells: Plasticity Works against Therapy. *Acta Naturae.* 2015;7(4):46-55.
65. Shackleton M, Quintana E, Fearon ER, Morrison SJ. Heterogeneity in cancer: cancer stem cells versus clonal evolution. *Cell.* 2009;138(5):822-9.
66. Adams JM, Strasser A. Is tumor growth sustained by rare cancer stem cells or dominant clones? *Cancer Res.* 2008;68(11):4018-21.
67. Salgia R, Kulkarni P. The Genetic/Non-genetic Duality of Drug 'Resistance' in Cancer. *Trends Cancer.* 2018;4(2):110-8.
68. Lengauer C, Kinzler KW, Vogelstein B. Genetic instabilities in human cancers. *Nature.* 1998;396(6712):643-9.
69. Nowell PC. The clonal evolution of tumor cell populations. *Science.* 1976;194(4260):23-8.
70. Greaves M, Maley CC. Clonal evolution in cancer. *Nature.* 2012;481(7381):306-13.
71. Meacham CE, Morrison SJ. Tumour heterogeneity and cancer cell plasticity. *Nature.* 2013;501(7467):328-37.

72. Lapidot T, Sirard C, Vormoor J, Murdoch B, Hoang T, Caceres-Cortes J, et al. A cell initiating human acute myeloid leukaemia after transplantation into SCID mice. *Nature*. 1994;367(6464):645-8.
73. Bonnet D, Dick JE. Human acute myeloid leukemia is organized as a hierarchy that originates from a primitive hematopoietic cell. *Nat Med*. 1997;3(7):730-7.
74. Reya T, Morrison SJ, Clarke MF, Weissman IL. Stem cells, cancer, and cancer stem cells. *Nature*. 2001;414(6859):105-11.
75. Lee G, Hall RR, Ahmed AU. Cancer Stem Cells: Cellular Plasticity, Niche, and its Clinical Relevance. *J Stem Cell Res Ther*. 2016;6(10).
76. Kreso A, Dick JE. Evolution of the cancer stem cell model. *Cell Stem Cell*. 2014;14(3):275-91.
77. Singh SK, Clarke ID, Hide T, Dirks PB. Cancer stem cells in nervous system tumors. *Oncogene*. 2004;23(43):7267-73.
78. Al-Hajj M, Wicha MS, Benito-Hernandez A, Morrison SJ, Clarke MF. Prospective identification of tumorigenic breast cancer cells. *Proc Natl Acad Sci U S A*. 2003;100(7):3983-8.
79. Ricci-Vitiani L, Lombardi DG, Pilozzi E, Biffoni M, Todaro M, Peschle C, et al. Identification and expansion of human colon-cancer-initiating cells. *Nature*. 2007;445(7123):111-5.
80. Singh SR. Gastric cancer stem cells: a novel therapeutic target. *Cancer Lett*. 2013;338(1):110-9.
81. Prince ME, Sivanandan R, Kaczorowski A, Wolf GT, Kaplan MJ, Dalerba P, et al. Identification of a subpopulation of cells with cancer stem cell properties in head and neck squamous cell carcinoma. *Proc Natl Acad Sci U S A*. 2007;104(3):973-8.
82. Hou Y, Zou Q, Ge R, Shen F, Wang Y. The critical role of CD133(+)CD44(+)/high tumor cells in hematogenous metastasis of liver cancers. *Cell Res*. 2012;22(1):259-72.
83. Eramo A, Lotti F, Sette G, Pilozzi E, Biffoni M, Di Virgilio A, et al. Identification and expansion of the tumorigenic lung cancer stem cell population. *Cell Death Differ*. 2008;15(3):504-14.
84. Schatton T, Murphy GF, Frank NY, Yamaura K, Waaga-Gasser AM, Gasser M, et al. Identification of cells initiating human melanomas. *Nature*. 2008;451(7176):345-9.
85. Zhang S, Balch C, Chan MW, Lai HC, Matei D, Schilder JM, et al. Identification and characterization of ovarian cancer-initiating cells from primary human tumors. *Cancer Res*. 2008;68(11):4311-20.
86. Li C, Heidt DG, Dalerba P, Burant CF, Zhang L, Adsay V, et al. Identification of pancreatic cancer stem cells. *Cancer Res*. 2007;67(3):1030-7.
87. Wang X, Kruithof-de Julio M, Economides KD, Walker D, Yu H, Halili MV, et al. A luminal epithelial stem cell that is a cell of origin for prostate cancer. *Nature*. 2009;461(7263):495-500.
88. Nunes T, Hamdan D, Leboeuf C, El Bouchtaoui M, Gapihan G, Nguyen TT, et al. Targeting Cancer Stem Cells to Overcome Chemoresistance. *Int J Mol Sci*. 2018;19(12).
89. Barbato L, Bocchetti M, Di Biase A, Regad T. Cancer Stem Cells and Targeting Strategies. *Cells*. 2019;8(8).
90. Tomita H, Tanaka K, Tanaka T, Hara A. Aldehyde dehydrogenase 1A1 in stem cells and cancer. *Oncotarget*. 2016;7(10):11018-32.
91. Rich JN. Cancer stem cells: understanding tumor hierarchy and heterogeneity. *Medicine (Baltimore)*. 2016;95(1 Suppl 1):S2-S7.
92. Nguyen LV, Vanner R, Dirks P, Eaves CJ. Cancer stem cells: an evolving concept. *Nat Rev Cancer*. 2012;12(2):133-43.
93. Gupta PB, Fillmore CM, Jiang G, Shapira SD, Tao K, Kuperwasser C, et al. Stochastic state transitions give rise to phenotypic equilibrium in populations of cancer cells. *Cell*. 2011;146(4):633-44.
94. van Neerven SM, Tieken M, Vermeulen L, Bijlsma MF. Bidirectional interconversion of stem and non-stem cancer cell populations: A reassessment of theoretical models for tumor heterogeneity. *Mol Cell Oncol*. 2016;3(2):e1098791.

95. Plaks V, Kong N, Werb Z. The cancer stem cell niche: how essential is the niche in regulating stemness of tumor cells? *Cell Stem Cell*. 2015;16(3):225-38.
96. Shackleton M. Normal stem cells and cancer stem cells: similar and different. *Semin Cancer Biol*. 2010;20(2):85-92.
97. Al-Hajj M, Clarke MF. Self-renewal and solid tumor stem cells. *Oncogene*. 2004;23(43):7274-82.
98. Takebe N, Miele L, Harris PJ, Jeong W, Bando H, Kahn M, et al. Targeting Notch, Hedgehog, and Wnt pathways in cancer stem cells: clinical update. *Nat Rev Clin Oncol*. 2015;12(8):445-64.
99. Gener P, Seras-Franzoso J, Callejo PG, Andrade F, Rafael D, Martínez F, et al. Dynamism, Sensitivity, and Consequences of Mesenchymal and Stem-Like Phenotype of Cancer Cells. *Stem Cells Int*. 2018;2018:4516454.
100. Shibue T, Weinberg RA. EMT, CSCs, and drug resistance: the mechanistic link and clinical implications. *Nat Rev Clin Oncol*. 2017;14(10):611-29.
101. Wilson MM, Weinberg RA, Lees JA, Guen VJ. Emerging Mechanisms by which EMT Programs Control Stemness. *Trends Cancer*. 2020;6(9):775-80.
102. Mani SA, Guo W, Liao MJ, Eaton EN, Ayyanan A, Zhou AY, et al. The epithelial-mesenchymal transition generates cells with properties of stem cells. *Cell*. 2008;133(4):704-15.
103. Jolly MK, Boareto M, Huang B, Jia D, Lu M, Ben-Jacob E, et al. Implications of the Hybrid Epithelial/Mesenchymal Phenotype in Metastasis. *Front Oncol*. 2015;5:155.
104. Sarrio D, Franklin CK, Mackay A, Reis-Filho JS, Isacke CM. Epithelial and mesenchymal subpopulations within normal basal breast cell lines exhibit distinct stem cell/progenitor properties. *Stem Cells*. 2012;30(2):292-303.
105. Poli V, Fagnocchi L, Zippo A. Tumorigenic Cell Reprogramming and Cancer Plasticity: Interplay between Signaling, Microenvironment, and Epigenetics. *Stem Cells Int*. 2018;2018:4598195.
106. Wang YH, Scadden DT. Harnessing the apoptotic programs in cancer stem-like cells. *EMBO Rep*. 2015;16(9):1084-98.
107. Vitale I, Manic G, De Maria R, Kroemer G, Galluzzi L. DNA Damage in Stem Cells. *Mol Cell*. 2017;66(3):306-19.
108. Srivastava AK, Han C, Zhao R, Cui T, Dai Y, Mao C, et al. Enhanced expression of DNA polymerase eta contributes to cisplatin resistance of ovarian cancer stem cells. *Proc Natl Acad Sci U S A*. 2015;112(14):4411-6.
109. Begicevic RR, Falasca M. ABC Transporters in Cancer Stem Cells: Beyond Chemoresistance. *Int J Mol Sci*. 2017;18(11).
110. Kathawala RJ, Gupta P, Ashby CR, Chen ZS. The modulation of ABC transporter-mediated multidrug resistance in cancer: a review of the past decade. *Drug Resist Updat*. 2015;18:1-17.
111. Gottesman MM, Fojo T, Bates SE. Multidrug resistance in cancer: role of ATP-dependent transporters. *Nat Rev Cancer*. 2002;2(1):48-58.
112. Ginestier C, Hur MH, Charafe-Jauffret E, Monville F, Dutcher J, Brown M, et al. ALDH1 is a marker of normal and malignant human mammary stem cells and a predictor of poor clinical outcome. *Cell Stem Cell*. 2007;1(5):555-67.
113. Najafi M, Farhood B, Mortezaee K, Kharazinejad E, Majidpoor J, Ahadi R. Hypoxia in solid tumors: a key promoter of cancer stem cell (CSC) resistance. *J Cancer Res Clin Oncol*. 2020;146(1):19-31.
114. Qian J, Rankin EB. Hypoxia-Induced Phenotypes that Mediate Tumor Heterogeneity. *Adv Exp Med Biol*. 2019;1136:43-55.
115. Wang P, Wan WW, Xiong SL, Feng H, Wu N. Cancer stem-like cells can be induced through dedifferentiation under hypoxic conditions in glioma, hepatoma and lung cancer. *Cell Death Discov*. 2017;3:16105.
116. Almog N. Molecular mechanisms underlying tumor dormancy. *Cancer Lett*. 2010;294(2):139-46.

117. Majmundar AJ, Wong WJ, Simon MC. Hypoxia-inducible factors and the response to hypoxic stress. *Mol Cell*. 2010;40(2):294-309.
118. Qin S, Jiang J, Lu Y, Nice EC, Huang C, Zhang J, et al. Emerging role of tumor cell plasticity in modifying therapeutic response. *Signal Transduct Target Ther*. 2020;5(1):228.
119. Moore N, Houghton J, Lyle S. Slow-cycling therapy-resistant cancer cells. *Stem Cells Dev*. 2012;21(10):1822-30.
120. Du L, Wang H, He L, Zhang J, Ni B, Wang X, et al. CD44 is of functional importance for colorectal cancer stem cells. *Clin Cancer Res*. 2008;14(21):6751-60.
121. Kurtova AV, Xiao J, Mo Q, Pazhanisamy S, Krasnow R, Lerner SP, et al. Blocking PGE2-induced tumour repopulation abrogates bladder cancer chemoresistance. *Nature*. 2015;517(7533):209-13.
122. Lagadec C, Vlashi E, Della Donna L, Meng Y, Dekmezian C, Kim K, et al. Survival and self-renewing capacity of breast cancer initiating cells during fractionated radiation treatment. *Breast Cancer Res*. 2010;12(1):R13.
123. Mitra A, Mishra L, Li S. EMT, CTCs and CSCs in tumor relapse and drug-resistance. *Oncotarget*. 2015;6(13):10697-711.
124. Eppert K, Takenaka K, Lechman ER, Waldron L, Nilsson B, van Galen P, et al. Stem cell gene expression programs influence clinical outcome in human leukemia. *Nat Med*. 2011;17(9):1086-93.
125. Li M, Zhang B, Zhang Z, Liu X, Qi X, Zhao J, et al. Stem cell-like circulating tumor cells indicate poor prognosis in gastric cancer. *Biomed Res Int*. 2014;2014:981261.
126. Annett S, Robson T. Targeting cancer stem cells in the clinic: Current status and perspectives. *Pharmacol Ther*. 2018;187:13-30.
127. Agliano A, Calvo A, Box C. The challenge of targeting cancer stem cells to halt metastasis. *Semin Cancer Biol*. 2017;44:25-42.
128. Rafael D, Gener P, Andrade F, Seras-Franzoso J, Montero S, Fernández Y, et al. AKT2 siRNA delivery with amphiphilic-based polymeric micelles show efficacy against cancer stem cells. *Drug Deliv*. 2018;25(1):961-72.
129. Deng CC, Liang Y, Wu MS, Feng FT, Hu WR, Chen LZ, et al. Nigericin selectively targets cancer stem cells in nasopharyngeal carcinoma. *Int J Biochem Cell Biol*. 2013;45(9):1997-2006.
130. Xu X, Liu Y, Su J, Li D, Hu J, Huang Q, et al. Downregulation of Bmi-1 is associated with suppressed tumorigenesis and induced apoptosis in CD44⁺ nasopharyngeal carcinoma cancer stem-like cells. *Oncol Rep*. 2016;35(2):923-31.
131. Bar EE, Chaudhry A, Lin A, Fan X, Schreck K, Matsui W, et al. Cyclopamine-mediated hedgehog pathway inhibition depletes stem-like cancer cells in glioblastoma. *Stem Cells*. 2007;25(10):2524-33.
132. Wu MS, Wang GF, Zhao ZQ, Liang Y, Wang HB, Wu MY, et al. Smac mimetics in combination with TRAIL selectively target cancer stem cells in nasopharyngeal carcinoma. *Mol Cancer Ther*. 2013;12(9):1728-37.
133. Reeves PM, Abbaslou MA, Kools FRW, Vutipongsatorn K, Tong X, Gavegnano C, et al. Correction: Ruxolitinib sensitizes ovarian cancer to reduced dose Taxol, limits tumor growth and improves survival in immune competent mice. *Oncotarget*. 2018;9(54):30472.
134. Metformin suppresses triple-negative breast cancer stem cells by targeting KLF5 for degradation. *Cancer Research*. 2017;77:147.
135. Smith KM, Datti A, Fujitani M, Grinshtein N, Zhang L, Morozova O, et al. Selective targeting of neuroblastoma tumour-initiating cells by compounds identified in stem cell-based small molecule screens. *EMBO Mol Med*. 2010;2(9):371-84.
136. Matsuda Y, Ishiwata T, Yoshimura H, Hagio M, Arai T. Inhibition of nestin suppresses stem cell phenotype of glioblastomas through the alteration of post-translational modification of heat shock protein HSPA8/HSC71. *Cancer Lett*. 2015;357(2):602-11.

137. Narita K, Matsuda Y, Seike M, Naito Z, Gemma A, Ishiwata T. Nestin regulates proliferation, migration, invasion and stemness of lung adenocarcinoma. *Int J Oncol*. 2014;44(4):1118-30.
138. Matsuda Y, Naito Z, Kawahara K, Nakazawa N, Korc M, Ishiwata T. Nestin is a novel target for suppressing pancreatic cancer cell migration, invasion and metastasis. *Cancer Biol Ther*. 2011;11(5):512-23.
139. Matsuda Y, Ishiwata T, Yoshimura H, Yamashita S, Ushijima T, Arai T. Systemic Administration of Small Interfering RNA Targeting Human Nestin Inhibits Pancreatic Cancer Cell Proliferation and Metastasis. *Pancreas*. 2016;45(1):93-100.
140. Han M, Liu M, Wang Y, Chen X, Xu J, Sun Y, et al. Antagonism of miR-21 reverses epithelial-mesenchymal transition and cancer stem cell phenotype through AKT/ERK1/2 inactivation by targeting PTEN. *PLoS One*. 2012;7(6):e39520.
141. Lin L, Hutzen B, Lee HF, Peng Z, Wang W, Zhao C, et al. Evaluation of STAT3 signaling in ALDH⁺ and ALDH⁺/CD44⁺/CD24⁻ subpopulations of breast cancer cells. *PLoS One*. 2013;8(12):e82821.
142. Li Y, Rogoff HA, Keates S, Gao Y, Murikipudi S, Mikule K, et al. Suppression of cancer relapse and metastasis by inhibiting cancer stemness. *Proc Natl Acad Sci U S A*. 2015;112(6):1839-44.
143. An H, Kim JY, Oh E, Lee N, Cho Y, Seo JH. Salinomycin Promotes Anoikis and Decreases the CD44⁺/CD24⁻ Stem-Like Population via Inhibition of STAT3 Activation in MDA-MB-231 Cells. *PLoS One*. 2015;10(11):e0141919.
144. Yamashita T, Honda M, Nio K, Nakamoto Y, Takamura H, Tani T, et al. Oncostatin m renders epithelial cell adhesion molecule-positive liver cancer stem cells sensitive to 5-Fluorouracil by inducing hepatocytic differentiation. *Cancer Res*. 2010;70(11):4687-97.
145. Yakisich JS, Azad N, Kaushik V, O'Doherty GA, Iyer AK. Nigericin decreases the viability of multidrug-resistant cancer cells and lung tumorspheres and potentiates the effects of cardiac glycosides. *Tumour Biol*. 2017;39(3):1010428317694310.
146. Smigiel JM, Parameswaran N, Jackson MW. Potent EMT and CSC Phenotypes Are Induced By Oncostatin-M in Pancreatic Cancer. *Mol Cancer Res*. 2017;15(4):478-88.
147. Yang L, Shi P, Zhao G, Xu J, Peng W, Zhang J, et al. Targeting cancer stem cell pathways for cancer therapy. *Signal Transduct Target Ther*. 2020;5(1):8.
148. Provenzano E, Ulaner GA, Chin SF. Molecular Classification of Breast Cancer. *PET Clin*. 2018;13(3):325-38.
149. Harbeck N, Penault-Llorca F, Cortes J, Gnant M, Houssami N, Poortmans P, et al. Breast cancer. *Nat Rev Dis Primers*. 2019;5(1):66.
150. Bertos NR, Park M. Breast cancer - one term, many entities? *J Clin Invest*. 2011;121(10):3789-96.
151. Waks AG, Winer EP. Breast Cancer Treatment: A Review. *JAMA*. 2019;321(3):288-300.
152. Li CI, Uribe DJ, Daling JR. Clinical characteristics of different histologic types of breast cancer. *Br J Cancer*. 2005;93(9):1046-52.
153. Dai X, Xiang L, Li T, Bai Z. Cancer Hallmarks, Biomarkers and Breast Cancer Molecular Subtypes. *J Cancer*. 2016;7(10):1281-94.
154. Fragomeni SM, Sciallis A, Jeruss JS. Molecular Subtypes and Local-Regional Control of Breast Cancer. *Surg Oncol Clin N Am*. 2018;27(1):95-120.
155. Slamon DJ, Clark GM, Wong SG, Levin WJ, Ullrich A, McGuire WL. Human breast cancer: correlation of relapse and survival with amplification of the HER-2/neu oncogene. *Science*. 1987;235(4785):177-82.
156. Oh DY, Bang YJ. HER2-targeted therapies - a role beyond breast cancer. *Nat Rev Clin Oncol*. 2020;17(1):33-48.
157. Yin L, Duan JJ, Bian XW, Yu SC. Triple-negative breast cancer molecular subtyping and treatment progress. *Breast Cancer Res*. 2020;22(1):61.

158. da Silva JL, Cardoso Nunes NC, Izetti P, de Mesquita GG, de Melo AC. Triple negative breast cancer: A thorough review of biomarkers. *Crit Rev Oncol Hematol*. 2020;145:102855.
159. Li CH, Karantza V, Aktan G, Lala M. Current treatment landscape for patients with locally recurrent inoperable or metastatic triple-negative breast cancer: a systematic literature review. *Breast Cancer Res*. 2019;21(1):143.
160. Bauer KR, Brown M, Cress RD, Parise CA, Caggiano V. Descriptive analysis of estrogen receptor (ER)-negative, progesterone receptor (PR)-negative, and HER2-negative invasive breast cancer, the so-called triple-negative phenotype: a population-based study from the California cancer Registry. *Cancer*. 2007;109(9):1721-8.
161. Marra A, Trapani D, Viale G, Criscitiello C, Curigliano G. Practical classification of triple-negative breast cancer: intratumoral heterogeneity, mechanisms of drug resistance, and novel therapies. *NPJ Breast Cancer*. 2020;6:54.
162. Wang DY, Jiang Z, Ben-David Y, Woodgett JR, Zacksenhaus E. Molecular stratification within triple-negative breast cancer subtypes. *Sci Rep*. 2019;9(1):19107.
163. Perou CM. Molecular stratification of triple-negative breast cancers. *Oncologist*. 2010;15 Suppl 5:39-48.
164. Lehmann BD, Bauer JA, Chen X, Sanders ME, Chakravarthy AB, Shyr Y, et al. Identification of human triple-negative breast cancer subtypes and preclinical models for selection of targeted therapies. *J Clin Invest*. 2011;121(7):2750-67.
165. Lehmann BD, Jovanović B, Chen X, Estrada MV, Johnson KN, Shyr Y, et al. Refinement of Triple-Negative Breast Cancer Molecular Subtypes: Implications for Neoadjuvant Chemotherapy Selection. *PLoS One*. 2016;11(6):e0157368.
166. Perou CM, Sørlie T, Eisen MB, van de Rijn M, Jeffrey SS, Rees CA, et al. Molecular portraits of human breast tumours. *Nature*. 2000;406(6797):747-52.
167. Hu Z, Fan C, Oh DS, Marron JS, He X, Qaqish BF, et al. The molecular portraits of breast tumors are conserved across microarray platforms. *BMC Genomics*. 2006;7:96.
168. Sørlie T, Perou CM, Tibshirani R, Aas T, Geisler S, Johnsen H, et al. Gene expression patterns of breast carcinomas distinguish tumor subclasses with clinical implications. *Proc Natl Acad Sci U S A*. 2001;98(19):10869-74.
169. Dai X, Li T, Bai Z, Yang Y, Liu X, Zhan J, et al. Breast cancer intrinsic subtype classification, clinical use and future trends. *Am J Cancer Res*. 2015;5(10):2929-43.
170. Sung H, Ferlay J, Siegel RL, Laversanne M, Soerjomataram I, Jemal A, et al. Global Cancer Statistics 2020: GLOBOCAN Estimates of Incidence and Mortality Worldwide for 36 Cancers in 185 Countries. *CA Cancer J Clin*. 2021;71(3):209-49.
171. Siegel RL, Miller KD, Goding Sauer A, Fedewa SA, Butterly LF, Anderson JC, et al. Colorectal cancer statistics, 2020. *CA Cancer J Clin*. 2020;70(3):145-64.
172. Ahmed M. Colon Cancer: A Clinician's Perspective in 2019. *Gastroenterology Res*. 2020;13(1):1-10.
173. Pan P, Yu J, Wang LS. Colon Cancer: What We Eat. *Surg Oncol Clin N Am*. 2018;27(2):243-67.
174. Pan P, Yu J, Wang LS. Diet and colon: what matters? *Curr Opin Gastroenterol*. 2019;35(2):101-6.
175. Kuipers EJ, Grady WM, Lieberman D, Seufferlein T, Sung JJ, Boelens PG, et al. Colorectal cancer. *Nat Rev Dis Primers*. 2015;1:15065.
176. Vatandoust S, Price TJ, Karapetis CS. Colorectal cancer: Metastases to a single organ. *World J Gastroenterol*. 2015;21(41):11767-76.
177. Chow FC, Chok KS. Colorectal liver metastases: An update on multidisciplinary approach. *World J Hepatol*. 2019;11(2):150-72.
178. Martini G, Dienstmann R, Ros J, Baraibar I, Cuadra-Urteaga JL, Salva F, et al. Molecular subtypes and the evolution of treatment management in metastatic colorectal cancer. *Ther Adv Med Oncol*. 2020;12:1758835920936089.
179. Weitz J, Knaebel HP, Büchler MW. Sporadic and hereditary colorectal cancer. Pathogenetically different with different therapeutic indications. *Chirurg*. 2003;74(8):717-25.

180. Yamagishi H, Kuroda H, Imai Y, Hiraishi H. Molecular pathogenesis of sporadic colorectal cancers. *Chin J Cancer*. 2016;35:4.
181. Hardiman KM. Update on Sporadic Colorectal Cancer Genetics. *Clin Colon Rectal Surg*. 2018;31(3):147-52.
182. Stoffel EM, Kastrinos F. Familial colorectal cancer, beyond Lynch syndrome. *Clin Gastroenterol Hepatol*. 2014;12(7):1059-68.
183. Jaspersion KW, Tuohy TM, Neklason DW, Burt RW. Hereditary and familial colon cancer. *Gastroenterology*. 2010;138(6):2044-58.
184. Pancione M, Remo A, Colantuoni V. Genetic and epigenetic events generate multiple pathways in colorectal cancer progression. *Patholog Res Int*. 2012;2012:509348.
185. Leslie A, Carey FA, Pratt NR, Steele RJ. The colorectal adenoma-carcinoma sequence. *Br J Surg*. 2002;89(7):845-60.
186. Kuipers EJ, Rösch T, Bretthauer M. Colorectal cancer screening--optimizing current strategies and new directions. *Nat Rev Clin Oncol*. 2013;10(3):130-42.
187. De Palma FDE, D'Argenio V, Pol J, Kroemer G, Maiuri MC, Salvatore F. The Molecular Hallmarks of the Serrated Pathway in Colorectal Cancer. *Cancers (Basel)*. 2019;11(7).
188. Pino MS, Chung DC. The chromosomal instability pathway in colon cancer. *Gastroenterology*. 2010;138(6):2059-72.
189. Gupta R, Sinha S, Paul RN. The impact of microsatellite stability status in colorectal cancer. *Curr Probl Cancer*. 2018;42(6):548-59.
190. Nojadeh JN, Behrouz Sharif S, Sakhinia E. Microsatellite instability in colorectal cancer. *EXCLI J*. 2018;17:159-68.
191. Kane AM, Fennell LJ, Liu C, Borowsky J, McKeone DM, Bond CE, et al. Alterations in signaling pathways that accompany spontaneous transition to malignancy in a mouse model of BRAF mutant microsatellite stable colorectal cancer. *Neoplasia*. 2020;22(2):120-8.
192. O'Brien MJ, Yang S, Mack C, Xu H, Huang CS, Mulcahy E, et al. Comparison of microsatellite instability, CpG island methylation phenotype, BRAF and KRAS status in serrated polyps and traditional adenomas indicates separate pathways to distinct colorectal carcinoma end points. *Am J Surg Pathol*. 2006;30(12):1491-501.
193. Kim SY, Kim TI. Serrated neoplasia pathway as an alternative route of colorectal cancer carcinogenesis. *Intest Res*. 2018;16(3):358-65.
194. Szyłberg Ł, Janiczek M, Popiel A, Marszałek A. Serrated polyps and their alternative pathway to the colorectal cancer: a systematic review. *Gastroenterol Res Pract*. 2015;2015:573814.
195. Nazemalhosseini Mojarad E, Kuppen PJ, Aghdaei HA, Zali MR. The CpG island methylator phenotype (CIMP) in colorectal cancer. *Gastroenterol Hepatol Bed Bench*. 2013;6(3):120-8.
196. Advani SM, Advani P, DeSantis SM, Brown D, VonVille HM, Lam M, et al. Clinical, Pathological, and Molecular Characteristics of CpG Island Methylator Phenotype in Colorectal Cancer: A Systematic Review and Meta-analysis. *Transl Oncol*. 2018;11(5):1188-201.
197. Guinney J, Dienstmann R, Wang X, de Reyniès A, Schlicker A, Soneson C, et al. The consensus molecular subtypes of colorectal cancer. *Nat Med*. 2015;21(11):1350-6.
198. Bae JM, Kim JH, Kwak Y, Lee DW, Cha Y, Wen X, et al. Distinct clinical outcomes of two CIMP-positive colorectal cancer subtypes based on a revised CIMP classification system. *Br J Cancer*. 2017;116(8):1012-20.
199. Wang W, Kandimalla R, Huang H, Zhu L, Li Y, Gao F, et al. Molecular subtyping of colorectal cancer: Recent progress, new challenges and emerging opportunities. *Semin Cancer Biol*. 2019;55:37-52.
200. Types of cancer treatment [online] NCI [Accessed 6th of June 2021] Available from: <https://www.cancer.gov/about-cancer/treatment/types>.

201. Vishnu P, Roy V. Safety and Efficacy of nab-Paclitaxel in the Treatment of Patients with Breast Cancer. *Breast Cancer (Auckl)*. 2011;5:53-65.
202. Kataja V, Castiglione M, Group EGW. Primary breast cancer: ESMO clinical recommendations for diagnosis, treatment and follow-up. *Ann Oncol*. 2009;20 Suppl 4:10-4.
203. Aparicio J, Esposito F, Serrano S, Falco E, Escudero P, Ruiz-Casado A, et al. Metastatic Colorectal Cancer. First Line Therapy for Unresectable Disease. *J Clin Med*. 2020;9(12).
204. Tournigand C, André T, Achille E, Lledo G, Flesh M, Mery-Mignard D, et al. FOLFIRI followed by FOLFOX6 or the reverse sequence in advanced colorectal cancer: a randomized GERCOR study. *J Clin Oncol*. 2004;22(2):229-37.
205. Tol J, Koopman M, Cats A, Rodenburg CJ, Creemers GJ, Schrama JG, et al. Chemotherapy, bevacizumab, and cetuximab in metastatic colorectal cancer. *N Engl J Med*. 2009;360(6):563-72.
206. Wang X, Zhang H, Chen X. Drug resistance and combating drug resistance in cancer. *Cancer Drug Resist*. 2019;2:141-60.
207. Esposito M, Ganesan S, Kang Y. Emerging strategies for treating metastasis. *Nat Cancer*. 2021;2(3):258-70.
208. Chemotherapy side effects [online] American Cancer Society [Accessed 6th of June 2021] Available from: <https://www.cancer.org/treatment/treatments-and-side-effects/treatment-types/chemotherapy/chemotherapy-side-effects.html>.
209. RP. F. There's plenty of room at the bottom. *Eng Sci* 1960;23:22–36
210. Bayda S, Adeel M, Tuccinardi T, Cordani M, Rizzolio F. The History of Nanoscience and Nanotechnology: From Chemical-Physical Applications to Nanomedicine. *Molecules*. 2019;25(1).
211. Taniguchi, N.; Arakawa, C.; Kobayashi, T. On the basic concept of nanotechnology. In *Proceedings of the International Conference on Production Engineering*, Tokyo, Japan, 26–9 August 1974.
212. Drexler, E.K. *Engines of Creation: The Coming Era of Nanotechnology*; Anchor Press: Garden City, NY, USA, 1986.
213. What is Nanotechnology? [online] National Nanotechnology Initiative (NNI) [Accessed 2nd of July 2021] Available from: <https://www.nano.gov/nanotech-101/what/definition>.
214. Guisbiers G. Size-dependent materials properties toward a universal equation. *Nanoscale Res Lett*. 2010;5(7):1132-6.
215. Patra JK, Das G, Fraceto LF, Campos EVR, Rodriguez-Torres MDP, Acosta-Torres LS, et al. Nano based drug delivery systems: recent developments and future prospects. *J Nanobiotechnology*. 2018;16(1):71.
216. Freitas RA. What is nanomedicine? *Nanomedicine*. 2005;1(1):2-9.
217. Wagner V, Dullaart A, Bock AK, Zweck A. The emerging nanomedicine landscape. *Nat Biotechnol*. 2006;24(10):1211-7.
218. Webster TJ. Nanomedicine: what's in a definition? *Int J Nanomedicine*. 2006;1(2):115-6.
219. ESF, European Science Foundation. 2004. *Nanomedicine – An ESF–European Medical Research Councils (EMRC) Forward Look Report*. Strasbourg cedex, France ESF.
220. Wu LP, Wang D, Li Z. Grand challenges in nanomedicine. *Mater Sci Eng C Mater Biol Appl*. 2020;106:110302.
221. Ragelle H, Danhier F, Préat V, Langer R, Anderson DG. Nanoparticle-based drug delivery systems: a commercial and regulatory outlook as the field matures. *Expert Opin Drug Deliv*. 2017;14(7):851-64.
222. Farjadian F, Ghasemi A, Gohari O, Roointan A, Karimi M, Hamblin MR. Nanopharmaceuticals and nanomedicines currently on the market: challenges and opportunities. *Nanomedicine (Lond)*. 2019;14(1):93-126.

223. 75 percent of nanopharmaceuticals are being developed for oncology [online] EPR [Accessed 6th of September 2021] Available from: <https://www.europeanpharmaceuticalreview.com/news/116562/75-percent-of-nanopharmaceuticals-are-being-developed-for-oncology/>.
224. Shi J, Kantoff PW, Wooster R, Farokhzad OC. Cancer nanomedicine: progress, challenges and opportunities. *Nat Rev Cancer*. 2017;17(1):20-37.
225. Barenholz Y. Doxil®--the first FDA-approved nano-drug: lessons learned. *J Control Release*. 2012;160(2):117-34.
226. Dogra P, Butner JD, Chuang YL, Caserta S, Goel S, Brinker CJ, et al. Mathematical modeling in cancer nanomedicine: a review. *Biomed Microdevices*. 2019;21(2):40.
227. Hoskins C. Cancer Nanomedicine. *Cancers (Basel)*. 2020;12(8).
228. Adams DJ. The Valley of Death in anticancer drug development: a reassessment. *Trends Pharmacol Sci*. 2012;33(4):173-80.
229. Fang J, Nakamura H, Maeda H. The EPR effect: Unique features of tumor blood vessels for drug delivery, factors involved, and limitations and augmentation of the effect. *Adv Drug Deliv Rev*. 2011;63(3):136-51.
230. Maeda H, Nakamura H, Fang J. The EPR effect for macromolecular drug delivery to solid tumors: Improvement of tumor uptake, lowering of systemic toxicity, and distinct tumor imaging in vivo. *Adv Drug Deliv Rev*. 2013;65(1):71-9.
231. Bielenberg DR, Zetter BR. The Contribution of Angiogenesis to the Process of Metastasis. *Cancer J*. 2015;21(4):267-73.
232. Golombek SK, May JN, Theek B, Appold L, Drude N, Kiessling F, et al. Tumor targeting via EPR: Strategies to enhance patient responses. *Adv Drug Deliv Rev*. 2018;130:17-38.
233. Li Y, Wang J, Wientjes MG, Au JL. Delivery of nanomedicines to extracellular and intracellular compartments of a solid tumor. *Adv Drug Deliv Rev*. 2012;64(1):29-39.
234. Blanco E, Shen H, Ferrari M. Principles of nanoparticle design for overcoming biological barriers to drug delivery. *Nat Biotechnol*. 2015;33(9):941-51.
235. Alexis F, Pridgen E, Molnar LK, Farokhzad OC. Factors affecting the clearance and biodistribution of polymeric nanoparticles. *Mol Pharm*. 2008;5(4):505-15.
236. Braet F, Wisse E, Bomans P, Frederik P, Geerts W, Koster A, et al. Contribution of high-resolution correlative imaging techniques in the study of the liver sieve in three-dimensions. *Microsc Res Tech*. 2007;70(3):230-42.
237. Cabral H, Matsumoto Y, Mizuno K, Chen Q, Murakami M, Kimura M, et al. Accumulation of sub-100 nm polymeric micelles in poorly permeable tumours depends on size. *Nat Nanotechnol*. 2011;6(12):815-23.
238. Ahsan SM, Rao CM, Ahmad MF. Nanoparticle-Protein Interaction: The Significance and Role of Protein Corona. *Adv Exp Med Biol*. 2018;1048:175-98.
239. Corbo C, Molinaro R, Parodi A, Toledano Furman NE, Salvatore F, Tasciotti E. The impact of nanoparticle protein corona on cytotoxicity, immunotoxicity and target drug delivery. *Nanomedicine (Lond)*. 2016;11(1):81-100.
240. Nel AE, Mädler L, Velegol D, Xia T, Hoek EM, Somasundaran P, et al. Understanding biophysicochemical interactions at the nano-bio interface. *Nat Mater*. 2009;8(7):543-57.
241. Pérez-Herrero E, Fernández-Medarde A. Advanced targeted therapies in cancer: Drug nanocarriers, the future of chemotherapy. *Eur J Pharm Biopharm*. 2015;93:52-79.
242. Pasut G, Paolino D, Celia C, Mero A, Joseph AS, Wolfram J, et al. Polyethylene glycol (PEG)-dendron phospholipids as innovative constructs for the preparation of super stealth liposomes for anticancer therapy. *J Control Release*. 2015;199:106-13.
243. D'souza AA, Shegokar R. Polyethylene glycol (PEG): a versatile polymer for pharmaceutical applications. *Expert Opin Drug Deliv*. 2016;13(9):1257-75.
244. Owens DE, Peppas NA. Opsonization, biodistribution, and pharmacokinetics of polymeric nanoparticles. *Int J Pharm*. 2006;307(1):93-102.

245. James AM, Ambrose EJ, Lowick JH. Differences between the electrical charge carried by normal and homologous tumour cells. *Nature*. 1956;177(4508):576-7.
246. Thurston G, McLean JW, Rizen M, Baluk P, Haskell A, Murphy TJ, et al. Cationic liposomes target angiogenic endothelial cells in tumors and chronic inflammation in mice. *J Clin Invest*. 1998;101(7):1401-13.
247. Al Tameemi W, Dale TP, Al-Jumaily RMK, Forsyth NR. Hypoxia-Modified Cancer Cell Metabolism. *Front Cell Dev Biol*. 2019;7:4.
248. Haider T, Sandha KK, Soni V, Gupta PN. Recent advances in tumor microenvironment associated therapeutic strategies and evaluation models. *Mater Sci Eng C Mater Biol Appl*. 2020;116:111229.
249. Mi P. Stimuli-responsive nanocarriers for drug delivery, tumor imaging, therapy and theranostics. *Theranostics*. 2020;10(10):4557-88.
250. Lee Y, Fukushima S, Bae Y, Hiki S, Ishii T, Kataoka K. A protein nanocarrier from charge-conversion polymer in response to endosomal pH. *J Am Chem Soc*. 2007;129(17):5362-3.
251. Yuan YY, Mao CQ, Du XJ, Du JZ, Wang F, Wang J. Surface charge switchable nanoparticles based on zwitterionic polymer for enhanced drug delivery to tumor. *Adv Mater*. 2012;24(40):5476-80.
252. Geng Y, Dalhaimer P, Cai S, Tsai R, Tewari M, Minko T, et al. Shape effects of filaments versus spherical particles in flow and drug delivery. *Nat Nanotechnol*. 2007;2(4):249-55.
253. Sun T, Zhang YS, Pang B, Hyun DC, Yang M, Xia Y. Engineered nanoparticles for drug delivery in cancer therapy. *Angew Chem Int Ed Engl*. 2014;53(46):12320-64.
254. Salvioni L, Rizzuto MA, Bertolini JA, Pandolfi L, Colombo M, Prosperi D. Thirty Years of Cancer Nanomedicine: Success, Frustration, and Hope. *Cancers (Basel)*. 2019;11(12).
255. Petros RA, DeSimone JM. Strategies in the design of nanoparticles for therapeutic applications. *Nat Rev Drug Discov*. 2010;9(8):615-27.
256. Mitchell MJ, Billingsley MM, Haley RM, Wechsler ME, Peppas NA, Langer R. Engineering precision nanoparticles for drug delivery. *Nat Rev Drug Discov*. 2021;20(2):101-24.
257. Lehner R, Wang X, Marsch S, Hunziker P. Intelligent nanomaterials for medicine: carrier platforms and targeting strategies in the context of clinical application. *Nanomedicine*. 2013;9(6):742-57.
258. Peer D, Karp JM, Hong S, Farokhzad OC, Margalit R, Langer R. Nanocarriers as an emerging platform for cancer therapy. *Nat Nanotechnol*. 2007;2(12):751-60.
259. Lee H, Shields AF, Siegel BA, Miller KD, Krop I, Ma CX, et al. Cu-MM-302 Positron Emission Tomography Quantifies Variability of Enhanced Permeability and Retention of Nanoparticles in Relation to Treatment Response in Patients with Metastatic Breast Cancer. *Clin Cancer Res*. 2017;23(15):4190-202.
260. Jain RK, Stylianopoulos T. Delivering nanomedicine to solid tumors. *Nat Rev Clin Oncol*. 2010;7(11):653-64.
261. Rosenblum D, Joshi N, Tao W, Karp JM, Peer D. Progress and challenges towards targeted delivery of cancer therapeutics. *Nat Commun*. 2018;9(1):1410.
262. Bertrand N, Wu J, Xu X, Kamaly N, Farokhzad OC. Cancer nanotechnology: the impact of passive and active targeting in the era of modern cancer biology. *Adv Drug Deliv Rev*. 2014;66:2-25.
263. Toporkiewicz M, Meissner J, Matuszewicz L, Czogalla A, Sikorski AF. Toward a magic or imaginary bullet? Ligands for drug targeting to cancer cells: principles, hopes, and challenges. *Int J Nanomedicine*. 2015;10:1399-414.
264. Duan H, Liu Y, Gao Z, Huang W. Recent advances in drug delivery systems for targeting cancer stem cells. *Acta Pharm Sin B*. 2021;11(1):55-70.
265. Karandish F, Froberg J, Borowicz P, Wilkinson JC, Choi Y, Mallik S. Peptide-targeted, stimuli-responsive polymersomes for delivering a cancer stemness inhibitor to cancer stem cell microtumors. *Colloids Surf B Biointerfaces*. 2018;163:225-35.

266. Li C, Liang Y, Cao J, Zhang N, Wei X, Tu M, et al. The Delivery of a Wnt Pathway Inhibitor Toward CSCs Requires Stable Liposome Encapsulation and Delayed Drug Release in Tumor Tissues. *Mol Ther*. 2019;27(9):1558-67.
267. Oak PS, Kopp F, Thakur C, Ellwart JW, Rapp UR, Ullrich A, et al. Combinatorial treatment of mammospheres with trastuzumab and salinomycin efficiently targets HER2-positive cancer cells and cancer stem cells. *Int J Cancer*. 2012;131(12):2808-19.
268. Ren Y, Wang R, Gao L, Li K, Zhou X, Guo H, et al. Sequential co-delivery of miR-21 inhibitor followed by burst release doxorubicin using NIR-responsive hollow gold nanoparticle to enhance anticancer efficacy. *J Control Release*. 2016;228:74-86.
269. Zhao P, Xia G, Dong S, Jiang ZX, Chen M. An iTEP-salinomycin nanoparticle that specifically and effectively inhibits metastases of 4T1 orthotopic breast tumors. *Biomaterials*. 2016;93:1-9.
270. Navya PN, Kaphle A, Srinivas SP, Bhargava SK, Rotello VM, Daima HK. Current trends and challenges in cancer management and therapy using designer nanomaterials. *Nano Converg*. 2019;6(1):23.
271. Domenico Lombardo MAK, and Maria Teresa Caccamo. Smart Nanoparticles for Drug Delivery Application: Development of Versatile Nanocarrier Platforms in Biotechnology and Nanomedicine. *Journal of Nanomaterials*. 2019;12:1-26.
272. Khalid K, Tan X, Mohd Zaid HF, Tao Y, Lye Chew C, Chu DT, et al. Advanced in developmental organic and inorganic nanomaterial: a review. *Bioengineered*. 2020;11(1):328-55.
273. Lohse SE, Murphy CJ. Applications of colloidal inorganic nanoparticles: from medicine to energy. *J Am Chem Soc*. 2012;134(38):15607-20.
274. Li M, Du C, Guo N, Teng Y, Meng X, Sun H, et al. Composition design and medical application of liposomes. *Eur J Med Chem*. 2019;164:640-53.
275. Bozzuto G, Molinari A. Liposomes as nanomedical devices. *Int J Nanomedicine*. 2015;10:975-99.
276. Akbarzadeh A, Rezaei-Sadabady R, Davaran S, Joo SW, Zarghami N, Hanifehpour Y, et al. Liposome: classification, preparation, and applications. *Nanoscale Res Lett*. 2013;8(1):102.
277. Sercombe L, Veerati T, Moheimani F, Wu SY, Sood AK, Hua S. Advances and Challenges of Liposome Assisted Drug Delivery. *Front Pharmacol*. 2015;6:286.
278. Anselmo AC, Mitragotri S. Nanoparticles in the clinic: An update. *Bioeng Transl Med*. 2019;4(3):e10143.
279. Northfelt DW, Dezube BJ, Thommes JA, Miller BJ, Fischl MA, Friedman-Kien A, et al. Pegylated-liposomal doxorubicin versus doxorubicin, bleomycin, and vincristine in the treatment of AIDS-related Kaposi's sarcoma: results of a randomized phase III clinical trial. *J Clin Oncol*. 1998;16(7):2445-51.
280. Mishra V, Bansal KK, Verma A, Yadav N, Thakur S, Sudhakar K, et al. Solid Lipid Nanoparticles: Emerging Colloidal Nano Drug Delivery Systems. *Pharmaceutics*. 2018;10(4).
281. Bayón-Cordero L, Alkorta I, Arana L. Application of Solid Lipid Nanoparticles to Improve the Efficiency of Anticancer Drugs. *Nanomaterials (Basel)*. 2019;9(3).
282. Westesen K, Bunjes H, Koch MHJ. Physicochemical characterization of lipid nanoparticles and evaluation of their drug loading capacity and sustained release potential. *J Control Release* 1997;48:223–36.
283. Müller RH, Shegokar R, Keck CM. 20 years of lipid nanoparticles (SLN and NLC): present state of development and industrial applications. *Curr Drug Discov Technol*. 2011;8(3):207-27.
284. Haider M, Abidin SM, Kamal L, Orive G. Nanostructured Lipid Carriers for Delivery of Chemotherapeutics: A Review. *Pharmaceutics*. 2020;12(3).
285. Belouqui A, Solinís M, Rodríguez-Gascón A, Almeida AJ, Préat V. Nanostructured lipid carriers: Promising drug delivery systems for future clinics. *Nanomedicine*. 2016;12(1):143-61.

286. Idrees H, Zaidi SZJ, Sabir A, Khan RU, Zhang X, Hassan SU. A Review of Biodegradable Natural Polymer-Based Nanoparticles for Drug Delivery Applications. *Nanomaterials (Basel)*. 2020;10(10).
287. Deshmukh AS, Chauhan PN, Noolvi MN, Chaturvedi K, Ganguly K, Shukla SS, et al. Polymeric micelles: Basic research to clinical practice. *Int J Pharm*. 2017;532(1):249-68.
288. Xiong XB, Falamarzian A, Garg SM, Lavasanifar A. Engineering of amphiphilic block copolymers for polymeric micellar drug and gene delivery. *J Control Release*. 2011;155(2):248-61.
289. Agrahari V. Advances and applications of block-copolymer-based nanoformulations. *Drug Discov Today*. 2018;23(5):1139-51.
290. Demina T, Grozdova I, Krylova O, Zhirnov A, Istratov V, Frey H, et al. Relationship between the structure of amphiphilic copolymers and their ability to disturb lipid bilayers. *Biochemistry*. 2005;44(10):4042-54.
291. Perin F, Motta A, Maniglio D. Amphiphilic copolymers in biomedical applications: Synthesis routes and property control. *Mater Sci Eng C Mater Biol Appl*. 2021;123:111952.
292. Xiong XB, Binkhathlan Z, Molavi O, Lavasanifar A. Amphiphilic block copolymers: preparation and application in nanodrug and gene delivery. *Acta Biomater*. 2012;8(6):2017-33.
293. Hussein YHA, Youssry M. Polymeric Micelles of Biodegradable Diblock Copolymers: Enhanced Encapsulation of Hydrophobic Drugs. *Materials (Basel)*. 2018;11(5).
294. Kwon G, Naito M, Yokoyama M, Okano T, Sakurai Y, Kataoka K. Micelles based on ab block copolymers of poly(ethylene oxide) and poly(L-benzyl L-aspartate). *Langmuir*. 1993;9:45-9.
295. Ghezzi M, Pescina S, Padula C, Santi P, Del Favero E, Cantù L, et al. Polymeric micelles in drug delivery: An insight of the techniques for their characterization and assessment in biorelevant conditions. *J Control Release*. 2021;332:312-36.
296. Owen SC CD, Schoichet M. Polymeric micelle stability. *Nanotoday*. 2012;7(1):53-65.
297. Jhaveri AM, Torchilin VP. Multifunctional polymeric micelles for delivery of drugs and siRNA. *Front Pharmacol*. 2014;5:77.
298. Hwang D, Ramsey JD, Kabanov AV. Polymeric micelles for the delivery of poorly soluble drugs: From nanoformulation to clinical approval. *Adv Drug Deliv Rev*. 2020;156:80-118.
299. Kwon GS. Polymeric micelles for delivery of poorly water-soluble compounds. *Crit Rev Ther Drug Carrier Syst*. 2003;20(5):357-403.
300. Kabanov AV, Batrakova EV, Alakhov VY. Pluronic block copolymers as novel polymer therapeutics for drug and gene delivery. *J Control Release*. 2002;82(2-3):189-212.
301. Batrakova EV, Kabanov AV. Pluronic block copolymers: evolution of drug delivery concept from inert nanocarriers to biological response modifiers. *J Control Release*. 2008;130(2):98-106.
302. Rafael D, Melendres MMR, Andrade F, Montero S, Martinez-Trucharte F, Vilar-Hernandez M, et al. Thermo-responsive hydrogels for cancer local therapy: Challenges and state-of-art. *Int J Pharm*. 2021;606:120954.
303. Ruel-Gariépy E, Leroux JC. In situ-forming hydrogels--review of temperature-sensitive systems. *Eur J Pharm Biopharm*. 2004;58(2):409-26.
304. Klouda L, Mikos AG. Thermoresponsive hydrogels in biomedical applications. *Eur J Pharm Biopharm*. 2008;68(1):34-45.
305. Zarrintaj P, Ramsey JD, Samadi A, Atoufi Z, Yazdi MK, Ganjali MR, et al. Poloxamer: A versatile tri-block copolymer for biomedical applications. *Acta Biomater*. 2020;110:37-67.

306. Pitto-Barry A BN. Pluronic® block-copolymers in medicine: From chemical and biological versatility to rationalisation and clinical advances. *Polymer Chemistry*. 2014;5:3291-7.
307. Bodratti AM, Alexandridis P. Formulation of Poloxamers for Drug Delivery. *J Funct Biomater*. 2018;9(1).
308. Dumortier G, Grossiord JL, Agnely F, Chaumeil JC. A review of poloxamer 407 pharmaceutical and pharmacological characteristics. *Pharm Res*. 2006;23(12):2709-28.
309. Rafael D Andrade F, Montero S, Gener P, Seras-Franzoso J. Rational design of a siRNA delivery system: ALOX5 and cancer stem cells as therapeutic targets. *Prec Nanomed*. 2018;1:86-105.
310. Alakhova DY, Kabanov AV. Pluronics and MDR reversal: an update. *Mol Pharm*. 2014;11(8):2566-78.
311. Xu C, Xu J, Zheng Y, Fang Q, Lv X, Wang X, et al. Active-targeting and acid-sensitive pluronic prodrug micelles for efficiently overcoming MDR in breast cancer. *J Mater Chem B*. 2020;8(13):2726-37.
312. Russo A, Pelloso DS, Pagliara V, Milone MR, Pucci B, Caetano W, et al. Biotin-targeted Pluronic® P123/F127 mixed micelles delivering niclosamide: A repositioning strategy to treat drug-resistant lung cancer cells. *Int J Pharm*. 2016;511(1):127-39.
313. Dehghan Kelishady P, Saadat E, Ravar F, Akbari H, Dorkoosh F. Pluronic F127 polymeric micelles for co-delivery of paclitaxel and lapatinib against metastatic breast cancer: preparation, optimization and in vitro evaluation. *Pharm Dev Technol*. 2015;20(8):1009-17.
314. Uz M, Kalaga M, Pothuraju R, Ju J, Junker WM, Batra SK, et al. Dual delivery nanoscale device for miR-345 and gemcitabine co-delivery to treat pancreatic cancer. *J Control Release*. 2019;294:237-46.
315. Santos A, Veiga F, Figueiras A. Dendrimers as Pharmaceutical Excipients: Synthesis, Properties, Toxicity and Biomedical Applications. *Materials (Basel)*. 2019;13(1).
316. Abbasi E, Aval SF, Akbarzadeh A, Milani M, Nasrabadi HT, Joo SW, et al. Dendrimers: synthesis, applications, and properties. *Nanoscale Res Lett*. 2014;9(1):247.
317. Wang H, Chang H, Zhang Q, Cheng Y. Fabrication of Low-Generation Dendrimers into Nanostructures for Efficient and Nontoxic Gene Delivery. *Top Curr Chem (Cham)*. 2017;375(3):62.
318. Chauhan AS. Dendrimers for Drug Delivery. *Molecules*. 2018;23(4).
319. Sherje AP, Jadhav M, Dravyakar BR, Kadam D. Dendrimers: A versatile nanocarrier for drug delivery and targeting. *Int J Pharm*. 2018;548(1):707-20.
320. Kim Y, Park EJ, Na DH. Recent progress in dendrimer-based nanomedicine development. *Arch Pharm Res*. 2018;41(6):571-82.
321. Janaszewska A, Lazniewska J, Trzapiński P, Marcinkowska M, Klajnert-Maculewicz B. Cytotoxicity of Dendrimers. *Biomolecules*. 2019;9(8).
322. He D, Lin H, Yu Y, Shi L, Tu J. Precisely Defined Polymers for Efficient Gene Delivery. *Top Curr Chem (Cham)*. 2018;376(1):2.
323. Zielińska A, Carreiró F, Oliveira AM, Neves A, Pires B, Venkatesh DN, et al. Polymeric Nanoparticles: Production, Characterization, Toxicology and Ecotoxicology. *Molecules*. 2020;25(16).
324. Pandey P, Dureja H. Recent Patents on Polymeric Nanoparticles for Cancer Therapy. *Recent Pat Nanotechnol*. 2018;12(2):155-69.
325. Crucho CIC, Barros MT. Polymeric nanoparticles: A study on the preparation variables and characterization methods. *Mater Sci Eng C Mater Biol Appl*. 2017;80:771-84.
326. Kothamasu P, Kanumur H, Ravur N, Maddu C, Parasuramrajam R, Thangavel S. Nanocapsules: the weapons for novel drug delivery systems. *Bioimpacts*. 2012;2(2):71-81.
327. Masood F. Polymeric nanoparticles for targeted drug delivery system for cancer therapy. *Mater Sci Eng C Mater Biol Appl*. 2016;60:569-78.

328. Kumari A, Yadav SK, Yadav SC. Biodegradable polymeric nanoparticles based drug delivery systems. *Colloids Surf B Biointerfaces*. 2010;75(1):1-18.
329. Krasia-Christoforou T, Georgiou TK. Polymeric theranostics: using polymer-based systems for simultaneous imaging and therapy. *J Mater Chem B*. 2013;1(24):3002-25.
330. Lazzari S, Moscatelli D, Codari F, Salmona M, Morbidelli M, Diomede L. Colloidal stability of polymeric nanoparticles in biological fluids. *J Nanopart Res*. 2012;14(6):920.
331. Hong S, Choi DW, Kim HN, Park CG, Lee W, Park HH. Protein-Based Nanoparticles as Drug Delivery Systems. *Pharmaceutics*. 2020;12(7).
332. Elzoghby AO, Samy WM, Elgindy NA. Protein-based nanocarriers as promising drug and gene delivery systems. *J Control Release*. 2012;161(1):38-49.
333. Martínez-López AL, Pangua C, Reboredo C, Campión R, Morales-Gracia J, Irache JM. Protein-based nanoparticles for drug delivery purposes. *Int J Pharm*. 2020;581:119289.
334. DeFrates K, Markiewicz T, Gallo P, Rack A, Weyhmler A, Jarmusik B, et al. Protein Polymer-Based Nanoparticles: Fabrication and Medical Applications. *Int J Mol Sci*. 2018;19(6).
335. Lohcharoenkal W, Wang L, Chen YC, Rojanasakul Y. Protein nanoparticles as drug delivery carriers for cancer therapy. *Biomed Res Int*. 2014;2014:180549.
336. Tarhini M, Greige-Gerges H, Elaissari A. Protein-based nanoparticles: From preparation to encapsulation of active molecules. *Int J Pharm*. 2017;522(1-2):172-97.
337. Varanko A, Saha S, Chilkoti A. Recent trends in protein and peptide-based biomaterials for advanced drug delivery. *Adv Drug Deliv Rev*. 2020;156:133-87.
338. Malafaya PB, Silva GA, Reis RL. Natural-origin polymers as carriers and scaffolds for biomolecules and cell delivery in tissue engineering applications. *Adv Drug Deliv Rev*. 2007;59(4-5):207-33.
339. Nanotechnology in Medical Applications: The Global Market [online] BBC Research [Accessed 5th of September 2021] Available from: <https://www.bccresearch.com/market-research/healthcare/nanotechnology-medical-applications-market.html>.
340. Ventola CL. Progress in Nanomedicine: Approved and Investigational Nanodrugs. *P T*. 2017;42(12):742-55.
341. Andrade F, Rafael D, Vilar-Hernández M, Montero S, Martínez-Trucharte F, Seras-Franzoso J, et al. Polymeric micelles targeted against CD44v6 receptor increase niclosamide efficacy against colorectal cancer stem cells and reduce circulating tumor cells in vivo. *J Control Release*. 2021;331:198-212.
342. Oncology products [online] Samyang [Accessed 6th of September 2021] Available from: <https://samyangbiopharm.com/eng/ProductIntroduce/injection>.
343. Kim TY, Kim DW, Chung JY, Shin SG, Kim SC, Heo DS, et al. Phase I and pharmacokinetic study of Genexol-PM, a cremophor-free, polymeric micelle-formulated paclitaxel, in patients with advanced malignancies. *Clin Cancer Res*. 2004;10(11):3708-16.
344. Lee KS, Chung HC, Im SA, Park YH, Kim CS, Kim SB, et al. Multicenter phase II trial of Genexol-PM, a Cremophor-free, polymeric micelle formulation of paclitaxel, in patients with metastatic breast cancer. *Breast Cancer Res Treat*. 2008;108(2):241-50.
345. Kim DW, Kim SY, Kim HK, Kim SW, Shin SW, Kim JS, et al. Multicenter phase II trial of Genexol-PM, a novel Cremophor-free, polymeric micelle formulation of paclitaxel, with cisplatin in patients with advanced non-small-cell lung cancer. *Ann Oncol*. 2007;18(12):2009-14.
346. Lee SW, Yun MH, Jeong SW, In CH, Kim JY, Seo MH, et al. Development of docetaxel-loaded intravenous formulation, Nanoxel-PM™ using polymer-based delivery system. *J Control Release*. 2011;155(2):262-71.
347. Danson S, Ferry D, Alakhov V, Margison J, Kerr D, Jowle D, et al. Phase I dose escalation and pharmacokinetic study of pluronic polymer-bound doxorubicin (SP1049C) in patients with advanced cancer. *Br J Cancer*. 2004;90(11):2085-91.

348. Valle JW, Armstrong A, Newman C, Alakhov V, Pietrzynski G, Brewer J, et al. A phase 2 study of SP1049C, doxorubicin in P-glycoprotein-targeting pluronics, in patients with advanced adenocarcinoma of the esophagus and gastroesophageal junction. *Invest New Drugs*. 2011;29(5):1029-37.
349. Houdaihed L, Evans JC, Allen C. Overcoming the Road Blocks: Advancement of Block Copolymer Micelles for Cancer Therapy in the Clinic. *Mol Pharm*. 2017;14(8):2503-17.
350. Matsumura Y, Hamaguchi T, Ura T, Muro K, Yamada Y, Shimada Y, et al. Phase I clinical trial and pharmacokinetic evaluation of NK911, a micelle-encapsulated doxorubicin. *Br J Cancer*. 2004;91(10):1775-81.
351. Gener P, Gouveia LP, Sabat GR, de Sousa Rafael DF, Fort NB, Arranja A, et al. Fluorescent CSC models evidence that targeted nanomedicines improve treatment sensitivity of breast and colon cancer stem cells. *Nanomedicine*. 2015;11(8):1883-92.
352. Croker AK, Allan AL. Inhibition of aldehyde dehydrogenase (ALDH) activity reduces chemotherapy and radiation resistance of stem-like ALDHhiCD44⁺ human breast cancer cells. *Breast Cancer Res Treat*. 2012;133(1):75-87.
353. Hellemans J, Mortier G, De Paepe A, Speleman F, Vandesompele J. qBase relative quantification framework and software for management and automated analysis of real-time quantitative PCR data. *Genome biology*. 2007;8(2):R19.
354. Steeg PS. Tumor metastasis: mechanistic insights and clinical challenges. *Nat Med*. 2006;12(8):895-904.
355. Varela-Moreira A, Shi Y, Fens MHAM, Lammers T, Hennink WE, Schiffelers RM. Clinical application of polymeric micelles for the treatment of cancer. *Materials Chemistry Frontiers*. 2017;1(8):1-35.
356. Dragu DL, Necula LG, Bleotu C, Diaconu CC, Chivu-Economescu M. Therapies targeting cancer stem cells: Current trends and future challenges. *World J Stem Cells*. 2015;7(9):1185-201.
357. Zhou HM, Zhang JG, Zhang X, Li Q. Targeting cancer stem cells for reversing therapy resistance: mechanism, signaling, and prospective agents. *Signal Transduct Target Ther*. 2021;6(1):62.
358. Funk CD, Hoshiko S, Matsumoto T, Rdmark O, Samuelsson B. Characterization of the human 5-lipoxygenase gene. *Proc Natl Acad Sci U S A*. 1989;86(8):2587-91.
359. Wisastra R, Dekker FJ. Inflammation, Cancer and Oxidative Lipoxygenase Activity are Intimately Linked. *Cancers (Basel)*. 2014;6(3):1500-21.
360. Wang D, Dubois RN. Eicosanoids and cancer. *Nat Rev Cancer*. 2010;10(3):181-93.
361. Chen Y, Li D, Li S. The Alox5 gene is a novel therapeutic target in cancer stem cells of chronic myeloid leukemia. *Cell Cycle*. 2009;8(21):3488-92.
362. Avis I, Hong SH, Martinez A, Moody T, Choi YH, Trepel J, et al. Five-lipoxygenase inhibitors can mediate apoptosis in human breast cancer cell lines through complex eicosanoid interactions. *FASEB J*. 2001;15(11):2007-9.
363. Sarveswaran S, Chakraborty D, Chitale D, Sears R, Ghosh J. Inhibition of 5-lipoxygenase selectively triggers disruption of c-Myc signaling in prostate cancer cells. *J Biol Chem*. 2015;290(8):4994-5006.
364. Zhou GX, Ding XL, Wu SB, Zhang HF, Cao W, Qu LS, et al. Inhibition of 5-lipoxygenase triggers apoptosis in pancreatic cancer cells. *Oncol Rep*. 2015;33(2):661-8.
365. Chen Y, Sullivan C, Peng C, Shan Y, Hu Y, Li D, et al. A tumor suppressor function of the Msr1 gene in leukemia stem cells of chronic myeloid leukemia. *Blood*. 2011;118(2):390-400.
366. Solzak JP, Atale RV, Hancock BA, Sinn AL, Pollok KE, Jones DR, et al. Dual PI3K and Wnt pathway inhibition is a synergistic combination against triple negative breast cancer. *NPJ Breast Cancer*. 2017;3:17.
367. Pohl SG, Brook N, Agostino M, Arfuso F, Kumar AP, Dharmarajan A. Wnt signaling in triple-negative breast cancer. *Oncogenesis*. 2017;6(4):e310.

368. Xia P, Xu XY. PI3K/Akt/mTOR signaling pathway in cancer stem cells: from basic research to clinical application. *Am J Cancer Res*. 2015;5(5):1602-9.
369. Chen Y, Hu Y, Zhang H, Peng C, Li S. Loss of the Alox5 gene impairs leukemia stem cells and prevents chronic myeloid leukemia. *Nat Genet*. 2009;41(7):783-92.
370. Chen Y, Peng C, Sullivan C, Li D, Li S. Novel therapeutic agents against cancer stem cells of chronic myeloid leukemia. *Anticancer Agents Med Chem*. 2010;10(2):111-5.
371. Dávalos V, Suárez-López L, Castaño J, Messent A, Abasolo I, Fernandez Y, et al. Human SMC2 protein, a core subunit of human condensin complex, is a novel transcriptional target of the WNT signaling pathway and a new therapeutic target. *J Biol Chem*. 2012;287(52):43472-81.
372. Losada A, Hirano T. Dynamic molecular linkers of the genome: the first decade of SMC proteins. *Genes Dev*. 2005;19(11):1269-87.
373. Fazzio TG, Panning B. Condensin complexes regulate mitotic progression and interphase chromatin structure in embryonic stem cells. *J Cell Biol*. 2010;188(4):491-503.
374. Kalitsis P, Zhang T, Marshall KM, Nielsen CF, Hudson DF. Condensin, master organizer of the genome. *Chromosome Res*. 2017;25(1):61-76.
375. Schmiesing JA, Ball AR, Gregson HC, Alderton JM, Zhou S, Yokomori K. Identification of two distinct human SMC protein complexes involved in mitotic chromosome dynamics. *Proc Natl Acad Sci U S A*. 1998;95(22):12906-11.
376. Wang HZ, Yang SH, Li GY, Cao X. Subunits of human condensins are potential therapeutic targets for cancers. *Cell Div*. 2018;13:2.
377. Ham MF, Takakuwa T, Rahadiani N, Tresnasari K, Nakajima H, Aozasa K. Condensin mutations and abnormal chromosomal structures in pyothorax-associated lymphoma. *Cancer Sci*. 2007;98(7):1041-7.
378. Kar SP, Beesley J, Amin AI Olama A, Michailidou K, Tyrer J, Kote-Jarai Z, et al. Genome-Wide Meta-Analyses of Breast, Ovarian, and Prostate Cancer Association Studies Identify Multiple New Susceptibility Loci Shared by at Least Two Cancer Types. *Cancer Discov*. 2016;6(9):1052-67.
379. Herheliuk T, Perepelytsina O, Ugnivenko A, Ostapchenko L, Sydorenko M. Investigation of multicellular tumor spheroids enriched for a cancer stem cell phenotype. *Stem Cell Investig*. 2019;6:21.
380. Gao W, Wu D, Wang Y, Wang Z, Zou C, Dai Y, et al. Development of a novel and economical agar-based non-adherent three-dimensional culture method for enrichment of cancer stem-like cells. *Stem Cell Res Ther*. 2018;9(1):243.
381. Gener P, Rafael D, Seras-Franzoso J, Perez A, Pindado LA, Casas G, et al. Pivotal Role of AKT2 during Dynamic Phenotypic Change of Breast Cancer Stem Cells. *Cancers (Basel)*. 2019;11(8).
382. G W Carter PRY, D H Albert, J Bouska, R Dyer, R L Bell, J B Summers, D W Brooks. 5-lipoxygenase inhibitory activity of zileuton. *Pharmacol Exp Ther*. 1991;256(3):929-37.
383. Gounaris E, Heiferman MJ, Heiferman JR, Shrivastav M, Vitello D, Blatner NR, et al. Zileuton, 5-lipoxygenase inhibitor, acts as a chemopreventive agent in intestinal polyposis, by modulating polyp and systemic inflammation. *PLoS One*. 2015;10(3):e0121402.
384. Poff CD, Balazy M. Drugs that target lipoxygenases and leukotrienes as emerging therapies for asthma and cancer. *Curr Drug Targets Inflamm Allergy*. 2004;3(1):19-33.
385. Corsello SM, Nagari RT, Spangler RD, Rossen J, Kocak M, Bryan JG, et al. Discovering the anti-cancer potential of non-oncology drugs by systematic viability profiling. *Nat Cancer*. 2020;1(2):235-48.
386. Li Y, Li PK, Roberts MJ, Arend RC, Samant RS, Buchsbaum DJ. Multi-targeted therapy of cancer by niclosamide: A new application for an old drug. *Cancer Lett*. 2014;349(1):8-14.

387. Wang LH, Xu M, Fu LQ, Chen XY, Yang F. The Antihelminthic Niclosamide Inhibits Cancer Stemness, Extracellular Matrix Remodeling, and Metastasis through Dysregulation of the Nuclear β -catenin/c-Myc axis in OSCC. *Sci Rep*. 2018;8(1):12776.
388. Shajari N, Mansoori B, Davudian S, Mohammadi A, Baradaran B. Overcoming the Challenges of siRNA Delivery: Nanoparticle Strategies. *Curr Drug Deliv*. 2017;14(1):36-46.
389. Ono T, Losada A, Hirano M, Myers MP, Neuwald AF, Hirano T. Differential contributions of condensin I and condensin II to mitotic chromosome architecture in vertebrate cells. *Cell*. 2003;115(1):109-21.
390. Hirota T, Gerlich D, Koch B, Ellenberg J, Peters JM. Distinct functions of condensin I and II in mitotic chromosome assembly. *J Cell Sci*. 2004;117(Pt 26):6435-45.
391. Andrade F, Fonte P, Oliva M, Videira M, Ferreira D, Sarmiento B. Solid state formulations composed by amphiphilic polymers for delivery of proteins: characterization and stability. *Int J Pharm*. 2015;486(1-2):195-206.
392. Andrade F, das Neves J, Gener P, Schwartz S, Ferreira D, Oliva M, et al. Biological assessment of self-assembled polymeric micelles for pulmonary administration of insulin. *Nanomedicine*. 2015;11(7):1621-31.
393. Scott AM, Wolchok JD, Old LJ. Antibody therapy of cancer. *Nat Rev Cancer*. 2012;12(4):278-87.
394. Carter PJ, Lazar GA. Next generation antibody drugs: pursuit of the 'high-hanging fruit'. *Nat Rev Drug Discov*. 2018;17(3):197-223.
395. Slastnikova TA, Ulasov AV, Rosenkranz AA, Sobolev AS. Targeted Intracellular Delivery of Antibodies: The State of the Art. *Front Pharmacol*. 2018;9:1208.
396. Trenevskaya I, Li D, Banham AH. Therapeutic Antibodies against Intracellular Tumor Antigens. *Front Immunol*. 2017;8:1001.
397. Batrakova EV, Li S, Alakhov VY, Miller DW, Kabanov AV. Optimal structure requirements for pluronic block copolymers in modifying P-glycoprotein drug efflux transporter activity in bovine brain microvessel endothelial cells. *J Pharmacol Exp Ther*. 2003;304(2):845-54.
398. Schwartz S. Unmet needs in developing nanoparticles for precision medicine. *Nanomedicine (Lond)*. 2017;12(4):271-4.
399. Hwang WL, Hwang KL, Miyamoto DT. The promise of circulating tumor cells for precision cancer therapy. *Biomark Med*. 2016;10(12):1269-85.
400. Housman G, Byler S, Heerboth S, Lapinska K, Longacre M, Snyder N, et al. Drug resistance in cancer: an overview. *Cancers (Basel)*. 2014;6(3):1769-92.
401. Gradishar WJ. Taxanes for the treatment of metastatic breast cancer. *Breast Cancer (Auckl)*. 2012;6:159-71.
402. Vinogradov S, Wei X. Cancer stem cells and drug resistance: the potential of nanomedicine. *Nanomedicine (Lond)*. 2012;7(4):597-615.
403. Shen J, Yin Q, Chen L, Zhang Z, Li Y. Co-delivery of paclitaxel and survivin shRNA by pluronic P85-PEI/TPGS complex nanoparticles to overcome drug resistance in lung cancer. *Biomaterials*. 2012;33(33):8613-24.
404. Wang Y, Hao J, Li Y, Zhang Z, Sha X, Han L, et al. Poly(caprolactone)-modified Pluronic P105 micelles for reversal of paclitaxel-resistance in SKOV-3 tumors. *Biomaterials*. 2012;33(18):4741-51.
405. Hamaguchi T, Matsumura Y, Suzuki M, Shimizu K, Goda R, Nakamura I, et al. NK105, a paclitaxel-incorporating micellar nanoparticle formulation, can extend in vivo antitumour activity and reduce the neurotoxicity of paclitaxel. *Br J Cancer*. 2005;92(7):1240-6.
406. Untch M, Jackisch C, Schneeweiss A, Conrad B, Aktas B, Denkert C, et al. Nab-paclitaxel versus solvent-based paclitaxel in neoadjuvant chemotherapy for early breast cancer (GeparSepto-GBG 69): a randomised, phase 3 trial. *Lancet Oncol*. 2016;17(3):345-56.

407. Nawara HM, Afify SM, Hassan G, Zahra MH, Seno A, Seno M. Paclitaxel-Based Chemotherapy Targeting Cancer Stem Cells from Mono- to Combination Therapy. *Biomedicines*. 2021;9(5).
408. Rodrigues P, Vanharanta S. Circulating Tumor Cells: Come Together, Right Now, Over Metastasis. *Cancer Discov*. 2019;9(1):22-4.

Annex

Article 3

Rational Design of a siRNA Delivery System: ALOX5 and Cancer Stem Cells as Therapeutic Targets

Diana Rafael^{1,2*}, Fernanda Andrade^{2,3*}, Sara Montero², Petra Gener^{2,3}, Joaquin Seras-Franzoso², Francesc Martínez², Patricia González^{2,3}, Helena Florindo¹, Diego Arango⁴, Joan Sayós⁵, Ibane Abasolo^{2,3,6}, *Mafalda Videira^{1,a}, and *Simó Schwartz Jr.^{2,3,b}.

¹ Research Institute for Medicines and Pharmaceutical Sciences, Faculdade de Farmácia, Universidade de Lisboa (iMed.Ulisboa), Lisbon, Portugal.

² Drug Delivery and Targeting Group, Molecular Biology and Biochemistry Research Centre for Nanomedicine (CIBBIM-Nanomedicine), Vall d'Hebron Institut de Recerca, Universitat Autònoma de Barcelona, Barcelona, Spain.

³ Networking Research Centre for Bioengineering, Biomaterials, and Nanomedicine (CIBER-BBN), Instituto de Salud Carlos III, Zaragoza, Spain.

⁴ Biomedical Research in Digestive Tract Tumors, CIBBIM-Nanomedicine, Vall d'Hebron Institut de Recerca, Universitat Autònoma de Barcelona, Barcelona, Spain.

⁵ Immune Regulation and Immunotherapy, CIBBIM-Nanomedicine, Vall d'Hebron Institut de Recerca, Universitat Autònoma de Barcelona, Barcelona, Spain.

⁶ Functional Validation & Preclinical Research (FVPR), CIBBIM-Nanomedicine, Vall d'Hebron Institut de Recerca, Universitat Autònoma de Barcelona, Barcelona, Spain.

* These authors contributed equally to this work.

Rational Design of a siRNA Delivery System: ALOX5 and Cancer Stem Cells as Therapeutic Targets

Submitted: June 22, 2018; Accepted: June 29, 2018; Posted July 13, 2018

Diana Rafael^{1,2*}, Fernanda Andrade^{2,3*}, Sara Montero², Petra Gener^{2,3}, Joaquin Seras-Franzoso², Francesc Martínez², Patricia González^{2,3}, Helena Florindo¹, Diego Arango⁴, Joan Sayós⁵, Ibane Abasolo^{2,3,6}, *Mafalda Videira^{1,a}, and *Simó Schwartz Jr.^{2,3,b}

¹Research Institute for Medicines and Pharmaceutical Sciences, Faculdade de Farmácia, Universidade de Lisboa (iMed.Ulisboa), Lisbon, Portugal

²Drug Delivery and Targeting Group, Molecular Biology and Biochemistry Research Centre for Nanomedicine (CIBBIM-Nanomedicine), Vall d'Hebron Institut de Recerca, Universitat Autònoma de Barcelona, Barcelona, Spain

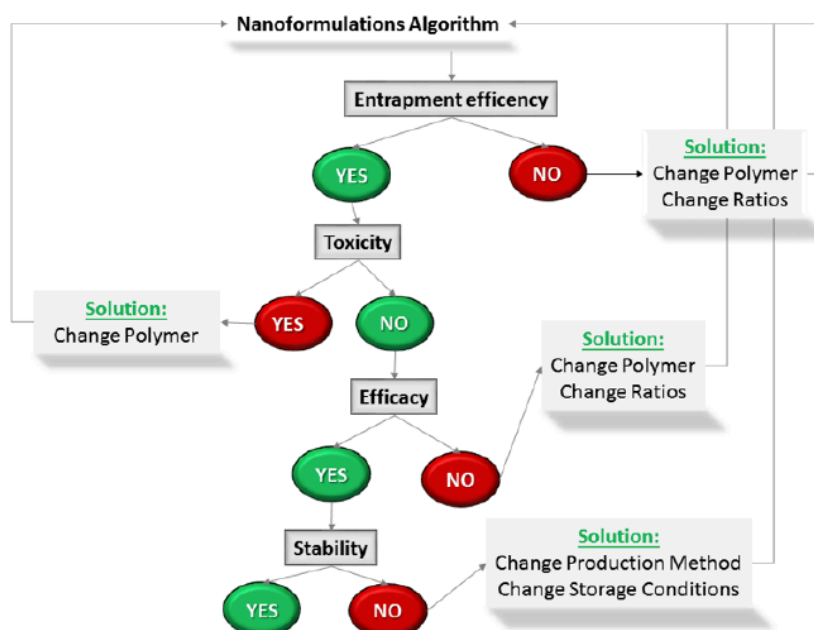
³Networking Research Centre for Bioengineering, Biomaterials, and Nanomedicine (CIBER-BBN), Instituto de Salud Carlos III, Zaragoza, Spain

⁴Biomedical Research in Digestive Tract Tumors, CIBBIM-Nanomedicine, Vall d'Hebron Institut de Recerca, Universitat Autònoma de Barcelona, Barcelona, Spain

⁵Immune Regulation and Immunotherapy, CIBBIM-Nanomedicine, Vall d'Hebron Institut de Recerca, Universitat Autònoma de Barcelona, Barcelona, Spain

⁶Functional Validation & Preclinical Research (FVPR), CIBBIM-Nanomedicine, Vall d'Hebron Institut de Recerca, Universitat Autònoma de Barcelona, Barcelona, Spain

*These authors contributed equally to this work.



^aMafalda Ascensão Videira, PhD, Assistant Professor of Pharmaceutics, iMed.Ulisboa Research Institute for Medicines, Pharmacological and Regulatory Sciences Group (PharmaRegSci), Faculdade de Farmácia da Universidade de Lisboa, Av. Prof. Gama Pinto, 1649-003 Lisboa, Portugal, mafaldavideira@campus.ul.pt

^b Simó Schwartz Jr, MD, PhD, Director, Molecular Biology and Biochemistry Research Center for Nanomedicine (CIBBIM-Nanomedicine), Vall d'Hebron Institut de Recerca (VHIR), Barcelona Vall d'Hebron Hospital Campus, Passeig de la Vall d'Hebron, 119-129 - 08035 Barcelona, Spain, simo.schwartz@vhir.org

Abbreviations:

- ALOX5 Arachidonate 5-lipoxygenase
- 5-DTAF 5-[4,6-dichlorotriazin-2-yl]amino)fluorescein hydrochloride
- AE Association efficiency
- ALDH1A1 Aldehyde dehydrogenase 1
- CMT Critical micellar temperature
- DAPI 4',6-diamidino-2-phenylindole
- DD Degree of deacetylation
- DLS Dynamic light scattering
- DM Direct Dissolution method
- EO Ethylene oxide
- EPR Enhanced permeability and retention effect
- ERK Extracellular signal-regulated kinases
- FACS Fluorescence-activated cell sorting
- FBS Fetal bovine serum
- FGFR Fibroblast growth factor receptors
- FH Thin-film hydration
- GADPH Glyceraldehyde 3-phosphate dehydrogenase
- GFP Green fluorescent protein
- MTT 3-(4,5-dimethylthiazol-2-yl)-2,5 diphenyl tetrazolium bromide
- PDI Polydispersity index
- PO Propylene oxide
- qRT-PCR Quantitative real time polymerase chain reaction
- ZP Zeta potential

Keywords:

Polymeric Micelles, Pluronic® F127, Gene Delivery, siRNA, ALOX5, Cancer Stem Cells.

Abstract

The search for an ideal gene delivery system is a long and laborious process in which several factors from the first idea to final formulation, including main challenges, peaks and troughs, should be deeply taken into consideration to ensure adequate biological safety and in vivo efficacy endpoints. Arachidonate 5-lipoxygenase (ALOX5), a crucial player related with cancer development and in particular with cancer stem cells malignancy. In this work we describe the process behind the development of a small interfering RNA (siRNA) delivery system to inhibit ALOX5 in cancer stem cells (CSC), as a model target gene. We started by screening chitosan polyplexes, among different types of chitosan in different complexation conditions. Due to the low silencing efficacy obtained, chitosan polyplexes were combined with Pluronic®-based polymeric micelles with recognized advantages regarding gene transfection. We tested different types of polymeric particles to improve the biological efficacy of chitosan polyplexes. Nevertheless, limited transfection efficiency was still detected. The well-established polyethylenimine (PEI) cationic polymer was used in substitution of chitosan, in combination with polymeric micelles, originating PEI-siRNA-Pluronic® systems. The presence of Pluronic® F127 in the formulation showed to be of utmost importance, because not only the silencing activity of the polyplexes was improved, but also PEI-associated toxicity was clearly reduced. This, allowed to increase the amount of PEI inside the system and its overall efficacy. Indeed, different types of PEI, N/P ratios and preparation methods were tested until an optimal formulation composed by PEI 10k branched-based polyplexes at an N/P ratio of 50 combined with micelles of Pluronic® F127 was selected. This combined micelle presented adequate technological properties, safety profile and biological efficacy, resulting in high ALOX5 gene silencing and strong reduction of invasion and transformation capabilities of a stem cell subpopulation isolated from MDA-MB-231 triple negative breast cancer cells.

Rationale and Purpose

The design and development of a nanoparticle-based drug delivery system is a long and complex process that is often not reflected in the literature. There are years of backstage work and a wide collection of negative results that are considered not publishable. However, this data gives crucial information for moving forward in the proper direction. Moreover, the publication of negative results, although not usual, is of great importance for time and resources optimization, by avoiding the repetition of similar errors by other research groups and, more importantly, by redefining the work plan priorities. Described in this work is the rational design and experimental sequence beyond the development of a nanocarrier system for siRNA intracellular delivery, with the negative results and the consequent modifications and improvements. The ultimate goal is the development of a new nanotechnology-based approach for cancer treatment.

Introduction

Despite of considerable number of advances achieved in the past decades, clinical use of nucleic acids as gene-based antitumor therapy is still precluded, mainly because of their poor cellular uptake, vulnerability to enzymatic degradation, and rapid renal clearance. Until now, most gene therapy strategies rely on the use of viral vectors, even though their use frequently raises important safety issues, challenging their clinical standardization as gene delivery vectors. Further, several limitations have also been identified in some non-viral vectors, such as low specificity, cellular toxicity, and limited transfection efficiencies (1, 2). Therefore, successful clinical application of gene therapy in the oncology field urgently demands the emergence of new and safer vehicles to first, enable oligonucleotides (OGN) to be effectively delivered into tumor target cells, and second, to overcome the well-known drawbacks of current vehicles (1, 3-6). Moreover, the design of a new vehicle has to take into account that an ideal gene delivery system should be efficient, stable, cost effective, and able to avoid rapid hepatic and renal clearance. Safety issues such as biocompatibility, biodegradability and lack of

immunogenicity are also critical, as well as the need of an appropriate balance between protection and release of the genetic material from the endosomes (e.g. proton-sponge effect) in order to ensure biological functionality (1, 7). Other characteristics such as particle size, surface charge, presence of moieties and also their interactions with the tumoral environment should be finely tuned in order to improve their biological behavior and efficacy (8, 9). Nanoparticles intended for gene delivery usually possess in its composition cationic polymers, such as chitosan (CS) and polyethylenimine (PEI) that condense negatively charged nucleic acids through electrostatic interactions (2, 10, 11).

CS is a natural cationic polysaccharide composed of glucosamine and N-acetyl glucosamine, whose ability to interact with negatively charged OGN depend, among other factors, on its Molecular Weight (MW) and Deacetylation Degree (DD). Whereas high DD enables better interaction with genetic material, high MW improves stability of the complexes, while low MW ameliorates intracellular release of OGN (12-14). Accordingly, DD and MW of CS should be adequately considered in order to ensure an appropriate balance between protection and release of OGN. In order to improve transfection efficiency of CS-based carriers, different chemical modifications as well as the use of the water-soluble salt forms of CS have been investigated (12, 13, 15-21). Regarding PEI and despite its high transfection efficiency, its use as a delivery vehicle is hampered because of its high cationic charge density (22-24). In fact, the transfection efficiency and cytotoxicity of these polymers are highly dependent on their linear versus branched structure, their branching degree and their MW (23, 25-28). PEI branched forms present higher transfection efficiencies than linear forms. Furthermore, higher MW PEI are frequently associated with higher buffering capacity, higher transfection efficiencies and also with increased cytotoxicity. An adequate ratio between the nitrogen content of the polymer and the number of phosphate groups from the OGN (N/P ratio) should be optimized for each formulation in order to find an equilibrium of charges and to achieve maximal efficacy with minor toxicity (23, 25, 27, 29).

Many different strategies have been explored in order to improve the efficiency of PEI transfection by reducing cytotoxicity, avoiding aggregation, and decreasing nonspecific interactions. Among them, grafting PEI with polyethyleneglycol (PEG) has become one of the most popular ones (30, 31).

In this study, both CS and PEI polycations have been used in combination with poloxamers (Pluronic®) based micelles (PM) in order to achieve an improvement of their transfection efficiency and toxicity profile, as well as their efficacy against cancer cells. Poloxamers are amphiphilic polymers consisting in ethylene oxide (EO) and propylene oxide (PO) chains arranged in an *a-b-a* triblock structure (EO-PO-EO) (32, 33). They have been included in the formulation due to their recognized ability to enhance transfection of genetic material (33-36). Because of their PEGylated surface, poloxamers offer stealth properties to the system and can be easily functionalized with different targeting moieties (37). Moreover, these polymers are approved for human administration due to their optimal water-solubility, biodegradability, and biocompatibility, as well as their low immunogenicity profile, which makes them a simple and safer approach for *in vitro* and *in vivo* gene transfection (38, 39). Several conditions and combinations have been tested to better define those which show the highest transfection efficiency and good antitumor efficacy in bioluminescent breast cancer models. Indeed, among the big challenges in cancer therapy are the avoidance of the metastatic spread of the disease, the appearance of multidrug resistance, and tumor recurrence as those features which are mostly related to the presence of CSC within a tumor (40). Arachidonate 5-lipoxygenase (ALOX5) silencing was selected as a candidate target due to its recognized key role in CSC survival and self-renewal (41). Our data show that poloxamer-PEI combinations with ALOX5-siRNA were effective in silencing ALOX5 in breast CSC and showed great therapeutic potential as anticancer treatment, significantly reducing cell malignant transformation and CSC invasion.

Materials and Methods

Materials

Different types of CS with DD of ~86% (Protasan Ultrapure) were gently provided by NovaMatriX (USA), namely, glutamate-CS low (G113 - 160 kDa) and high (G213 - 470 kDa) MW, and hydrochloride-CS low (CL113 - 110 kDa) and high (CL213 - 270 kDa) MW. Glycol-CS was purchased from Sigma Aldrich (Madrid, Spain). Pluronic® F68, F108 and F127 were kindly provided by BASF (Ludwigshafen, Germany), while 10k branched and 25k branched PEI were provided by Alfa Aesar (Thermo Fisher GmbH, Karlsruhe, Germany) and Sigma-Aldrich (Madrid, Spain), respectively. siRNA against gree fluorescent protein (GFP-siRNA) and the scramble sequence (siC) were provided by LifeTechnologies (Spain). The sense anti-ALOX5 siRNA sequence used was 5'-CUGAGCGCAACAAGAAGAATT-3', while a non-specific sequence, 5'-UUCUCCGAACGUGUCACGUTT-3', was used as negative control. MDA-MB-231 (ATCC number HTB-26) cell line was obtained from American Type Culture Collection (ATCC, LGC Standards, Barcelona, Spain), and RXO-C colon cancer cells expressing GFP were generously provided by Dr. Diego Arango (CIBBIM-Nanomedicine). RPMI medium, phosphate buffered saline (PBS), and fetal bovine serum (FBS) were purchase from Lonza (Barcelona, Spain). Penicillin-streptomycin, L-glutamine, non-essential amino acids, sodium pyruvate, 0.25% Trypsin-EDTA, Lipofectamine® 2000, 4',6-diamidino-2-phenylindole (DAPI), and LysoTracker® Red were brought from Life Technologies Ltd. (Madrid, Spain). Other reagents used were methanol, ethanol, dimethyl sulfoxide (DMSO), 3-(4,5-dimethylthiazol-2-yl)-2,5-diphenyl tetrazolium bromide (MTT), gelatin, paraformaldehyde, Triton X-100, and 5-([4,6-dichlorotriazin-2-yl]amino)fluorescein hydrochloride (5-DTAF) from Sigma-Aldrich (Madrid, Spain), and Type 1 ultrapure water (18.2 MΩ.cm at 25 °C, Milli-Q®, Billerica, MA, USA).

Methods

Polyplex Preparation

Polymer-siRNA complexes were prepared by simple complexation, adding the polymer

solution dropwise to an equal volume of siRNA solution. The mixture was quickly vortexed during few seconds and incubated at room temperature for 30 minutes. CS-siRNA complexes were prepared at different N/P ratios calculated according to Equation 1 (mass per charge of phosphate = 330 g/mol and mass per charge of Nitrogen = 160 g/mol) and at different conditions (Table 2).

$$\frac{N}{P} \text{ ratio} = \frac{\frac{\text{Mass of polycation}}{\text{Mass per charge of Nitrogen}}}{\frac{\text{Mass of siRNA}}{\text{Mass per charge of Phosphate}}}$$

Equation 1

For the PEI-based polyplexes, two types of branched PEI, namely 10k and 25k, were used. Different N/P ratios were tested ranging from 5 to 75 (Table 4) and calculated according to Equation 1 (Considering mass per charge of phosphate = 330 g/mol and mass per charge of nitrogen = 43 g/mol).

Micelles Preparation through the Direct Dissolution Method (DM)

The amphiphilic polymer was dissolved overnight (O/N) under agitation in aqueous solution, and added dropwise to the polyplexes solution, previously prepared. After vortexing, the mixture was left to incubate for 30 minutes and filtered through a 0.22 µm syringe filter.

Micelles Preparation through the Thin-Film Hydration (FH) Technique

The amphiphilic polymers were individually weighted and dissolved in a mixture of methanol:ethanol=1:1. This mixture of solvents was chosen because the polymers are insoluble in ethanol alone (Class 3 solvent), but soluble in methanol (Class 2 solvent). By mixing both solvents it was possible to solubilize the polymers and reduce the use of methanol, as previously described. Then, the solvent was removed under vacuum and the formed film was left to dry at room temperature to eliminate any remaining solvent. Afterwards, the film was hydrated with PBS for empty micelles or with the previously prepared polymer-siRNA polyplexes and vortexed for 1 minute. The obtained dispersion was filtered through a 0.22 µm syringe filter to remove possible aggregates.

Association Efficiency (AE)

The non-associated siRNA present in the aqueous phase of the polyplexes was separated by centrifugation with filtration (10,000 rpm, 10 minutes) using a 100K membrane (Nanosep® Centrifugal Devices, Millipore, USA) and measured by spectrophotometry (Nanodrop NP-1000, Thermo Scientific, USA). AE was calculated according to Equation 2, and also assessed by agarose gel electrophoresis. Polyplexes were loaded onto 1% agarose gel with 6X loading buffer. The mixture was separated in 0.5X Tris/Borate/EDTA (TBE) buffer at 100V for 25 minutes. siRNA bands were visualized using an ultra violet imaging system (Uvidoc, UVItect Ltd, Cambridge, UK).

$$AE = \frac{\text{Total amount of siRNA-Free siRNA in filtrate}}{\text{Total amount of siRNA}} \times 100$$

Equation 2

Particles Physicochemical Characterization

Particles mean hydrodynamic diameter (md) and polydispersity index (PDI) were measured by dynamic light scattering (DLS). Zeta potential was assessed by laser Doppler micro-electrophoresis using NanoZS (Malvern Instruments, UK). For each formulation, at least three batches were produced and analyzed. Particle shape and morphology were observed by transmission electron microscopy (external services from IBMC, University of Porto, Portugal).

Serum Stability

To assess the stability of formulations in the presence of serum, particles were incubated in a proportion of 1:1 with 50% FBS culture medium. Mean diameter was measured by DLS at 0, 6, 12, and 24 hours.

Cell Lines Culture Conditions

RXO-C and MDA-MB-231 breast cancer cell lines were cultured in RPMI medium supplemented with 10% FBS, 1% penicillin-streptomycin, 1% L-glutamine, 1% non-essential amino acids and 1% of sodium pyruvate. CSC subpopulation from MDA-MB-231 cell line was isolated using a model previously validated by our group (42). Briefly, the model is based on the expression of tdTomato under the control of a CSC specific promoter (ALDH1A1), which allows the separation of CSC among the bulk tumor cells population and the study of the biological

efficacy of the developed therapeutic system in this subpopulation of cells. Blasticidin (0.5 mg/mL) was used as a selective antibiotic for ALDH1A1/tomato cell lines. All cell lines were kept at 37°C under 5% CO₂ saturated atmosphere. Cell medium was changed every other day and, upon confluence, cells were harvested from plates with 0.25% trypsin-EDTA.

Cell Transfection

Different siRNA formulations were transfected into cells according to the conditions shown in Table 1. For silencing experiments, the medium was changed after 4 hours of incubation with

polyplexes and PM-polyplexes. For the toxicity assays, cells were left 24 hours in contact with formulations, while for internalization assays, cells were incubated over 4 hours. Cells were harvested 24 to 72 hours after transfection. For internalization experiments, particles were diluted at a ratio of 1:10. Lipofectamine® 2000 was used as positive control for transfection according to suppliers' protocols and in order to obtain a final siRNA concentration in the well of 200 nM. For all experiments, cells were transfected at the same conditions using a scrambled siRNA sequence (siC).

Table 1. Transfection Conditions for the Different Experiments

Plates	Day 0: before transfection		Day 1: during transfection time (4 hours)		
	Cells seeded (cells/well)	Volume of medium (μl)	Volume of medium (μl)	Volume of formulation (μl)	Final siRNA concentration (nM)
96 well	5.0×10 ³	100	50	50	200
24 well	5.0×10 ⁴	1000	100	100	200
6 well	2.0×10 ⁵	2000	250	250	200

GFP Reporter Gene Silencing Assay

RXO-C cancer cells expressing GFP were used as a model to assess the silencing efficacy of the different nanosystems. Polyplexes and micelles prepared using a GFP-siRNA and different cationic polymers were transfected to cells previously seeded in 96 well plates. Complexes formed between Lipofectamine® 2000 and GFP-siRNA were used as positive controls. The expression of GFP in cells after transfection was assessed with fluorescence microscopy (Olympus, USA). The intensity of cells fluorescence was also measured using an FLX800 Fluorescent Microplate Reader (BioTek, Germany).

In vitro Cytotoxicity Assay

The cytotoxicity of different components was assessed in MDA-MB-231 breast cancer cells using the MTT assay. Briefly, cells previously seeded in 96-well plates were incubated in the presence and absence of increasing concentrations of polymers/formulations for 24 hours. After the incubation time, medium was changed, and cells left for additional 72 hours. Complete medium was used as negative control and 10% DMSO as positive control of toxicity.

After 72 hours of incubation, 0.5 mg/mL of MTT was added to each well. Plates were incubated for additional 4 hours at 37°C, the medium discarded, and the formazan crystals produced by mitochondrial succinate dehydrogenase dissolved with DMSO. The absorbance of each well was read on a microplate reader (ELx800 absorbance reader, BioTek, Germany) at 590 nm and cell viability calculated accordingly. Cell viability data were used to determine IC₅₀ value by nonlinear regression of the dose-effect curve fit, using Prism 6.02 software (GraphPad Software, Inc., CA, USA).

Conjugation of F127 with 5-DTAF

F127 was fluorescently conjugated with 5-DTAF in an aqueous medium via nucleophilic aromatic substitution by an addition-elimination pathway, as previously described.⁴⁴ Briefly, a stock solution of 20 g/L 5-DTAF in DMSO was diluted in 0.1M sodium bicarbonate (pH 9.3) and added to a 6% (w/v) F127 solution in 0.1M sodium bicarbonate (pH 9.3) to a final molar ratio of 1:2 (F127:5-DTAF). The reaction was left overnight in the dark, at room temperature. Unreacted 5-DTAF was washed out by dialysis (12,000–14,000 MWCO

Spectra/Por® membrane from Spectrum Europe BV, The Netherlands) against type I ultrapure water. Dialyzed polymer solutions were lyophilized and stored in closed containers protected from light (Virtis Benchtop Freeze Dryer, SP Scientific).

Internalization Assays

Flow cytometry and confocal microscopy were used to assess quantitatively and qualitatively the internalization capacity of the nanosystem into MDA-MB-231 breast cancer cells. For quantitative Fluorescence-activated cell sorting (FACS) assays, 2×10^5 cells were seeded in 6 well plates and incubated for 24 hours. After incubation, 5-DTAF-labelled micelles were added to cells and incubated for 4 hours, and washed with $1 \times$ PBS, detached with 0.25% trypsin-EDTA, and re-suspended in PBS supplemented with 10% FBS. Cells were then stained with DAPI (1 μ g/mL). Plates were then analyzed in a Fortessa cytometer (BD Biosciences, San Jose, California, USA). Data were analyzed with FCS Express 4 Flow Research Edition software (De Novo Software, Los Angeles, USA). Contaminants were removed by forward and side scatter gating. For each sample, at least 10000 individual cells were collected to measure mean fluorescence intensity. For qualitative confocal microscopy assay (Spectral Confocal Microscope MFV1000 Olympus, USA), cells were cultured in 0.1% gelatin-treated coverslips at a density of 2.5×10^5 cells per well in 6 well plates. After 24 hours, cells were incubated with 5-DTAF labelled-PM for 4 hours, and further incubated for 30 minutes with LysoTracker® Red. Subsequently, cells were fixed using 4% paraformaldehyde. Finally, nuclei were stained with DAPI (0.2 mg/mL) for 5 minutes in the dark and further visualized.

Cell sorting

FACS was used to sort CSC and non-CSC subpopulations from a heterogeneous population MDA-MB-231 cells. For cell sorting, a starting amount of 5×10^6 cells was used. Cells were detached with 0.25% trypsin-EDTA and re-suspended in PBS supplemented with 10% FBS and DAPI (1 μ g/mL) used for vital staining. Cells were sorted according to tdTomato expression and DAPI staining in a FACS Aria cell sorter (BD Biosciences, Madrid, Spain). Sorted cells were collected in

complete medium without antibiotic and stored.⁴⁴

RNA Extraction and Quantitative RT-PCR (qRT-PCR)

Total RNA was extracted from cells using RNeasy Micro Kit (Qiagen, Madrid, Spain). RNA was reverse transcribed with High Capacity cDNA Reverse Transcription Kit (Applied Biosystems, Madrid, Spain) according to manufacturer instructions. The cDNA reverse transcription product was amplified with specific primers for ALOX5 (hALOX5 F:

5' AGAACCTGGCCAACAAGATTGT A 3'; hALOX5 R:

5' TCTGGTGGACGTGGAAGTCA 3') GADPH (hGADPH F: 5' ACC CAC TCC TCC ACC TTT GAC;

hGADPH R:

5' CAT ACC AGG AAA TGA GCT TGA CAA 3') and

Actin (hActin F:

5' CAT CCA CGA AAC TAC CTT CAA CTC C 3';

hActin R:

5' GAG CCG CCG ATC CAC AC 3') by qPCR using the SYBR Green method. The reaction was performed in triplicate in a 7500 Real-Time PCR system (Applied Biosystems, Madrid, Spain). Actin and GADPH, were used as endogenous controls. Relative mRNA levels were calculated using the comparative Ct method ($2^{-\Delta\Delta Ct}$).

Cell Transformation Assay (Anchorage-Independent Growth Assay)

Anchorage-independent growth of the different breast cancer cell lines was assessed by CytoSelect™ Cell Transformation Assay Kit (Cell Biolabs, San Diego, CA, USA). A semisolid agar media was prepared according to manufacturer prior addition of PM-siALOX5 or PM-siC to each well. After 6–8 days of incubation, colonies were observed under optical microscopy and viable transformed cells counted using trypan blue.

Invasion Assay

Cells invasiveness was assessed using CytoSelect™ Laminin Cell Invasion Assay Kit (Cell Biolabs, San Diego, CA, USA) accordingly to manufacturer instructions. Briefly, inserts were placed in 24 well plates

and 2.5×10^4 cells previously transfected (24 hours before) with PM-siALOX5 and PM-siC, added to the upper chamber. After 48 hours incubation, invasive cells were dissociated from the membrane, lysed, and quantified with CyQuant® GR Fluorescent Dye using an FLX800 Fluorescent Microplate Reader (BioTek, Germany).

Statistical Analysis

At least three batches from each polyplex and PM were produced and characterized, and results expressed as mean \pm standard deviation (SD). For biological studies, at least 3 replicates, each involving at least two technical replicates, were involved. Final results were also expressed as mean \pm SD. Statistical analysis

was performed in Microsoft Office Excel™ 2010 using unpaired Student's t-test. Differences were considered as statistically significant when p-values were smaller than 0.05.

Results

CS-Based Systems

Due to known advantages of CS and its derivatives for gene delivery, a screening for the best CS polyplexes with optimal transfection conditions was performed. GFP silencing efficacy of different conditions and combinations were also tested (Table 2). For all CS showing high AE *in vitro* cytotoxicity was also assessed.

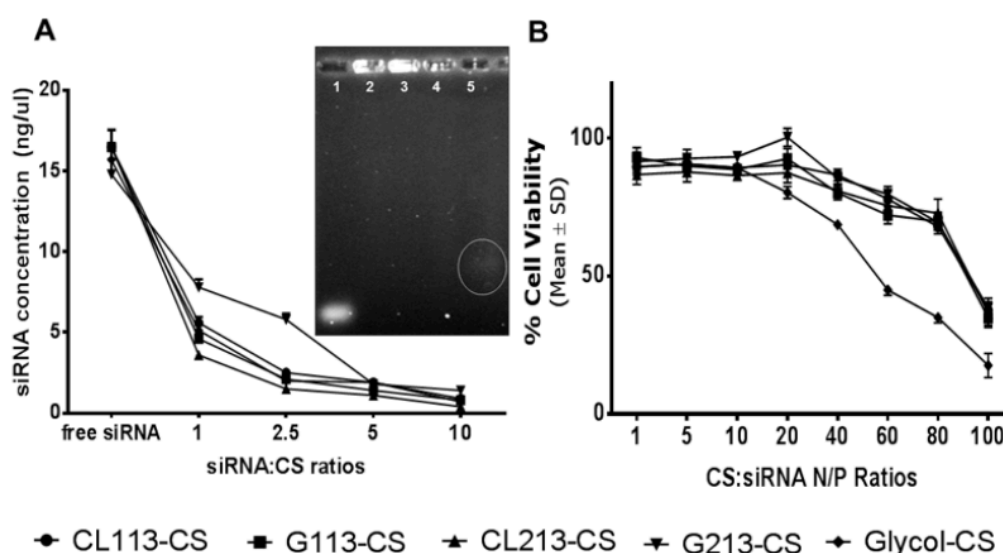


Figure 1. A, *In vitro* cytotoxicity of CS-siRNA polyplexes at different N/P ratios in MDA-MB-231 cells. B, Polyplexes association efficiency. The graph represents the concentration of free siRNA detected in the supernatant by spectrophotometry after formulation filtration by centrifugation using different N/P ratios. Agarose gel electrophoresis for the CL213-based polyplex. 1 – free siRNA; 2 – 1:10 ratio; 3 – 1:5 ratio; 4 – 1:2.5 ratio; 5 – 1:1 ratio. Free siRNA was observed in siRNA:CS ratio of 5:1 (encircled).

According to our data, all CS were able to efficiently complex with siRNA (Figure 1A). A decrease in the concentration of free siRNA was observed upon complexation with CS even at low ratios. Additionally, in the agarose gel assay, a small amount of free siRNA was only detected in CS:siRNA 1:1 ratio. Nonetheless, low N/P ratios are not enough to produce biological efficacy, thus higher N/P ratios were

further tested in terms of cell toxicity. Figure 1B demonstrates that CL113, G113, CL213 and G213 have a similar toxicity pattern, being an N/P ratio of 80 the maximum N/P ratio that can be used without causing severe toxicity. Glycol-CS causes higher toxicity even at lower N/P ratios.

Table 2. Summary of the Different Conditions Tested on CS-Based Polyplexes

Tested Conditions		Observations
siRNA final conc. in the well	50 nM	No effect
	100 nM	No effect
	200 nM	Effective (at certain conditions)
Polyplexes	Glycol-CS	Toxic (at ratios > 60)
	G113	No effect
	CL113	No effect
	G213	Effective (at certain conditions)
	CL213	Effective (at certain conditions)
N/P ratios	<10	No effect
	20	No effect
	30	No effect
	40	No effect
	60	No effect
	80	Knockdown detected (at certain toxicity)
	100	Toxicity
	>100	Highly toxic
pH	4.5 (in acetate buffer)	Higher efficacy
	7 (in water)	Low effect
Time-points	24 hours	No effect
	48 hours	No effect
	72 hours	Knockdown detected
Micelles	CL213 (N/P 80, pH 4.5) + F127 (1%) Time-point 72 hours	Effect < than Lipofectamine® 2000

As described in Table 2, the most promising polyplexes, such as those able to cause a visible decrease in the number of cells expressing GFP without promoting significant toxicity, were obtained with the following conditions: GFP-siRNA at a final concentration of 200 nM per well, complexed with CL213 and G213 CS at a N/P ratio of 80 and pH 4.5, observed in a post-transfection incubation time of 72 hours.

Results depicting the silencing efficacy of CL213-based GFP-siRNA polyplexes produced at optimal conditions, are showed in Figure 2A. A partial silencing of the expression

of GFP at 72 hours after transfection, was observed. Nonetheless, a significantly stronger silencing was observed in cells transfected with Lipofectamine® 2000. On the contrary, no decrease of GFP expression was observed in cells transfected with siC. Similar results were obtained with the polyplexes composed by G213. No significant silencing efficacy was observed with other types of CS tested. CS-siRNA polyplexes produced with CL213-CS were further characterized resulting in 17nm size, positive charge (+ 15 mV) and spherical shape (Table 3).

Table 3. Physicochemical Characterization of Polyplexes using CL213 CS

Parameters	CL113-CS polyplexes
Md (nm)	16.6 ± 0.8
PDI	0.19 ± 0.07
Zp (mV)	+15.2 ± 1.7

Md = mean diameter; PDI = polydispersity index; Zp = Zeta potential. Md, PDI, and Zp values for Cs-siRNA polyplexes are expressed as mean±SD, n=3.

Table 4. Physicochemical Characterization of Different Pluronic®-Based Micelles

Polymer	Md (nm)	PDI	Zp (mV)	IC ₅₀ (mg/mL)
F68	228.6 ± 31.2	0.5 ± 0.2	2.9±1.0	n.d.
F108	130.2 ± 18.4	0.4 ± 0.2	2.1±1.2	>10
F127	68.5 ± 9.4	0.2 ± 0.1	2.7±1.8	>10

Md=Mean diameter; PDI=polydispersity index; Zp=Zeta potential. Md, PDI and Zp values for polyplexes Cs-siRNA are expressed as mean±SD, n=3.

Different Pluronic®-based PM obtained by direct DM were tested with the objective to ensure protection of the siRNA sequence and to increase the biological efficacy of these polyplexes. All micelles presented sizes under 250 nm (lower than 75 nm for Pluronic® F127) and nearly a neutral surface charge (Table 4).

Due to high polydispersity and low reproducibility of micelles obtained with F68, this polymer was discarded from the further studies. Regarding cytotoxicity assessment, both Pluronic® F108 and F127 presented IC₅₀ higher than 10 mg/mL (Table 4). Because Pluronic® F127 micelles showed the smallest

size and lowest polydispersity, it was selected to produce micelles combined with CL213-CS-based polyplexes (CS-siRNA-Pluronic®). In the biological assessment, we observed better silencing of GFP expression from CS-siRNA-Pluronic®-polyplexes compared to CS-polyplexes (Figure 2B). Conversely, no silencing was noticed in cells transfected with siC. However, despite the improvement in gene silencing promoted by the presence of Pluronic® F127, silencing efficacy of this system is still lower than the one obtained using Lipofectamine® 2000, as positive control.

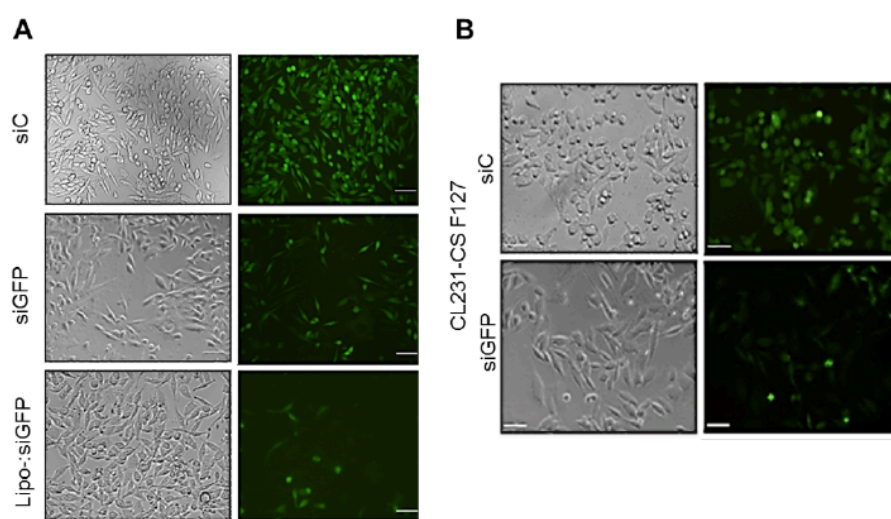


Figure 2. A, Silencing efficacy of CS-siRNA polyplexes at 72 hours after transfection in RXO-C cells expressing green fluorescent protein (GFP). Biological activity was assessed based on GFP expression reduction in cells transfected with CS polyplexes loaded with GFP-siRNA versus siC, using a fluorescence microscope. Lipofectamine® 2000-based complexes were used as positive control. B, GFP silencing efficacy of CS-siRNA-Pluronic® micelles 72 hours post-transfection, using siGFP and siC in RXO-C cells, respectively (results are expressed as mean±SD, n=3).

PEI-based Systems: DM

As cationic polymers, CS show advantages related with siRNA complexation efficiency and biological safety but fail in biological gene silencing efficacy. Therefore, the substitution of CS by PEI as cationic polymer was tested. Despite its potential cytotoxicity effects, PEI is

also known for its endosomal membrane disruptive properties and high transfection ability. Pluronic® F127 PM were maintained as part of the formulation with the intention to reduce the required amount of PEI to obtain the desired biological effect, thus reducing PEI-associated toxicity (Table 5).

Table 5. Summary of the Different Tested Conditions Regarding the Branched PEI-Based Systems

Tested Conditions		Observations
siRNA final conc. in the well	200 nM	Effective (at certain conditions)
Polymers combinations	PEI 10K	Low effect
	PEI 25K	Low effect
	PEI 10K + F127 (0.5%)	Effect < than Lipofectamine® 2000
	PEI 25 K + F127 (0.5%)	Effect < than Lipofectamine® 2000
	PEI 10K + F127 (1%)	Effective (at N/P 50)
	PEI 25 K + F127 (1%)	Effective (at N/P 25 and 50)
N/P ratios PEI:siRNA	5	No effect
	25	Effective only for PEI 25K
	50	Effective
	75	Toxic

Formulations composed by PEI:siRNA polyplexes of N/P ratio 50 presented higher transfection efficacy than polyplexes with lower N/P ratios (Figure 3A). No significant differences were observed between both types of PEI (Figure 3A). The 10K branched PEI. was chosen as cationic polymer because of its lower toxicity profile.^{46,47} As observed for CS-polyplexes, the presence of 1% Pluronic® F127 in the formation of micelles (prepared by DM) improved significantly the transfection efficiency of PEI-polyplexes (Figure 3B). Moreover, Pluronic® F127 reduces the cytotoxicity of PEI-polyplexes (Figure 4B).

Therefore, Pluronic® 127 micelles associated with PEI:siRNA polyplexes at a N/P ratio 50 were selected for further studies, and characterized in terms of their internalization profile, physicochemical features and serum stability. The internalization of PEI-siRNA-Pluronic® micelles was qualitatively assessed by confocal microscopy (Figure 4A). For that, MDA-MB-231 cells were incubated with 5-DTAF-labeled micelles for 4 hours. Internalization of PM was observed after incubation time, as well as co-localization with cytoplasmic endosomal vesicles (Figure 4A).

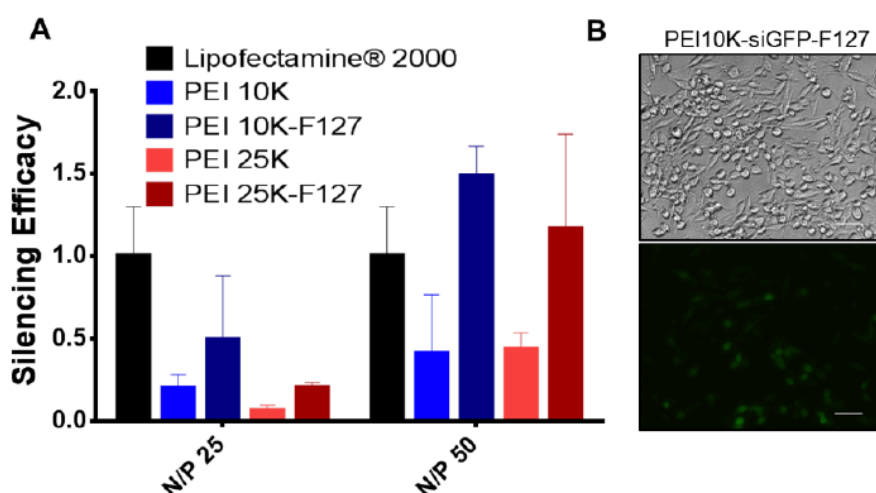


Figure 3. A, Green fluorescent protein (GFP) silencing efficacy of polyethylenimine (PEI)-siRNA polyplexes and PEI-siRNA-Pluronic® micelles (obtained by DM) in GFP expressing RXO-C cells. Lipofectamine® 2000 was used as reference to determine differences on the intensity of GFP expression upon incubation with different formulations. GFP silencing values are normalized to Lipofectamine® 2000 as control. Results are expressed as mean±SD (n≥3). * p≤0.05 compared to the polyplexes without Pluronic® F127. B, Fluorescent microscopy of GFP silencing efficacy of PEI10K-siGFP-F127 formulation.

Despite the adequate association efficiency (>93%), cytotoxicity ($IC_{50} > 10\text{mg/mL}$), and biological efficacy, the physicochemical characterization of this formulation showed increased polydispersity and aggregation over

time, under storage. (Table 6). Moreover, serum stability studies showed an increase in the mean diameter of particles after the first 6 hours of incubation, clearly indicating their opsonization by serum proteins (Figure 4C).

Table 6. Physicochemical Characterization of PEI-siRNA-Pluronic® Micelles

Sample	Md (nm)	PDI	ZP (mV)	AE (%)
PM-siRNA	60.28 ± 8.65	0.51 ± 0.07	-0.21 ± 0.06	93.02 ± 0.12
PM	73.22 ± 9.54	0.28 ± 0.078	3.81 ± 0.96	

AE=association efficiency; Md=mean diameter; PDI=polydispersity index; ZP=zeta potential. AE values are calculated by undirected method previously described. Results are expressed as mean \pm SD, n=3.

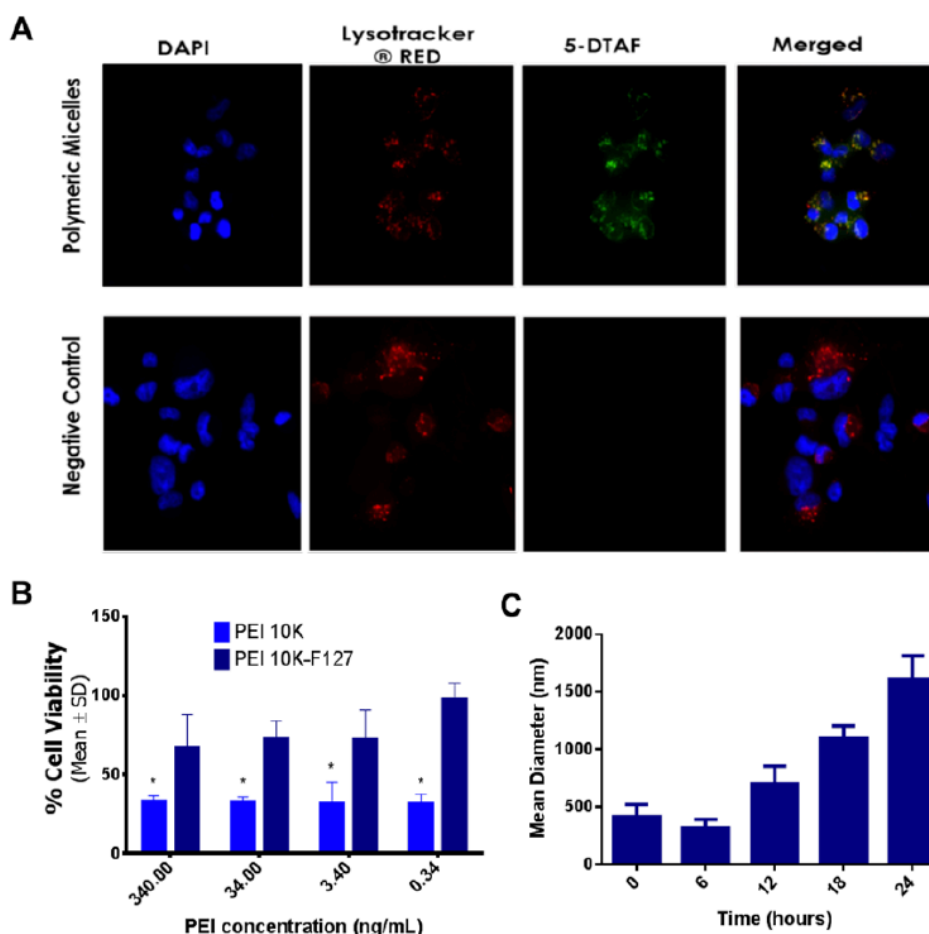


Figure 4. A, Comparative cytotoxicity of formulations with and without Pluronic® F127, at different concentrations. B, Confocal microscopy analysis of labelled particles. Internalization after 4 hours of incubation showing DAPI stained nuclei (blue), nanoparticles labelled with DTAF (green) and endocytic vesicles (LysoTracker [DND-99] red). C, Serum stability of PEI-siRNA-Pluronic® formulation. The graphic shows mean diameter values of micelles after incubation with serum at different time-points. Results are expressed as mean \pm SD, n=3. DAPI = 4',6-diamidino-2-phenylindole; DTAF = ([4,6-dichlorotriazin-2-yl]amino) fluorescein hydrochloride; PEI = polyethylenimine.

Based on these results, it is possible to conclude that even though the combination of polymers in optimized ratios could be promising, unfortunately, the production method of PM by direct dissolution did not generate nanoparticles with adequate physicochemical features. The production of micelles by thin-FH technique was evaluated as an alternative, in order to improve their physicochemical characteristics.

PEI-based Systems for siALOX5 Delivery, as Model Gene: FH Technique

Next, we generated a system for siRNA delivery combining (1) polyplexes formed by electrostatic interaction of negatively charged siRNA molecules and positively charged chains of PEI-10K, and (2) Pluronic® F127-based PM obtained by FH method, which yields better

physicochemical characteristics (Figure 5A, Table 7).

Table 7. MD and PDI of loaded and unloaded formulations, as well as a loaded formulation stored 30 Days at 4°C.

Sample	Md (nm) ± SD	PDI ± SD
PM-Empty	23.93 ± 0.65	0.250 ± 0.007
PM-siALOX5	24.51 ± 0.53	0.276 ± 0.035
PM-siALOX5 (30 days)	27.72 ± 1.16	0.231 ± 0.070

Md=mean diameter; PDI=polydispersity index. Results are expressed as mean±SD, n=3.

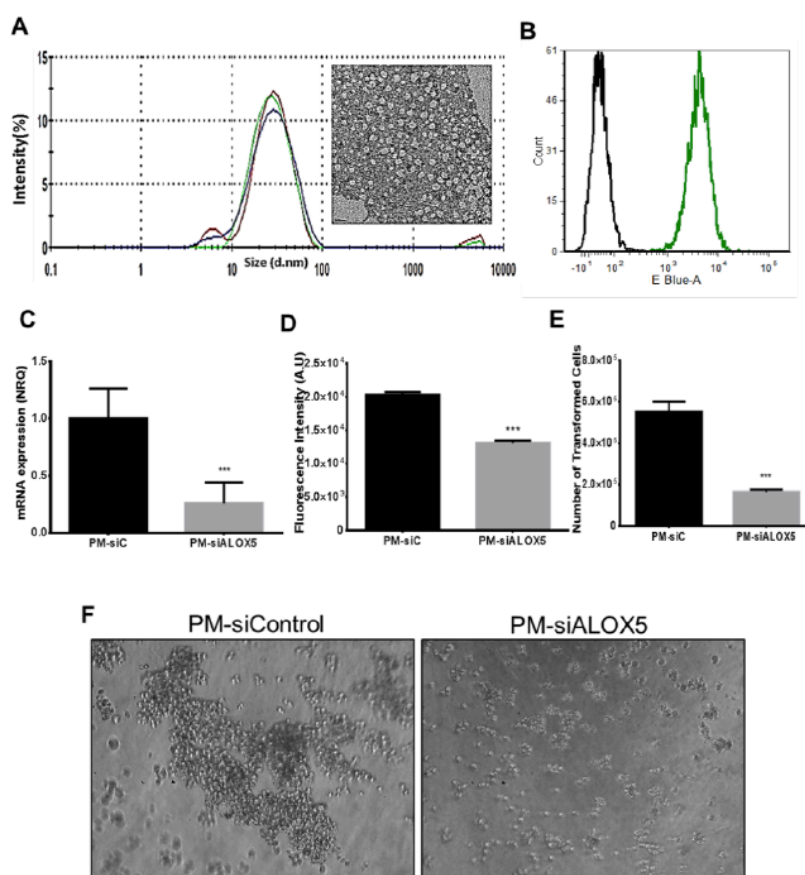


Figure 5. A, Physicochemical characterization of PM-siALOX5. B, Flow cytometry analysis of PEI-siRNA-Pluronic® internalization in MDA-MB-231 cells, after 4 hours of incubation with 5-DTAF labelled particles (green line). The black line corresponds to the negative control. C, ALOX5 downregulation in CSC population from the MDA-MB-231 cell line after treatment with PM-siALOX5. ALOX5 expression was analyzed by qPCR. D, Invasion Assay: the number of invasive cells was quantified after 24 hours of incubation with PM-siC and PM-siALOX5 in MDA-MB-231 CSC. E, Transformation Assay: transformed cells were quantified after 8 days of incubation with PM-siC and PM-siALOX5 in MDA-MB-231-ALDH1A1/tdTomato cell line. Pictures were taken at 10× in optical microscope and represent colonies formed within soft agar matrix after a 7 day of incubation. Results are expressed as mean ± SEM (n=3), *** $p < 0.001$, ** $p < 0.01$, * $p < 0.05$.

ALOX5, a gene involved in CSC homeostasis was chosen as a model gene to test our siRNA system (siALOX5). PM-siALOX5 showed a Md value of 24 nm and a low PDI (≤ 0.2). Moreover, after 30 days of storage no significant aggregation of particles was detected (Figure 5A, Table 7). Further, PM were easily internalized in MDA-MB-231 breast cancer cells with more than 98% of positive cells, after 4 hours of incubation (Figure 5B).

Biological efficacy of our system was also tested in breast CSC. PM-siALOX5 were transfected into CSC population isolated from MDA-MB-231 cell line. ALOX5 mRNA levels were quantified by qPCR. As shown in Figure 5C an encouraging significant silencing of ALOX5 expression was achieved. Furthermore, the effects of PM-siALOX5 transfection in CSC invasion and transformation capacity were also assessed. Accordingly, the invasive potential of breast CSC was significantly decreased ($p \leq 0.001$) after transfection with PM-siALOX5 (Figure 5D), as well as their anchorage-independent growth ability (Figure 5E), showing that treatment with PM-siALOX5 reduced not only the number of transformed cells but also inhibits proper colony formation (Figure 5F).

Discussion

The present work aimed to develop an efficient and safe siRNA delivery system. Most gene delivery systems require the use of cationic components able to complex and condense genetic material, in order to facilitate their cellular internalization and biological effects (46-48). The use of cationic polymers however exhibit several drawbacks, particularly, exceeding levels of undesired toxicity. Because of this, different polymeric-based formulations were designed and tested overtime in order to select the best performing system with optimal characteristics for siRNA delivery. As a result, several formulations were discarded due to their toxicity and/or low biological efficacy. As shown, our first approach consisted in the complexation of siRNA in polyplexes composed by CS (CS-siRNA), a well-established biopolymer with recognized advantages in terms of gene delivery (49,50).

Using Lipofectamine® 2000 as positive control, different types of CS were tested at different

conditions regarding concentration, pH and N/P ratio, in order to achieve the correct silencing efficacy/toxicity balance. RXO-C cells expressing GFP were used to test the silencing efficacy of polyplexes loaded with siRNA against GFP. Biological activity was assessed based on visual reduction of GFP expression in cells transfected with CS-siGFP versus CS-siC, using fluorescence microscopy. Regarding association efficiency of polyplexes, different polymer:siRNA ratios were also tested. As previously reported, our data also show the so well recognized capacity of CS to complex OGN, even at lower ratios (51, 52). Although a 1:2.5 ratio showed to be enough to complex siRNA, GFP reporter silencing assays demonstrate that in order to promote endosomal swelling and to obtain biological efficacy, higher polymer concentrations are required. This highlights that complexation is not the unique condition for the existence of biological effect, despite being essential for proper delivery of genetic material. In fact, N/P ratio proved to be an essential factor affecting complexation efficiency of polyplexes. Moreover, complexes formed at low molar ratio in the range of 2-5 tend to aggregate due to hydrophobic interactions, thus hampering its efficient transfection. In contrast, higher N/P ratios reduce aggregation as a result of electrostatic repulsion of higher positive surface charges of the complexes (49, 50). In agreement with this, an N/P ratio of 80 was required to observe biological efficacy, despite the low ratios required to ensure siRNA complexation.

According to our data, CS with higher MW presented the best results regarding transfection efficacy, which could be explained by its higher positive charge and capacity to better complex and protect siRNA. Similar data has been also provided by others using plasmids and siRNA (51-54). However, the biological efficacy observed with CS polyplexes showed to be insufficient. Although higher MW CS seem to better condense and protect siRNA for cellular delivery, it is possible that concurrent strong interactions of the system result in lower dissociation between CS and the genetic material after endosomal disruption, rendering low biological efficacy. As referred previously, it is of utmost importance to find a balance between MW and DD to efficiently complex

and protect genetic material, promote its endosomal escape, and allow cytoplasmic release of OGN (53, 54).

In order to increase the biological efficacy, the most effective polyplex (CL213-CS) was posteriorly combined with Pluronic® micelles. This type of polymer has already been described as an enhancer of transfection of genetic material. Although not completely understood and explained, poloxamers interfere with cell membranes reducing their structure and microviscosity/fluidity and allowing escape from the endosomal compartment via membrane disruption and pore formation (55, 56). Different Pluronic® (F68, F108, F127) were tested, with Pluronic® F127 being the one selected due to its better technological features. The smaller size and PDI of F127-based micelles can be explained by their lower critical micellar concentration (CMC), hydrophilic-lipophilic balance (HLB) and critical micellization temperature (CMT) (24 °C for 1% w/v solutions (57)), whereas F68 presents the highest CMC and CMT (54-56.21 °C for 1% w/v solutions (58)) and consequently, higher diameter. Similar data has been reported previously (59). Further, poloxamers with intermediate HLB values like F127 (HLB=18-23), have shown higher ability to interfere with membranes than poloxamers with higher HLB values like F68 and F108 (HLB>24) (60, 61). Thus, higher biological efficacy of the system containing Pluronic® F127 is expected.

Although the silencing efficiency of CS-based polyplexes appears to improve with the presence of Pluronic® F127 in the formulation, it is still substantially lower than those obtained with Lipofectamine® 2000. Taking into account that the presence of Pluronic® improves the transfection efficiency of CS-based polyplexes, the substitution of CS for another cationic polymer, in this case PEI, was addressed. In order to rapidly screen different formulation compositions regarding their transfection efficiency, the reduction of GFP fluorescence in RXO-C/GFP expressing cells was quantified. Our data show that PEI-based polyplexes were able to reduce gene expression, being the transfection efficiency more significant for the polyplexes with an N/P ratio of 50 than N/P ratio 25. Because no significant differences in terms of biological efficacy were observed between both types of PEI, the 10K branched

PEI was chosen due to its recognized lower toxicity profile (44). Interestingly, the presence of 1% Pluronic® (w/v) in the form of micelles improves significantly the transfection efficiency of the polyplexes as observed both, quantitatively and qualitatively by a higher GFP gene expression inhibition. The formulation where PEI 10k was complexed with siRNA at an N/P ratio of 50 and further incorporated into 1% (m/v) Pluronic® F127-based PM, presented similar transfection efficacy and GFP silencing than Lipofectamine® 2000. Contrarily to the need of complex chemical modifications proposed by other studies (62, 63), in this work we used a simple association of PEI-based polyplexes with Pluronic® F127-based PM. The micelles prepared by DM present the great advantage of being prepared by a simpler method, importantly avoiding the use of organic solvents. This is a relevant issue in terms of future translatability to the clinical practice. Unfortunately, higher sizes and polydispersity were shown, as well as lower reproducibility and stability, suffering aggregation in the presence of serum and also under storage. To overcome these technological drawbacks, we changed to the FH technique as production method (64). This method allowed the production of micelles with better physicochemical features (lower size (<30nm) and PDI, as well as neutral zeta potential). A better control and more effective formation of micelles and association of PEI-polyplexes might explain this. Further, the importance of nanoparticles design for gene therapy is not only related with the condensation of genetic material but also with the prevention of its potential degradation. In our case, the particles obtained using the FH method present higher storage stability (64).

Oncology is certainly one of the fields that is most benefiting from the application of nanotechnology to drug and gene delivery. As a result of their malignant phenotype and resistance to conventional therapies, special attention has been given to CSC and to their specific targeting. An anti-CSC therapy, with a delivery system able to effectively reach them, is highly desirable. Otherwise, a reservoir of resistant CSC can cause recurrence and metastatic growth of a more aggressive form of cancer. In this work we used a CSC model we

previously validated both *in vitro* and *in vivo* (42). To specifically target CSC, we selected siRNA against the gene ALOX5 as model gene. It has been shown that inhibition of ALOX5 is a promising strategy to hamper tumor development, due to its recognized role in CSC survival (41, 65, 66). Our data show that PM-siALOX5 were quickly and effectively internalized in breast cancer cells and did not present significant toxicity *in vitro* for the working concentrations. We also confirmed that the presence of F127 was essential to reduce PEI-related cytotoxicity.

Downregulation of ALOX5 after treatment with PM-siALOX5 was studied by qPCR. A significant reduction of ALOX5 mRNA expression was observed. To study the effects of PM-siALOX5 on the metastatic potential of isolated CSC, functional assays were performed. Interestingly, a significant impairment of CSC invasion capacity and anchorage-independent growth ability was observed. Cell neoplastic transformation and

invasive potential are two important hallmarks for CSC aggressive behavior, thus the strategy of silencing ALOX5 using PEI10K-siALOX5-F127 could be a promising and successful future antitumor therapy, particularly in advanced cancers.

In vivo toxicity of this formulation was tested through a maximum tolerated dose assay, and any change of body weight or any adverse effect was detected (64). This formulation was able to extravasate from blood circulation to the tumor mass (64). Moreover, with a F127 based delivery system with similar physicochemical features we assessed the biodistribution of the formulation in a breast cancer model and we obtained high percentages of tumor accumulation (10 to 15%) mainly due to the enhanced permeability effect associated with the small size of the micelles (data not shown), which demonstrates the potentiality of these delivery systems in the field of cancer treatment.

Conclusions

In this work different cationic polymers were tested for the production of polyplexes and different polymeric systems. The choice of PM composed by Pluronic® F127 was based on their capacity to improve transfection efficiency of polyplexes and reduce toxicity. The amphiphilic properties of the system opened the possibility to design a multifunctional-targeted particle for combined therapies, such as a combination of gene- and chemotherapies in one single nanoparticle formulation. Two different PM preparation methods were also compared. The DM technique was the easiest and less time-consuming method to prepare micelles and avoid organic solvents; however, it had important disadvantages regarding the technological features when compared with micelles obtained by the FH technique. Finally, a promising vehicle with adequate physicochemical and biological properties for gene delivery (siRNA-ALOX5) was selected after screening different formulations. Following the concept of precision nanomedicine, the effective gene silencing of our system opens the door to design better gene delivery strategies to specifically target cancer genes, and therefore, benefit specific groups of patients according to their cancer type or genetic profiles.

Acknowledgments

This work was partially supported by grants PI14/02079 and PI17/02242 from Fondo de Investigaciones Sanitarias (FIS) of Instituto Carlos III (ISCIII), co-financed by the European Regional Development Fund (FEDER), and grant AC15/00092 (Target4Cancer project) from EuroNanoMed II to SS and grant 337/C/2013 (PENTRI project) from Fundació Marató TV3 (Catalonia, Spain) to IA. This study was also supported by the Portuguese Science and Technology Foundation (FCT) (PTDC/SAU-FAR/120453/2010) and in part, by iMed.Ulisboa, Portugal (UID/DTP/04138/2013). FCT supported DR with a predoctoral grant (SFRH/BD/76270/2011) and the Spanish Asociación Española Contra el Cáncer (AECC) supported JSF with a postdoctoral fellowship.

Bibliography

1. Wang D, Gao G. State-of-the-art human gene therapy: Part I. gene delivery technologies. *Discov Med*. 2014;18(97):67-77. PubMed PMID: 25091489; PubMed Central PMCID: PMC4440413.
2. Li L, Wei Y, Gong C. Polymeric Nanocarriers for Non-Viral Gene Delivery. *J Biomed Nanotechnol*. 2015;11(5):739-70. PubMed PMID: 26349389.
3. Kaufmann KB, Büning H, Galy A, Schambach A, Grez M. Gene therapy on the move. *EMBO Mol Med*. 2013;5(11):1642-61. doi: 10.1002/emmm.201202287. PubMed PMID: 24106209; PubMed Central PMCID: PMC3840483.
4. Videira M, Arranja A, Rafael D, Gaspar R. Preclinical development of siRNA therapeutics: towards the match between fundamental science and engineered systems. *Nanomedicine*. 2014;10(4):689-702. doi: 10.1016/j.nano.2013.11.018. PubMed PMID: 24333589.
5. Wasungu L, Hoekstra D. Cationic lipids, lipoplexes and intracellular delivery of genes. *J Control Release*. 2006;116(2):255-64. doi: 10.1016/j.jconrel.2006.06.024. PubMed PMID: 16914222.
6. Eliyahu H, Joseph A, Schillemans JP, Azzam T, Domb AJ, Barenholz Y. Characterization and in vivo performance of dextran-spermine polyplexes and DOTAP/cholesterol lipoplexes administered locally and systemically. *Biomaterials*. 2007;28(14):2339-49. doi: 10.1016/j.biomaterials.2006.09.001. PubMed PMID: 17298842.
7. Chira S, Jackson CS, Oprea I, Ozturk F, Pepper MS, Diaconu I, et al. Progresses towards safe and efficient gene therapy vectors. *Oncotarget*. 2015;6(31):30675-703. PubMed PMID: 26362400; PubMed Central PMCID: PMC4741561.
8. Xiong XB, Falamarzian A, Garg SM, Lavasanifar A. Engineering of amphiphilic block copolymers for polymeric micellar drug and gene delivery. *J Control Release*. 2011;155(2):248-61. doi: S0168-3659(11)00243-4 [pii] 10.1016/j.jconrel.2011.04.028. PubMed PMID: 21621570.
9. Ozpolat B, Sood AK, Lopez-Berestein G. Nanomedicine based approaches for the delivery of siRNA in cancer. *Journal of internal medicine*. 2010;267(1):44-53. Epub 2010/01/12. doi: 10.1111/j.1365-2796.2009.02191.x. PubMed PMID: 20059643.
10. Dizaj SM, Jafari S, Khosroushahi AY. A sight on the current nanoparticle-based gene delivery vectors. *Nanoscale Res Lett*. 2014;9(1):252. doi: 10.1186/1556-276X-9-252. PubMed PMID: 24936161; PubMed Central PMCID: PMC4046008.
11. Nayerossadat N, Maedeh T, Ali PA. Viral and nonviral delivery systems for gene delivery. *Adv Biomed Res*. 2012;1:27. doi: 10.4103/2277-9175.98152. PubMed PMID: 23210086; PubMed Central PMCID: PMC403507026.
12. Mao S, Sun W, Kissel T. Chitosan-based formulations for delivery of DNA and siRNA. *Adv Drug Deliv Rev*. 2010;62(1):12-27. doi: S0169-409X(09)00281-6 [pii] 10.1016/j.addr.2009.08.004. PubMed PMID: 19796660.
13. Rudzinski WE, Aminabhavi TM. Chitosan as a carrier for targeted delivery of small interfering RNA. *Int J Pharm*. 2010;399(1-2):1-11. doi: S0378-5173(10)00627-7 [pii] 10.1016/j.ijpharm.2010.08.022. PubMed PMID: 20732398.
14. Holzer P, Ajdini B, Heusermann W, Bruno K, Schuleit M, Meinel L, et al. Biophysical properties of chitosan/siRNA polyplexes: profiling the polymer/siRNA interactions and bioactivity. *J Control Release*. 2012;157(2):297-304. doi: 10.1016/j.jconrel.2011.08.023. PubMed PMID: 21884740.
15. Park IK, Park YH, Shin BA, Choi ES, Kim YR, Akaike T, et al. Galactosylated chitosan-graft-dextran as hepatocyte-targeting DNA carrier. *J Control Release*. 2000;69(1):97-108. PubMed PMID: 11018549.
16. Kim TH, Ihm JE, Choi YJ, Nah JW, Cho CS. Efficient gene delivery by urocanic acid-modified chitosan. *J Control Release*. 2003;93(3):389-402. PubMed PMID: 14644588.
17. Kim TH, Kim SI, Akaike T, Cho CS. Synergistic effect of poly(ethylenimine) on the transfection efficiency of galactosylated chitosan/DNA complexes. *J Control Release*. 2005;105(3):354-66. doi: S0168-3659(05)00133-1 [pii] 10.1016/j.jconrel.2005.03.024. PubMed PMID: 15949861.
18. Wong K, Sun G, Zhang X, Dai H, Liu Y, He C, et al. PEI-g-chitosan, a novel gene delivery system with transfection efficiency comparable to polyethylenimine in vitro and after liver administration in vivo. *Bioconjug Chem*. 2006;17(1):152-8. doi: 10.1021/bc0501597. PubMed PMID: 16417264.

19. Lin A, Liu Y, Huang Y, Sun J, Wu Z, Zhang X, et al. Glycyrrhizin surface-modified chitosan nanoparticles for hepatocyte-targeted delivery. *Int J Pharm.* 2008;359(1-2):247-53. doi: 10.1016/j.ijpharm.2008.03.039. PubMed PMID: 18457928.
20. Gabizon A, Shmeeda H, Horowitz AT, Zalipsky S. Tumor cell targeting of liposome-entrapped drugs with phospholipid-anchored folic acid-PEG conjugates. *Adv Drug Deliv Rev.* 2004;56(8):1177-92. doi: 10.1016/j.addr.2004.01.011. PubMed PMID: 15094214.
21. Moreira C, Oliveira H, Pires LR, Simões S, Barbosa MA, Pêgo AP. Improving chitosan-mediated gene transfer by the introduction of intracellular buffering moieties into the chitosan backbone. *Acta Biomater.* 2009;5(8):2995-3006. doi: S1742-7061(09)00176-7 [pii] 10.1016/j.actbio.2009.04.021. PubMed PMID: 19427930.
22. Akinc A, Thomas M, Klibanov AM, Langer R. Exploring polyethylenimine-mediated DNA transfection and the proton sponge hypothesis. *J Gene Med.* 2005;7(5):657-63. doi: 10.1002/jgm.696. PubMed PMID: 15543529.
23. Roesler S, Koch FP, Schmehl T, Weissmann N, Seeger W, Gessler T, et al. Amphiphilic, low molecular weight poly(ethylene imine) derivatives with enhanced stability for efficient pulmonary gene delivery. *J Gene Med.* 2011;13(2):123-33. doi: 10.1002/jgm.1538. PubMed PMID: 21308899.
24. Martin I, Dohmen C, Mas-Moruno C, Troiber C, Kos P, Schaffert D, et al. Solid-phase-assisted synthesis of targeting peptide-PEG-oligo(ethane amino)amides for receptor-mediated gene delivery. *Org Biomol Chem.* 2012;10(16):3258-68. doi: 10.1039/c2ob06907e. PubMed PMID: 22407126.
25. Godbey WT, Wu KK, Mikos AG. Size matters: molecular weight affects the efficiency of poly(ethylenimine) as a gene delivery vehicle. *J Biomed Mater Res.* 1999;45(3):268-75. PubMed PMID: 10397985.
26. Thomas M, Klibanov AM. Enhancing polyethylenimine's delivery of plasmid DNA into mammalian cells. *Proc Natl Acad Sci U S A.* 2002;99(23):14640-5. doi: 10.1073/pnas.192581499. PubMed PMID: 12403826; PubMed Central PMCID: PMC137472.
27. Mao S, Neu M, Gernershaus O, Merkel O, Sitterberg J, Bakowsky U, et al. Influence of polyethylene glycol chain length on the physicochemical and biological properties of poly(ethylene imine)-graft-poly(ethylene glycol) block copolymer/siRNA polyplexes. *Bioconj Chem.* 2006;17(5):1209-18. doi: 10.1021/bc060129j. PubMed PMID: 16984130.
28. Dehshahri A, Oskuee RK, Shier WT, Hatefi A, Ramezani M. Gene transfer efficiency of high primary amine content, hydrophobic, alkyl-oligoamine derivatives of polyethylenimine. *Biomaterials.* 2009;30(25):4187-94. doi: 10.1016/j.biomaterials.2009.04.036. PubMed PMID: 19464054.
29. Grayson AC, Doody AM, Putnam D. Biophysical and structural characterization of polyethylenimine-mediated siRNA delivery in vitro. *Pharm Res.* 2006;23(8):1868-76. doi: 10.1007/s11095-006-9009-2. PubMed PMID: 16845585.
30. Oskuee RK, Philipp A, Dehshahri A, Wagner E, Ramezani M. The impact of carboxyalkylation of branched polyethylenimine on effectiveness in small interfering RNA delivery. *J Gene Med.* 2010;12(9):729-38. Epub 2010/08/05. doi: 10.1002/jgm.1490. PubMed PMID: 20683834.
31. Malek A, Czubayko F, Aigner A. PEG grafting of polyethylenimine (PEI) exerts different effects on DNA transfection and siRNA-induced gene targeting efficacy. *Journal of Drug Targeting.* 2008;16(2):124-39. Epub 2008/02/16. doi: 10.1080/10611860701849058. PubMed PMID: 18274933.
32. Moghimi SM, Hunter AC. Poloxamers and poloxamines in nanoparticle engineering and experimental medicine. *Trends Biotechnol.* 2000;18(10):412-20. doi: S0167-7799(00)01485-2 [pii]. PubMed PMID: 10998507.
33. Kabanov AV, Batrakova EV, Alakhov VY. Pluronic block copolymers as novel polymer therapeutics for drug and gene delivery. *J Control Release.* 2002;82(2-3):189-212. doi: S0168365902000093 [pii]. PubMed PMID: 12175737.
34. Batrakova EV, Kabanov AV. Pluronic block copolymers: evolution of drug delivery concept from inert nanocarriers to biological response modifiers. *J Control Release.* 2008;130(2):98-106. doi: 10.1016/j.jconrel.2008.04.013. PubMed PMID: 18534704; PubMed Central PMCID: PMC137472.
35. Chen YC, Jiang LP, Liu NX, Ding L, Liu XL, Wang ZH, et al. Enhanced gene transduction into skeletal muscle of mice in vivo with pluronic block copolymers and ultrasound exposure. *Cell Biochem Biophys.* 2011;60(3):267-73. doi: 10.1007/s12013-010-9149-1. PubMed PMID: 21253893.
36. Wang F, Li K, Chen Y. Gene transfection mediated by ultrasound and Pluronic P85 in HepG2 cells. *J Huazhong Univ Sci Technolog Med Sci.* 2007;27(6):700-2. doi: 10.1007/s11596-007-0621-0. PubMed PMID: 18231747.

37. Kabanov A, Zhu J, Alakhov V. Pluronic block copolymers for gene delivery. *Advances in genetics*. 2005;53:231-61. Epub 2005/10/26. PubMed PMID: 16240996.
38. Wang M, Wu B, Lu P, Tucker JD, Milazi S, Shah SN, et al. Pluronic-PEI copolymers enhance exon-skipping of 2'-O-methyl phosphorothioate oligonucleotide in cell culture and dystrophic mdx mice. *Gene Ther*. 2014;21(1):52-9. doi: 10.1038/gt.2013.57. PubMed PMID: 24131982.
39. Kuo JH. Effect of Pluronic-block copolymers on the reduction of serum-mediated inhibition of gene transfer of polyethyleneimine-DNA complexes. *Biotechnol Appl Biochem*. 2003;37(Pt 3):267-71. doi: BA20020123 [pii] 10.1042/BA20020123. PubMed PMID: 12597775.
40. Yang F, Xu J, Tang L, Guan X. Breast cancer stem cell: the roles and therapeutic implications. *Cellular and molecular life sciences : CMLS*. 2017;74(6):951-66. doi: 10.1007/s00018-016-2334-7. PubMed PMID: 27530548.
41. Chen Y, Shan Y, Lu M, DeSouza N, Guo Z, Hoffman R, et al. Alox5 Blockade Eradicates JAK2V617F-Induced Polycythemia Vera in Mice. *Cancer research*. 2017;77(1):164-74. doi: 10.1158/0008-5472.CAN-15-2933. PubMed PMID: 27784744; PubMed Central PMCID: PMC5217717.
42. Gener P, Gouveia LP, Sabat GR, de Sousa Rafael DF, Fort NB, Arranja A, et al. Fluorescent CSC models evidence that targeted nanomedicines improve treatment sensitivity of breast and colon cancer stem cells. *Nanomedicine*. 2015;11(8):1883-92. doi: 10.1016/j.nano.2015.07.009. PubMed PMID: 26238079.
43. Andrade F, das Neves J, Gener P, Schwartz S, Ferreira D, Oliva M, et al. Biological assessment of self-assembled polymeric micelles for pulmonary administration of insulin. *Nanomedicine*. 2015;11(7):1621-31. doi: 10.1016/j.nano.2015.05.006. PubMed PMID: 26049134.
44. Paul A, Eun C-J, Song JM. Cytotoxicity mechanism of non-viral carriers polyethylenimine and poly-L-lysine using real time high-content cellular assay. *Polymer*. 2014;55(20):5178-88.
45. Symonds P, Murray JC, Hunter AC, Debska G, Szewczyk A, Moghimi SM. Low and high molecular weight poly(L-lysine)s/poly(L-lysine)-DNA complexes initiate mitochondrial-mediated apoptosis differently. *FEBS Lett*. 2005;579(27):6191-8. doi: 10.1016/j.febslet.2005.09.092. PubMed PMID: 16243317.
46. Tros de Ilarduya C, Sun Y, Düzgüneş N. Gene delivery by lipoplexes and polyplexes. *Eur J Pharm Sci*. 2010;40(3):159-70. doi: 10.1016/j.ejps.2010.03.019. PubMed PMID: 20359532.
47. Iyer AK, Duan Z, Amiji MM. Nanodelivery systems for nucleic acid therapeutics in drug resistant tumors. *Molecular pharmaceutics*. 2014;11(8):2511-26. Epub 2014/03/26. doi: 10.1021/mp500024p. PubMed PMID: 24661041.
48. Rafael DF, Andrade F, Arranja A, Luís AS, Videira M. Lipoplexes and Polyplexes: Gene Delivery Applications. . *Encyclopedia Biomedical Polymers and Polymeric Biomaterials*, Taylor and Francis Group 2014.
49. Huang M, Fong CW, Khor E, Lim LY. Transfection efficiency of chitosan vectors: effect of polymer molecular weight and degree of deacetylation. *J Control Release*. 2005;106(3):391-406. doi: S0168-3659(05)00232-4 [pii] 10.1016/j.jconrel.2005.05.004. PubMed PMID: 15967533.
50. Lavertu M, Méthot S, Tran-Khanh N, Buschmann MD. High efficiency gene transfer using chitosan/DNA nanoparticles with specific combinations of molecular weight and degree of deacetylation. *Biomaterials*. 2006;27(27):4815-24. doi: 10.1016/j.biomaterials.2006.04.029. PubMed PMID: 16725196.
51. Mao S, Sun W, Kissel T. Chitosan-based formulations for delivery of DNA and siRNA. *Adv Drug Deliv Rev*. 2010;62(1):12-27. doi: 10.1016/j.addr.2009.08.004. PubMed PMID: 19796660.
52. Rudzinski WE, Aminabhavi TM. Chitosan as a carrier for targeted delivery of small interfering RNA. *International journal of pharmaceutics*. 2010;399(1-2):1-11. Epub 2010/08/25. doi: 10.1016/j.ijpharm.2010.08.022. PubMed PMID: 20732398.
53. Köping-Höggård M, Tubulekas I, Guan H, Edwards K, Nilsson M, Vårnum KM, et al. Chitosan as a nonviral gene delivery system. Structure-property relationships and characteristics compared with polyethylenimine in vitro and after lung administration in vivo. *Gene Ther*. 2001;8(14):1108-21. doi: 10.1038/sj.gt.3301492. PubMed PMID: 11526458.
54. Köping-Höggård M, Vårnum KM, Issa M, Danielsen S, Christensen BE, Stokke BT, et al. Improved chitosan-mediated gene delivery based on easily dissociated chitosan polyplexes of highly defined chitosan oligomers. *Gene Ther*. 2004;11(19):1441-52. doi: 10.1038/sj.gt.3302312. PubMed PMID: 15269712.

55. Demina T, Grozdova I, Krylova O, Zhirnov A, Istratov V, Frey H, et al. Relationship between the structure of amphiphilic copolymers and their ability to disturb lipid bilayers. *Biochemistry*. 2005;44(10):4042-54. doi: 10.1021/bi048373q. PubMed PMID: 15751981.
56. Batrakova EV, Li S, Alakhov VY, Miller DW, Kabanov AV. Optimal structure requirements for pluronic block copolymers in modifying P-glycoprotein drug efflux transporter activity in bovine brain microvessel endothelial cells. *The Journal of pharmacology and experimental therapeutics*. 2003;304(2):845-54. Epub 2003/01/23. doi: 10.1124/jpet.102.043307. PubMed PMID: 12538842.
57. Lin Y, Alexandridis P. Temperature-dependent adsorption of Pluronic F127 block copolymers onto carbon black particles dispersed in aqueous media. *J Phys Chem B*. 2002;106:10834-44.
58. Tsui H-W, Wang J-H, Hsu Y-H, Chen L-J. Study of heat of micellization and phase separation for Pluronic aqueous solutions by using a high sensitivity differential scanning calorimetry. *Colloid and Polymer Science*. 2010;288:1687-96.
59. Andrade F, Fonte P, Oliva M, Videira M, Ferreira D, Sarmiento B. Solid state formulations composed by amphiphilic polymers for delivery of proteins: characterization and stability. *International Journal of Pharmaceutics*. 2015;486(1-2):195-206. doi: 10.1016/j.ijpharm.2015.03.050. PubMed PMID: WOS:000353999100022.
60. Chen J, Luo J, Zhao Y, Pu L, Lu X, Gao R, et al. Increase in transgene expression by pluronic L64-mediated endosomal/lysosomal escape through its membrane-disturbing action. *ACS applied materials & interfaces*. 2015;7(13):7282-93. Epub 2015/03/20. doi: 10.1021/acsami.5b00486. PubMed PMID: 25786540.
61. Katas H, Alpar HO. Development and characterisation of chitosan nanoparticles for siRNA delivery. *J Control Release*. 2006;115(2):216-25. doi: 10.1016/j.jconrel.2006.07.021. PubMed PMID: 16959358.
62. Hu Y, Zhou D, Li C, Zhou H, Chen J, Zhang Z, et al. Gene delivery of PEI incorporating with functional block copolymer via non-covalent assembly strategy. *Acta biomaterialia*. 2013;9(2):5003-12. Epub 2012/10/06. doi: 10.1016/j.actbio.2012.09.033. PubMed PMID: 23036947.
63. Wen Y, Pan S, Luo X, Zhang W, Shen Y, Feng M. PEG- and PDMAEG-graft-modified branched PEI as novel gene vector: synthesis, characterization and gene transfection. *Journal of biomaterials science Polymer edition*. 2010;21(8-9):1103-26. Epub 2010/05/29. doi: 10.1163/092050609X12459295750316. PubMed PMID: 20507711.
64. Rafael D, Gener P, Andrade F, Seras-Franzoso J, Montero S, Fernandez Y, et al. AKT2 siRNA delivery with amphiphilic-based polymeric micelles show efficacy against cancer stem cells. *Drug delivery*. 2018;25(1):961-72. doi: 10.1080/10717544.2018.1461276. PubMed PMID: 29667444.
65. Chen Y, Li D, Li S. The Alox5 gene is a novel therapeutic target in cancer stem cells of chronic myeloid leukemia. *Cell cycle*. 2009;8(21):3488-92. doi: 10.4161/cc.8.21.9852. PubMed PMID: 19823023.
66. Chen Y, Hu Y, Zhang H, Peng C, Li S. Loss of the Alox5 gene impairs leukemia stem cells and prevents chronic myeloid leukemia. *Nature genetics*. 2009;41(7):783-92. doi: 10.1038/ng.389. PubMed PMID: 19503090; PubMed Central PMCID: PMC2887745.

Quote As: Rafael D, Andrade F, Montero S, Gener P, Seras-Franzoso J, Martínez F, González P, Florindo H, Arango D, Sayós J, Abasolo I, Videira M, and Schwartz Jr. S. Rational Design of a siRNA Delivery System: ALOX5 and Cancer Stem Cells as Therapeutic Targets, *Prec. Nanomed*. 2018 July;1(2):86-105 DOI:[10.29016/180629.1](https://doi.org/10.29016/180629.1)

